Western Graduate&PostdoctoralStudies

Western University
Scholarship@Western

Electronic Thesis and Dissertation Repository

7-4-2019 11:00 AM

Nonlinear Attitude and Pose Filters with Superior Convergence Properties

Hashim Abdellah Hashim Mohamed, *The University of Western Ontario*

Supervisor: Brown, Lyndon J., *The University of Western Ontario*
Co-Supervisor: McIsaac, Kenneth, *The University of Western Ontario*
A thesis submitted in partial fulfillment of the requirements for the Doctor of Philosophy degree in Electrical and Computer Engineering
© Hashim Abdellah Hashim Mohamed 2019

Follow this and additional works at: https://ir.lib.uwo.ca/etd

Part of the Controls and Control Theory Commons, Navigation, Guidance, Control and Dynamics Commons, and the Robotics Commons

Recommended Citation

Mohamed, Hashim Abdellah Hashim, "Nonlinear Attitude and Pose Filters with Superior Convergence Properties" (2019). *Electronic Thesis and Dissertation Repository*. 6244.
https://ir.lib.uwo.ca/etd/6244

This Dissertation/Thesis is brought to you for free and open access by Scholarship@Western. It has been accepted for inclusion in Electronic Thesis and Dissertation Repository by an authorized administrator of Scholarship@Western. For more information, please contact wlswadmin@uwo.ca.

Abstract

In this thesis, several deterministic and stochastic attitude filtering solutions on the special orthogonal group $\mathbb{SO}(3)$ are proposed. Firstly, the attitude estimation problem is approached on the basis of nonlinear deterministic filters on $\mathbb{SO}(3)$ with guaranteed transient and steady-state measures. The second solution to the attitude estimation problem considers nonlinear stochastic filters on $\mathbb{SO}(3)$ with superior convergence properties with two filters being developed in the sense of Ito, and one in the sense of Stratonovich. This thesis also presents several deterministic and stochastic pose filtering solutions developed on the special Euclidean group $\mathbb{SE}(3)$. The first solution includes two nonlinear deterministic pose filters on $\mathbb{SE}(3)$ with predefined transient as well as steady-state performance, while the second one involves a nonlinear stochastic filter on $\mathbb{SE}(3)$ in the sense of Stratonovich. The proposed nonlinear deterministic filters on $\mathbb{SO}(3)$ and $\mathbb{SE}(3)$ guarantee that attitude and pose error are trapped to initially start within a known large set and converge systematically and asymptotically to the equilibrium point from almost any initial condition, respectively. The proposed stochastic filters ensure that errors of the estimates and attitude or errors of the estimates and pose are semi-globally uniformly ultimately bounded in mean square, and they converge to a small neighborhood of the origin from almost any initial condition. The output performance of the proposed filters is examined and simulated considering high level of uncertainties in the measurements and large error in initialization. The above-mentioned consideration makes the proposed filters a good fit for measurements obtained from low-cost inertial measurement units or low-cost inertial vision systems.

Keywords: Observer, estimator, estimate, attitude, position, pose, stochastic differential equations, Ito, Stratonovich, noise, Wong-Zakai, transient error, steady-state, error, prescribed performance function, special orthogonal group, special Euclidean group, IMUs, SDEs, SO(3), SE(3).

Summary for Lay Audience

Nowadays, the research of autonomous vehicles is on the rise. In the coming years, unmanned aerial vehicles, for example, are predicted to become an indispensable part of our daily life. The applications of such vehicles include mail and food delivery as well as a multitude of other military and civil applications. However, to make the wide usage possible the price of the vehicle has to be affordable. Therefore, this work proposes a set of algorithms which help the vehicle to achieve great performance even with cheap sensors. The function of the sensors attached to the vehicle is to collect information about its orientation and position. However, because of their simple structure the information they collect is noisy. The proposed algorithms allow to filter out the noise, and therefore successfully control the movement of the vehicle.

Statement of Co-Authorship

The following thesis contains materials from published papers as well as manuscripts submitted for publication that have been co-authored by Hashim A. Hashim Mohamed, Dr. Lyndon J. Brown, and Dr. Kenneth McIsaac. All the work presented in this thesis has been done under the supervision of Dr. Lyndon J. Brown, and Dr. Kenneth McIsaac with the exception of the preliminaries of the work in Chapter 4 which have been done under the supervision of Dr. Abdelhamid Tayebi. All the research, developments, work, results and simulations presented here were carried out by Hashim A. Hashim Mohamed under the guidance of Dr. Lyndon J. Brown and Dr. Kenneth McIsaac. The original manuscripts which make up Chapters 1-8 of this thesis were also written by Hashim A. Hashim Mohamed.

Dedication

To my beloved parents, brother, wife and to the gentle reader

Acknowledgements

I would like to thank my supervisors, Lyndon J. Brown and Kenneth McIsaac, for their support, guidance, and constructive suggestions. I am also grateful to Lydon J. Brown for an opportunity to work as a teaching assistant which was very beneficial for my academic growth.

I also would like to thank Western University for the funding that allowed me to publish multiple research articles and write this thesis. I also would like to thank the school of Graduate and Postdoctoral Studies for their help and support.

I want to thank my wife for proofreading every chapter of this thesis and all the published articles related to this thesis. I am grateful to my wife for her help and support without whom I would not have completed this thesis within a short period of time.

Forever and ever I am indebted to my lovely **parents** and they are the main reason for every success in my life. I want to thank my **parents** and **brother** whose love and support have always guided me forward and without whom I would not have achieved any success. I also want to thank my relatives and friends who have all been important parts of my life.

Table of Contents

Page

Abstract . . . . . **i**

Lay Summary . . . . . **ii**

Statement of Co-Authorship . . . . . **iii**

Dedication . . . . . **iv**

Acknowledgements . . . . . **v**

List of Figures . . . . . **ix**

List of Tables . . . . . **xi**

List of Symbols . . . . . **xii**

1 Introduction **1**

1.1 General Overview 2

1.2 Background of Attitude Filtering Methods 3

1.2.1 Earliest attitude filtering 3

1.2.2 Gaussian attitude filtering 4

1.2.3 Nonlinear deterministic attitude filtering 6

1.2.4 Attitude filtering: Nonlinear deterministic vs Gaussian 8

1.3 Background of Pose Filtering Methods 8

1.3.1 Gaussian pose filtering and challenges 9

1.3.2 Nonlinear deterministic pose filtering 10

1.4 Scope of Thesis: Nonlinear Attitude and Pose Filtering Design Challenges 11

1.4.1 Nonlinear deterministic attitude filtering challenges 11

1.4.2 Nonlinear deterministic pose filtering challenges 12

1.4.3 Nonlinear deterministic filters with prescribed performance . . 12

1.4.4 Nonlinear stochastic attitude filtering challenges 13

1.4.5 Nonlinear stochastic pose filtering challenges 13

1.5 Statement of Contributions 14

1.5.1 List of publications 19

1.6 Thesis Outline 21

2 Preliminaries and Notation **24**
2.1 Math Notation 24
2.2 $\mathbb{SO}(3)$ and $\mathbb{SE}(3)$ Preliminaries 24

3 Nonlinear Attitude Filters on $\mathbb{SO}(3)$ with Prescribed Performance **29**
3.1 Introduction 29
3.2 Problem Formulation with Prescribed Performance 30
3.2.1 Attitude Kinematics and Measurements 30
3.2.2 Estimator Structure and Error Criteria 32
3.2.3 Prescribed Performance 34
3.3 Nonlinear Complementary Filters On $\mathbb{SO}(3)$ with Prescribed Performance 37
3.3.1 Semi-direct Attitude Filter with Prescribed Performance . . . 38
3.3.2 Direct Attitude Filter with Prescribed Performance 40
3.4 Simulations 47
3.4.1 Proposed Filters vs Nonlinear Attitude Filters 51
3.4.2 Proposed Filters vs Gaussian Attitude Filters 54
3.5 Conclusion 55

4 Nonlinear Stochastic Filters on $\mathbb{SO}(3)$: Ito and Stratonovich . . . **57**
4.1 Introduction 57
4.2 Problem Formulation in Stochastic Sense 58
4.3 Stochastic Complementary Filters On $\mathbb{SO}(3)$ 62
4.3.1 Nonlinear Deterministic Attitude Filter 63
4.3.2 Nonlinear Stochastic Attitude Filter in Ito Sense 65
4.3.3 Nonlinear Stochastic Attitude Filter in Stratonovich Sense . . 71
4.3.4 Stochastic Attitude Filters: Ito vs Stratonovich 78
4.4 Simulations 79
4.5 Conclusion 84

5 Nonlinear Explicit Stochastic Attitude Filter on $\mathbb{SO}(3)$ **85**
5.1 Introduction 85
5.2 Problem Formulation 86
5.3 Nonlinear Stochastic Filter on $\mathbb{SO}(3)$ 89
5.4 Simulation 98
5.5 Conclusion 99

6 Nonlinear Pose Filters on $\mathbb{SE}(3)$ with Prescribed Performance . . 101
6.1 Introduction . . . 101
6.2 Problem Formulation with Prescribed Performance . . . 102
6.2.1 Pose Kinematics and Measurements . . . 102
6.2.2 Prescribed Performance . . . 107
6.3 Nonlinear Complementary Pose Filters On $\mathbb{SE}(3)$ with Prescribed Performance . . . 111
6.3.1 Semi-direct Pose Filter with Prescribed Performance . . . 112
6.3.2 Direct Pose Filter with Prescribed Performance . . . 115
6.3.3 Simplified steps of the proposed pose filters . . . 123
6.4 Simulations . . . 124
6.5 Conclusion . . . 129

7 Nonlinear Stochastic Pose Filter on $\mathbb{SE}(3)$ . . . 131
7.1 Introduction . . . 131
7.2 Problem Formulation in Stochastic Sense . . . 131
7.3 Nonlinear Stochastic Complementary Filter on $\mathbb{SE}(3)$ . . . 139
7.3.1 Nonlinear Deterministic Pose Filter . . . 140
7.3.2 Nonlinear Stochastic Pose Filter in Stratonovich Sense . . . 144
7.4 Simulations . . . 157
7.5 Conclusion . . . 164

8 Conclusion . . . 165
8.1 Future Work . . . 168

A Proof of Lemma 3.1, 5.1 and 6.1 . . . 176

B An Overview of Attitude Reconstruction via SVD . . . 180

C Detailed proofs . . . 181

Curriculum Vitae . . . 188

List of Figures

Section **Page**

1.1 Relative applications for attitude and pose. 2

3.1 The relative orientation between body-frame and inertial-frame of a rigid-body. 30
3.2 A detailed representation of tracking normalized Euclidean distance error $||\tilde{R}(t)||_I$ with PPF satisfying (a) Eq. (3.17); (b) Eq. (3.18). . . 35
3.3 True and measured angular velocities. 49
3.4 Body-frame vectorial measurements: true and measured. 49
3.5 Transient and steady-state performance of normalized Euclidean distance. 50
3.6 Tracking performance of Euler angles (roll (ϕ) and pitch (θ), yaw (ψ)). 50
3.7 The estimated bias of the proposed filters. 51
3.8 Transient and steady-state performance of normalized Euclidean distance: Semi-direct filter vs literature Mahony, Hamel, and Pflimlin (2008). 52
3.9 Transient and steady-state performance of normalized Euclidean distance: Direct filter vs MEKF Markley (2003). 55

4.1 The orientation of a 3D rigid-body in body-frame relative to inertial-frame. 58
4.2 True and measured angular velocities. 81
4.3 True and measured body-frame vectorial measurements. 81
4.4 Tracking performance of Euler angles. 82
4.5 Rodriguez vector square error $\tilde{\rho}^2$. 82
4.6 Tracking performance of normalized Euclidean distance error $||\tilde{R}||_I$. . 83
4.7 Estimates of stochastic attitude filters ($\hat{b}$). 83
4.8 Estimates of stochastic attitude filters ($\hat{\sigma}$). 84

5.1 True values and measurements of Ω, $\upsilon_1^{\mathcal{B}(R)}$, and $\upsilon_2^{\mathcal{B}(R)}$. 99
5.2 Tracking performance of normalized Euclidean distance error. 100
5.3 Tracking performance of Euler angles, proposed filter performance vs true trajectories. 100

6.1 Pose estimation problem of a rigid-body in 3D space. 102
6.2 Graphical representation of the systematic convergence of tracking error $\boldsymbol{e}_i$ with PPF satisfying (a) Eq. (6.21); (b) Eq. (6.22). 108

6.3 Measured and true values of angular velocities. 126
6.4 Measured and true values of translational velocities. 127
6.5 True and measured body-frame vectorial measurements. 127
6.6 True and estimated Euler angles of the rigid-body. 128
6.7 True and estimated rigid-body positions in 3D space. 128
6.8 Systematic convergence of the error trajectories within the prescribed performance boundaries. 129
6.9 The estimated bias of the proposed filters. 129

7.1 Pose estimation problem of a rigid-body moving in 3D space. 133
7.2 True and measured angular velocities. 160
7.3 True and measured translational velocities. 160
7.4 True values and vectorial measurements of the body-frame. 161
7.5 Tracking performance of Euler angles of the stochastic filter. 161
7.6 Tracking performance of x, y and z trajectory of the stochastic filter in 3D space. 162
7.7 Tracking performance of normalized Euclidean distance error of $||\tilde{R}||_I$ and Euclidean distance $||P - \hat{P}||$. 162

List of Tables

Section **Page**

3.1 Statistical analysis of $||\tilde{R}||_I$ of the proposed two filters. 51
3.2 Statistical analysis of $||\tilde{R}||_I$ of the semi-direct filter vs literature. . . . 53
3.3 MEKF design parameters. 54

4.1 Statistical analysis of $||\tilde{R}||_I$ of the two proposed filter. 81

7.1 Statistical analysis of the noise and bias in input measurements and output data of the proposed filter. 163

List of Symbols

$\mathbb{R}$	:	The set of real numbers
$\mathbb{S}^2$	:	Two-sphere, $\mathbb{S}^2 = \left\{ x = [x_1, x_2, x_3]^\top \in \mathbb{R}^3 \middle\vert \, \|x\| = 1 \right\}$
$\mathbf{I}_n$	:	Identity matrix with dimension n-by-n, $\mathbf{I}_n \in \mathbb{R}^{n \times n}$
$\underline{\mathbf{0}}_n$	:	Zero vector, $\underline{\mathbf{0}}_n \in \mathbb{R}^n$
$\{\mathcal{I}\}$	:	Inertial-frame of reference
$\{\mathcal{B}\}$	:	Body-frame of reference
$\mathbb{GL}\,(3)$	:	Three dimensional General Linear Group
$\mathbb{O}\,(3)$	:	Orthogonal Group
$\mathbb{SO}\,(3)$	:	Special Orthogonal Group
$\mathbb{SE}\,(3)$	:	Special Euclidean Group
$\mathfrak{so}\,(3)$	:	The space of 3×3 skew-symmetric matrices, and Lie-algebra of $\mathbb{SO}\,(3)$
R	:	Rotational matrix (Attitude), $R \in \mathbb{SO}\,(3)$
P	:	Position of a rigid-body, $P \in \mathbb{R}^3$
$\boldsymbol{T}$	:	Homogeneous transformation matrix, $\boldsymbol{T} \in \mathbb{SE}\,(3)$
$\hat{R}$	:	Estimate of attitude, $\hat{R} \in \mathbb{SO}\,(3)$
$\hat{P}$	:	Estimate of position, $\hat{P} \in \mathbb{R}^3$
$\hat{\boldsymbol{T}}$	:	Estimate of homogeneous transformation matrix, $\hat{\boldsymbol{T}} \in \mathbb{SE}\,(3)$
$\tilde{R}$	:	Error of attitude, $\tilde{R} \in \mathbb{SO}\,(3)$
$\tilde{P}$	:	Error of position, $\tilde{P} \in \mathbb{R}^3$
$\tilde{\boldsymbol{T}}$	:	Error of homogeneous transformation matrix, $\tilde{\boldsymbol{T}} \in \mathbb{SE}\,(3)$
Ω	:	True angular velocity vector, $\Omega \in \mathbb{R}^3$
V	:	True translational velocity vector, $V \in \mathbb{R}^3$
Ω_m	:	Angular velocity measurement, $\Omega_m \in \mathbb{R}^3$
V_m	:	Translational velocity measurement, $V_m \in \mathbb{R}^3$
$\mathrm{v}^{\mathcal{I}(\mathrm{R})}$	:	Inertial-frame vector associated with attitude, $\mathrm{v}^{\mathcal{I}(\mathrm{R})} \in \mathbb{R}^3$
$\mathrm{v}^{\mathcal{B}(\mathrm{R})}$	:	Body-frame vector associated with attitude, $\mathrm{v}^{\mathcal{B}(\mathrm{R})} \in \mathbb{R}^3$
$\mathrm{v}^{\mathcal{I}(\mathrm{L})}$	:	Inertial-frame vector associated with landmark, $\mathrm{v}^{\mathcal{I}(\mathrm{L})} \in \mathbb{R}^3$
$\mathrm{v}^{\mathcal{B}(\mathrm{L})}$	:	Body-frame vector associated with landmark, $\mathrm{v}^{\mathcal{B}(\mathrm{L})} \in \mathbb{R}^3$

u	:	Unit vector (axis of parameterization), $u \in \mathbb{S}^2$
α	:	Angle of rotation, $\alpha \in \mathbb{R}$
$\mathcal{R}_\alpha(\alpha, u)$	:	Attitude representation using angle-axis components
ρ	:	Rodriguez vector, $\rho \in \mathbb{R}^3$
$\mathcal{R}_\rho(\rho)$	:	Attitude representation using Rodriguez vector
$\tilde{\rho}$	:	Rodriguez vector error, $\tilde{\rho} \in \mathbb{R}^3$
b	:	Constant bias vector
$\hat{b}$	:	Estimate of bias
$\tilde{b}$	:	Bias vector error
W	:	Correction factor
ω	:	Noise vector
$\boldsymbol{e}_i$	:	Error of the ith element
$\mathcal{E}_i$	:	Transformed error of the ith element
ξ_i	:	Preformance function of the ith element

Chapter 1
Introduction

This thesis concerns the problems of nonlinear deterministic and stochastic attitude and pose filters. The attitude and pose kinematics are naturally nonlinear and their natural configuration spaces are modelled on the Lie group of the special orthogonal group $\mathbb{SO}(3)$ and the special Euclidean group $\mathbb{SE}(3)$, respectively. Accordingly, the attitude and pose filtering problems are tackled by utilizing nonlinear filters evolved directly on $\mathbb{SO}(3)$ and $\mathbb{SE}(3)$, respectively. Attitude and pose estimation are fundamental sub-tasks in the majority of automated and semi-automated robotic applications. Knowledge of attitude or pose of the rigid-body in space is indispensable for the control process of any robotic application. This information is mandatory such that the robotic application can attain the designated task accurately and efficiently. In particular, rigid-bodies such as rotating radars, satellites and fast dynamical systems such as manoeuvring spacecrafts, underwater vehicles, unmanned aerial vehicles (UAVs), mobile robots, and others require reliable attitude or pose estimate as depicted in Figure 1.1.

Depending on the application, any degradation of attitude or pose estimate could cause the overall system to go unstable. Thereby, attitude and pose filtering algorithms accurate and robust with respect to large initialization errors and uncertain measurements are needed to ensure that the overall system meets the desirable performance characteristics.

The main focus of this thesis is to provide theoretical results for nonlinear deterministic and stochastic attitude and pose filters, which commonly used in a variety of applications. The theoretical results of nonlinear attitude and pose filters developed directly on $\mathbb{SO}(3)$ and $\mathbb{SE}(3)$, respectively. In spite of the purely theoretical nature of the problem, the proposed filters demonstrate impressive output performance considering large initialization errors and high level of uncertainties in measurements with superior convergence properties. In fact, the presented results are strongly motivated

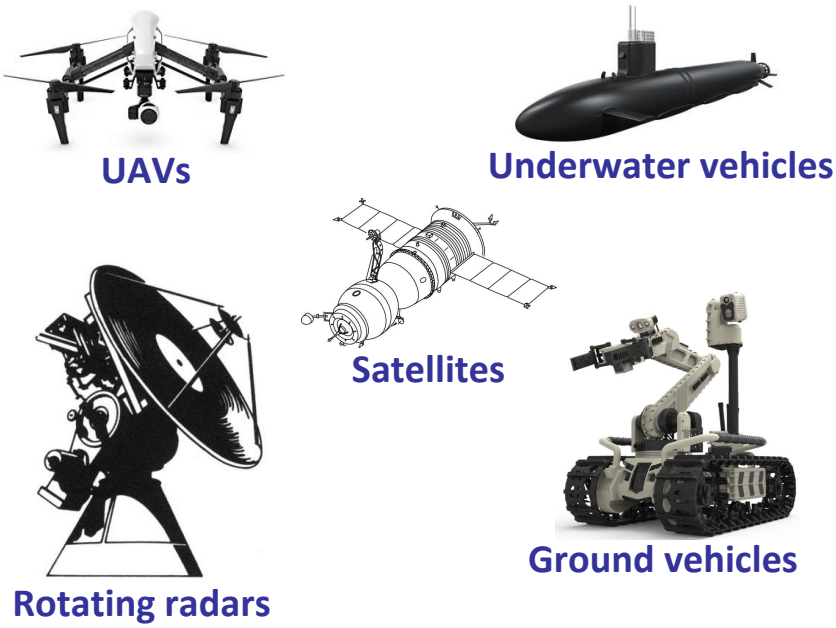

Figure 1.1: Relative applications for attitude and pose.

by many applications in automated robotic systems. In the next section a general overview of attitude and pose filtering problems is presented. It is followed by an overview of attitude and pose filtering approaches. Next, the challenges are defined and discussed. Finally, the problems considered and the results of this thesis as well as the thesis contributions are further detailed.

1.1 General Overview

Attitude and pose (i.e, attitude and position) estimation are critical elements in the majority of robotic applications. The orientation of a rigid-body in 3D space is often referred to as attitude, therefore, in this thesis orientation and attitude will be used interchangeably. Attitude represents the orientation of a body-fixed frame attached to a moving object relative to an inertial-fixed frame. The attitude of a rigid-body in 3D space is described by a 3 by 3 orthogonal matrix whose determinant equals 1. In fact, the attitude matrix consists of three orthogonal unit vectors or, in other words, the orientation serves as a linear transformation from a set of axes in a coordinate frame to a set of axes in a rotated coordinate frame. On the other side, the pose

of a rigid-body consists of two elements: orientation and position and it encodes the attitude along with the linear translation of the body-fixed frame relative to the inertial-fixed frame.

Control of automated and semi-automated robotic applications relies on the knowledge of attitude or pose of the rigid-body in the space. For example, flight manoeuvres could lead to very fast dynamics of attitude, consequently an accurate attitude estimate is essential to guarantee that the overall control task has been accomplished successfully. Historically, attitude or pose of the rigid-body used to be obtained from high quality measurement units. Therefore, conventional attitude or pose filtering methods are efficient only when coupled with high quality measurements obtained from the above-mentioned filters. However, these units have three main shortcomings: large size, considerable weight and high cost. On the other side, small size, light weight and low-cost sensors produce measurements corrupted with high level of uncertainties. These uncertainties consist of slowly time-varying or constant bias and a wide-band of random Gaussian noise. Furthermore, the initial value of attitude or pose may not be accurately known. These challenges have inspired different directions of research within the control communityaiming to develop attitude and pose estimation algorithms that would be robust against high level of uncertainties in measurements and large error in initialization that would demonstrate superior convergence properties and produce accurate attitude or pose estimates similar to those obtained from high quality measurement units. These estimation algorithms will be developed according to the perceived gap in the existing literature.

1.2 Background of Attitude Filtering Methods

1.2.1 Earliest attitude filtering

As previously mentioned, attitude estimation is an integral component of most robotics and control applications. The attitude can be constructed from a set of vector measurements made on body-frame and reference-frame as it acts as a linear transformation from one frame to the other. In general terms, the attitude estimation algorithms aim to minimize a cost function such as Wahba's Problem (Wahba (1965)). The earliest work done by Wahba (1965) was purely algebraic. Several alternative methods

attempted to reconstruct the attitude simply and statically by solving a set of inertial and body-frame measurements known simultaneously, for instance, TRIAD or QUEST algorithms (Black (1964); Shuster and Oh (1981)) and singular value decomposition (SVD) (Markley (1988)). However, it is important to note that vector measurements are subject to significant noise and bias components. Therefore, the category of static estimation proposed by Black (1964); Markley (1988); Shuster and Oh (1981) gives poor results in this case, in particular, if the moving body is equipped with low-cost measurement units. Consequently, the attitude estimation problem used to be tackled either by Gaussian or nonlinear deterministic filters.

1.2.2 Gaussian attitude filtering

In the last few decades, several Gaussian filters have been developed mainly to obtain higher estimation performance with noise reduction. Many attitude estimation algorithms are based on optimal stochastic filtering for linear systems known as Kalman filter (KF) (Kalman (1960)). The linearized version of KF can be modified in a certain way for nonlinear systems to obtain the extended Kalman filter (EKF) (Anderson and Moore (1979)). An early survey of attitude observers was presented with the structure of EKF in Lefferts, Markley, and Shuster (1982) and a more recent overview on attitude estimation was introduced in Crassidis, Markley, and Cheng (2007). Over the last three decades, several nonlinear filters have been proposed to estimate the attitude of spacecrafts. However, EKF and especially the multiplicative extended Kalman filter (MEKF) is highly recommended and considered as a standard in most spacecraft applications (Crassidis et al. (2007)). Generally, the covariance of any noise components introduced in angular velocity measurements is taken into account during filter design. The family of KFs parameterize the global attitude problem using unit-quaternion. The unit-quaternion provides a nonsingular attitude parameterization of attitude matrix (Shuster (1993)). Also, the unit-quaternion kinematics and measurement models of the attitude can be defined by a linear set of equations dependent on the quaternion state through EKF. This advantage motivated researchers to employ the unit-quaternion in attitude representation (for example Lefferts et al. (1982); Markley (2003)). Although EKF is subject to theoretical and practical problems, the estimated state vector with the approximated covariance matrix gives a reasonable estimate of uncertainties in the dynamics. In general, a four-dimensional vector is used

to describe a three-dimensional one. Since, the covariance matrix associated with the quaternion vector is 4×4, whereas the noise vector is 3×1, the covariance is assumed to have rank 3. Generally, the state vector is 7×1 as it includes the four quaternion elements and the three bias components. One of the earliest detailed derivations of EKF attitude design was presented in Lefferts et al. (1982). However, the unit-quaternion kinematics and measurement models can be modified to suit KF with a linear set of equations (Choukroun, Bar-Itzhack, and Oshman (2006)). The KF in Choukroun et al. (2006) has the same state dimensions as EKF and to some degree, it can outperform the EKF. MEKF (Markley (2003)) is the modified version of EKF and is highly recommended for spacecraft applications. In MEKF, the true attitude state is the product of reference and estimated error quaternion. The estimated error in quaternion is parameterized from a three-dimensional vector in the body-frame, and the error is estimated using EKF. Next, the MEKF is used to multiply the estimated error and the reference quaternion. The estimated error should be selected in such a way that it yields identity when multiplied by the reference quaternion. The EKF can be modified into invariant extended Kalman filter (IEKF), which has two groups of operations. The right IEKF considers the errors modeled in the inertial-frame and the left IEKF matches with the MEKF (Bonnable, Martin, and Salaun (2009)). IEKF has autonomous error and its evolution error does not depend on the system trajectory (Barrau and Bonnabel (2015)). Recently, a group of IEKF has been presented on Lie groups (Barrau and Bonnabel (2017)). Another recently proposed attitude filtering solution known as geometric approximate minimum-energy filter (GAMEF) approach (Zamani, Trumpf, and Mahony (2013)) is based on Mortensen's deterministic minimum-energy filtering (Mortensen (1968)). The minimum-energy attitude filter is formulated as an optimal control problem and depends on the Hessian of the value function of the optimal control problem. With the aid of a matrix representation of the Hessian, a Riccati equation is obtained to approximate GAMEF by disregarding the higher order derivatives than two of the value function. Unlike KF, EKF, IEKF, and MEKF, which are quaternion based, the GAMEF kinematics are posed directly on $\mathbb{SO}(3)$. In addition, KF, EKF, and IEKF are based on first order optimal minimum-energy which makes them simpler in computation and implementation. In contrast, MEKF and GAMEF are second order optimal minimum-energy, and therefore they require more calculation steps and more computational power. The Unscented Kalman filter (UKF) uses unit-quaternion kinematics, and its structure is

nearly similar to KF. However, UKF utilizes a set of sigma points to enhance the probability distribution (Crassidis and Markley (2003); Hashim, Brown, and McIsaac (2018b); Menegaz, Ishihara, Borges, and Vargas (2015)). The advantages of UKF can be listed as follows: it requires less theoretical knowledge, it could approximate the nonlinear equations of the system dynamics by using higher order moments to fit the unknown probability distribution which in turn allows achieving lower error bounds, and it demonstrate faster convergence rate than EKF and MEKF. As such, UKF has the potential to outperform EKF in simulations. However, the main drawbacks of UKF include more computational power required for the propagation of UKF compared to EKF, while the sigma points could add complexity to the implementation process (Haykin et al. (2001)). In addition, the measure of how close UKF to the optimal solution is not known. The family of KF assumes the noise signals to be Gaussian. Particle filters (PFs), on the contrary, although belonging to the family of stochastic filters, do not follow the Gaussian assumptions (Arulampalam, Maskell, Gordon, and Clapp (2002)). The main idea of PFs is the use of Monte-Carlo simulations for the weighted particle approximation of the nonlinear distribution. In fact, PFs outperform EKF in terms of lower error bounds and faster convergence rate. However, they have higher computational cost, and they are unsuitable for the small scale systems (Crassidis et al. (2007); Hashim et al. (2018b)). Moreover, they do not have a clear measure of how close the solution is to the optimal one. Quaternion based attitude PF showed a better performance than UKF with higher processing cost (Cheng and Crassidis (2004)). All the Gaussian filters described above as well as PFs are based on unit-quaternion, except for GAMEF in Zamani et al. (2013) and the group of IEKF in Barrau and Bonnabel (2017) which are $\mathbb{SO}(3)$ based. The main advantage of unit-quaternion based filters is non-singularity in attitude parameterization, while the main drawback is non-uniqueness in representation. In addition, unit-quaternion based filters could require normalization to maintain the property of unit norm of the quaternion estimate.

1.2.3 Nonlinear deterministic attitude filtering

Nonlinear deterministic filtering is an alternative approach to attitude estimation which aims to establish convergence bounds with stable performance. Nonlinear deterministic filters based on unit-quaternion were introduced in (Salcudean (1991);

Thienel and Sanner (2003)). Indeed, the development of microelectromenchanical systems (MEMS) devices has paved the way to propose a range of units, termed inertial measurement units (IMUs), which have the following three advantages: low-cost, light weight and small size. Since a wide range of small objects, for instance, robotic toys and low cost mini-aerial-vehicles, can be fitted with IMUs, IMUs have a prominent role in enriching the research of attitude estimation. However, the measurements obtained by low-cost IMUs systems are characterized by low-resolution signals. These signals are subject to high levels of wide-band random noise as well as slowly time-varying or constant bias. The IMUs output signals and angular velocity measurements have to be processed to establish an estimate of the attitude. Thus, the process of attitude reconstruction is vulnerable to the effects of noise and bias contaminating the body-frame and angular velocity measurements. The merits and challenges offered by low-cost IMUs devices fostered researchers to propose nonlinear deterministic complementary filters on $\mathbb{SO}(3)$ since these filters can be easily fitted knowing a rate gyroscope measurement and two or more vector measurements. In particular, the tracking performance of Gaussian attitude filters coupled with measurements obtained from low-cost IMUs devices is an issue (Crassidis et al. (2007); Hashim et al. (2018b)). One of the earliest observer design techniques with measurements from low-cost sensors fused through linear complementary filters is proposed in Baerveldt and Klang (1997). Later the above-mentioned design technique was modified into a nonlinear complementary filter (Vik and Fossen (2001)). The nonlinear filter is termed nonlinear complementary filter if it recaptures the structure of a classical complementary filter, (Appendix A Mahony et al. (2008)). Nonlinear filters with low-cost IMUs devices low-pass sensors has been considered in Rehbinder and Hu (2000) as well as partial attitude estimation (Rehbinder and Hu (2004)). A new form of an error function was needed mainly to reduce the error bounds at the steady-state to lower levels. Accordingly, over the last few years, a group of nonlinear complementary attitude filters developed directly on $\mathbb{SO}(3)$ (for example, Grip, Fossen, Johansen, and Saberi (2012); Hamel and Mahony (2006); Lee (2012); Mahony, Hamel, and Pflimlin (2005); Mahony et al. (2008); Zlotnik and Forbes (2017)). These filters on $\mathbb{SO}(3)$ might need the attitude to be reconstructed in addition to obtaining angular velocity measurements (Lee (2012); Mahony et al. (2005, 2008)) or alternatively they can operate using body-frame vector measurements and angular velocity measurements directly without the need of attitude reconstruction (Mahony

et al. (2008); Zlotnik and Forbes (2017)). Also, the work done in Mahony et al. (2008) provides the filter kinematics in quaternion representation. In general, nonlinear deterministic filters achieve almost global asymptotic stability as they disregard the noise impact in filter derivation. It is worth mentioning that the convergence behavior of nonlinear attitude filters is primarily attributed to the careful selection of the error function (Hashim, Brown, and McIsaac (2018a); Hashim et al. (2018b)).

1.2.4 Attitude filtering: Nonlinear deterministic vs Gaussian

When comparing nonlinear deterministic attitude filters against Gaussian attitude filters or PFs, it can be noticed that nonlinear deterministic attitude filters have the following three distinctive advantages over Gaussian attitude filters:

1) Better tracking performance.

2) Less computational power.

3) Simplicity in derivation.

Furthermore, no sensor knowledge is required for nonlinear deterministic filters, due to the fact that they omit the noise component in filter derivation (Hashim et al. (2018a, 2018b)). Also, PFs have higher computational cost, and they do not fit small scale systems. As such, it can be concluded that nonlinear deterministic attitude filters outperform Gaussian attitude filters and PFs Hashim et al. (2018a, 2018b).

1.3 Background of Pose Filtering Methods

Pose estimation is an essential sub-task in the field of robotics and control applications of any object rotating and translating in 3D space. These applications include manipulation and registration (Srivatsan, Rosen, Mohamed, and Choset (2016)), sensor calibration (Keskin, Kirac, Kara, and Akarun (2013); Srivatsan et al. (2016)), and object tracking (Blanco (2010); Choi and Christensen (2012); Kwon, Choi, Park, and

Chun (2007)). The pose of a rigid body in 3D space consists of two elements: attitude and position. The pose can be reconstructed from a set of vector measurements made on body-frame and reference-frame. According to the discussion in Subsection 1.2.1, vector measurements are susceptible to the attached noise and bias components. Therefore, the category of static attitude reconstruction proposed in Black (1964); Markley (1988); Shuster and Oh (1981) would lead to poor pose results, especially, if the moving body is equipped with low-cost measurement units. As a result, the pose estimation problem used to be tackled either using Gaussian filters or nonlinear deterministic filters.

1.3.1 Gaussian pose filtering and challenges

In comparison with nonlinear deterministic pose filters, relatively few studies have been done on Gaussian pose filters and particle pose filters, examples include (Chiuso and Soatto (2000); Choi and Christensen (2012); Goodarzi and Lee (2016); Kwon et al. (2007); Srivatsan et al. (2016)). One of the earliest particle pose filter on $\mathbb{SE}(3)$ was presented by Chiuso and Soatto (2000). Later, the problem was generalized to include object tracking and needle steering in Kwon et al. (2007) which was followed by an implementation of first order autoregressive state dynamics used to propagate particles of the filter Choi and Christensen (2012). On the other side, the novel KF with a linear set of equations for attitude problem in Choukroun et al. (2006) has been modified to tackle the pose filtering problem in Srivatsan et al. (2016). Since the pose filter in Srivatsan et al. (2016) is quaternion-based, a modified EKF on $\mathbb{SE}(3)$ has been presented in Goodarzi and Lee (2016).

In spite of the fact that Gaussian pose filters used for the estimation of $\mathbb{SE}(3)$ elements have linear structure, the filter updates are nonlinear and the estimates are often inaccurate. As such, the pose filter may diverge in particular if the initial estimation error is significantly high. Also, particle filters require higher processing cost, and they are not optimal fit for small scale systems (Crassidis et al. (2007); Hashim et al. (2018a, 2018b)). Since attitude is a fundamental part of the pose problem and nonlinear deterministic attitude filters outperform Gaussian attitude filters as given in Subsection 1.2.4, especially, in case when low cost IMUs systems are used, it is better to address the pose filtering problem using a nonlinear filter

on $\mathbb{SE}(3)$ to accommodate for the nonlinear nature of the pose kinematics on $\mathbb{SE}(3)$ (Hashim, Brown, and McIsaac (2019d)).

1.3.2 Nonlinear deterministic pose filtering

The pose estimation problem relies on filters evolved on $\mathbb{SE}(3)$ which require measurements derived from a group velocity vector, vector measurements that could be provided by low-cost IMUs systems, landmark measurements collected, for example, by a computer vision system, and an estimate of the bias associated with velocity measurements (Hashim, Brown, and McIsaac (2019d)). The low-cost IMUs and an on-board camera measurements could be combined in one unit termed low-cost inertial vision system (Hashim, Brown, and McIsaac (2019d)). Landmark based navigation estimation is known by a motion estimation using dynamic vision. An early derivation of a nonlinear pose filter with the implementation of an inertial vision system was presented by Rehbinder and Ghosh (2003). This work was followed by an extension of the nonlinear deterministic attitude filter on $\mathbb{SO}(3)$ in Hamel and Mahony (2006); Mahony et al. (2005) to nonlinear deterministic pose filter on $\mathbb{SE}(3)$ in Baldwin, Mahony, Trumpf, Hamel, and Cheviron (2007). The filters in Hamel and Mahony (2006); Mahony et al. (2005) and Baldwin et al. (2007) were termed passive complementary filters since they require attitude and pose reconstruction for the implementation, respectively. Nonetheless, the nonlinear filter in Baldwin et al. (2007) can be modified to function based solely on a set of vector measurements avoiding the need for pose reconstruction (Baldwin, Mahony, and Trumpf (2009); Hua, Zamani, Trumpf, Mahony, and Hamel (2011); Vasconcelos, Cunha, Silvestre, and Oliveira (2010)). Also, the pose filtering problem could be formulated as an optimal control problem which depends on deterministic Riccati observer design framework (Hua and Allibert (2018)). The nonlinear pose filters in Baldwin et al. (2009, 2007); Hua et al. (2011); Vasconcelos et al. (2010) have been proven to be almost globally asymptotically stable.

1.4 Scope of Thesis: Nonlinear Attitude and Pose Filtering Design Challenges

Motivating by the above presented survey of attitude and pose filters, the definition of many challenging problems associated with filtering design will be introduced aiming to fill a perceived gap in the existing literature. Two topics related to nonlinear attitude filtering are explored in this thesis: nonlinear deterministic attitude filters on $\mathbb{SO}(3)$ with predefined transient and steady-state characteristics and nonlinear stochastic attitude filters on $\mathbb{SO}(3)$. Also, this thesis examines two topics associated with nonlinear pose filtering: nonlinear deterministic pose filters on $\mathbb{SE}(3)$ with predefined transient and steady-state measures and nonlinear stochastic pose filter on $\mathbb{SE}(3)$. In the following subsections, the four topics are discussed and the perceived gaps and challenges are highlighted.

1.4.1 Nonlinear deterministic attitude filtering challenges

The transient convergence behavior and steady-state performance of nonlinear attitude filters are mainly attributed to the careful selection of the error function. The selected error function in Mahony et al. (2005) underwent slight modifications in Grip et al. (2012); Hamel and Mahony (2006); Mahony et al. (2008), overall performance, however, was not significantly changed. The main problem of the error function in Grip et al. (2012); Hamel and Mahony (2006); Mahony et al. (2005, 2008) consists in the slow convergence, especially with large initial attitude error. A new form of the error function presented in Lee (2012); Zlotnik and Forbes (2017) offered faster error convergence to the origin. However, no systematic convergence is observed in Lee (2012); Zlotnik and Forbes (2017). In other words, the transient performance does not follow a predefined trajectory and the steady-state error cannot be controlled (Hashim, Brown, and McIsaac (2019a, 2019c)). Thus, the prediction of transient and steady-state error performance is almost impossible (Hashim, Brown, and McIsaac (2019a, 2019c); Hashim, El-Ferik, Ayinde, and Abido (2017); Hashim, El-Ferik, and Lewis (2017)).

1.4.2 Nonlinear deterministic pose filtering challenges

In spite of the simplicity of the filter design in Baldwin et al. (2009, 2007); Hua et al. (2011), numerical results show high sensitivity to the uncertain components attached to the measurements. Also, the main concern of the selected error function in Baldwin et al. (2009, 2007); Hua et al. (2011) consists in the slow convergence, in particular, if the pose error initiated at a significantly large value. To the best of our knowledge, no new error function has been proposed to offer faster rate of error convergence to the origin than the one presented in Baldwin et al. (2009, 2007); Hua et al. (2011). In addition, no systematic convergence is observed in Baldwin et al. (2009, 2007); Dominguez (2017); Hua and Allibert (2018); Hua et al. (2011); Rehbinder and Ghosh (2003); Vasconcelos et al. (2010), such that the tracking error does not follow a predefined transient and steady-state measures (Hashim, Brown, and McIsaac (2019c)). Accordingly, successful pose estimation for spacecraft control applications cannot be achieved without pose filters which are robust against uncertain measurements, demonstrate fast tracking performance, and satisfy a certain level of transient and steady-state characteristics (Hashim, Brown, and McIsaac (2019c)).

1.4.3 Nonlinear deterministic filters with prescribed performance

Prescribed performance (Bechlioulis and Rovithakis (2008); Mohamed (2014)) signifies trapping the error to start arbitrarily within a given large set and reduce systematically and smoothly to a given small residual set. The convergence of the error is constrained by a specified range during transient as well as steady-state performance. The aim of prescribed performance is to relax the constrained error and transform it to a new unconstrained form termed transformed error through a prescribed performance function (PPF). Accordingly, the new form allows one to keep the error below the predefined value which could be useful in the estimation and control process. Prescribed performance has been implemented successfully in many control applications such as two degrees of freedom planar robot (Bechlioulis and Rovithakis (2008); Mohamed (2014)), uncertain dynamics of underwater vehicles (He, Dai, and Luo (2018)), and robust adaptive control of uncertain multi-agent systems (El-Ferik, Hashim, and Lewis (2018); Hashim, El-Ferik, and Lewis (2017, 2019)). Attitude and

pose error functions are essential for the construction of nonlinear attitude and pose filters, respectively, as the error function is directly related to the convergence behavior of the error trajectory (Hashim, Brown, and McIsaac (2019a, 2019c)). Therefore, the merits offered by prescribed performance could help in tackling the challenges of nonlinear deterministic attitude and pose filtering described in Subsection 1.4.1 and 1.4.2, respectively.

1.4.4 Nonlinear stochastic attitude filtering challenges

Two major factors have to be taken into account when designing the attitude estimator: 1) the attitude problem of the rigid-body, modeled on the Lie group of $\mathbb{SO}(3)$, is naturally nonlinear; and 2) the true attitude kinematics rely on angular velocity Hashim et al. (2018b). In spite of the remarkable advantages offered by nonlinear deterministic attitude filters when compared to Gaussian filters or PFs (Crassidis et al. (2007); Hashim et al. (2018b)), design of nonlinear deterministic attitude filter kinematics takes into account only constant bias disregarding the random noise attached to angular velocity measurements . However, randomness woth consideration (Eltoukhy, Chan, Chung, Niu, and Wang (2017); Eltoukhy, Wang, Chan, and Chung (2018); Hashim (2019); Hashim, El-Ferik, Ayinde, and Abido (2017); Mohamed (2014)), the environment is noisy (Eltoukhy, Chan, and Chung (2017); Eltoukhy, Chan, Chung, and Niu (2018); Eltoukhy, Wang, Chan, and Fu (2019); Hashim and Abido (2015); Hashim, El-Ferik, and Abido (2015); Hashim, El-Ferik, and Lewis (2019)) andRemove comment the attitude problem should be considered in its natural stochastic sense. Therefore, successful attitude estimation can be achieved when nonlinear filter design takes into consideration both noise and bias components (Hashim et al. (2018b)) to the angular velocity measurements. Likewise, it is essential that the estimator design considers any noise and/or bias components introduced during the measurement process.

1.4.5 Nonlinear stochastic pose filtering challenges

Despite the simplicity of the filter design in Baldwin et al. (2009, 2007); Hua et al. (2011), simulation results illustrated remarkable sensitivity to noise and bias intro-

duced in the measurements Hashim, Brown, and McIsaac (2019c, 2019d). Moreover, pose estimators such as Baldwin et al. (2009, 2007); Dominguez (2017); Hua et al. (2011); Rehbinder and Ghosh (2003); Vasconcelos et al. (2010) disregard the noise in the filter design assuming only constant bias introduced in the measuring process Hashim, Brown, and McIsaac (2019d). Therefore, successful spacecraft control applications cannot be achieved without pose filters being robust against high level of uncertainties in measurements and large error in initialization Hashim, Brown, and McIsaac (2019c, 2019d). Consequently, in order to develop successful pose estimator, we need to realize that 1) the pose problem is naturally nonlinear on $\mathbb{SE}(3)$; and 2) the true pose kinematics rely on angular and translational velocity Hashim, Brown, and McIsaac (2019d). Furthermore, the velocity vector is subject to slowly time-variant bias and random noise components. As such, it is necessary that the pose filter design addresses any noise and/or bias components introduced during the measurement process.

1.5 Statement of Contributions

In this thesis, several contributions to deterministic and stochastic attitude filtering on $\mathbb{SO}(3)$, and deterministic and stochastic pose filtering on $\mathbb{SE}(3)$ are presented. Different filter schemes are formulated to achieve superior convergence properties of attitude and pose filters. As for attitude filters, nonlinear deterministic and stochastic attitude filters on $\mathbb{SO}(3)$ robust against high level of uncertainties in the measurements and a large initial attitude error are proposed. As for pose filters, robust nonlinear deterministic and stochastic pose filters on $\mathbb{SE}(3)$ are introduced considering high level of uncertainties in the measurements and a large initial pose error. The principle of transformed error acting as an auxiliary component to force the error function to obey dynamically decreasing boundaries is applied to nonlinear deterministic filters.

The contributions presented in this thesis are briefly summarized as follows:

1. Two novel nonlinear attitude filters on $\mathbb{SO}(3)$ with predefined transient and steady-state characteristics are presented. These filters provide reliable attitude estimates with remarkable convergence properties when measurements ob-

tained from low quality sensors such as low-cost inertial measurement units are being used. In general, successful nonlinear attitude filter could be achieved via careful selection of the error function. Thus, in this thesis a new attitude error function is defined in terms of normalized Euclidean distance. The error function is constrained to initially start within a known large set and reduce systematically and smoothly to a given small set. In order for the error to be constrained by dynamically reducing boundaries, the constrained error is relaxed and transformed to a new unconstrained form, named transformed error. The transformed error helps to ensure boundedness of the closed loop error signals with normalized Euclidean distance of attitude error being regulated asymptotically to the origin. Also, transformed error allows the attitude estimators to ensure faster convergence properties and satisfy prescribed performance. The fast convergence is mainly associated with the dynamic gains of the estimator.

Unlike nonlinear deterministic attitude filters on $\mathbb{SO}(3)$ described in the literature, the proposed filters design methods allow to handle high level of uncertainty in angular velocity as well as body-frame vector measurements. In addition, they allow handling large error in initialization with error function being constrained by dynamically reducing boundaries and achieving almost global asymptotic stability results. This remarkable advantage was not offered in other deterministic attitude filters such as Grip et al. (2012); Hamel and Mahony (2006); Lee (2012); Mahony et al. (2005, 2008); Zlotnik and Forbes (2017). The above-listed results are detailed in ***Chapter*** 3 and published in Hashim, Brown, and McIsaac (2019a).

2. Due to the fact that attitude kinematics are nonlinear and rely on angular velocity, the attitude estimator kinematics should also be nonlinear and rely on angular velocity measurements. Hence, it is essential that any noise and/or bias components introduced during the angular velocity measurement process are considered in the estimator design. Furthermore, any noise component is characterized by randomness and irregular behavior which may impair the estimation process and cause the estimated attitude to drift away from the true attitude. Therefore, two nonlinear stochastic complementary filters on $\mathbb{SO}(3)$ based on two different approaches of stochastic integrals are proposed to improve the overall estimation quality. The first nonlinear stochastic filter is driven

in the sense of Ito (Ito and Rao (1984)) and the second one is developed in the sense of Stratonovich (Stratonovich (1967)). Superior filtering outcome was achieved by studying one of the traditional potential functions of nonlinear deterministic complimentary filters evolved on $\mathbb{SO}(3)$ (for example Crassidis et al. (2007); Mahony et al. (2008)) and taking into consideration the fact that angular velocity measurements are corrupted with bias and noise components. This study established that selecting the potential function in an alternative way could allow to diminish the noise attached to measurements.
In contrast to nonlinear deterministic attitude filters on $\mathbb{SO}(3)$ described in the literature, the proposed filters are able to 1) steer the error vector towards an arbitrarily small neighborhood of the origin/(identity) in probability; 2) attenuate the noise impact to a very low level for known or unknown bounded covariance; and 3) make the error semi-globally/(almost semi-globally) uniformly ultimately bounded in mean square in case when angular velocity measurement is contaminated not only with a constant bias but also with a wide-band of random Gaussian noise, as far as the Rodriquez vector/($\mathbb{SO}(3)$) is concerned. A comparison between the two proposed filters is given. An in-depth description of the results presented above can be found in ***Chapter*** 4 and is published in Hashim et al. (2018b).

3. The filters outlined in the previous section ***Chapter*** 4 demonstrate impressive estimation of the true attitude in case when high level of uncertainties in measurements and large error in initialization are observed. However, the above-mentioned filters (***Chapter*** 4) require an online reconstruction of the uncertain attitude which could add computational complexity. Therefore, the uncertain behavior in measurements and the added computational cost inspired the proposal of an explicit nonlinear stochastic attitude filter on $\mathbb{SO}(3)$ which is based on the selection of a new potential function.
This explicit non-linear stochastic attitude filter on SO(3) is able to avoid the need for online reconstruction of the uncertain attitude and guarantee that, 1) the error is regulated to an arbitrarily small neighborhood of the equilibrium point in probability; and 2) the error is semi-globally uniformly ultimately bounded in mean square in the case where angular velocity measurements are contaminated with a constant bias and a wide-band of random Gaussian noise. The results obtained in this section are reported in ***Chapter*** 5 and published

in Hashim et al. (2018a).

4. No nonlinear pose filters described in literature demonstrate systematic convergence, and therefore the tracking error cannot be guaranteed to follow predefined transient and steady-state measures. Moreover, successful nonlinear pose filters should be characterized by the following features: robust against uncertain measurements, demonstrate fast tracking performance, and satisfy a certain level of transient and steady-state characteristics. In order to address the three aforementioned challenges effectively, two robust nonlinear pose filters on $\mathbb{SE}(3)$ with predefined transient as well as steady-state measures are proposed. These filters provide reliable pose estimates with superior convergence properties when using measurements obtained from low quality sensors such as vision systems and low-cost inertial measurement units. The error trajectory is constrained by a prescribed performance function to satisfy transient as well as steady-state performance. The main objective is to relax the constrained error to its unconstrained form, termed transformed error, which allows to keep the error within the dynamically decaying boundaries.
   The main contributions are as follows: 1) The proposed filters guarantee boundedness of the closed loop error signals with constrained error and unconstrained transformed error being proven to be almost globally asymptotically stable such that the error in the homogeneous transformation matrix is regulated asymptotically to the identity from almost any initial condition. 2) The proposed filters guarantee systematic convergence of the error controlled by the dynamically reducing boundaries forcing the error to initiate within a predefined large set and decrease systematically and smoothly to a residual small set. As a result, the transient error is less than predefined value and the steady-state error does not exceed known small value, unlike (Baldwin et al. (2009, 2007); Hua et al. (2011); Rehbinder and Ghosh (2003); Vasconcelos et al. (2010)). 3) The proposed pose filters are more efficient at ensuring fast convergence compared to similar estimators described in the literature, for instance Baldwin et al. (2009, 2007); Hua et al. (2011); Rehbinder and Ghosh (2003); Vasconcelos et al. (2010). The fast convergence is mainly attributed to the dynamic behavior of the estimator gains. The first filter requires a group of velocity vectors and a set of measurements to obtain an online algebraic reconstruction of the pose. The second filter uses a group of velocity vector and a set of vector measurements

directly, alleviating the need for pose reconstruction. The above-listed results are given in ***Chapter*** 6 and published in Hashim, Brown, and McIsaac (2019b, 2019c).

5. Since the pose kinematics are nonlinear and rely on translational and angular velocity, the pose estimator kinematics should also be nonlinear and should rely on translational and angular velocity measurement. However, the velocity vector is subject to slowly time-variant bias and random noise components. In addition, the noise components are characterized by uncertain behavior which could negatively impact the estimation process and deviate the estimated pose from the true pose. As such, a nonlinear stochastic position and attitude filter is developed on $\mathbb{SE}(3)$ in the sense of Stratonovich (Stratonovich (1967)). The proposed approach is successfully achieved by studying common potential functions of nonlinear deterministic pose filters evolved on $\mathbb{SE}(3)$ (for instance Baldwin et al. (2009, 2007); Hua et al. (2011)) and taking into account the fact that velocity measurements are corrupted with bias and noise components. Accordingly, the selected potential function has been modified which allows the noise attached to measurements to be diminished.
   The problem is mapped from $\mathbb{SE}(3)$ to vector form which includes position and Rodriquez vector such that $X : \mathbb{SE}(3) \to \mathbb{R}^6$. In the case where the velocity measurements are corrupted with a constant bias and a wide-band of random Gaussian noise, the proposed nonlinear stochastic pose filter guarantees that 1) the error vectors steers towards an arbitrarily small neighborhood of the origin in probability; 2) the noise impact associated with velocity measurement is attenuated for known or unknown bounded covariance; and 3) the error in X and estimates is shown to be semi-globally uniformly ultimately bounded (SGUUB) in mean square. The results obtained in this part are reported in ***Chapter*** 7 and published in Hashim, Brown, and McIsaac (2019d).

In summary, the proposed nonlinear deterministic attitude and pose filters comply with the desired prescribed performance set by the user. In particular, the transient and steady-state performance truly respect the dynamically reducing boundaries. Thus, the proposed nonlinear deterministic attitude and pose filters are characterized with guaranteed performance. In addition, the natural configuration space of the attitude and pose filters is posed on the Lie group of $\mathbb{SO}(3)$ and $\mathbb{SE}(3)$, respectively.

The proposed filters are robust with respect to large initialization and measurement errors. Another advantage of the proposed nonlinear deterministic attitude and pose filters with guaranteed performance is that the gains of the estimates and the correction factors are functions of the transformed error. Also, the transformed error relies on the error function such that the gains are tuned adaptively and their values become increasingly aggressive as the error value increases. Their dynamic behavior is essential for forcing the proposed filters to obey the prescribed performance constraints. An additional advantage to note is that no sensor knowledge is required for nonlinear deterministic filters. Nonetheless, they have a significant shortcoming, namely, the noise component associated with the angular velocity measurements is disregarded in filter derivation. The proposed nonlinear stochastic attitude and pose filters, on the contrary, although structurally similar to nonlinear deterministic attitude and pose filters, account for both constant bias and the wide-band of random Gaussian noise associated with angular velocity measurements. They have the natural configuration space of the attitude and pose motion as they are developed on the Lie group of $\mathbb{SO}(3)$ and $\mathbb{SE}(3)$, respectively. They are robust with respect to large initialization and measurement errors. Moreover, the gains of the estimates and correction factors are dynamic and their values become increasingly aggressive as the error value increases. Also, no sensor knowledge is required in the proposed nonlinear stochastic filters.

1.5.1 List of publications

The publications listed below include my papers published in the period between January 2018 and April 2019 which are summarized in this thesis:

Journal publications:

- Hashim, H. A., Brown, L. J., & McIsaac, K. (2018). Nonlinear Stochastic Attitude Filters on the Special Orthogonal Group 3: Ito and Stratonovich. IEEE Transactions on Systems, Man, and Cybernetics: Systems, PP(PP), 1-13.

- Hashim, H. A., Brown, L. J., & McIsaac, K. (2019). Nonlinear stochastic

position and attitude filter on the special euclidean group 3. Journal of the Franklin Institute, 356(7), 4144-4173.

- Hashim, H. A., Brown, L. J., & McIsaac, K. (2019). Guaranteed performance of nonlinear attitude filters on the special orthogonal group 3. IEEE Access, 7(1), 3731–3745.
- Hashim, H. A., Brown, L. J., & McIsaac, K. (2019). Nonlinear Pose Filters on the Special Euclidean Group SE(3) with Guaranteed Transient and Steady-state Performance. IEEE Transactions on Systems, Man, and Cybernetics: Systems, PP(PP), 1-14.

Refereed conference publications:

- Hashim, H. A., Brown, L. J., & McIsaac, K. (2018). Nonlinear explicit stochastic attitude filter on SO(3). In Proceedings of the 57th IEEE conference on decision and control (CDC), Miami Beach, FL, USA, 1210-1216.
- Hashim, H. A., Brown, L. J., & McIsaac, K. (2019). Guaranteed performance of nonlinear pose filter on SE(3). In Proceedings of the american control conference, (ACC), Philadelphia, PA, USA, 1-6.

In addition, the following publications were produced and/or published during the course of my study at Western University. The topics covered are adaptive and neuro-adaptive tracking control of nonlinear heterogeneous multi-agent systems and application of artificial intelligence in the field of communication networks.

Journal Publications:

- Hashim, H. A., El-Ferik, S., & Lewis, F. L. (2019). Neuro-adaptive cooperative tracking control with prescribed performance of unknown higher-order nonlinear multi-agent systems. International Journal of Control, 92(2), 445-460(Hashim, El-Ferik, and Lewis (2019)).
- Hashim, H. A., Abido, M. A. (2019). Location Management in LTE Networks using Multi-Objective Particle Swarm Optimization. Computer Networks, 157(1), 78-88(Hashim and Abido (2019)).

- Aqeeli, E., Hashim, H. A., Haque, A., & Shami, A. (2019). Optimal Location Management in LTE Networks using Evolutionary Techniques. International Journal of Communication Systems, PP(PP), 1-17(Aqeeli, Hashim, Anwer, and Shami (2019)).

- Ayinde, B. O., & Hashim, H. A. (2018). Energy-efficient Deployment of Relay Nodes in Wireless Sensor Networks using Evolutionary Techniques. International Journal of Wireless Information Networks, 25(1), 157-172(Ayinde and Hashim (2018)).

- El-Ferik, S., Hashim, H. A., & Lewis, F. L. (2017). Neuro-adaptive distributed control with prescribed performance for the synchronization of unknown nonlinear networked systems. IEEE Transactions on Systems, Man, and Cybernetics: Systems, 48(12), 2135-2144 (El-Ferik et al. (2018)).

- Hashim, H. A., El-Ferik, S., & Lewis, F. L. (2017). Adaptive synchronisation of unknown nonlinear networked systems with prescribed performance. International Journal of Systems Science, 48(4), 885-898(Hashim, El-Ferik, and Lewis (2017)).

- Hashim, H. A., Ayinde, B. O., & Abido, M. A. (2016). Optimal placement of relay nodes in wireless sensor network using artificial bee colony algorithm. Journal of Network and Computer Applications, 64, 239-248 (Hashim, Ayinde, and Abido (2016)).

1.6 Thesis Outline

The rest of the thesis is organized as follows:

Chapter 2 contains the mathematical notation and preliminaries used throughout the thesis. Also, it presents the special orthogonal group $\mathbb{SO}(3)$, the special Euclidean group $\mathbb{SE}(3)$, and some helpful properties associated with $\mathbb{SO}(3)$ and $\mathbb{SE}(3)$ which will be used in the subsequent chapters.

Chapter 3 introduces two robust nonlinear deterministic attitude filters on $\mathbb{SO}(3)$

with predefined transient as well as steady-state characteristics. It presents an alternate attitude error function which is defined in terms of normalized Euclidean distance. It shows that the introduced error function is forced to be contained within a predefined large set and reduce systematically and smoothly to a known small set. It presents the stability analysis and illustrates that the proposed filters ensure boundedness of the closed loop error signals with attitude error being regulated asymptotically to the origin.

Chapter 4 studies one of the traditional potential functions of nonlinear deterministic complimentary filters evolved on $\mathbb{SO}(3)$ taking into consideration the fact that angular velocity measurements are corrupted with bias and noise components. It formulates the attitude kinematics in the stochastic sense and proposes two nonlinear stochastic complementary filters on $\mathbb{SO}(3)$ with one filter being driven in the sense of Ito, while the second one being developed in the sense of Stratonovich. It presents the stability results and shows that in case when angular velocity measurement is contaminated with noise, the proposed filters are able to make the error semi-globally uniformly ultimately bounded in mean square, as far as the Rodriquez vector is concerned.

Chapter 5 demonstrates the weakness of the explicit nonlinear deterministic complimentary filters on $\mathbb{SO}(3)$ for the case when angular velocity measurements are corrupted with bias and noise components. To avoid the attitude reconstruction of nonlinear stochastic attitude filter proposed in ***Chapter*** 4, an explicit nonlinear stochastic complementary filter on $\mathbb{SO}(3)$ is introduced. The chapter also contains the stability results and demonstrates that the proposed filter is able to make the error semi-globally uniformly ultimately bounded in mean square in presence of noise in the angular velocity measurements, as far as the Rodriquez vector is concerned.

Chapter 6 proposes two robust nonlinear deterministic pose filters on $\mathbb{SE}(3)$ with predefined transient as well as steady-state measures. It shows that the proposed filters guarantee boundedness of the closed loop error signals such that the error in the homogeneous transformation matrix is regulated asymptotically to the identity from almost any initial condition. It presents the stability analysis and shows that the proposed filters ensure fast systematic convergence of the error controlled by the

dynamically reducing boundaries which force it to start within a predefined large set and decrease systematically and smoothly to a residual small set.

Chapter 7 presents a nonlinear stochastic position and attitude filter on $\mathbb{SE}(3)$ in the sense of Stratonovich. The pose problem is mapped from $\mathbb{SE}(3)$ to vector form which includes position and Rodriquez vector such that $X : \mathbb{SE}(3) \to \mathbb{R}^6$. It demonstrates that when velocity measurements are corrupted with noise, the error vectors steer towards an arbitrarily small neighborhood of the origin in probability; and the error of X and estimates is semi-globally uniformly ultimately bounded in mean square.

Chapter 8 summarizes the thesis and provides concluding remarks on deterministic and stochastic attitude filters proposed in this thesis.

Appendix A presents detailed proofs of Lemma 3.1, 5.1, and 6.1 stated in ***Chapter*** 3, 5, and 6, respectively.

Appendix B provides an overview of the singular value decomposition algorithm used for attitude reconstruction.

Appendix C includes detailed proofs of final formulas stated throughout this thesis.

Chapter 2
Preliminaries and Notation

2.1 Math Notation

Throughout this thesis, $\mathbb{R}_+$ denotes the set of nonnegative real numbers. $\mathbb{R}^n$ is the real n-dimensional space while $\mathbb{R}^{n\times m}$ denotes the real $n \times m$ dimensional space. For $x \in \mathbb{R}^n$, the Euclidean norm is defined as $\|x\| = \sqrt{x^\top x}$, where $^\top$ denotes transpose of the associated component. $\mathcal{C}^n$ denotes the set of functions with continuous nth partial derivatives. $\mathcal{K}$ denotes a set of continuous and strictly increasing functions such that $\gamma : \mathbb{R}_+ \to \mathbb{R}_+$ and vanishes only at zero. $\mathcal{K}_\infty$ denotes a set of continuous and strictly increasing functions which belongs to class $\mathcal{K}$ and are unbounded. $\mathbb{P}\{\cdot\}$ denotes probability, $\mathbb{E}[\cdot]$ denotes an expected value, and $\exp(\cdot)$ refers to an exponential of associated component. $\lambda(\cdot)$ is the set of singular values of the associated matrix with $\underline{\lambda}(\cdot)$ being the minimum value. $\mathbf{I}_n$ denotes identity matrix with dimension n-by-n, and $\underline{\mathbf{0}}_n$ is a zero vector with n-rows and one column. V denotes a potential function and for any $V(x)$ we denote $V_x = \partial V/\partial x$ and $V_{xx} = \partial^2 V/\partial x^2$.

2.2 $\mathbb{SO}(3)$ and $\mathbb{SE}(3)$ Preliminaries

Define $\mathbb{GL}(3)$ as a 3-dimensional general linear group which is a Lie group with smooth multiplication and inversion. The orthogonal group 3, denoted by $\mathbb{O}(3)$, is a subgroup of $\mathbb{GL}(3)$ defined by

$$\mathbb{O}(3) = \left\{ M \in \mathbb{R}^{3\times 3} \middle| M^\top M = M M^\top = \mathbf{I}_3 \right\}$$

with $\mathbf{I}_3$ being a 3-by-3 identity matrix. Let $\mathbb{SO}(3)$ denote the Special Orthogonal Group 3 which is a subgroup of $\mathbb{O}(3)$. The orientation of a rigid-body in 3D space is

termed attitude, denoted by R, and defined as follows:

$$\mathbb{SO}(3) = \left\{ R \in \mathbb{R}^{3\times 3} \middle| RR^\top = R^\top R = \mathbf{I}_3,\, \det(R) = +1 \right\}$$

with $\det(\cdot)$ being the determinant of the associated matrix. $\mathbb{SE}(3)$ stands for the Special Euclidean Group 3, a subset of the affine group $\mathbb{GA}(3) = \mathbb{SO}(3) \times \mathbb{R}^3$ defined by

$$\mathbb{SE}(3) = \left\{ \boldsymbol{T} \in \mathbb{R}^{4\times 4} \middle| R \in \mathbb{SO}(3), P \in \mathbb{R}^3 \right\}$$

where $\boldsymbol{T} \in \mathbb{SE}(3)$, termed a homogeneous transformation matrix, represents the pose of a rigid-body in 3D space with

$$\boldsymbol{T} = \begin{bmatrix} R & P \\ \underline{\mathbf{0}}_3^\top & 1 \end{bmatrix} \in \mathbb{SE}(3) \tag{2.1}$$

where $P \in \mathbb{R}^3$ and $R \in \mathbb{SO}(3)$ denote position and attitude of a rigid-body in 3D space, respectively, and $\underline{\mathbf{0}}_3^\top$ is a zero row. $\mathfrak{so}(3)$ is a Lie-algebra related to $\mathbb{SO}(3)$ defined by

$$\mathfrak{so}(3) = \left\{ A \in \mathbb{R}^{3\times 3} \middle| A^\top = -A \right\}$$

where A is a skew symmetric matrix. Define the map $[\cdot]_\times : \mathbb{R}^3 \to \mathfrak{so}(3)$ as

$$A = [\alpha]_\times = \begin{bmatrix} 0 & -\alpha_3 & \alpha_2 \\ \alpha_3 & 0 & -\alpha_1 \\ -\alpha_2 & \alpha_1 & 0 \end{bmatrix} \in \mathfrak{so}(3), \quad \alpha = \begin{bmatrix} \alpha_1 \\ \alpha_2 \\ \alpha_3 \end{bmatrix}$$

For any $\alpha, \beta \in \mathbb{R}^3$, we define $[\alpha]_\times \beta = \alpha \times \beta$ with $\times$ being the cross product. The wedge operator is denoted by $\wedge$, and for any $\mathcal{Y} = \left[y_1^\top, y_2^\top \right]^\top$ with $y_1, y_2 \in \mathbb{R}^3$ the wedge map $[\cdot]_\wedge : \mathbb{R}^6 \to \mathfrak{se}(3)$ is defined by

$$[\mathcal{Y}]_\wedge = \begin{bmatrix} [y_1]_\times & y_2 \\ \underline{\mathbf{0}}_3^\top & 0 \end{bmatrix} \in \mathfrak{se}(3)$$

$\mathfrak{se}(3)$ is a Lie algebra of $\mathbb{SE}(3)$ and can be expressed as

$$\mathfrak{se}(3) = \left\{ [\mathcal{Y}]_\wedge \in \mathbb{R}^{4\times 4} \middle| \exists y_1, y_2 \in \mathbb{R}^3 : [\mathcal{Y}]_\wedge = \begin{bmatrix} [y_1]_\times & y_2 \\ \underline{0}_3^\top & 0 \end{bmatrix} \right\}$$

Let the vex operator be the inverse of $[\cdot]_\times$, denoted by $\mathbf{vex} : \mathfrak{so}(3) \to \mathbb{R}^3$ such that for $\alpha \in \mathbb{R}^3$ and $A = [\alpha]_\times \in \mathfrak{so}(3)$ we have

$$\mathbf{vex}(A) = \mathbf{vex}\left([\alpha]_\times\right) = \alpha \in \mathbb{R}^3$$

Let $\boldsymbol{\mathcal{P}}_a$ denote the anti-symmetric projection operator on the Lie-algebra $\mathfrak{so}(3)$, defined by $\boldsymbol{\mathcal{P}}_a : \mathbb{R}^{3\times 3} \to \mathfrak{so}(3)$ such that

$$\boldsymbol{\mathcal{P}}_a(M) = \frac{1}{2}\left(M - M^\top\right) \in \mathfrak{so}(3), \; M \in \mathbb{R}^{3\times 3} \tag{2.2}$$

Let us define $\boldsymbol{\Upsilon}_a(\cdot)$ as the composition mapping such that $\boldsymbol{\Upsilon}_a = \mathbf{vex} \circ \boldsymbol{\mathcal{P}}_a$. Hence, $\boldsymbol{\Upsilon}_a(M)$ can be expressed for $M \in \mathbb{R}^{3\times 3}$ as

$$\boldsymbol{\Upsilon}_a(M) = \mathbf{vex}\left(\boldsymbol{\mathcal{P}}_a(M)\right) \in \mathbb{R}^3 \tag{2.3}$$

Consider $\boldsymbol{\mathcal{P}} : \mathbb{R}^{4\times 4} \to \mathfrak{se}(3)$ denoting the projection operator on the space of the Lie algebra $\mathfrak{se}(3)$ such that for $\mathcal{M} = \begin{bmatrix} M & m_x \\ m_y^\top & m_z \end{bmatrix} \in \mathbb{R}^{4\times 4}$ with $M \in \mathbb{R}^{3\times 3}$, $m_x, m_y \in \mathbb{R}^3$ and $m_z \in \mathbb{R}$, we have

$$\boldsymbol{\mathcal{P}}(\mathcal{M}) = \boldsymbol{\mathcal{P}}\left(\begin{bmatrix} M & m_x \\ m_y^\top & m_z \end{bmatrix}\right) = \begin{bmatrix} \boldsymbol{\mathcal{P}}_a(M) & m_x \\ \underline{0}_3^\top & 0 \end{bmatrix} \in \mathfrak{se}(3) \tag{2.4}$$

For any $\mathcal{M} \in \mathbb{R}^{4\times 4}$, we define the operator $\boldsymbol{\Upsilon}(\cdot)$ as follows

$$\boldsymbol{\Upsilon}(\mathcal{M}) = \begin{bmatrix} \boldsymbol{\Upsilon}_a(M) \\ m_x \end{bmatrix} \in \mathbb{R}^6 \tag{2.5}$$

The normalized Euclidean distance of a rotation matrix on $\mathbb{SO}(3)$ is defined by

$$\|R\|_I = \frac{1}{4}\mathrm{Tr}\left\{\mathbf{I}_3 - R\right\} \tag{2.6}$$

such that $\mathrm{Tr}\{\cdot\}$ is the trace of the associated matrix, while the normalized Euclidean distance of $R \in \mathbb{SO}(3)$ is $\|R\|_I \in [0,1]$. The orientation of a rigid-body rotating in a 3D-space can be established according to its angle of rotation $\alpha \in \mathbb{R}$ and its axis parameterization $u \in \mathbb{R}^3$. Such parameterization is termed angle-axis parameterization Shuster (1993). Mapping from angle-axis parameterization to $\mathbb{SO}(3)$ is given by $\mathcal{R}_\alpha : \mathbb{R} \times \mathbb{R}^3 \to \mathbb{SO}(3)$ such that

$$\mathcal{R}_\alpha(\alpha, u) = \mathbf{I}_3 + \sin(\alpha)[u]_\times + (1 - \cos(\alpha))[u]_\times^2 \in \mathbb{SO}(3) \tag{2.7}$$

Let us consider the transformation matrix in (2.1) with $\boldsymbol{T} \in \mathbb{SE}(3)$. The adjoint map for any $\boldsymbol{T} \in \mathbb{SE}(3)$ and $\mathcal{M} \in \mathfrak{se}(3)$ is given by

$$\mathbf{Ad}_{\boldsymbol{T}}(\mathcal{M}) = \boldsymbol{T}\mathcal{M}\boldsymbol{T}^{-1} \in \mathfrak{se}(3) \tag{2.8}$$

Let us define another adjoint map for any $\boldsymbol{T} \in \mathbb{SE}(3)$ by

$$\overline{\breve{\mathbf{Ad}}}_{\boldsymbol{T}} = \begin{bmatrix} R & \mathbf{0}_{3\times3} \\ [P]_\times R & R \end{bmatrix} \in \mathbb{R}^{6\times6} \tag{2.9}$$

One can easily verify that the vex operator in (2.5) can be combined with the results in (2.8) and (2.9) to show (Appendix C)

$$\boldsymbol{\Upsilon}(\mathbf{Ad}_{\boldsymbol{T}}(\mathcal{M})) = \overline{\breve{\mathbf{Ad}}}_{\boldsymbol{T}}\boldsymbol{\Upsilon}(\mathcal{M}) \in \mathbb{R}^6$$

thus

$$\boldsymbol{T}[\mathcal{Y}]_\wedge \boldsymbol{T}^{-1} = \left[\overline{\breve{\mathbf{Ad}}}_{\boldsymbol{T}}\mathcal{Y}\right]_\wedge \in \mathbb{SE}(3), \quad \mathcal{Y} \in \mathbb{R}^6, \boldsymbol{T} \in \mathbb{SE}(3) \tag{2.10}$$

which will be useful for the filter derivation and further analysis, for more details visit Appendix C. For $\alpha, \beta \in \mathbb{R}^3$, $R \in \mathbb{SO}(3)$, $A \in \mathbb{R}^{3\times3}$ and $B = B^\top \in \mathbb{R}^{3\times3}$ the following mathematical identities

$$[\alpha \times \beta]_\times = \beta\alpha^\top - \alpha\beta^\top \tag{2.11}$$

$$[R\alpha]_\times = R[\alpha]_\times R^\top \tag{2.12}$$

$$B[\alpha]_\times + [\alpha]_\times B = \mathrm{Tr}\{B\}[\alpha]_\times - [B\alpha]_\times \tag{2.13}$$

$$[\alpha]_\times^2 = -\alpha^\top\alpha\mathbf{I}_3 + \alpha\alpha^\top \tag{2.14}$$

$$\mathrm{Tr}\left\{B\left[\alpha\right]_{\times}\right\} = 0 \tag{2.15}$$

$$\mathrm{Tr}\left\{A\left[\alpha\right]_{\times}\right\} = \mathrm{Tr}\left\{\boldsymbol{\mathcal{P}}_a\left(A\right)\left[\alpha\right]_{\times}\right\} = -2\mathbf{vex}\left(\boldsymbol{\mathcal{P}}_a\left(A\right)\right)^{\top}\alpha \tag{2.16}$$

$$\overline{\breve{\mathbf{Ad}}}_{\boldsymbol{T}_1\boldsymbol{T}_2} = \overline{\breve{\mathbf{Ad}}}_{\boldsymbol{T}_1}\overline{\breve{\mathbf{Ad}}}_{\boldsymbol{T}_2}, \quad \boldsymbol{T}_1, \boldsymbol{T}_2 \in \mathbb{SE}\left(3\right) \tag{2.17}$$

$$\overline{\breve{\mathbf{Ad}}}_{\boldsymbol{T}}\overline{\breve{\mathbf{Ad}}}_{\boldsymbol{T}^{-1}} = \overline{\breve{\mathbf{Ad}}}_{\boldsymbol{T}^{-1}}\overline{\breve{\mathbf{Ad}}}_{\boldsymbol{T}} = \mathbf{I}_6, \quad \boldsymbol{T} \in \mathbb{SE}\left(3\right) \tag{2.18}$$

will be used in the subsequent derivations. Proof of (2.17) and (2.18) is given in Appendix C.

Chapter 3
Nonlinear Attitude Filters on $\mathbb{SO}(3)$ with Prescribed Performance

3.1 Introduction

This chapter proposes two novel nonlinear attitude filters evolved directly on the Special Orthogonal Group $\mathbb{SO}(3)$ able to ensure prescribed measures of transient and steady-state performance. The tracking performance of the normalized Euclidean distance of attitude error is trapped to initially start within a large set and converge systematically and asymptotically to the origin. The convergence rate is guaranteed to be less than the prescribed value and the steady-state error does not exceed a predefined small value. The first filter uses a set of vectorial measurements with the need for attitude reconstruction. The second filter does not require attitude reconstruction and instead uses only a rate gyroscope measurement and two or more vectorial measurements. These filters provide good attitude estimates with superior convergence properties and can be applied to measurements obtained from low cost inertial measurement units. Simulation results illustrate the robustness and effectiveness of the proposed attitude filters with guaranteed performance considering high level of uncertainty in angular velocity along with body-frame vector measurements. The results of this chapter were first published in Hashim, Brown, and McIsaac (2019a).

The remainder of the chapter is organized as follows: Section 3.2 formulates the attitude problem, presents the estimator structure and error criteria, and formulates the attitude error in terms of prescribed performance. The two proposed filters and the associated stability analysis are demonstrated in Section 3.3. Section 3.4 illustrates through simulation the effectiveness and robustness of the proposed filters. Finally, Section 3.5 summarizes the work with concluded remarks.

3.2 Problem Formulation with Prescribed Performance

Attitude estimator relies on a collection of inertial-frame and body-frame vectorial measurements. In this section, the attitude problem is defined, and body-frame and gyroscope measurements are presented. Next, the attitude error is defined and reformulated to satisfy a desired measure of transient and steady-state performance.

3.2.1 Attitude Kinematics and Measurements

$R \in \mathbb{SO}(3)$ stands for the rotation matrix, and therefore the orientation of the rigid-body in the body-frame $\{\mathcal{B}\}$ relative to the inertial-frame $\{\mathcal{I}\}$ can be represented by the attitude matrix R as illustrated in Figure 3.1.

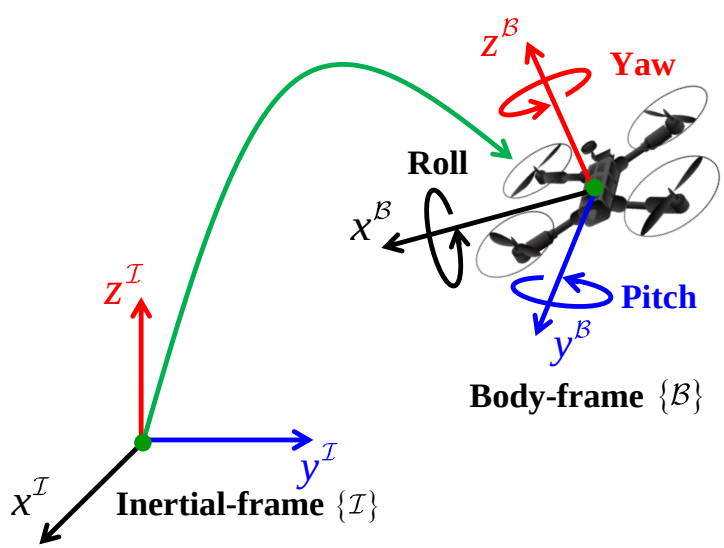

Figure 3.1: The relative orientation between body-frame and inertial-frame of a rigid-body.

Let the superscripts $\mathcal{I}$ and $\mathcal{B}$ denote a vector associated with the inertial-frame and body-frame, respectively. Consider $\mathrm{v}_i^{\mathcal{I}(\mathrm{R})} \in \mathbb{R}^3$ to be a known vector in the inertial-frame and to be measured in the coordinate system fixed to the rigid-body such that

$$\mathrm{v}_i^{\mathcal{B}(\mathrm{R})} = R^\top \mathrm{v}_i^{\mathcal{I}(\mathrm{R})} + \mathrm{b}_i^{\mathcal{B}(\mathrm{R})} + \omega_i^{\mathcal{B}(\mathrm{R})} \tag{3.1}$$

where $\mathrm{v}_i^{\mathcal{B}(\mathrm{R})} \in \mathbb{R}^3$ is the ith body-frame measurement associated with $\mathrm{v}_i^{\mathcal{I}(\mathrm{R})}$. $\mathrm{b}_i^{\mathcal{B}(\mathrm{R})} \in \mathbb{R}^3$ stands for the bias component, and $\omega_i^{\mathcal{B}(\mathrm{R})} \in \mathbb{R}^3$ denotes the noise component attached to the ith body-frame measurement for $i = 1, 2, \ldots, n$. Suppose that the instantaneous set of size $n \geq 2$ consisting of known inertial-frame and measured body-frame vectors is non-collinear. Therefore, the attitude can be established. Moreover, two non-collinear vectors ($n = 2$) are sufficient for attitude reconstruction, e.g., Crassidis et al. (2007); Hashim et al. (2018a, 2018b); Hashim, Brown, and McIsaac (2019d); Mahony et al. (2008); Shuster and Oh (1981). In case when $n = 2$, the third inertial-frame and body-frame vectors can be obtained by the cross product such that $\mathrm{v}_3^{\mathcal{I}(\mathrm{R})} = \mathrm{v}_1^{\mathcal{I}(\mathrm{R})} \times \mathrm{v}_2^{\mathcal{I}(\mathrm{R})}$ and $\mathrm{v}_3^{\mathcal{B}(\mathrm{R})} = \mathrm{v}_1^{\mathcal{B}(\mathrm{R})} \times \mathrm{v}_2^{\mathcal{B}(\mathrm{R})}$, respectively. The inertial-frame and body-frame vectors can be normalized and their normalized values can be implemented in the estimation of the attitude in the following manner

$$\upsilon_i^{\mathcal{I}(\mathrm{R})} = \frac{\mathrm{v}_i^{\mathcal{I}(\mathrm{R})}}{||\mathrm{v}_i^{\mathcal{I}(\mathrm{R})}||}, \quad \upsilon_i^{\mathcal{B}(\mathrm{R})} = \frac{\mathrm{v}_i^{\mathcal{B}(\mathrm{R})}}{||\mathrm{v}_i^{\mathcal{B}(\mathrm{R})}||} \tag{3.2}$$

Hence, the attitude can be obtained knowing $\upsilon_i^{\mathcal{I}(\mathrm{R})}$ and $\upsilon_i^{\mathcal{B}(\mathrm{R})}$. For simplicity, it is considered that the body frame vector ($\mathrm{v}_i^{\mathcal{B}(\mathrm{R})}$) is noise and bias free in the stability analysis. The Simulation Section, on the other hand, takes noise and bias associated with the measurements into account. The angular velocity of the moving body relative to the inertial-frame is measured by the rate gyros as

$$\Omega_m = \Omega + b + \omega \tag{3.3}$$

where $\Omega \in \mathbb{R}^3$ is the true value of angular velocity and b and ω denote the bias and noise components, respectively, attached to the measurement of angular velocity for all $b, \omega \in \mathbb{R}^3$. The true rotational kinematics are described by

$$\dot{R} = R\,[\Omega]_\times \tag{3.4}$$

where $\Omega \in \{\mathcal{B}\}$. Considering the normalized Euclidean distance of R in (2.6) and the identity in (2.16), the kinematics of the true attitude in (3.4) can be defined in terms

of normalized Euclidean distance as

$$\begin{aligned}\frac{d}{dt}||R||_I &= -\frac{1}{4}\mathrm{Tr}\left\{\dot{R}\right\} \\ &= -\frac{1}{4}\mathrm{Tr}\left\{\boldsymbol{\mathcal{P}}_a\left(R\right)\left[\Omega\right]_\times\right\} \\ &= \frac{1}{2}\mathbf{vex}\left(\boldsymbol{\mathcal{P}}_a\left(R\right)\right)^\top\Omega \end{aligned} \tag{3.5}$$

For the sake of simplicity, let us neglect the noise attached to angular velocity measurements such that the kinematics of the normalized Euclidean distance in (3.5) become

$$\frac{d}{dt}||R||_I = \frac{1}{2}\mathbf{vex}\left(\boldsymbol{\mathcal{P}}_a\left(R\right)\right)^\top\left(\Omega_m - b\right) \tag{3.6}$$

Now, we introduce Lemma 3.1 which is going to be applicable in the subsequent filter derivation.

Lemma 3.1 *Let $R \in \mathbb{SO}(3)$, $M^{\mathcal{B}} = \left(M^{\mathcal{B}}\right)^\top \in \mathbb{R}^{3\times 3}$, $M^{\mathcal{B}}$ be nonsingular, $\mathrm{Tr}\left\{M^{\mathcal{B}}\right\} = 3$, and $\bar{\mathbf{M}}^{\mathcal{B}} = \mathrm{Tr}\left\{M^{\mathcal{B}}\right\}\mathbf{I}_3 - M^{\mathcal{B}}$, while the minimum singular value of $\bar{\mathbf{M}}^{\mathcal{B}}$ is $\underline{\lambda} := \underline{\lambda}\left(\bar{\mathbf{M}}^{\mathcal{B}}\right)$. Then, the following holds:*

$$||\mathbf{vex}\left(\boldsymbol{\mathcal{P}}_a\left(R\right)\right)||^2 = 4\left(1 - ||R||_I\right)||R||_I \tag{3.7}$$

$$\frac{2}{\underline{\lambda}}\frac{||\mathbf{vex}\left(\boldsymbol{\mathcal{P}}_a\left(M^{\mathcal{B}}R\right)\right)||^2}{1 + \mathrm{Tr}\left\{\left(M^{\mathcal{B}}\right)^{-1}M^{\mathcal{B}}R\right\}} \geq \left\|M^{\mathcal{B}}R\right\|_I \tag{3.8}$$

Proof. See Appendix A.

3.2.2 Estimator Structure and Error Criteria

The goal of the attitude estimator in this work is to achieve accurate estimate of the true attitude satisfying transient as well as steady-state performance characteristics. In this subsection a general framework of the nonlinear attitude filter on $\mathbb{SO}(3)$ is introduced. Next, the error dynamics are expressed with respect to normalized Euclidean distance. Let $\hat{R}$ denote the estimate of the true attitude R and $\tilde{R} = R^\top\hat{R}$ denote the attitude error between body-frame and estimator-frame. Consider the

following nonlinear attitude filter on $\mathbb{SO}(3)$

$$\dot{\hat{R}} = \hat{R}\left[\Omega_m - \hat{b} - W\right]_\times, \quad \hat{R}(0) = \hat{R}_0 \tag{3.9}$$

$$\dot{\hat{b}} = \frac{1}{2}\mathbf{K}_b \mathbf{vex}\left(\boldsymbol{\mathcal{P}}_a(\boldsymbol{\Phi})\right), \quad \hat{b}(0) = \hat{b}_0 \tag{3.10}$$

$$W = 2\mathbf{K}_W \mathbf{vex}\left(\boldsymbol{\mathcal{P}}_a(\boldsymbol{\Phi})\right) \tag{3.11}$$

with $\hat{b}$ being the estimate of the true rate-gyro bias b, $\mathbf{K}_b$ being a time-variant gain associated with $\hat{b}$, $\mathbf{K}_W$ being a time-variant gain associated with the correction factor W, and $\boldsymbol{\Phi}$ being a matrix associated with attitude error $\tilde{R}$. Define the unstable set $\mathcal{U} \subseteq \mathbb{SO}(3)$ by $\mathcal{U} := \left\{\tilde{R}_0 \middle| \operatorname{Tr}\left\{\tilde{R}_0\right\} = -1\right\}$ with $\tilde{R}_0 = \tilde{R}(0)$. $\mathbf{K}_b$, $\mathbf{K}_W$, and $\boldsymbol{\Phi}$ will be defined subsequently. In particular, the dynamic gains $\mathbf{K}_b$ and $\mathbf{K}_W$ will be selected such that their values become increasingly aggressive as $\tilde{R}$ approaches the unstable equilibria $\operatorname{Tr}\left\{\tilde{R}_0\right\} \to -1$, and reduce significantly as $\tilde{R}$ approaches $\mathbf{I}_3$.

Remark 3.1 *In the conventional design of nonlinear attitude filters, for example Crassidis et al. (2007); Grip et al. (2012); Hamel and Mahony (2006); Mahony et al. (2008), $\mathbf{K}_b$ and $\mathbf{K}_W$ are selected as positive constant gains. However, the weakness of the conventional design of nonlinear attitude filters is that smaller values of $\mathbf{K}_b$ and $\mathbf{K}_W$ result in slower transient performance with less oscillatory behavior in the steady-state. In contrast, higher values of $\mathbf{K}_b$ and $\mathbf{K}_W$ generate faster transient performance with higher oscillation in the steady-state.*

Consider the attitude error defined as

$$\tilde{R} = R^\top \hat{R} \tag{3.12}$$

Also, define the error in bias estimation by

$$\tilde{b} = b - \hat{b} \tag{3.13}$$

From (3.4) and (3.9) the error dynamics can be found to be

$$\begin{aligned}\dot{\tilde{R}} &= R^\top \hat{R}\left[\Omega_m - \hat{b} - W\right]_\times - [\Omega]_\times R^\top \hat{R} \\ &= \tilde{R}\left[\tilde{b} - W\right]_\times + \tilde{R}[\Omega]_\times - [\Omega]_\times \tilde{R}\end{aligned} \tag{3.14}$$

Considering (3.4) and (3.5), the error dynamics in (3.14) are represented with regards to normalized Euclidean distance

$$\begin{aligned}\frac{d}{dt}||\tilde{R}||_I &= \frac{d}{dt}\frac{1}{4}\mathrm{Tr}\left\{\mathbf{I}_3 - \tilde{R}\right\} \\ &= -\frac{1}{4}\mathrm{Tr}\left\{\tilde{R}\left[\tilde{b} - W\right]_\times\right\} - \frac{1}{4}\mathrm{Tr}\left\{\left[\tilde{R}, [\Omega]_\times\right]\right\} \\ &= \frac{1}{2}\mathbf{vex}\left(\boldsymbol{\mathcal{P}}_a\left(\tilde{R}\right)\right)^\top\left(\tilde{b} - W\right) \end{aligned} \tag{3.15}$$

where $\mathrm{Tr}\left\{\tilde{R}\left[\tilde{b}\right]_\times\right\} = -2\mathbf{vex}\left(\boldsymbol{\mathcal{P}}_a\left(\tilde{R}\right)\right)^\top\tilde{b}$ as given in (2.16) and $\mathrm{Tr}\left\{\left[\tilde{R}, [\Omega]_\times\right]\right\} = 0$ as defined in (2.15).

3.2.3 Prescribed Performance

This subsection aims to reformulate the problem such that the normalized Euclidean distance of the attitude error $||\tilde{R}(t)||_I$ satisfies the predefined transient as well as steady-state measures set by the user. Initially, the error $||\tilde{R}(t)||_I$ is contained within a predefined large set and decreases systematically and smoothly to a predefined narrow set through a prescribed performance function (PPF) Bechlioulis and Rovithakis (2008). This is accomplished by first defining a configuration error function Bechlioulis and Rovithakis (2008); Hashim, El-Ferik, and Lewis (2017, 2019). Let $\xi(t)$ be a positive smooth and time-decreasing performance function such that $\xi : \mathbb{R}_+ \to \mathbb{R}_+$ and $\lim_{t\to\infty} \xi(t) = \xi_\infty > 0$. The general expression of the PPF is as follows

$$\xi(t) = (\xi_0 - \xi_\infty)\exp(-\ell t) + \xi_\infty \tag{3.16}$$

where $\xi_0 = \xi(0)$ is the upper bound of the predefined large set, also known to be the initial value of the PPF, ξ_∞ is the upper bound of the small set such that the steady-state error is confined by $\pm\xi_\infty$, while ℓ is a positive constant controlling the convergence rate of the set boundaries $\xi(t)$ with respect to time from ξ_0 to ξ_∞. It is sufficient to force $||\tilde{R}(t)||_I$ to obey a predefined transient and steady-state charac-

teristics, if the following conditions are met:

$$-\delta\xi(t) < ||\tilde{R}(t)||_I < \xi(t), \text{ if } ||\tilde{R}(0)||_I \geq 0, \forall t \geq 0 \tag{3.17}$$

$$-\xi(t) < ||\tilde{R}(t)||_I < \delta\xi(t), \text{ if } ||\tilde{R}(0)||_I < 0, \forall t \geq 0 \tag{3.18}$$

where δ is selected such that $1 \geq \delta \geq 0$. The tracking error $||\tilde{R}(t)||_I$, with PPF decreasing systematically from a known large set to a known small set in accordance with (3.17) and (3.18) is illustrated in Figure 3.2.

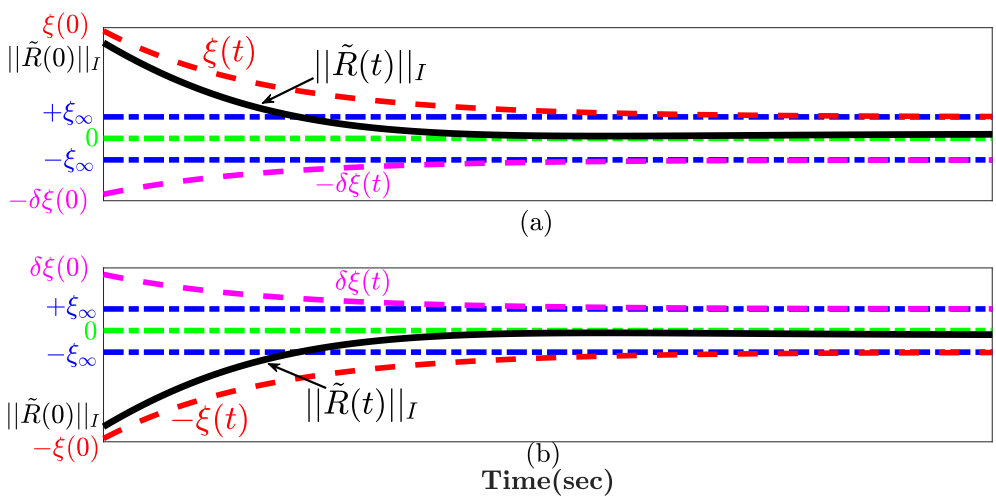

Figure 3.2: A detailed representation of tracking normalized Euclidean distance error $||\tilde{R}(t)||_I$ with PPF satisfying (a) Eq. (3.17); (b) Eq. (3.18).

Remark 3.2 *As explained in Bechlioulis and Rovithakis (2008); Hashim, El-Ferik, and Lewis (2017, 2019), knowing the sign of $||\tilde{R}(0)||_I$ is sufficient to satisfy the performance constraints and maintain the error convergence within the predefined dynamically decreasing boundaries for all $t > 0$. Since $||\tilde{R}(0)||_I \in [0, 1]$, $||\tilde{R}(0)||_I$ is guaranteed to be greater than or equal to 0 for any attitude initialization, and therefore the only possible condition is (3.17). If the condition in (3.17) is met, the maximum steady-state error will be less than ξ_∞, the maximum overshoot will be less than $-\delta\xi(0)$, and $||\tilde{R}(t)||_I$ will be confined between $\xi(t)$ and $\delta\xi(t)$ as given in the upper portion of Figure 3.2.*

Let us define

$$||\tilde{R}(t)||_I = \xi(t)\,\mathcal{Z}(\mathcal{E}) \tag{3.19}$$

with $\xi(t) \in \mathbb{R}$ being given in (3.16), $\mathcal{E} \in \mathbb{R}$ being a transformed error, and $\mathcal{Z}(\mathcal{E})$ being a smooth function which satisfies Assumption 3.1:

Assumption 3.1 *The smooth function $\mathcal{Z}(\mathcal{E})$ must satisfy Bechlioulis and Rovithakis (2008):*

P 1) $\mathcal{Z}(\mathcal{E})$ is smooth and strictly increasing.

P 2) $\mathcal{Z}(\mathcal{E})$ is bounded between two predefined bounds
$-\underline{\delta} < \mathcal{Z}(\mathcal{E}) < \bar{\delta}, for ||\tilde{R}(0)||_I \geq 0$
with $\bar{\delta}$ and $\underline{\delta}$ being positive constants and $\underline{\delta} \leq \bar{\delta}$.

P 3) $\lim_{\mathcal{E}\to-\infty} \mathcal{Z}(\mathcal{E}) = -\underline{\delta}$ and $\lim_{\mathcal{E}\to+\infty} \mathcal{Z}(\mathcal{E}) = \bar{\delta}$ where

$$\mathcal{Z}(\mathcal{E}) = \frac{\bar{\delta}\exp(\mathcal{E}) - \underline{\delta}\exp(-\mathcal{E})}{\exp(\mathcal{E}) + \exp(-\mathcal{E})} \tag{3.20}$$

One could find the transformed error to be

$$\mathcal{E}\left(||\tilde{R}(t)||_I, \xi(t)\right) = \mathcal{Z}^{-1}\left(\frac{||\tilde{R}(t)||_I}{\xi(t)}\right) \tag{3.21}$$

where $\mathcal{E} \in \mathbb{R}$, $\mathcal{Z} \in \mathbb{R}$ and $\mathcal{Z}^{-1} \in \mathbb{R}$ are smooth functions. For clarity, let $\xi := \xi(t)$, $||\tilde{R}||_I := ||\tilde{R}(t)||_I$ and $\mathcal{E} := \mathcal{E}(\cdot,\cdot)$. The transformed error $\mathcal{E}$ plays a prominent role driving the error dynamics from constrained form in either (3.17) or (3.18) to that in (3.21) which is unconstrained. One can find from (3.20) that the transformed error is

$$\mathcal{E} = \frac{1}{2}\ln\frac{\underline{\delta} + ||\tilde{R}||_I/\xi}{\bar{\delta} - ||\tilde{R}||_I/\xi} \tag{3.22}$$

Remark 3.3 *Consider the transformed error in (3.22). If $\mathcal{E}(t)$ is guaranteed to be bounded for all $t \geq 0$, the performance function $\xi(t)$ can be used to bound the transient and steady-state of the tracking error ($||\tilde{R}||_I$) allowing it to achieve the prescribed performance.*

Proposition 3.1 *Consider the normalized Euclidean distance error $||\tilde{R}||_I$ being defined by (2.6) and from (3.19), (3.20), (3.21) let the transformed error be given as in (3.22) with $\underline{\delta} = \bar{\delta}$. Then the following statements hold.*

(i) The transformed error $\mathcal{E} > 0 \forall ||\tilde{R}||_I \neq 0$ and $\mathcal{E} = 0$ only at $||\tilde{R}||_I = 0$.

(ii) The critical point of $\mathcal{E}$ satisfies $||\tilde{R}||_I = 0$.

(iii) The only critical point of $\mathcal{E}$ is $\tilde{R} = \mathbf{I}_3$.

Proof. Letting $\underline{\delta} = \bar{\delta}$ with the prescribed performance constraints $||\tilde{R}||_I \leq \xi$, the expression $\left(\underline{\delta} + ||\tilde{R}||_I/\xi\right) / \left(\bar{\delta} - ||\tilde{R}||_I/\xi\right)$ in (3.22) is always greater than or equal to 1. Accordingly, $\mathcal{E} > 0 \forall ||\tilde{R}||_I \neq 0$ and $\mathcal{E} = 0$ at $||\tilde{R}||_I = 0$ which proves (i). For (ii) and (iii), from (2.6), $||\tilde{R}||_I = 0$ if and only if $\tilde{R} = \mathbf{I}_3$. Thus, the critical point of $\mathcal{E}$ satisfies $\tilde{R} = \mathbf{I}_3$ and, consequently, also satisfies $||\tilde{R}||_I = 0$ which proves (ii) and (iii). Let us define a new variable $\mu := \mu\left(||\tilde{R}||_I, \xi\right)$ such that

$$\begin{aligned} \mu &= \frac{1}{2\xi} \frac{\partial \mathcal{Z}^{-1}\left(||\tilde{R}||_I/\xi\right)}{\partial\left(||\tilde{R}||_I/\xi\right)} \\ &= \frac{1}{2\xi}\left(\frac{1}{\underline{\delta} + ||\tilde{R}||_I/\xi} + \frac{1}{\bar{\delta} - ||\tilde{R}||_I/\xi}\right) \end{aligned} \tag{3.23}$$

Consequently, the derivative of the transformed error is governed by

$$\begin{aligned} \dot{\mathcal{E}} &= \frac{1}{2\xi}\left(\frac{1}{\underline{\delta} + ||\tilde{R}||_I/\xi} + \frac{1}{\bar{\delta} - ||\tilde{R}||_I/\xi}\right)\left(\frac{d}{dt}||\tilde{R}||_I - \frac{\dot{\xi}}{\xi}||\tilde{R}||_I\right) \\ &= \mu\left(\frac{1}{2}\mathbf{vex}\left(\boldsymbol{\mathcal{P}}_a\left(\tilde{R}\right)\right)^\top\left(\tilde{b} - W\right) - \frac{\dot{\xi}}{\xi}||\tilde{R}||_I\right) \end{aligned} \tag{3.24}$$

with direct substitution of (3.15) in (3.24). The next section presents two nonlinear attitude filters on $\mathbb{SO}(3)$ with prescribed performance which guarantees $\mathcal{E} \in \mathcal{L}_\infty, \forall t \geq 0$ and, thus, satisfies (3.17) provided that $0 \leq ||\tilde{R}(0)||_I < \xi(0)$.

3.3 Nonlinear Complementary Filters On $\mathbb{SO}(3)$ with Prescribed Performance

The primary objective of this section is to propose two nonlinear attitude estimators on $\mathbb{SO}(3)$ with normalized Euclidean distance error satisfying a predefined transient

as well as steady-state performance given by the user. The constrained error $||\tilde{R}||_I$ is relaxed to unconstrained $\mathcal{E}$. The first filter is termed a semi-direct attitude filter with prescribed performance because it requires the attitude to be reconstructed via the set of vectorial measurements as defined in (3.2), in addition to the measurement of the angular velocity in (3.3). The second filter is called a direct attitude filter with prescribed performance because it uses the vectorial measurements in (3.2) and the angular velocity measurement in (3.3) directly without the need for attitude reconstruction.

3.3.1 Semi-direct Attitude Filter with Prescribed Performance

Let R_y denote the reconstructed attitude of R. There are many methods to reconstruct R_y, for instance, TRIAD Black (1964), QUEST Shuster and Oh (1981), or SVD Markley (1988). Consider the following filter kinematics

$$\dot{\hat{R}} = \hat{R}\left[\Omega_m - \hat{b} - W\right]_\times, \quad \hat{R}(0) = \hat{R}_0 \tag{3.25}$$

$$\dot{\hat{b}} = \frac{1}{2}\gamma\mu\mathcal{E}\mathbf{vex}\left(\boldsymbol{\mathcal{P}}_a\left(\tilde{R}\right)\right), \quad \hat{b}(0) = \hat{b}_0, \tilde{R} = R_y^\top \hat{R} \tag{3.26}$$

$$W = 2\frac{k_w\mu\mathcal{E} - \dot{\xi}/4\xi}{1 - ||\tilde{R}||_I}\mathbf{vex}\left(\boldsymbol{\mathcal{P}}_a\left(\tilde{R}\right)\right), \quad \tilde{R} = R_y^\top \hat{R} \tag{3.27}$$

with $\mathcal{E}$ and μ being defined in (3.22) and (3.23), respectively, k_w and γ being positive constants, $||\tilde{R}||_I = \frac{1}{4}\mathrm{Tr}\left\{\mathbf{I}_3 - \tilde{R}\right\}$ being defined in (2.6), ξ being PPF defined in (3.16), and $\hat{b}$ being the estimate of b.

Theorem 3.1 *Consider the rotation kinematics in (3.4), measurements of angular velocity in (3.3) with no noise associated with the measurement $\Omega_m = \Omega + b$, in addition to two or more non-collinear vector measurements given in (3.1) coupled with the filter in (3.25), (3.26) and (3.27). Define $\mathcal{U} \subseteq \mathbb{SO}(3) \times \mathbb{R}^3$ by*

$$\mathcal{U} := \left\{\left(\tilde{R}_0, \tilde{b}_0\right) \middle| \mathrm{Tr}\left\{\tilde{R}_0\right\} = -1, \tilde{b}_0 = \underline{\mathbf{0}}_3\right\}$$

with $\tilde{R}_0 = \tilde{R}(0)$ and $\tilde{b}_0 = \tilde{b}(0)$. For almost any initial condition such that $\tilde{R}_0 \notin \mathcal{U}$ and $||\tilde{R}(0)||_I < \xi(0)$, then, all signals in the closed loop are bounded, $\lim_{t\to\infty}\mathcal{E}(t) = 0$

and $\tilde{R}$ asymptotically approaches $\mathbf{I}_3$.

Theorem 3.1 guarantees that the observer dynamics in (3.25), (3.26) and (3.27) are stable with $\mathcal{E}(t)$ approaching asymptotically the origin. Since, $\mathcal{E}(t)$ is bounded, $||\tilde{R}||_I$ obeys the prescribed transient and steady-state performance introduced in (3.16).

Proof. Let the error in attitude and bias be defined by $\tilde{R} = R^\top \hat{R}$ and $\tilde{b} = b - \hat{b}$ similar to (3.12) and (3.13), respectively. From (3.4) and (3.25), the error dynamics can be obtained as in (3.14). Also, in view of (3.4) and (3.5), the error dynamics are analogous to (3.15) in terms of normalized Euclidean distance. Therefore, considering (3.5) and (3.24), the derivative of the transformed error can be found to be

$$\dot{\mathcal{E}} = \mu \left(\frac{1}{2} \mathbf{vex} \left(\boldsymbol{\mathcal{P}}_a \left(\tilde{R} \right) \right)^\top \left(\tilde{b} - W \right) - \frac{\dot{\xi}}{\xi} ||\tilde{R}||_I \right) \tag{3.28}$$

Consider the following candidate Lyapunov function

$$V\left(\mathcal{E}, \tilde{b}\right) = \frac{1}{2}\mathcal{E}^2 + \frac{1}{2\gamma}||\tilde{b}||^2 \tag{3.29}$$

Differentiating V in (3.29) and substituting for $\dot{\hat{b}}$ and W in (3.26), and (3.27), respectively, one obtains

$$\begin{aligned} \dot{V} =& \mathcal{E}\dot{\mathcal{E}} - \frac{1}{\gamma}\tilde{b}^\top \dot{\hat{b}} \\ =& \mu\mathcal{E} \left(\frac{1}{2} \mathbf{vex} \left(\boldsymbol{\mathcal{P}}_a \left(\tilde{R} \right) \right)^\top \left(\tilde{b} - W \right) - \frac{\dot{\xi}}{\xi} ||\tilde{R}||_I \right) - \frac{1}{\gamma}\tilde{b}^\top \dot{\hat{b}} \\ =& -\mathcal{E}\mu \left(\frac{k_w \mu \mathcal{E} - \dot{\xi}/4\xi}{1 - ||\tilde{R}||_I} \left\| \mathbf{vex} \left(\boldsymbol{\mathcal{P}}_a \left(\tilde{R} \right) \right) \right\|^2 + \frac{\dot{\xi}}{\xi} ||\tilde{R}||_I \right) \end{aligned} \tag{3.30}$$

Substituting for $\left\| \mathbf{vex} \left(\boldsymbol{\mathcal{P}}_a \left(\tilde{R} \right) \right) \right\|^2 = 4 \left(1 - ||\tilde{R}||_I \right) ||\tilde{R}||_I$ as defined in (3.7), the expression in (3.30) becomes

$$\dot{V} = -4k_w ||\tilde{R}||_I \mu^2 \mathcal{E}^2 \tag{3.31}$$

This implies that $V(t) \leq V(0), \forall t \geq 0$. Given $\tilde{R}_0 \notin \mathcal{U}$ implies that $\tilde{b}$ remains bounded for all $t \geq 0$, and, therefore, $\mathcal{E}$ is bounded and well defined for all $t \geq 0$. It

can be shown that

$$\ddot{V} = -4k_w \left(2\left(\mathcal{E}\dot{\mathcal{E}}\mu^2 + \mathcal{E}^2\mu\dot{\mu}\right)||\tilde{R}||_I + \mathcal{E}^2\mu^2||\dot{\tilde{R}}||_I\right) \tag{3.32}$$

From (3.23), it can be found that

$$\dot{\mu} = -\frac{1}{2}\frac{\underline{\delta}\dot{\xi} + ||\dot{\tilde{R}}||_I}{\left(\underline{\delta}\xi + ||\tilde{R}||_I\right)^2} - \frac{1}{2}\frac{\bar{\delta}\dot{\xi} - ||\dot{\tilde{R}}||_I}{\left(\bar{\delta}\xi - ||\tilde{R}||_I\right)^2} \tag{3.33}$$

where $\dot{\xi} = -\ell\left(\xi^0 - \xi^\infty\right)\exp\left(-\ell t\right)$. Since $||\dot{\tilde{R}}||_I$ is bounded, $\dot{\mu}$ is bounded which shows that $\ddot{V}$ is bounded for all $t \geq 0$. Consequently, $\dot{V}$ is uniformly continuous, and according to Barbalat Lemma, $\dot{V} \to 0$ indicates that one or more of the following conditions are true

1. $||\mathcal{E}|| \to 0$.
2. $||\tilde{R}||_I \to 0$.
3. $||\mathcal{E}|| \to 0$ and $||\tilde{R}||_I \to 0$.

as $t \to \infty$. According to property (i) and (ii) of Proposition 3.1, $||\mathcal{E}|| \to 0$ means $||\tilde{R}||_I \to 0$ and vice versa. Therefore, $\dot{V} \to 0$ as $t \to \infty$ strictly indicates that $||\mathcal{E}|| \to 0$ and $||\tilde{R}||_I \to 0$. As stated by property (iii) of Proposition 3.1, $||\mathcal{E}|| \to 0$ implies that $\tilde{R}$ asymptotically approaches $\mathbf{I}_3$. Hence, $\dot{V} \to 0$ means that $\tilde{R}$ asymptotically approaches $\mathbf{I}_3$, which completes the proof.

3.3.2 Direct Attitude Filter with Prescribed Performance

Let R_y denote the reconstructed attitude of R obtained through a set of vectorial measurements in (3.2). Although there are many methods to reconstruct R_y, this may add computational cost. The filter proposed in the previous Subsection 3.3.1 requires R_y to obtain the attitude error $\tilde{R} = R_y^\top \hat{R}$, for example (the Appendix in Hashim et al. (2018b); Hashim, Brown, and McIsaac (2019d)). In this Subsection the aforementioned weakness is eliminated by proposing a nonlinear filter with prescribed performance in terms of direct measurements from the inertial and body-frame units.

Let us recall $\upsilon_i^{\mathcal{I}(\mathrm{R})}$ and $\upsilon_i^{\mathcal{B}(\mathrm{R})}$ from (3.1) and (3.2) for $i = 1, \ldots, n$. Let us define

$$\begin{aligned} M^{\mathcal{I}} &= \left(M^{\mathcal{I}}\right)^{\top} = \sum_{i=1}^{n} s_i \upsilon_i^{\mathcal{I}(\mathrm{R})} \left(\upsilon_i^{\mathcal{I}(\mathrm{R})}\right)^{\top} \\ M^{\mathcal{B}} &= \left(M^{\mathcal{B}}\right)^{\top} = \sum_{i=1}^{n} s_i \upsilon_i^{\mathcal{B}(\mathrm{R})} \left(\upsilon_i^{\mathcal{B}(\mathrm{R})}\right)^{\top} \\ &= R^{\top} M^{\mathcal{I}} R \end{aligned} \tag{3.34}$$

where $s_i > 0$ refers to confidence level of the ith sensor measurements, and in this work s_i is selected such that $\sum_{i=1}^{n} s_i = 3$. According to (3.34), $M^{\mathcal{I}}$ and $M^{\mathcal{B}}$ are symmetric matrices. Assume that at least two non-collinear inertial-frame and measured body-frame vectors are available. If two typical vectors are available for measurements, $n = 2$, the third vector is obtained by the cross product as mentioned in Subsection 3.2.1. Thereby, the set of vectors is non-collinear and $M^{\mathcal{B}}$ is nonsingular with rank $\left(M^{\mathcal{B}}\right) = 3$. Hence, the three eigenvalues of $M^{\mathcal{B}}$ are greater than zero. Let $\bar{\mathbf{M}}^{\mathcal{B}} = \mathrm{Tr}\left\{M^{\mathcal{B}}\right\}\mathbf{I}_3 - M^{\mathcal{B}} \in \mathbb{R}^{3\times 3}$, provided that rank $\left(M^{\mathcal{B}}\right) = 3$, then, the following three statements hold (Bullo and Lewis (2004) page. 553):

1. $\bar{\mathbf{M}}^{\mathcal{B}}$ is a symmetric and positive-definite matrix.
2. The eigenvectors of $M^{\mathcal{B}}$ coincide with the eigenvectors of $\bar{\mathbf{M}}^{\mathcal{B}}$.
3. Define the three eigenvalues of $M^{\mathcal{B}}$ by $\lambda\left(M^{\mathcal{B}}\right) = \{\lambda_1, \lambda_2, \lambda_3\}$, then $\lambda\left(\bar{\mathbf{M}}^{\mathcal{B}}\right) = \{\lambda_3 + \lambda_2, \lambda_3 + \lambda_1, \lambda_2 + \lambda_1\}$ such that the minimum singular value $\underline{\lambda}\left(\bar{\mathbf{M}}^{\mathcal{B}}\right) > 0$.

In the remainder of this section, we assume that rank $\left(M^{\mathcal{B}}\right) = 3$, and accordingly the three above-mentioned statements are true. Define

$$\hat{\upsilon}_i^{\mathcal{B}(\mathrm{R})} = \hat{R}^{\top} \upsilon_i^{\mathcal{I}(\mathrm{R})} \tag{3.35}$$

Define the error in attitude and bias by $\tilde{R} = R^{\top}\hat{R}$ and $\tilde{b} = b - \hat{b}$ which is similar to (3.12) and (3.13), respectively. In order to derive the explicit filter, it is necessary to present the following equations expressed in terms of vector measurements. From identity (2.11), one can find

$$\begin{aligned}\left[\sum_{i=1}^{n}\frac{s_i}{2}\hat{\upsilon}_i^{\mathcal{B}(\mathrm{R})}\times\upsilon_i^{\mathcal{B}(\mathrm{R})}\right]_{\times} &= \sum_{i=1}^{n}\frac{s_i}{2}\left(\upsilon_i^{\mathcal{B}(\mathrm{R})}\left(\hat{\upsilon}_i^{\mathcal{B}(\mathrm{R})}\right)^{\top}-\hat{\upsilon}_i^{\mathcal{B}(\mathrm{R})}\left(\upsilon_i^{\mathcal{B}(\mathrm{R})}\right)^{\top}\right)\\ &= \frac{1}{2}R^{\top}M^{\mathcal{I}}R\tilde{R}-\frac{1}{2}\tilde{R}^{\top}R^{\top}M^{\mathcal{I}}R\\ &= \boldsymbol{\mathcal{P}}_a\left(M^{\mathcal{B}}\tilde{R}\right)\end{aligned}$$

such that

$$\mathbf{vex}\left(\boldsymbol{\mathcal{P}}_a\left(M^{\mathcal{B}}\tilde{R}\right)\right)=\sum_{i=1}^{n}\frac{s_i}{2}\hat{\upsilon}_i^{\mathcal{B}(\mathrm{R})}\times\upsilon_i^{\mathcal{B}(\mathrm{R})} \tag{3.36}$$

The normalized Euclidean distance of $M^{\mathcal{B}}\tilde{R}$ can be found to be

$$\begin{aligned}||M^{\mathcal{B}}\tilde{R}||_I &= \frac{1}{4}\mathrm{Tr}\left\{\mathbf{I}_3-M^{\mathcal{B}}\tilde{R}\right\}\\ &= \frac{1}{4}\mathrm{Tr}\left\{\mathbf{I}_3-\sum_{i=1}^{n}s_i\upsilon_i^{\mathcal{B}(\mathrm{R})}\left(\hat{\upsilon}_i^{\mathcal{B}(\mathrm{R})}\right)^{\top}\right\}\\ &= \frac{1}{4}\sum_{i=1}^{n}s_i\left(1-\left(\hat{\upsilon}_i^{\mathcal{B}(\mathrm{R})}\right)^{\top}\upsilon_i^{\mathcal{B}(\mathrm{R})}\right)\end{aligned} \tag{3.37}$$

Let us introduce the following variable

$$\begin{aligned}\boldsymbol{\Upsilon}\left(M^{\mathcal{B}},\tilde{R}\right) &= \mathrm{Tr}\left\{\left(M^{\mathcal{B}}\right)^{-1}M^{\mathcal{B}}\tilde{R}\right\}\\ &= \mathrm{Tr}\left\{\left(\sum_{i=1}^{n}s_i\upsilon_i^{\mathcal{B}(\mathrm{R})}\left(\upsilon_i^{\mathcal{B}(\mathrm{R})}\right)^{\top}\right)^{-1}\sum_{i=1}^{n}s_i\upsilon_i^{\mathcal{B}(\mathrm{R})}\left(\hat{\upsilon}_i^{\mathcal{B}(\mathrm{R})}\right)^{\top}\right\}\end{aligned} \tag{3.38}$$

Consequently, any $\mathbf{vex}\left(\boldsymbol{\mathcal{P}}_a\left(M^{\mathcal{B}}\tilde{R}\right)\right)$, $||M^{\mathcal{B}}\tilde{R}||_I$ and $\boldsymbol{\Upsilon}\left(M^{\mathcal{B}},\tilde{R}\right)$ will be obtained via a set of vectorial measurements as given in (3.36), (3.37), and (3.38), respectively, in all the subsequent calculations and derivations. Let us define the minimum singular value of $\bar{\mathbf{M}}^{\mathcal{B}}$ as $\underline{\lambda}:=\underline{\lambda}\left(\bar{\mathbf{M}}^{\mathcal{B}}\right)$, $\mathcal{E}:=\mathcal{E}\left(||M^{\mathcal{B}}\tilde{R}||_I,\xi\right)$, and $\mu:=\mu\left(||M^{\mathcal{B}}\tilde{R}||_I,\xi\right)$, and

consider the following filter kinematics

$$\dot{\hat{R}} = \hat{R}\left[\Omega_m - \hat{b} - W\right]_\times, \quad \hat{R}(0) = \hat{R}_0 \tag{3.39}$$

$$\dot{\hat{b}} = \frac{1}{2}\gamma\mu\mathcal{E}\mathbf{vex}\left(\boldsymbol{\mathcal{P}}_a\left(M^{\mathcal{B}}\tilde{R}\right)\right), \quad \hat{b}(0) = \hat{b}_0 \tag{3.40}$$

$$W = \frac{4}{\lambda}\frac{k_w\mu\mathcal{E} - \dot{\xi}/\xi}{1 + \boldsymbol{\Upsilon}\left(M^{\mathcal{B}}, \tilde{R}\right)}\mathbf{vex}\left(\boldsymbol{\mathcal{P}}_a\left(M^{\mathcal{B}}\tilde{R}\right)\right) \tag{3.41}$$

where $\boldsymbol{\Upsilon}\left(M^{\mathcal{B}}, \tilde{R}\right)$ and $\mathbf{vex}\left(\boldsymbol{\mathcal{P}}_a\left(M^{\mathcal{B}}\tilde{R}\right)\right)$ are defined in terms of vectorial measurements in (3.38) and (3.36), respectively, ξ is a PPF defined in (3.16), $\mathcal{E}$ and μ are defined in (3.22) and (3.23), respectively, with every $||\tilde{R}||_I$ being replaced by $||M^{\mathcal{B}}\tilde{R}||_I$, k_w and γ are positive constants, and $\hat{b}$ is the estimate of b.

Theorem 3.2 *Consider the filter in (3.39), (3.40) and (3.41) to be coupled with the normalized vector measurements in (3.2) and angular velocity measurements in (3.3) with the assumption that no noise is associated with the measurement $\Omega_m = \Omega + b$. Let two or more body-frame non-collinear vectors be available for measurements such that $M^{\mathcal{B}}$ is nonsingular. Define $\mathcal{U} \subseteq \mathbb{SO}(3) \times \mathbb{R}^3$ by*

$$\mathcal{U} := \left\{\left(\tilde{R}_0, \tilde{b}_0\right) \middle| \operatorname{Tr}\left\{\tilde{R}_0\right\} = -1, \tilde{b}_0 = \underline{\mathbf{0}}_3\right\}$$

with $\tilde{R}_0 = \tilde{R}(0)$ and $\tilde{b}_0 = \tilde{b}(0)$. If $\tilde{R}_0 \notin \mathcal{U}$ and $\mathcal{E}(0) \in \mathcal{L}_\infty$, then, all error signals are bounded, while $\mathcal{E}(t)$ asymptotically approaches 0 and $\tilde{R}$ asymptotically approaches $\mathbf{I}_3$.

The observer dynamics in (3.39), (3.40) and (3.41) are guaranteed by Theorem 3.2 to be stable as $\mathcal{E}(t)$ approaches the origin asymptotically. It follows that $\mathcal{E}(t)$ is bounded, which in turn causes $||\tilde{R}||_I$ to obey the prescribed transient and steady-state performance as described in (3.16) in consistence with Remark 3.3.

Proof. Consider the error in attitude and bias being defined similar to (3.12) and (3.13), respectively. From (3.4) and (3.25), the error dynamics can be found to

be analogous to (3.14). From (3.34), one can find the derivative of $M^{\mathcal{B}}$ to be

$$\begin{aligned}\dot{M}^{\mathcal{B}} &= \dot{R}^\top M^{\mathcal{I}} R + R^\top M^{\mathcal{I}} \dot{R} \\ &= -\left[\Omega\right]_\times R^\top M^{\mathcal{I}} R + R^\top M^{\mathcal{I}} R \left[\Omega\right]_\times \\ &= -\left[\Omega\right]_\times M^{\mathcal{B}} + M^{\mathcal{B}} \left[\Omega\right]_\times \end{aligned} \tag{3.42}$$

Therefore, from (3.14) and (3.42), the derivative of $||M^{\mathcal{B}}\tilde{R}||_I$ can be expressed as

$$\begin{aligned}\frac{d}{dt}||M^{\mathcal{B}}\tilde{R}||_I =& -\frac{1}{4}\mathrm{Tr}\left\{M^{\mathcal{B}}\dot{\tilde{R}} + \dot{M}^{\mathcal{B}}\tilde{R}\right\} \\ =& -\frac{1}{4}\mathrm{Tr}\left\{M^{\mathcal{B}}\left(\left[\tilde{R}, \left[\Omega\right]_\times\right] + \tilde{R}\left[\tilde{b} - W\right]_\times\right)\right\} \\ & -\frac{1}{4}\mathrm{Tr}\left\{\left(-\left[\Omega\right]_\times M^{\mathcal{B}} + M^{\mathcal{B}}\left[\Omega\right]_\times\right)\tilde{R}\right\} \\ =& -\frac{1}{4}\mathrm{Tr}\left\{M^{\mathcal{B}}\tilde{R}\left[\tilde{b} - W\right]_\times\right\} - \frac{1}{4}\mathrm{Tr}\left\{\left[M^{\mathcal{B}}\tilde{R}, \left[\Omega\right]_\times\right]\right\} \\ =& \frac{1}{2}\mathbf{vex}\left(\boldsymbol{\mathcal{P}}_a\left(M^{\mathcal{B}}\tilde{R}\right)\right)^\top\left(\tilde{b} - W\right)\end{aligned} \tag{3.43}$$

where $\mathrm{Tr}\left\{M^{\mathcal{B}}\tilde{R}\left[\tilde{b}\right]_\times\right\} = -2\mathbf{vex}\left(\boldsymbol{\mathcal{P}}_a\left(M^{\mathcal{B}}\tilde{R}\right)\right)^\top\tilde{b}$ as given in (2.16), and $\mathrm{Tr}\left\{\left[M^{\mathcal{B}}\tilde{R}, \left[\Omega\right]_\times\right]\right\} = 0$ as defined in (2.15). Thus, in view of (3.5) and (3.24), the derivative of the transformed error in the sense of (3.15) can be found to be

$$\dot{\mathcal{E}} = \frac{\mu}{2}\mathbf{vex}\left(\boldsymbol{\mathcal{P}}_a\left(M^{\mathcal{B}}\tilde{R}\right)\right)^\top\left(\tilde{b} - W\right) - \mu\frac{\dot{\xi}}{\xi}||M^{\mathcal{B}}\tilde{R}||_I \tag{3.44}$$

Define the following candidate Lyapunov function as

$$V\left(\mathcal{E}, \tilde{b}\right) = \frac{1}{2}\mathcal{E}^2 + \frac{1}{2\gamma}||\tilde{b}||^2 \tag{3.45}$$

The derivative of $V := V\left(\mathcal{E}, \tilde{b}\right)$ in (3.45) can be expressed as

$$\begin{aligned}\dot{V} =& \mathcal{E}\dot{\mathcal{E}} - \frac{1}{\gamma}\tilde{b}^\top\dot{\tilde{b}} \\ =& \mathcal{E}\mu\left(\frac{1}{2}\mathbf{vex}\left(\boldsymbol{\mathcal{P}}_a\left(M^{\mathcal{B}}\tilde{R}\right)\right)^\top\left(\tilde{b} - W\right) - \frac{\dot{\xi}}{\xi}||M^{\mathcal{B}}\tilde{R}||_I\right) - \frac{1}{\gamma}\tilde{b}^\top\dot{\tilde{b}}\end{aligned} \tag{3.46}$$

Directly substituting for $\dot{\hat{b}}$ and W in (3.40), and (3.41), respectively, one obtains

$$\begin{aligned}\dot{V} \leq & \frac{\dot{\xi}}{\xi}\left(\frac{2}{\underline{\lambda}}\frac{\left\|\mathbf{vex}\left(\boldsymbol{\mathcal{P}}_a\left(M^{\mathcal{B}}\tilde{R}\right)\right)\right\|^2}{1+\boldsymbol{\Upsilon}\left(M^{\mathcal{B}},\tilde{R}\right)} - \left\|M^{\mathcal{B}}\tilde{R}\right\|_I\right)\mu\mathcal{E} \\ & - \frac{2}{\underline{\lambda}}\frac{k_w\mu^2\mathcal{E}^2}{1+\boldsymbol{\Upsilon}\left(M^{\mathcal{B}},\tilde{R}\right)}\left\|\mathbf{vex}\left(\boldsymbol{\mathcal{P}}_a\left(M^{\mathcal{B}}\tilde{R}\right)\right)\right\|^2 \end{aligned} \tag{3.47}$$

One can also easily find

$$\frac{\dot{\xi}}{\xi}\left(\frac{2}{\underline{\lambda}}\frac{\left\|\mathbf{vex}\left(\boldsymbol{\mathcal{P}}_a\left(M^{\mathcal{B}}\tilde{R}\right)\right)\right\|^2}{1+\boldsymbol{\Upsilon}\left(M^{\mathcal{B}},\tilde{R}\right)} - \left\|M^{\mathcal{B}}\tilde{R}\right\|_I\right)\mu\mathcal{E} \leq 0 \tag{3.48}$$

where $\mathcal{E} > 0 \forall ||M^{\mathcal{B}}\tilde{R}||_I \neq 0$ and $\mathcal{E} = 0$ at $||M^{\mathcal{B}}\tilde{R}||_I = 0$ as given in (i) Proposition 3.1, and $\mu > 0 \forall t \geq 0$ as given in (3.23). Also, $\dot{\xi}$ is a negative strictly increasing component which satisfies $\dot{\xi} \to 0$ as $t \to \infty$, and $\xi : \mathbb{R}_+ \to \mathbb{R}_+$ such that $\xi \to \xi_\infty$ as $t \to \infty$. Thus, $\dot{\xi}/\xi \leq 0$. In addition, consider (3.8) in Lemma 3.1, the expression in (3.48) is negative semi-definite. Consequently, the inequality in (3.47) can be expressed as

$$\dot{V} \leq -k_w\mu^2\mathcal{E}^2\left\|M^{\mathcal{B}}\tilde{R}\right\|_I \tag{3.49}$$

This implies that $V(t) \leq V(0), \forall t \geq 0$. Given that $\tilde{R}_0 \notin \mathcal{U}$, $\tilde{b}$ is bounded for $t \geq 0$, and $\mathcal{E} \in \mathcal{L}_\infty, \forall t \geq 0$. As such, $\mathcal{E}$ remains bounded and well-defined for all $t \geq 0$. In order to prove asymptotic convergence of $\mathcal{E}$ to the origin and $\tilde{R}$ to the identity for all $\tilde{R}_0 \notin \mathcal{U}$, one obtains the second derivative of (3.45) as

$$\ddot{V} \leq -2k_w\left(\mathcal{E}\dot{\mathcal{E}}\mu^2 + \mathcal{E}^2\mu\dot{\mu}\right)||M^{\mathcal{B}}\tilde{R}||_I - k_w\mathcal{E}^2\mu^2\frac{d}{dt}||M^{\mathcal{B}}\tilde{R}||_I \tag{3.50}$$

Consider the result in (3.23), as such, it can be shown that

$$\dot{\mu} = -\frac{1}{2}\frac{\underline{\delta}\dot{\xi} + \frac{d}{dt}||M^{\mathcal{B}}\tilde{R}||_I}{\left(\underline{\delta}\xi + ||\tilde{R}||_I\right)^2} - \frac{1}{2}\frac{\bar{\delta}\dot{\xi} - \frac{d}{dt}||M^{\mathcal{B}}\tilde{R}||_I}{\left(\bar{\delta}\xi - ||\tilde{R}||_I\right)^2} \tag{3.51}$$

with $\dot{\xi} = -\ell\left(\xi^0 - \xi^\infty\right)\exp\left(-\ell t\right)$. Due to the fact that $||\dot{\tilde{R}}||_I$ is bounded, $\dot{\mu}$ is bounded

and in turn $\ddot{V}$ is bounded for all $t \geq 0$. Thus, $\dot{V}$ is uniformly continuous and in accordance with Barbalat Lemma, $\dot{V} \to 0$ implies that either $||\mathcal{E}|| \to 0$ or $||M^{\mathcal{B}}\tilde{R}||_I \to 0$ or both $||\mathcal{E}|| \to 0$ and $||M^{\mathcal{B}}\tilde{R}||_I \to 0$ as $t \to \infty$. From property (i) and (ii) of Proposition 3.1, $||\mathcal{E}|| \to 0$ indicates that $||M^{\mathcal{B}}\tilde{R}||_I \to 0$ and vice versa. Thus, $\dot{V} \to 0$ implies that $||\mathcal{E}|| \to 0$ and $||M^{\mathcal{B}}\tilde{R}||_I \to 0$, which means that $\tilde{R}$ asymptotically approaches $\mathbf{I}_3$ consistent with property (iii) of Proposition 3.1, which completes the proof.

It is clear that the gains associated with the vex operator of $\dot{\hat{b}}$ and W in (3.26), and (3.27), or in (3.40), and (3.41), respectively, are dynamic. Their values rely on μ, $\mathcal{E}$ and $||\tilde{R}||_I$ or $||M^{\mathcal{B}}\tilde{R}||_I$. Their dynamic behavior has the essential role of forcing the proposed observer to comply with the prescribed performance constraints. Thus, the proposed filter has a remarkable advantage which is reflected in the dynamic gains becoming increasingly aggressive as $||\tilde{R}||_I$ approaches the unstable equilibria $+1$. On the other side, these gains reduce significantly as $\mathcal{E} \to 0$. These dynamic gains directly impact the proposed nonlinear filter forcing it to adhere to the predefined prescribed performance features imposed by the user and thereby satisfying the predefined measures of transient as well as steady-state measures.

Remark 3.4 ***(Notes on filter design parameters)*** *$\bar{\delta}$, $\underline{\delta}$, and ξ_0 define the dynamic boundaries of the transformed error $\mathcal{E}$. ξ_0 and ξ_∞ refer to the boundaries of the large and small sets, respectively. ℓ controls the convergence rate of the dynamic boundaries from large to narrow set. The asymptotic convergence of $||\tilde{R}||_I$ or $||M^{\mathcal{B}}\tilde{R}||_I$ is guaranteed by selecting $\bar{\delta} = \underline{\delta}$. Also, increasing the value of ℓ would lead to faster rate of convergence of $||\tilde{R}||_I$ or $||M^{\mathcal{B}}\tilde{R}||_I$ to the origin. It should be noted that if the initial value of $||\tilde{R}(0)||_I$ or $||M^{\mathcal{B}}\tilde{R}(0)||_I$ are unknown, the user could select $\bar{\delta}$, $\underline{\delta}$, and ξ_0 based on the highest value of $||\tilde{R}(0)||_I$, therefore accounting for the worst possible scenario, since $||\tilde{R}(0)||_I \in [0, 1]$, and thus the prescribed performance is guaranteed.*

The filter design algorithm proposed in Subsection 3.3.2 can be summarized briefly as

A.1 Select $\bar{\delta} = \underline{\delta} > ||M^{\mathcal{B}}\tilde{R}(0)||_I$, the ultimate bound of the small set of the desired steady-state error ξ_∞ and the desired convergence rate ℓ.

A.2 Evaluate the vex operator $\mathbf{vex}\left(\boldsymbol{\mathcal{P}}_a\left(M^{\mathcal{B}}\tilde{R}\right)\right)$, the normalized Euclidean distance error $||M^{\mathcal{B}}\tilde{R}||_I$, and $\boldsymbol{\Upsilon}\left(M^{\mathcal{B}},\tilde{R}\right)$ from (3.36), (3.37), and (3.38), respectively, in the form of vector measurements.

A.3 Evaluate the prescribed performance function ξ from equation (3.16).

A.4 Evaluate $\mu\left(||M^{\mathcal{B}}\tilde{R}||_I,\xi\right)$ and $\mathcal{E}\left(||M^{\mathcal{B}}\tilde{R}||_I,\xi\right)$ from equations (3.23) and (3.22), respectively.

A.5 Evaluate the filter design $\dot{\hat{R}}$, $\dot{\hat{b}}$ and W from (3.39), (3.40), and (3.41), respectively.

A.6 Go to **A.2**.

The same steps can be applied for the filter design in Subsection 3.3.1.

3.4 Simulations

The performance of the two proposed nonlinear attitude filters on $\mathbb{SO}(3)$ with predefined measures is presented in this section considering large error initialization and high level of noise and bias in the measurements. In this regard, consider the set of measurements given as follows:

$$\begin{cases} \mathrm{v}_i^{\mathcal{B}(\mathrm{R})} & = R^\top \mathrm{v}_i^{\mathcal{I}(\mathrm{R})} + \mathrm{b}_i^{\mathcal{B}(\mathrm{R})} + \omega_i^{\mathcal{B}(\mathrm{R})} \\ \Omega_m & = \Omega + b + \omega \end{cases}$$

which exemplifies a set measurements obtained from a low-cost IMUs module, for all $i = 1, 2$. Let the rotational matrix R be acquired from attitude dynamics in equation (3.4) and suppose that the input signal of the angular velocity is given by

$$\Omega = \begin{bmatrix} \sin(0.7t) \\ 0.7\sin(0.5t+\pi) \\ 0.5\sin\left(0.3t+\frac{\pi}{3}\right) \end{bmatrix} (\mathrm{rad/sec})$$

with $R(0) = \mathbf{I}_3$ being the initial attitude. Consider that a wide-band of a zero mean random noise process vector with standard deviation (STD) of $0.2\,(\mathrm{rad/sec})$

and bias $b = 0.1\,[1, -1, 1]^\top$ is contaminating the true angular velocity (Ω) such that $\Omega_m = \Omega + b + \omega$. Let two non-collinear inertial frame vectors be given by $\mathrm{v}_1^{\mathcal{I}(\mathrm{R})} = \frac{1}{\sqrt{3}}\,[1, -1, 1]^\top$ and $\mathrm{v}_2^{\mathcal{I}(\mathrm{R})} = [0, 0, 1]^\top$, whereas the body-frame vectors $\mathrm{v}_1^{\mathcal{B}(\mathrm{R})}$ and $\mathrm{v}_2^{\mathcal{B}(\mathrm{R})}$ are given by $\mathrm{v}_i^{\mathcal{B}(\mathrm{R})} = R^\top \mathrm{v}_i^{\mathcal{I}(\mathrm{R})} + \mathrm{b}_i^{\mathcal{B}(\mathrm{R})} + \omega_i^{\mathcal{B}(\mathrm{R})}$ for all $i = 1, 2$. Similarly, suppose that an additional zero mean Gaussian white noise vector $\omega_i^{\mathcal{B}(\mathrm{R})}$ with STD =0.08 corrupts the body-frame vector measurements with bias components $\omega_1^{\mathcal{B}(\mathrm{R})} = 0.1\,[-1, 1, 0.5]^\top$ and $\omega_2^{\mathcal{B}(\mathrm{R})} = 0.1\,[0, 0, 1]^\top$. $\mathrm{v}_i^{\mathcal{I}(\mathrm{R})}$ and $\mathrm{v}_i^{\mathcal{B}(\mathrm{R})}$ are normalized and the third vector is extracted by $\upsilon_3^{\mathcal{I}(\mathrm{R})} = \upsilon_1^{\mathcal{I}(\mathrm{R})} \times \upsilon_2^{\mathcal{I}(\mathrm{R})}$ and $\upsilon_3^{\mathcal{B}(\mathrm{R})} = \upsilon_1^{\mathcal{B}(\mathrm{R})} \times \upsilon_2^{\mathcal{B}(\mathrm{R})}$. The confidence level of body-frame measurements was chosen as $s_1 = 1.4$, $s_2 = 1.4$, and $s_3 = 0.2$. For the semi-direct filter in Subsection 3.3.1, the corrupted reconstructed attitude R_y is defined using SVD in Appendix B or see the Appendix in Hashim et al. (2018b); Hashim, Brown, and McIsaac (2019d) where $\tilde{R} = R_y^\top \hat{R}$.

To illustrate the robustness of the proposed filtering algorithms, a very large initial attitude error is considered. The initial rotation of the attitude estimate is defined in accordance with angle-axis parameterization in (2.7) as $\hat{R}(0) = \mathcal{R}_\alpha(\alpha, u/||u||)$ with $\alpha = 178\,(\mathrm{deg})$ and $u = [4, 1, 5]^\top$. As such, $||\tilde{R}||_I \approx 0.9999$ which is very close to the unstable equilibria. Initial bias estimate is $\hat{b}(0) = [0, 0, 0]^\top$. The design parameters are chosen as $\gamma = 1$, $k_w = 3$, $\bar{\delta} = \underline{\delta} = 1.2$, $\xi_0 = 1.2$, $\xi_\infty = 0.05$, and $\ell = 3$. The total time of the simulation is 15 seconds.

The color notation is as follows: green color represents a true value, red depicts the performance of the nonlinear semi-direct filter on $\mathbb{SO}(3)$ derived using a group of vectorial measurements and reconstructed attitude as described in Subsection 3.3.1, and blue demonstrates the performance of the direct filter characterized in Subsection 3.3.2 which does not demand attitude reconstruction. Also, magenta describes a measured value while orange and purple refer to prescribed performance response.

Figure 3.3 and 3.4 illustrate high values of noise and bias components present in angular velocity and body-frame vector measurements plotted against the true values. Figure 3.5 illustrates the systematic and smooth convergence of the normalized Euclidean distance error $||\tilde{R}||_I$. It can be noticed in Figure 3.5 that the error function for $||\tilde{R}||_I = \frac{1}{4}\mathrm{Tr}\left\{\mathbf{I}_3 - R^\top \hat{R}\right\}$ started very near to the unstable equilibria within a given large set and ended within a given small residual set obeying the PPF. Thus, Figure 3.5 confirms the stability analysis discussed in the previous section and illus-

trates the robustness of the proposed filter. The output performance of the proposed filters in Euler angles representation is shown in Figure 3.6. The three Euler angles (ϕ, θ, ψ) in Figure 3.6 show impressive tracking performance with fast convergence to the true angles. Finally, the boundedness of the estimated bias $\hat{b}$ is illustrated in Figure 3.7.

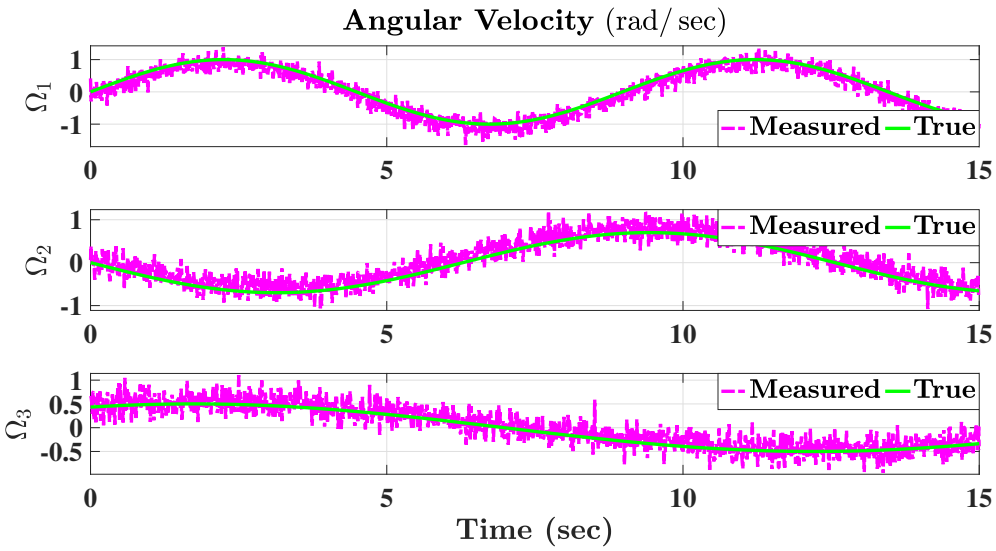

Figure 3.3: True and measured angular velocities.

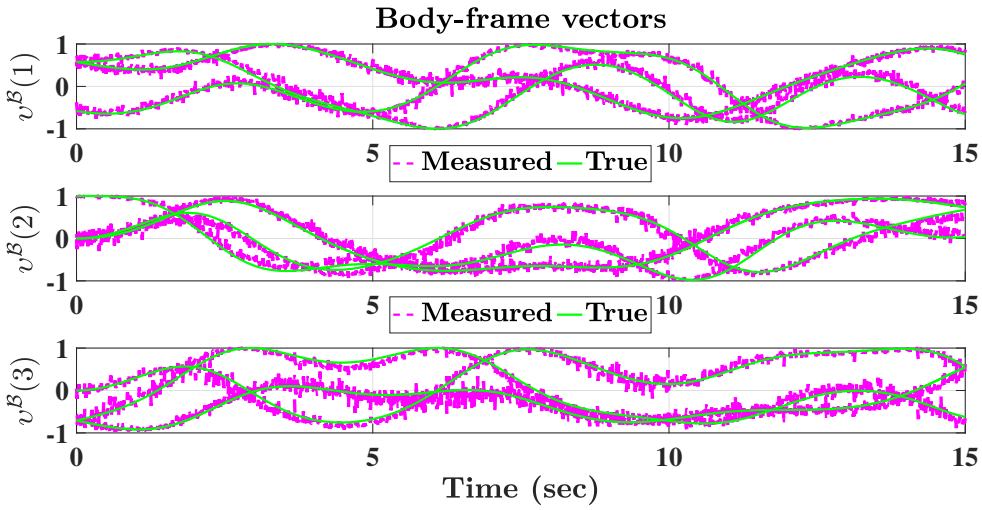

Figure 3.4: Body-frame vectorial measurements: true and measured.

Table 3.1 contains a synopsis of statistical details of the mean and the STD of the error $(||\tilde{R}||_I)$. These details facilitate the comparison of the steady-state performance

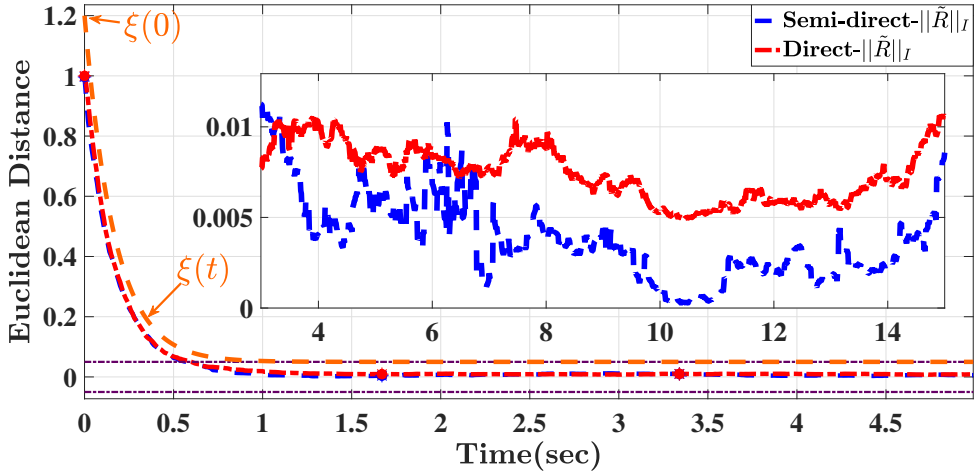

Figure 3.5: Transient and steady-state performance of normalized Euclidean distance.

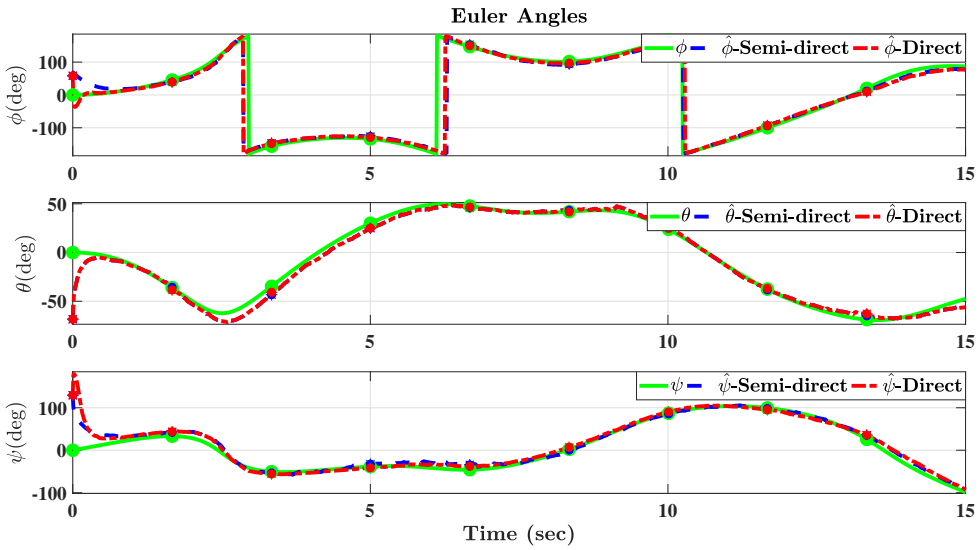

Figure 3.6: Tracking performance of Euler angles (roll (ϕ) and pitch (θ), yaw (ψ)).

of the two filters proposed in this paper with respect to $||\tilde{R}||_I$. In spite of the fact that both filters have extremely small mean of $||\tilde{R}||_I$, the semi-direct attitude filter with prescribed performance showed a remarkably smaller mean errors and STD when compared to the direct attitude filter with prescribed performance. Numerical results outlined in Table 3.1 demonstrate effectiveness and robustness of the proposed nonlinear attitude filters against large error initialization and uncertainties in sensor

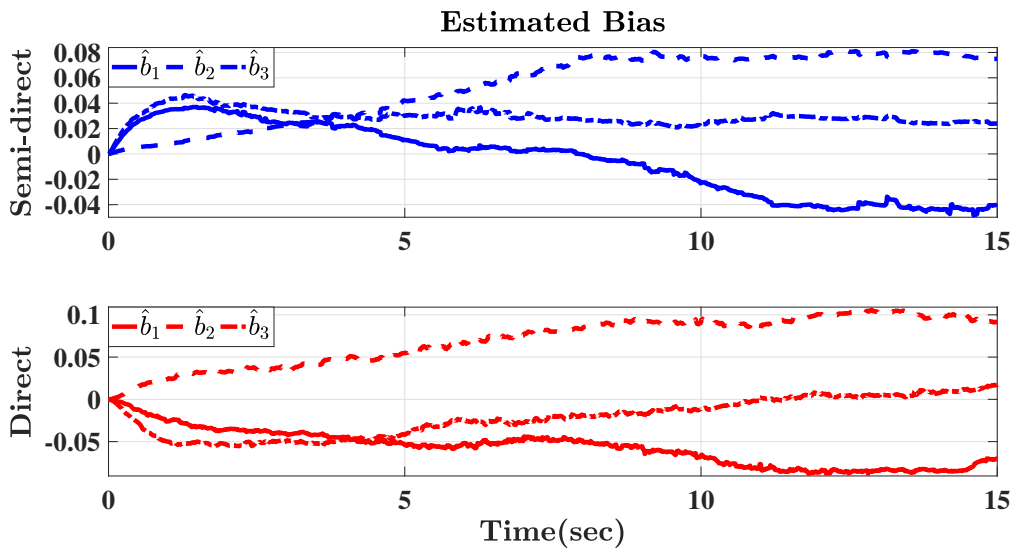

Figure 3.7: The estimated bias of the proposed filters.

measurements as illustrated in Figure 3.3, 3.4, 3.5, 3.6, and 3.7.

Table 3.1: Statistical analysis of $||\tilde{R}||_I$ of the proposed two filters.

Output data of $||\tilde{R}||_I$ over the period (1-15 sec)		
Filter	Semi-direct	Direct
Mean	4.2×10^{-3}	6.9×10^{-3}
STD	2.5×10^{-3}	2.1×10^{-3}

The robustness and the superior convergence properties of the proposed nonlinear attitude filters with guaranteed performance are presented and compared to a well-known nonlinear attitude complimentary filter termed nonlinear passive complementary filter Mahony et al. (2008) as well as to a standard attitude filter which belongs to the family of Gaussian attitude filters and is termed multiplicative extended Kalman filter (MEKF) Markley (2003) in Subsection 3.4.1 and 3.4.2, respectively.

3.4.1 Proposed Filters vs Nonlinear Attitude Filters

To further illustrate the robustness and the superior convergence properties of the proposed nonlinear attitude filters as opposed to the conventional nonlinear attitude

filters, a fair comparison is presented. Consider the following nonlinear passive complementary filter given in Mahony et al. (2008)

$$\begin{cases} \dot{\hat{R}} & = \hat{R}\left[\Omega_m - \hat{b} - W\right]_\times, \quad \hat{R}(0) = \hat{R}_0 \\ \dot{\hat{b}} & = k_1 \mathbf{vex}\left(\boldsymbol{\mathcal{P}}_a\left(\tilde{R}\right)\right), \quad \hat{b}(0) = \hat{b}_0, \tilde{R} = R_y^\top \hat{R} \\ W & = k_1 \mathbf{vex}\left(\boldsymbol{\mathcal{P}}_a\left(\tilde{R}\right)\right), \tilde{R} = R_y^\top \hat{R} \end{cases} \tag{3.52}$$

where $k_1 > 0$. A fair comparison between the proposed semi-direct attitude filter and the nonlinear passive complementary filter in Mahony et al. (2008) is attainable due to the shared structure of the filters. Consider initializing the nonlinear passive complementary filter analogously to the semi-direct attitude filter given at the beginning of the Simulation Section. To ensure validity of the comparison, three variations of the design parameter k_1 in (3.52) namely, $k_1 = 1$, $k_1 = 10$ and $k_1 = 100$. In this Subsection, the color notation is as follows: black solid and dashed lines

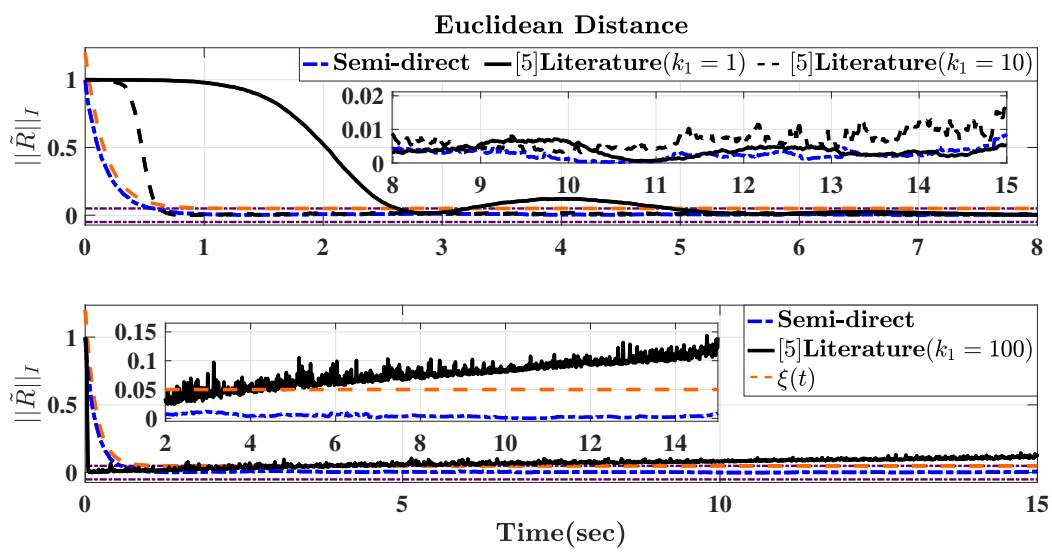

Figure 3.8: Transient and steady-state performance of normalized Euclidean distance: Semi-direct filter vs literature Mahony et al. (2008).

describe the performance of the nonlinear passive complementary filter, blue center line depicts the proposed semi-direct attitude filter while orange and purple refer to the prescribed performance response. It can be noticed in the upper portion of Figure 3.8 that smaller value of k_1 results in slower transient performance with less oscillatory behavior in the steady-state. In contrast, the lower portion of Figure 3.8

illustrates that higher value of k_1 leads to faster transient performance with higher levels of oscillation in the steady-state. Moreover, Figure 3.8 shows that the predefined measure of transient performance cannot be achieved for low value of k_1, since the transient performance of the passive complementary filter violates the dynamic reducing boundaries. In the same spirit, the predefined characteristics of steady-state performance cannot be achieved for high value of k_1. These results confirm Remark 3.1.

Therefore, the nonlinear attitude filters given in the literature, for example Grip et al. (2012); Hamel and Mahony (2006); Lee (2012); Mahony et al. (2005, 2008); Zlotnik and Forbes (2017) cannot guarantee a predefined measure of convergence properties. The semi-direct attitude filter, on the other side, obeys the dynamically reducing boundaries and allows to achieve a desired level of prescribed performance.

Table 3.2 compares the statistical details, namely the mean and the STD of $||\tilde{R}||_I$, of the proposed semi-direct attitude filter and the nonlinear passive complementary filter. The above-mentioned statistics describe the output performance with respect to $||\tilde{R}||_I$ over the steady-state period of time depicted in Figure 3.8. The semi-direct attitude filter displays smaller values of mean and STD of $||\tilde{R}||_I$ when compared to the passive complementary filter for all the considered cases of $k_1 = 1$, $k_1 = 10$ and $k_1 = 100$. Moreover, the numerical results listed in Table 3.2 illustrate the effectiveness and robustness of the proposed nonlinear attitude filters against large error initialization and uncertainties in sensor measurements which make them a good fit for measurements obtained from low-cost IMUs modules.

Table 3.2: Statistical analysis of $||\tilde{R}||_I$ of the semi-direct filter vs literature.

Output data of $\|\|\tilde{R}\|\|_I$ over the period (7-15 sec)				
Filter	Semi-direct	Passive Filter Mahony et al. (2008)		
		$k_1 = 1$	$k_1 = 10$	$k_1 = 100$
Mean	2.7×10^{-3}	4.5×10^{-3}	6.9×10^{-3}	91.9×10^{-3}
STD	1.4×10^{-3}	2.9×10^{-3}	2.7×10^{-3}	14.2×10^{-3}

3.4.2 Proposed Filters vs Gaussian Attitude Filters

In this subsection the effectiveness and the high convergence capabilities of the proposed nonlinear attitude filters are compared to the performance of a Gaussian attitude filter. A comparison between the proposed direct attitude filter and the MEKF in Appendix C (Hashim, Brown, and McIsaac (2019a)) is presented. Consider the MEKF in Appendix C (Hashim, Brown, and McIsaac (2019a)) initialized similar to the direct attitude filter given at the beginning of the Simulation Section. To guarantee validity of the comparison, three cases of the design parameters of MEKF have been detailed in Table 3.3.

Table 3.3: MEKF design parameters.

Case	Design Parameters		
Case 1	$\bar{\mathcal{Q}}_{v(i)} = \mathbf{I}_3$	$\bar{\mathcal{Q}}_{\omega} = \mathbf{I}_3$	$\bar{\mathcal{Q}}_{b} = \mathbf{I}_3$
Case 2	$\bar{\mathcal{Q}}_{v(i)} = 0.1\mathbf{I}_3$	$\bar{\mathcal{Q}}_{\omega} = 10\mathbf{I}_3$	$\bar{\mathcal{Q}}_{b} = 10\mathbf{I}_3$
Case 3	$\bar{\mathcal{Q}}_{v(i)} = 0.01\mathbf{I}_3$	$\bar{\mathcal{Q}}_{\omega} = 100\mathbf{I}_3$	$\bar{\mathcal{Q}}_{b} = 100\mathbf{I}_3$

In this Subsection, the color notation is as follows: black solid and dashed lines represent the performance of the MEKF, blue center line refers to the proposed direct attitude filter while orange and purple depict the prescribed performance response. It can be noticed in the upper portion of Figure 3.9 that cases 1 and 2 show slower transient performance with less oscillatory behavior in the steady-state. In contrast, the lower portion of Figure 3.9 illustrates that case 3 results in faster transient performance with higher levels of oscillation in the steady-state. As such, a desired measure of transient and stead-state error cannot be guaranteed in case of MEKF. The direct attitude filter, on the other side, follows the dynamically reducing boundaries achieving a desired level of prescribed performance set by the user.

The simulation results presented in this section validate the stable performance and robustness of the two proposed filters against uncertain measurements and large initialized errors. The two filters comply with the constraints imposed by the user indicating guaranteed prescribed performance measures in transient as well as steady-state performance. This remarkable advantage was not offered in other nonlinear deterministic attitude filters such as Grip et al. (2012); Hamel and Mahony (2006);

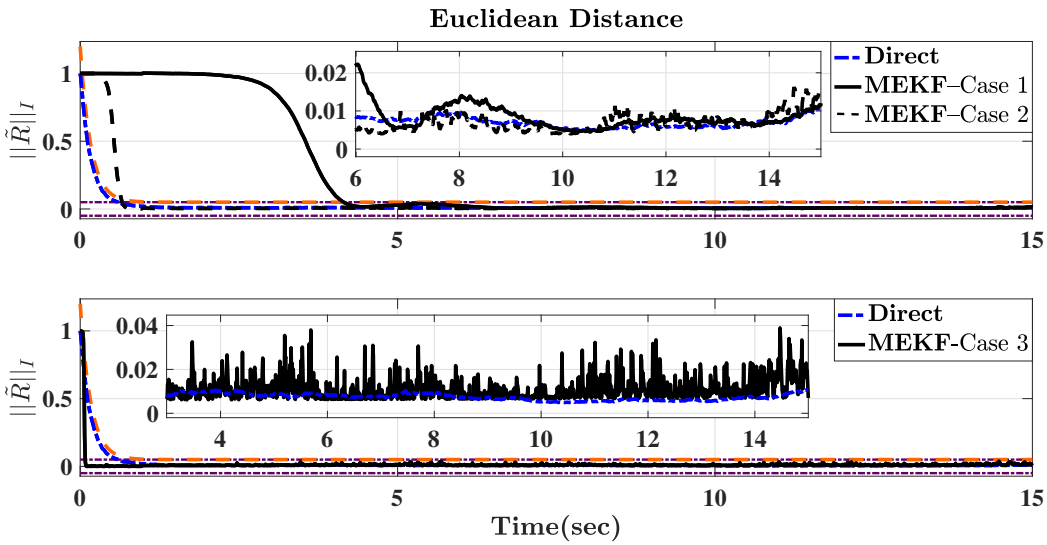

Figure 3.9: Transient and steady-state performance of normalized Euclidean distance: Direct filter vs MEKF Markley (2003).

Hashim et al. (2018a, 2018b); Lee (2012); Mahony et al. (2005, 2008) as well as Gaussian attitude filters such as Choukroun et al. (2006); Lefferts et al. (1982); Markley (2003). Semi-direct attitude filter with prescribed performance requires attitude reconstruction, for instance in our case we employed Singular Value Decomposition (SVD) Appendix B, or visit (Hashim et al. (2018b)), to obtain $\tilde{R} = R_y^\top \hat{R}$. This adds complexity, and therefore the semi-direct attitude filter requires more computational power in comparison with direct attitude filter with prescribed performance. However, both proposed filters showed remarkable convergence as detailed in Table 3.1.

3.5 Conclusion

In this chapter, two nonlinear attitude filters with prescribed performance characteristics have been considered. The filters are evolved directly on $\mathbb{SO}(3)$. Attitude error has been defined in terms of normalized Euclidean distance such that innovation term has been selected to ensure predefined characteristics of transient and steady-state performance. Consequently, the proposed filters achieve superior convergence properties with transient error being less than a predefined dynamic decreasing constrained

function and steady-state error being confined by a known lower bound. The constrained error is transformed to its unconstrained form which is sufficient to solve the attitude problem in prescribed performance sense. The filters are deterministic while the stability analysis ensure boundedness of all closed loop signals with asymptotic convergence of the normalized Euclidean distance of attitude error to the origin. Simulation example illustrated the robustness of the proposed filters in their response to the predefined constraints in case when high level of uncertainties is present in the measurements and a large initial attitude error is observed.

Chapter 4
Nonlinear Stochastic Filters on $\mathbb{SO}(3)$: Ito and Stratonovich

4.1 Introduction

This chapter formulates the attitude filtering problem as a nonlinear stochastic filter problem evolved directly on the Special Orthogonal Group $\mathbb{SO}(3)$. One of the traditional potential functions for nonlinear deterministic complimentary filters is studied and examined against angular velocity measurements corrupted with noise. This work demonstrates that the careful selection of the attitude potential function allows to attenuate the noise associated with the angular velocity measurements and results into superior convergence properties of estimator and correction factor. The problem is formulated as a stochastic problem through mapping $\mathbb{SO}(3)$ to Rodriguez vector parameterization. Two nonlinear stochastic complimentary filters are developed on $\mathbb{SO}(3)$. The first stochastic filter is driven in the sense of Ito and the second one considers Stratonovich. The two proposed filters guarantee that errors in the Rodriguez vector and estimates are semi-globally uniformly ultimately bounded in mean square, and they converge to a small neighborhood of the origin. Simulation results are presented to illustrate the effectiveness of the proposed filters considering high level of uncertainties in angular velocity as well as body-frame vector measurements. The results of this chapter were first published in Hashim et al. (2018b).

The rest of the chapter is organized as follows: Attitude estimation dynamic problem in Rodriguez vector with Gaussian noise vector which satisfies the Brownian motion process is formulated in Section 4.2. The nonlinear stochastic filters on $\mathbb{SO}(3)$ and the stability analysis are presented in Section 4.3. Section 4.4 shows the output performance and discusses the simulation results of the proposed filters. Finally, Section 4.5 draws a conclusion of this work.

4.2 Problem Formulation in Stochastic Sense

Let $R \in \mathbb{SO}(3)$ denote the attitude (rotational) matrix, which describes the relative orientation of the body-frame $\{\mathcal{B}\}$ with respect to the inertial-frame $\{\mathcal{I}\}$ as given in Figure 4.1.

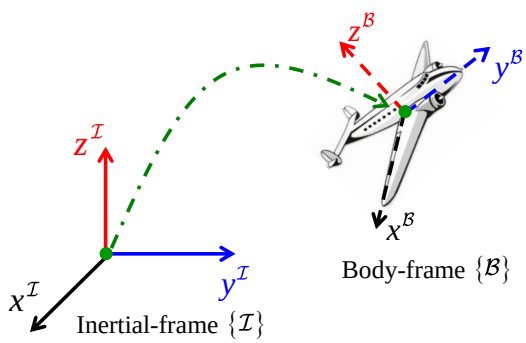

Figure 4.1: The orientation of a 3D rigid-body in body-frame relative to inertial-frame.

The attitude can be extracted from n-known non-collinear inertial vectors which are measured in a coordinate system fixed to the rigid body. Let $\mathrm{v}_i^{\mathcal{B}(\mathrm{R})} \in \mathbb{R}^3$ for $i = 1, 2, \ldots, n$, be vectors measured in the body-fixed frame. Let $R \in \mathbb{SO}(3)$, the body fixed-frame vector $\mathrm{v}_i^{\mathcal{B}(\mathrm{R})} \in \mathbb{R}^3$ is defined by

$$\mathrm{v}_i^{\mathcal{B}(\mathrm{R})} = R^\top \mathrm{v}_i^{\mathcal{I}(\mathrm{R})} + \mathrm{b}_i^{\mathcal{B}(\mathrm{R})} + \omega_i^{\mathcal{B}(\mathrm{R})} \tag{4.1}$$

where $\mathrm{v}_i^{\mathcal{I}(\mathrm{R})} \in \mathbb{R}^3$ denotes the inertial fixed-frame vector for $i = 1, 2, \ldots, n$. $\mathrm{b}_i^{\mathcal{B}(\mathrm{R})}$ and $\omega_i^{\mathcal{B}(\mathrm{R})}$ denote the additive bias and noise components of the associated body-frame vector, respectively, for all $\mathrm{b}_i^{\mathcal{B}(\mathrm{R})}, \omega_i^{\mathcal{B}(\mathrm{R})} \in \mathbb{R}^3$. The assumption that $n \geq 2$ is necessary for instantaneous three-dimensional attitude determination. In case when $n = 2$, the cross product of the two measured vectors can be accounted as the third vector measurement such that $\mathrm{v}_3^{\mathcal{I}(\mathrm{R})} = \mathrm{v}_1^{\mathcal{I}(\mathrm{R})} \times \mathrm{v}_2^{\mathcal{I}(\mathrm{R})}$ and $\mathrm{v}_3^{\mathcal{B}(\mathrm{R})} = \mathrm{v}_1^{\mathcal{B}(\mathrm{R})} \times \mathrm{v}_2^{\mathcal{B}(\mathrm{R})}$. It is common to employ the normalized values of inertial and body-frame vectors in the process of attitude estimation such as

$$\upsilon_i^{\mathcal{I}(\mathrm{R})} = \frac{\mathrm{v}_i^{\mathcal{I}(\mathrm{R})}}{\left\|\mathrm{v}_i^{\mathcal{I}(\mathrm{R})}\right\|}, \quad \upsilon_i^{\mathcal{B}(\mathrm{R})} = \frac{\mathrm{v}_i^{\mathcal{B}(\mathrm{R})}}{\left\|\mathrm{v}_i^{\mathcal{B}(\mathrm{R})}\right\|} \tag{4.2}$$

In this manner, the attitude can be defined knowing $\upsilon_i^{\mathcal{I}(\mathrm{R})}$ and $\upsilon_i^{\mathcal{B}(\mathrm{R})}$. Gyroscope or the rate gyros measures the angular velocity vector in the body-frame relative to the inertial-frame. The measurement vector of angular velocity $\Omega_m \in \mathbb{R}^3$ is

$$\Omega_m = \Omega + b + \omega \tag{4.3}$$

where $\Omega \in \mathbb{R}^3$ denotes the true value of angular velocity, b denotes an unknown constant (bias) or slowly time-varying vector, while ω denotes the noise component associated with angular velocity measurements, for all $b, \omega \in \mathbb{R}^3$. The noise vector ω is assumed to be Gaussian. The true attitude dynamics and the associated Rodriguez vector dynamics are given in (4.4) and (4.5), respectively, as

$$\dot{R} = R\,[\Omega]_\times \tag{4.4}$$

$$\dot{\rho} = \frac{1}{2}\left(\mathbf{I}_3 + [\rho]_\times + \rho\rho^\top\right)\Omega \tag{4.5}$$

In general, the measurement of angular velocity vector is subject to additive noise and bias components. These components are characterized by randomness and unknown behavior. In view of the fact that any unknown components in angular velocity measurements may impair the estimation process of the true attitude dynamics in (4.4) or (4.5), it is necessary to assume that the attitude dynamics are excited by a wide-band of random Gaussian noise process with zero mean. Combining angular velocity measurement in (4.3) and the attitude dynamics in (4.5), the attitude dynamics can be expressed as follows

$$\dot{\rho} = \frac{1}{2}\left(\mathbf{I}_3 + [\rho]_\times + \rho\rho^\top\right)(\Omega_m - b - \omega) \tag{4.6}$$

where $\omega \in \mathbb{R}^3$ is a bounded continuous Gaussian random noise vector with zero mean. The fact that derivative of any Gaussian process yields Gaussian process allows us to write the stochastic attitude dynamics as a function of Brownian motion process vector $d\beta/dt \in \mathbb{R}^3$ (Jazwinski (2007); Khasminskii (1980)). Let $\{\omega, t \geq t_0\}$ be a vector process of independent Brownian motion process such that

$$\omega = \mathcal{Q}\frac{d\beta}{dt} \tag{4.7}$$

where $\mathcal{Q} \in \mathbb{R}^{3\times 3}$ is an unknown time-variant matrix with only nonzero and nonnega-

tive bounded components in the diagonal. The covariance component associated with the noise ω can be defined by $\mathcal{Q}^2 = \mathcal{Q}\mathcal{Q}^\top$. The properties of Brownian motion process are defined as (Deng, Krstic, and Williams (2001); Ito and Rao (1984); Jazwinski (2007))

$$\mathbb{P}\left\{\beta\left(0\right)=0\right\}=1, \quad \mathbb{E}\left[d\beta/dt\right]=0, \quad \mathbb{E}\left[\beta\right]=0$$

Let the attitude dynamics of Rodriguez vector in (4.5) be defined in the sense of Ito (Ito and Rao (1984)). Considering the attitude dynamics in (4.6) and substituting ω by $\mathcal{Q}d\beta/dt$ as in (4.7), the stochastic differential equation of (4.5) in view of (4.6) can be expressed by

$$d\rho = f\left(\rho, b\right)dt + g\left(\rho\right)\mathcal{Q}d\beta \tag{4.8}$$

Similarly, the stochastic dynamics of (4.4) become

$$dR = R\left[\Omega_m - b\right]_\times dt - R\left[\mathcal{Q}d\beta\right]_\times \tag{4.9}$$

where b was defined in (4.3), $g\left(\rho\right) := -\frac{1}{2}\left(\mathbf{I}_3 + \left[\rho\right]_\times + \rho\rho^\top\right)$ and $f\left(\rho, b\right) := -g\left(\rho\right)\left(\Omega_m - b\right)$ with $g : \mathbb{R}^3 \to \mathbb{R}^{3\times 3}$ and $f : \mathbb{R}^3 \times \mathbb{R}^3 \to \mathbb{R}^3$. $g\left(\rho\right)$ is locally Lipschitz in ρ, and $f\left(\rho, b\right)$ is locally Lipschitz in ρ and b. Accordingly, the dynamic system in (4.8) has a solution for $t \in \left[t_0, T\right] \forall t_0 \leq T < \infty$ in the mean square sense and for any $\rho\left(t\right) \in \mathbb{R}^3$ such that $t \neq t_0$, $\rho - \rho_0$ is independent of $\left\{\beta\left(\tau\right), \tau \geq t\right\}, \forall t \in \left[t_0, T\right]$ (Theorem 4.5 Jazwinski (2007)). Now the aim is to achieve adaptive stabilization of an unknown bias and unknown time-variant covariance matrix. Let σ be the upper bound of $\mathcal{Q}^2$ such that

$$\sigma = \left[\max\left\{\mathcal{Q}^2_{1,1}\right\}, \max\left\{\mathcal{Q}^2_{2,2}\right\}, \max\left\{\mathcal{Q}^2_{3,3}\right\}\right]^\top \in \mathbb{R}^3 \tag{4.10}$$

where $\max\left\{\cdot\right\}$ is the maximum value of an element.

Assumption 4.1 *(Uniform boundedness of unknown parameters b and σ) Let the vector b and the nonnegative vector σ belong to a given compact set Δ where $b, \sigma \in \Delta \subset \mathbb{R}^3$, and b and σ are upper bounded by a scalar Γ such that $\|\Delta\| \leq \Gamma < \infty$.*

Definition 4.1 *Consider the stochastic differential system in (4.8). For a given func-*

tion $V(\rho) \in \mathcal{C}^2$, the differential operator $\mathcal{L}V$ is given by

$$\mathcal{L}V(\rho) = V_\rho^\top f(\rho, b) + \frac{1}{2}\mathrm{Tr}\left\{g(\rho)\,\mathcal{Q}^2 g^\top(\rho)\,V_{\rho\rho}\right\}$$

such that $V_\rho = \partial V/\partial\rho$, and $V_{\rho\rho} = \partial^2 V/\partial\rho^2$.

Definition 4.2 *(Ji and Xi (2006)) The trajectory ρ of the stochastic differential system in (4.8) is said to be semi-globally uniformly ultimately bounded (SGUUB) if for some compact set $\Lambda \in \mathbb{R}^3$ and any $\rho_0 = \rho(t_0)$, there exists a constant $\kappa > 0$, and a time constant $T = T(\kappa, \rho_0)$ such that $\mathbb{E}[\|\rho\|] < \kappa, \forall t > t_0 + T$.*

Lemma 4.1 *(Deng and Krsti (1997); Deng et al. (2001)) Let the dynamic system in (4.8) be assigned a potential function $V \in \mathcal{C}^2$ such that $V : \mathbb{R}^3 \to \mathbb{R}_+$, class $\mathcal{K}_\infty$ function $\bar{\alpha}_1(\cdot)$ and $\bar{\alpha}_2(\cdot)$, constants $c_1 > 0$ and $c_2 \geq 0$ and a nonnegative function $\mathbf{Z}(\|\rho\|)$ such that*

$$\bar{\alpha}_1(\|\rho\|) \leq V(\rho) \leq \bar{\alpha}_2(\|\rho\|) \tag{4.11}$$

$$\begin{aligned}\mathcal{L}V(\rho) =& V_\rho^\top f(\rho, b) + \frac{1}{2}\mathrm{Tr}\left\{g(\rho)\,\mathcal{Q}^2 g^\top(\rho)\,V_{\rho\rho}\right\} \\ \leq& -c_1\mathbf{Z}(\|\rho\|) + c_2\end{aligned} \tag{4.12}$$

then for $\rho_0 \in \mathbb{R}^3$, there exists almost a unique strong solution on $[0, \infty)$ for the dynamic system in (4.8), the solution ρ is bounded in probability such that

$$\mathbb{E}[V(\rho)] \leq V(\rho_0)\exp(-c_1 t) + \frac{c_2}{c_1} \tag{4.13}$$

Furthermore, if the inequality in (4.13) holds, then ρ in (4.8) is SGUUB in the mean square. In addition, when $c_2 = 0$, $f(0, b) = \underline{\mathbf{0}}_3$, $g(0) = \mathbf{0}_{3\times 3}$, and $\mathbf{Z}(\|\rho\|)$ is continuous, the equilibrium point $\rho = 0$ is globally asymptotically stable in probability and the solution of ρ satisfies

$$\mathbb{P}\left\{\lim_{t\to\infty}\mathbf{Z}(\|\rho\|) = 0\right\} = 1, \quad \forall\rho_0 \in \mathbb{R}^3 \tag{4.14}$$

The proof of this lemma and existence of a unique solution can be found in Deng et al. (2001). For a rotation matrix $R \in \mathbb{SO}(3)$, let us define $\mathcal{U} \subseteq \mathbb{SO}(3)$ by $\mathcal{U} :=$

$\{R|\operatorname{Tr}\{R\} = -1, \boldsymbol{\mathcal{P}}_a(R) = 0\}$. We have $-1 \leq \operatorname{Tr}\{R\} \leq 3$ such that the set $\mathcal{U}$ is forward invariant and unstable for the dynamic system in (4.4) which implies that $\rho = \infty$. For almost any initial condition such that $R_0 \notin \mathcal{U}$ or $\rho_0 \in \mathbb{R}^3$, we have $-1 < \operatorname{Tr}\{R_0\} \leq 3$ and the trajectory of ρ is semi-globally uniformly ultimately bounded in mean square.

Lemma 4.2 *(Young's inequality) Let x and y be $x, y \in \mathbb{R}^n$. Then, for any $c > 1$ and $d > 1$ satisfying $(c-1)(d-1) = 1$ with a small positive constant ε, the following holds*

$$x^\top y \leq (1/c)\,\varepsilon^c \|x\|^c + (1/d)\,\varepsilon^{-d} \|y\|^d \tag{4.15}$$

In the next section, the presence of noise will be examined in light of a traditional form of potential function. The concept of an alternate potential function with specific characteristics able to attenuate the noise behavior will be carefully elucidated.

4.3 Stochastic Complementary Filters On $\mathbb{SO}(3)$

The main goal of attitude estimation is to derive the attitude estimate $\hat{R} \to R$. Let's define the error in attitude estimate from the body-frame to estimator-frame by

$$\tilde{R} = R^\top \hat{R} \tag{4.16}$$

Let $\hat{b}$ and $\hat{\sigma}$ be estimates of unknown parameters b and σ, respectively. Define the error in vector b and σ by

$$\tilde{b} = b - \hat{b} \tag{4.17}$$

$$\tilde{\sigma} = \sigma - \hat{\sigma} \tag{4.18}$$

Thus, driving $\hat{R} \to R$ ensures that $\tilde{R} \to \mathbf{I}_3$ and $\tilde{\rho} \to \underline{\mathbf{0}}_3$ where $\tilde{\rho}$ is Rodriguez error vector associated with $\tilde{R}$. In this section, two nonlinear stochastic complementary filters are developed on the Special Orthogonal Group $\mathbb{SO}(3)$. These filters in the sense of Rodriguez vector guarantee that the error vector is SGUUB in mean square for the case of noise contamination of the angular velocity measurements.

4.3.1 Nonlinear Deterministic Attitude Filter

In this subsection, we aim to study the behavior of nonlinear deterministic filter on $\mathbb{SO}(3)$ with noise introduced in angular velocity measurements. The attitude R can be reconstructed through a set of measurements in (4.2) to obtain R_y, for instance (Black (1964); Markley (1988); Shuster and Oh (1981)). R_y is corrupted with noise and bias greatly increase the difference between R_y and the true R. The filter design aims to use the angular velocity measurements and the given R_y to obtain good estimate of R. Consider the following filter design

$$\dot{\hat{R}} = \hat{R}\left[\Omega_m - \hat{b} - W\right]_\times, \quad \hat{R}(0) = \hat{R}_0 \tag{4.19}$$

$$\dot{\hat{b}} = \gamma_1 \boldsymbol{\Upsilon}_a(\tilde{R}), \quad \hat{b}(0) = \hat{b}_0, \tilde{R} = R_y^\top \hat{R} \tag{4.20}$$

$$W = k_1 \boldsymbol{\Upsilon}_a(\tilde{R}), \quad \tilde{R} = R_y^\top \hat{R} \tag{4.21}$$

where Ω_m is angular velocity measurement, $\hat{b} \in \mathbb{R}^3$ is the estimate of the unknown bias b, and $\boldsymbol{\Upsilon}_a(\tilde{R}) = \mathbf{vex}\left(\boldsymbol{\mathcal{P}}_a(\tilde{R})\right)$ was given in (A.4). Also, $\gamma_1 > 0$ is an adaptation gain and k_1 is a positive constant.

Let the error in vector b be defined as in (4.17) and assume that no noise was introduced to the dynamics ($\omega = \underline{\mathbf{0}}_3$). The derivative of attitude error in (4.16) can be obtained from (4.4) and (4.19) as

$$\dot{\tilde{R}} = \tilde{R}\left[\Omega - \tilde{R}^\top \Omega + \tilde{b} - W\right]_\times \tag{4.22}$$

where $\left[\tilde{R}^\top \Omega\right]_\times = \tilde{R}^\top [\Omega]_\times \tilde{R}$. Hence, in view of (4.9) and (4.8), the error dynamic in (4.22) can be expressed in Rodriguez error vector dynamic by

$$\dot{\tilde{\rho}} = \frac{1}{2}\left(\mathbf{I}_3 + [\tilde{\rho}]_\times + \tilde{\rho}\tilde{\rho}^\top\right)\left(\Omega - \tilde{R}^\top \Omega + \tilde{b} - W\right) \tag{4.23}$$

From literature, one of traditional potential functions for adaptive filter estimation is $V\left(\tilde{R}, \tilde{b}\right) = \frac{1}{4}\mathrm{Tr}\left\{\mathbf{I}_3 - \tilde{R}\right\} + \frac{1}{2\gamma_1}\tilde{b}^\top \tilde{b}$ (for example (Crassidis et al. (2007); Mahony et al. (2008))). The equivalent of the aforementioned function in form of Rodriguez

error is

$$V\left(\tilde{\rho},\tilde{b}\right)=\frac{\|\tilde{\rho}\|^2}{1+\|\tilde{\rho}\|^2}+\frac{1}{2\gamma_1}\tilde{b}^\top\tilde{b} \tag{4.24}$$

let $\tilde{f}:=\frac{1}{2}\left(\mathbf{I}_3+[\tilde{\rho}]_\times+\tilde{\rho}\tilde{\rho}^\top\right)\left(\Omega-\tilde{R}^\top\Omega+\tilde{b}-W\right)$. For $V:=V\left(\tilde{\rho},\tilde{b}\right)$, the derivative of (4.24) is

$$\begin{aligned}\dot{V}&=V_{\tilde{\rho}}^\top\tilde{f}-\frac{1}{\gamma_1}\tilde{b}^\top\dot{\tilde{b}}\\&=\boldsymbol{\Upsilon}_a(\tilde{R})^\top\left(\tilde{b}-W\right)-\frac{1}{\gamma_1}\tilde{b}^\top\dot{\tilde{b}}\end{aligned} \tag{4.25}$$

where $\frac{1}{2}V_{\tilde{\rho}}^\top\left(\mathbf{I}_3+[\tilde{\rho}]_\times+\tilde{\rho}\tilde{\rho}^\top\right)\left(\Omega-\tilde{R}^\top\Omega\right)=0$, see Appendix C, which was obtained by substitution of $\tilde{R}=\mathcal{R}_{\tilde{\rho}}(\tilde{\rho})$ in (A.1). Substituting for $\dot{\tilde{b}}$ and W in (4.20) and (4.21), respectively, yields

$$\dot{V}=-k_1\left\|\boldsymbol{\Upsilon}_a(\tilde{R})\right\|^2=-4k_1\frac{\|\tilde{\rho}\|^2}{\left(1+\|\tilde{\rho}\|^2\right)^2} \tag{4.26}$$

Lyapunov's direct method ensures that for $\mathrm{Tr}\left\{\tilde{R}_0\right\}\neq-1$, $\boldsymbol{\Upsilon}_a(\tilde{R})$ converges asymptotically to zero. As such, $(\mathbf{I}_3,\underline{\mathbf{0}}_3)$ is an isolated equilibrium point and $\left(\tilde{R},\tilde{b}\right)\to(\mathbf{I}_3,\underline{\mathbf{0}}_3)$ for $\omega=\underline{\mathbf{0}}_3$ (Mahony et al. (2008)). If angular velocity measurements (Ω_m) are contaminated with noise $(\omega\neq\underline{\mathbf{0}}_3)$, it is more convenient to represent the differential operator in (4.25) in the form of Definition 4.1. Hence, the following extra term will appear

$$\frac{1}{2}\mathrm{Tr}\left\{\tilde{g}^\top V_{\tilde{\rho}\tilde{\rho}}\tilde{g}\mathcal{Q}^2\right\}=\frac{1}{4\left(1+\|\tilde{\rho}\|^2\right)}\mathrm{Tr}\left\{\left(\mathbf{I}_3-3\tilde{\rho}\tilde{\rho}^\top\right)\mathcal{Q}^2\right\}$$

In this case, the operator $\mathcal{L}V(0,0)=\frac{1}{4}\mathrm{Tr}\left\{\mathcal{Q}^2\right\}$ which implies that the significant impact of covariance matrix $\mathcal{Q}^2$ cannot be lessened. One way to attenuate the noise associated with the angular velocity measurements is to chose a potential function in the sense of Rodriguez error vector $\tilde{\rho}$ of order higher than two. It is worth mentioning that the deterministic filter in (4.19), (4.20) and (4.21) is known as a passive complementary filter proposed in Mahony et al. (2008).

4.3.2 Nonlinear Stochastic Attitude Filter in Ito Sense

Generally, the assumption behind nonlinear deterministic filters is that angular velocity vector measurements are joined with constant or slowly time-variant bias (Crassidis et al. (2007); Mahony et al. (2008)). However, angular velocity vector measurements are typically subject to additive noise components which may weaken the estimation process of the true attitude dynamics in (4.4). Therefore, we aim to design a nonlinear stochastic filter in Ito sense taking into consideration that angular velocity vector measurements are subject to a constant bias and a wide-band of Gaussian random with zero mean such that $\mathbb{E}[\omega] = 0$. Let the true inertial vector $\mathrm{v}_i^{\mathcal{I}(\mathrm{R})}$ and body-frame vector $\mathrm{v}_i^{\mathcal{B}(\mathrm{R})}$ be defined as in (4.1). Let the error in attitude estimate be similar to (4.16).

Consider the nonlinear stochastic filter design

$$\dot{\hat{R}} = \hat{R}\left[\Omega_m - \hat{b} - W\right]_\times, \quad \hat{R}(0) = \hat{R}_0 \tag{4.27}$$

$$\dot{\hat{b}} = \gamma_1 ||\tilde{R}||_I \boldsymbol{\Upsilon}_a(\tilde{R}) - \gamma_1 k_b \hat{b}, \quad \hat{b}(0) = \hat{b}_0 \tag{4.28}$$

$$\dot{\hat{\sigma}} = k_1\gamma_2 ||\tilde{R}||_I \mathcal{D}_\Upsilon^\top \boldsymbol{\Upsilon}_a(\tilde{R}) - \gamma_2 k_\sigma \hat{\sigma}, \quad \hat{\sigma}(0) = \hat{\sigma}_0 \tag{4.29}$$

$$W = \frac{k_1}{\varepsilon}\frac{2 - ||\tilde{R}||_I}{1 - ||\tilde{R}||_I}\boldsymbol{\Upsilon}_a(\tilde{R}) + k_2 \mathcal{D}_\Upsilon \hat{\sigma} \tag{4.30}$$

where Ω_m is angular velocity measurement defined in (4.3), $\hat{b}$ is the estimate of the unknown bias b, $\hat{\sigma}$ is the estimate of σ which includes the upper bound of $\mathcal{Q}^2$ as given in (4.10), $\tilde{R} = R_y^\top \hat{R}$ with R_y being the reconstructed attitude, $\boldsymbol{\Upsilon}_a(\tilde{R}) = \mathbf{vex}\left(\boldsymbol{\mathcal{P}}_a(\tilde{R})\right)$ as given in (A.4), $\mathcal{D}_\Upsilon = \left[\boldsymbol{\Upsilon}_a(\tilde{R}), \boldsymbol{\Upsilon}_a(\tilde{R}), \boldsymbol{\Upsilon}_a(\tilde{R})\right]$, and $||\tilde{R}||_I$ is the Euclidean distance of $\tilde{R}$ as defined in (A.2). Also, $\gamma_1 > 0$ and $\gamma_2 > 0$ are adaptation gains, $\varepsilon > 0$ is a small constant, while k_b, k_σ, k_1 and k_2 are positive constants.

Theorem 4.1 *Consider the rotation dynamics in (4.9), angular velocity measurements in (4.3) in addition to other given vectorial measurements in (4.2) coupled with the observer (4.27), (4.28), (4.29), and (4.30). Assume that two or more body-frame non-collinear vectors are available for measurements and the design parameters γ_1 , γ_2 , ε, k_b, k_σ, k_1, and k_2 are chosen appropriately with ε being selected sufficiently small. Then, for angular velocity measurements contaminated with noise ($\omega \neq \underline{\mathbf{0}}_3$), all the signals in the closed-loop system is semi-globally uniformly ultimately bounded*

in mean square. In addition, the observer errors can be minimized by the appropriate selection of the design parameters.

Proof: Let the error in vector b be defined as in (4.17). Therefore, the derivative of attitude error in incremental form of (4.16) can be obtained from (4.8) and (4.27) by

$$\begin{aligned} d\tilde{R} =& R^\top \hat{R}\left[\Omega_m - \hat{b} - W\right]_\times dt + [\Omega]_\times^\top R^\top \hat{R} dt \\ =& \left(\tilde{R}\,[\Omega]_\times + [\Omega]_\times^\top \tilde{R} + \tilde{R}\left[\tilde{b} - W\right]_\times\right) dt + \tilde{R}\,[\mathcal{Q} d\beta]_\times \\ =& \tilde{R}\left[\Omega - \tilde{R}^\top \Omega + \tilde{b} - W\right]_\times dt + \tilde{R}\,[\mathcal{Q} d\beta]_\times \end{aligned} \tag{4.31}$$

Similar extraction of Rodriguez error vector dynamic in view of (4.9) to (4.8) can be expressed from (4.31) to (4.32) in Ito's representation (Ito and Rao (1984)) as

$$d\tilde{\rho} = \tilde{f} dt + \tilde{g}\mathcal{Q} d\beta \tag{4.32}$$

where $\tilde{\rho}$ is the Rodriguez error vector associated with $\tilde{R}$. Let $\tilde{g} = \frac{1}{2}\left(\mathbf{I}_3 + [\tilde{\rho}]_\times + \tilde{\rho}\tilde{\rho}^\top\right)$ and $\tilde{f} = \tilde{g}\left(\Omega - \tilde{R}^\top \Omega + \tilde{b} - W\right)$. Consider the following potential function

$$V\left(\tilde{\rho}, \tilde{b}, \tilde{\sigma}\right) = \left(\frac{\|\tilde{\rho}\|^2}{1 + \|\tilde{\rho}\|^2}\right)^2 + \frac{1}{2\gamma_1}\tilde{b}^\top \tilde{b} + \frac{1}{2\gamma_2}\tilde{\sigma}^\top \tilde{\sigma} \tag{4.33}$$

For $V := V\left(\tilde{\rho}, \tilde{b}, \tilde{\sigma}\right)$, the differential operator $\mathcal{L}V$ in Definition 4.1 for the dynamic system in (4.32) can be expressed as

$$\mathcal{L}V = V_{\tilde{\rho}}^\top \tilde{f} + \frac{1}{2}\mathrm{Tr}\left\{\tilde{g}^\top V_{\tilde{\rho}\tilde{\rho}} \tilde{g}\mathcal{Q}^2\right\} - \frac{1}{\gamma_1}\tilde{b}^\top \dot{\tilde{b}} - \frac{1}{\gamma_2}\tilde{\sigma}^\top \dot{\tilde{\sigma}} \tag{4.34}$$

where $V_{\tilde{\rho}} = \partial V / \partial \tilde{\rho}$ and $V_{\tilde{\rho}\tilde{\rho}} = \partial V^2 / \partial^2 \tilde{\rho}$. The first and the second partial derivatives

of (4.33) with respect to $\tilde{\rho}$ can be obtained as follows

$$V_{\tilde{\rho}} = 4\frac{\|\tilde{\rho}\|^2}{\left(1+\|\tilde{\rho}\|^2\right)^3}\tilde{\rho} \tag{4.35}$$

$$V_{\tilde{\rho}\tilde{\rho}} = 4\frac{\left(1+\|\tilde{\rho}\|^2\right)\|\tilde{\rho}\|^2\mathbf{I}_3 + \left(2-4\|\tilde{\rho}\|^2\right)\tilde{\rho}\tilde{\rho}^\top}{\left(1+\|\tilde{\rho}\|^2\right)^4} \tag{4.36}$$

substituting $\tilde{R} = \mathcal{R}_{\tilde{\rho}}(\tilde{\rho})$ in (A.1), one can verify that (Appendix C)

$$\frac{1}{2}V_{\tilde{\rho}}^\top\left(\mathbf{I}_3 + [\tilde{\rho}]_\times + \tilde{\rho}\tilde{\rho}^\top\right)\left(\Omega - \tilde{R}^\top\Omega\right) = 0$$

Hence, the first part of the differential operator $\mathcal{L}V$ in (4.34) can be evaluated by

$$V_{\tilde{\rho}}^\top\tilde{f} = 2\frac{\|\tilde{\rho}\|^2}{\left(1+\|\tilde{\rho}\|^2\right)^2}\tilde{\rho}^\top\left(\tilde{b} - W\right) \tag{4.37}$$

Keeping in mind the identity in (2.14) and $\tilde{g}$ in (4.32) and combining them with (4.36), the component $\mathrm{Tr}\left\{\tilde{g}^\top V_{\tilde{\rho}\tilde{\rho}}\tilde{g}\mathcal{Q}^2\right\}$ can be simplified and expressed as

$$\begin{aligned}\frac{1}{2}\mathrm{Tr}\left\{\tilde{g}^\top V_{\tilde{\rho}\tilde{\rho}}\tilde{g}\mathcal{Q}^2\right\} =& \frac{1}{2\left(1+\|\tilde{\rho}\|^2\right)^3}\mathrm{Tr}\left\{\left(1+\|\tilde{\rho}\|^2\right)\|\tilde{\rho}\|^2\mathcal{Q}^2\right.\\ &\left.+\left(2-\|\tilde{\rho}\|^2-3\|\tilde{\rho}\|^4\right)\tilde{\rho}\tilde{\rho}^\top\mathcal{Q}^2\right\}\end{aligned} \tag{4.38}$$

Let $\bar{q} = \left[\mathcal{Q}_{1,1}, \mathcal{Q}_{2,2}, \mathcal{Q}_{3,3}\right]^\top$ and σ be similar to (4.10). From (4.37) and (4.38), one can write the operator $\mathcal{L}V$ in (4.34) as

$$\begin{aligned}\mathcal{L}V =& 2\frac{\|\tilde{\rho}\|^2\tilde{\rho}^\top\left(\tilde{b}-W\right)}{\left(1+\|\tilde{\rho}\|^2\right)^2} + \frac{\mathrm{Tr}\left\{\left(2-\|\tilde{\rho}\|^2-3\|\tilde{\rho}\|^4\right)\tilde{\rho}\tilde{\rho}^\top\mathcal{Q}^2\right\}}{2\left(1+\|\tilde{\rho}\|^2\right)^3} + \frac{\mathrm{Tr}\left\{\|\tilde{\rho}\|^2\mathcal{Q}^2\right\}}{2\left(1+\|\tilde{\rho}\|^2\right)^2}\\ &-\frac{1}{\gamma_1}\tilde{b}^\top\dot{\tilde{b}} - \frac{1}{\gamma_2}\tilde{\sigma}^\top\dot{\tilde{\sigma}}\end{aligned} \tag{4.39}$$

Since $\|\bar{q}\|^2 = \mathrm{Tr}\left\{\mathcal{Q}^2\right\}$ and $\mathrm{Tr}\left\{\tilde{\rho}\tilde{\rho}^\top \mathcal{Q}^2\right\} \leq \|\tilde{\rho}\|^2 \|\bar{q}\|^2$, we have

$$\begin{aligned}\mathcal{L}V \leq & 2\frac{\|\tilde{\rho}\|^2 \tilde{\rho}^\top \left(\tilde{b} - W\right)}{\left(1 + \|\tilde{\rho}\|^2\right)^2} + \frac{\|\tilde{\rho}\|^4 \mathrm{Tr}\left\{\mathcal{Q}^2\right\} + 3\|\tilde{\rho}\|^2 \|\bar{q}\|^2}{2\left(1 + \|\tilde{\rho}\|^2\right)^3} \\ & - \frac{\left(1 + 3\|\tilde{\rho}\|^2\right)\|\tilde{\rho}\|^2 \tilde{\rho}^\top \mathcal{Q}^2 \tilde{\rho}}{2\left(1 + \|\tilde{\rho}\|^2\right)^3} - \frac{1}{\gamma_1}\tilde{b}^\top \dot{\hat{b}} - \frac{1}{\gamma_2}\tilde{\sigma}^\top \dot{\hat{\sigma}}\end{aligned} \tag{4.40}$$

According to Lemma 4.2, the following equation holds

$$\begin{aligned}\frac{3\|\tilde{\rho}\|^2 \|\bar{q}\|^2}{2\left(1 + \|\tilde{\rho}\|^2\right)^3} &\leq \frac{9\|\tilde{\rho}\|^4}{8\left(1 + \|\tilde{\rho}\|^2\right)^6 \varepsilon} + \frac{\varepsilon}{2}\|\bar{q}\|^4 \\ &\leq \frac{9\|\tilde{\rho}\|^4}{8\left(1 + \|\tilde{\rho}\|^2\right)^3 \varepsilon} + \frac{\varepsilon}{2}\left(\sum_{i=1}^{3} \sigma_i\right)^2\end{aligned} \tag{4.41}$$

where ε is a sufficiently small positive constant. Combining (4.41) with (4.40) yields

$$\begin{aligned}\mathcal{L}V \leq & 2\frac{\|\tilde{\rho}\|^2 \tilde{\rho}^\top \left(\tilde{b} - W\right)}{\left(1 + \|\tilde{\rho}\|^2\right)^2} + 2\frac{\frac{1}{4}\sum_{i=1}^{3}\sigma_i + \frac{9}{16\varepsilon}}{\left(1 + \|\tilde{\rho}\|^2\right)^3}\|\tilde{\rho}\|^4 - \frac{1}{\gamma_1}\tilde{b}^\top \dot{\hat{b}} - \frac{1}{\gamma_2}\tilde{\sigma}^\top \dot{\hat{\sigma}} \\ & - \frac{\left(1 + 3\|\tilde{\rho}\|^2\right)\|\tilde{\rho}\|^2 \tilde{\rho}^\top \mathcal{Q}^2 \tilde{\rho}}{2\left(1 + \|\tilde{\rho}\|^2\right)^3} + \frac{\varepsilon}{2}\left(\sum_{i=1}^{3}\sigma_i\right)^2\end{aligned} \tag{4.42}$$

Define $\bar{\sigma} = \sum_{i=1}^{3}\sigma_i$. Substitute $\dot{\hat{b}}$, $\dot{\hat{\sigma}}$, and W from (4.28), (4.29), and (4.30), respectively, in (4.42). Also, $||\tilde{R}||_I = \|\tilde{\rho}\|^2 / \left(1 + \|\tilde{\rho}\|^2\right)$ and $\boldsymbol{\Upsilon}_a(\tilde{R}) = 2\tilde{\rho}/\left(1 + \|\tilde{\rho}\|^2\right)$ as defined in (A.2) and (A.4), respectively. Hence, (4.42) yields

$$\mathcal{L}V \leq -4\left(\frac{8k_2-1}{8}\bar{\sigma}+\frac{32k_1-9}{32\varepsilon}\right)\frac{\|\tilde{\rho}\|^4}{\left(1+\|\tilde{\rho}\|^2\right)^3}-\frac{4k_1}{\varepsilon}\frac{\|\tilde{\rho}\|^4}{\left(1+\|\tilde{\rho}\|^2\right)^2}$$
$$-\frac{\left(1+3\|\tilde{\rho}\|^2\right)\|\tilde{\rho}\|^2\tilde{\rho}^\top\mathcal{Q}^2\tilde{\rho}}{2\left(1+\|\tilde{\rho}\|^2\right)^3}+k_b\tilde{b}^\top\hat{b}+k_\sigma\tilde{\sigma}^\top\hat{\sigma}+\frac{\varepsilon}{2}\bar{\sigma}^2 \tag{4.43}$$

from (4.43) $k_b\tilde{b}^\top\hat{b}=-k_b||\tilde{b}||^2+k_b\tilde{b}^\top b$ and $k_\sigma\tilde{\sigma}^\top\hat{\sigma}=-k_\sigma\|\tilde{\sigma}\|^2+k_\sigma\tilde{\sigma}^\top\sigma$. Combining this result with Young's inequality yields

$$k_b\tilde{b}^\top b\leq\frac{k_b}{2}||\tilde{b}||^2+\frac{k_b}{2}\|b\|^2$$
$$k_\sigma\tilde{\sigma}^\top\sigma\leq\frac{k_\sigma}{2}\|\tilde{\sigma}\|^2+\frac{k_\sigma}{2}\|\sigma\|^2$$

thereby, the differential operator in (4.43) results in

$$\mathcal{L}V \leq -4\left(\frac{8k_2-1}{8}\bar{\sigma}+\frac{32k_1-9}{32\varepsilon}\right)\frac{\|\tilde{\rho}\|^4}{\left(1+\|\tilde{\rho}\|^2\right)^3}-\frac{\left(1+3\|\tilde{\rho}\|^2\right)\|\tilde{\rho}\|^2\tilde{\rho}^\top\mathcal{Q}^2\tilde{\rho}}{2\left(1+\|\tilde{\rho}\|^2\right)^3}$$
$$-\frac{4k_1}{\varepsilon}\frac{\|\tilde{\rho}\|^4}{\left(1+\|\tilde{\rho}\|^2\right)^2}-\frac{k_b}{2}||\tilde{b}||^2-\frac{k_\sigma}{2}\|\tilde{\sigma}\|^2+\frac{k_b}{2}\|b\|^2+\frac{k_\sigma}{2}\|\sigma\|^2+\frac{\varepsilon}{2}\bar{\sigma}^2 \tag{4.44}$$

such that (4.44) in $\mathbb{SO}(3)$ form is equivalent to

$$\mathcal{L}V \leq -\left(\frac{8k_2-1}{8}\bar{\sigma}+\frac{32k_1-9}{32\varepsilon}\right)||\tilde{R}||_I\left\|\boldsymbol{\Upsilon}_a(\tilde{R})\right\|^2$$
$$-\left(\frac{1}{8}+\frac{3}{8}\frac{||\tilde{R}||_I}{1-||\tilde{R}||_I}\right)||\tilde{R}||_I\boldsymbol{\Upsilon}_a(\tilde{R})^\top\mathcal{Q}^2\boldsymbol{\Upsilon}_a(\tilde{R})$$
$$-\frac{4k_1}{\varepsilon}||\tilde{R}||_I^2-\frac{k_b}{2}||\tilde{b}||^2-\frac{k_\sigma}{2}\|\tilde{\sigma}\|^2+\frac{k_b}{2}\|b\|^2+\frac{k_\sigma}{2}\|\sigma\|^2+\frac{\varepsilon}{2}\bar{\sigma}^2 \tag{4.45}$$

Setting $\gamma_1\geq 1$, $\gamma_2\geq 1$, $k_1\geq\frac{9}{32}$, $k_2\geq\frac{1}{8}$, $k_b>0$, $k_\sigma>0$, and the positive constant ε sufficiently small with $\mathcal{Q}^2:\mathbb{R}_+\to\mathbb{R}^{3\times 3}$ being bounded, the operator $\mathcal{L}V$ in (4.44) becomes similar to (4.12) in Lemma 4.1. Define $c_2=\frac{k_b}{2}\|b\|^2+\frac{1}{2}(k_\sigma+\varepsilon)\bar{\sigma}^2$ which is governed by the unknown constant bias b and the the upper bound of covariance σ.

Let $\tilde{X} = \left[\frac{\|\tilde{\rho}\|^2}{1+\|\tilde{\rho}\|^2}, \frac{1}{\sqrt{2\gamma_1}}\tilde{b}^\top, \frac{1}{\sqrt{2\gamma_2}}\tilde{\sigma}^\top\right]^\top \in \mathbb{R}^7$ and

$$\mathcal{H} = \begin{bmatrix} 4k_1/\varepsilon & \underline{\mathbf{0}}_3^\top & \underline{\mathbf{0}}_3^\top \\ \underline{\mathbf{0}}_3 & \gamma_1 k_b \mathbf{I}_3 & \mathbf{0}_{3\times 3} \\ \underline{\mathbf{0}}_3 & \mathbf{0}_{3\times 3} & \gamma_2 k_\sigma \mathbf{I}_3 \end{bmatrix} \in \mathbb{R}^{7\times 7}$$

Hence, the differential operator in (4.44) can be expressed as

$$\begin{aligned}\mathcal{L}V \leq &-4\left(\frac{8k_2-1}{8}\bar{\sigma} + \frac{32k_1-9}{32\varepsilon}\right)\frac{\|\tilde{\rho}\|^4}{\left(1+\|\tilde{\rho}\|^2\right)^3} - \frac{\left(1+3\|\tilde{\rho}\|^2\right)\|\tilde{\rho}\|^2\,\tilde{\rho}^\top\mathcal{Q}^2\tilde{\rho}}{2\left(1+\|\tilde{\rho}\|^2\right)^3} \\ &- \tilde{X}^\top\mathcal{H}\tilde{X} + c_2 \end{aligned} \tag{4.46}$$

or more simply

$$\mathcal{L}V \leq -h\left(\|\tilde{\rho}\|\right) - \underline{\lambda}\left(\mathcal{H}\right)V + c_2 \tag{4.47}$$

such that $h(\cdot)$ is a class $\mathcal{K}$ function which includes the first two components in (4.46), and $\underline{\lambda}(\cdot)$ denotes the minimum eigenvalue of a matrix. Based on (4.47), one easily obtains

$$\frac{d\left(\mathbb{E}\left[V\right]\right)}{dt} = \mathbb{E}\left[\mathcal{L}V\right] \leq -\underline{\lambda}\left(\mathcal{H}\right)\mathbb{E}\left[V\right] + c_2 \tag{4.48}$$

Consider $\mathrm{K} = \mathbb{E}\left[V(t)\right]$; thus $\frac{d(\mathbb{E}[V])}{dt} \leq 0$ for $\underline{\lambda}(\mathcal{H}) > \frac{c_2}{\mathrm{K}}$. Hence, $V \leq \mathrm{K}$ is an invariant set and for $\mathbb{E}\left[V(0)\right] \leq \mathrm{K}$ there is $\mathbb{E}\left[V(t)\right] \leq \mathrm{K}\forall t > 0$. Based on Lemma 4.1, the inequality in (4.48) holds for $V(0) \leq \mathrm{K}$ and for all $t > 0$ such that

$$0 \leq \mathbb{E}\left[V(t)\right] \leq V(0)\exp\left(-\underline{\lambda}\left(\mathcal{H}\right)t\right) + \frac{c_2}{\underline{\lambda}\left(\mathcal{H}\right)},\ \forall t \geq 0 \tag{4.49}$$

The above-mentioned inequality implies that $\mathbb{E}\left[V(t)\right]$ is eventually bounded by $c_2/\underline{\lambda}(\mathcal{H})$ indicating that $\tilde{X}$ is SGUUB in the mean square. Let us define $\tilde{Y} = \left[\tilde{\rho}^\top, \tilde{b}^\top, \tilde{\sigma}^\top\right]^\top \in \mathbb{R}^9$. Since $\tilde{X}$ is SGUUB, $\tilde{Y}$ is SGUUB in the mean square. For a rotation matrix $R \in \mathbb{SO}(3)$, let us define $\mathcal{U}_0 \subseteq \mathbb{SO}(3) \times \mathbb{R}^3 \times \mathbb{R}^3$ as

$$\mathcal{U}_0 = \left\{\left(\tilde{R}_0, \tilde{b}_0, \tilde{\sigma}_0\right) \middle| \operatorname{Tr}\left\{\tilde{R}_0\right\} = -1, \tilde{b}_0 = \underline{\mathbf{0}}_3, \tilde{\sigma}_0 = \underline{\mathbf{0}}_3\right\}$$

The set $\mathcal{U}_0$ is forward invariant and unstable for the dynamic system in (4.4). From al-

most any initial condition such that $\tilde{R}_0 \notin \mathcal{U}_0$ or, equivalently, $\tilde{\rho}_0 \in \mathbb{R}^3$, the trajectory of $\tilde{X}$ is SGUUB in the mean square.

4.3.3 Nonlinear Stochastic Attitude Filter in Stratonovich Sense

Stochastic differential equations can be defined and solved in the sense of Ito integral (Ito and Rao (1984)). Alternatively, Stratonovich integral (Stratonovich (1967)) can be employed for solving stochastic differential equations. The common feature between Stratonovich and Ito integral is that if the associated function multiplied by $d\beta$ is continuous and Lipschitz, the mean square limit exists. The Ito integral is defined for functional on $\{\beta(\tau), \tau \leq t\}$ which is more natural but does not obey the chain rule. Conversely, Stratonovich is a well-defined Riemann integral for the sampled function, it has a continuous partial derivative with respect to β, it obeys the chain rule and it is more convenient for colored noise (Jazwinski (2007); Stratonovich (1967)). Hence, the Stratonovich integral is defined for explicit functions of β. In case when angular velocity measurements are contaminated with a wide-band of random colored noise process, the solution of (4.6) for $\rho(t_0) = 0$ is defined by

$$\rho(t) = \int_{t_0}^{t} f(\rho(\tau), b(\tau))\, d\tau + \int_{t_0}^{t} g(\rho(\tau))\, \mathcal{Q} d\beta \tag{4.50}$$

according to subsection 4.3.2, the expected value of (4.50) is

$$\mathbb{E}[\rho] \neq \int_{t_0}^{t} \mathbb{E}[f(\rho(\tau), b(\tau))]\, d\tau$$

Thus, Stratonovich introduced the Wong-Zakai correction factor which can help in designing an adaptive estimate for the covariance component. Let us assume that the attitude dynamic in (4.8) was defined in the sense of Stratonovich (Stratonovich (1967)), hence, its equivalent Ito (Ito and Rao (1984); Jazwinski (2007); Khasminskii

(1980)) can be defined by

$$[d\rho]_i = [f(\rho, b)]_i \, dt + \sum_{k=1}^{3} \sum_{j=1}^{3} \frac{\mathcal{Q}_{j,j}^2}{2} g_{kj}(\rho) \frac{\partial g_{ij}(\rho)}{\partial \rho_k} dt + [g(\rho) \mathcal{Q} d\beta]_i \tag{4.51}$$

where both $f(\rho, b)$ and $g(\rho)$ are defined in (4.8), $i, j, k = 1, 2, 3$ denote ith, jth and kth element components of the associate vector or matrix. The term

$$\sum_{k=1}^{3} \sum_{j=1}^{3} \frac{\mathcal{Q}_{j,j}^2}{2} g_{kj}(\rho) \frac{\partial g_{ij}(\rho)}{\partial \rho_k}$$

denotes the Wong-Zakai correction factor of stochastic differential equations (SDEs) in the sense of Ito's representations (Wong and Zakai (1965)). Let

$$\boldsymbol{\mathcal{W}}_i(\rho) = \sum_{k=1}^{3} \sum_{j=1}^{3} \frac{\mathcal{Q}_{j,j}^2}{2} g_{kj}(\rho) \frac{\partial g_{ij}(\rho)}{\partial \rho_k}$$

accordingly, one can find that for $i = 1$

$$\sum_{k=1}^{3} \sum_{j=1}^{3} \frac{\mathcal{Q}_{j,j}^2}{2} g_{kj}(\rho) \frac{\partial g_{ij}(\rho)}{\partial \rho_k} = \frac{1}{4} \Big(\left(1 + \rho_1^2\right) \rho_1 \mathcal{Q}_{1,1}^2 + \\ (\rho_1 \rho_2 - \rho_3) \rho_2 \mathcal{Q}_{2,2}^2 + (\rho_2 + \rho_1 \rho_3) \rho_3 \mathcal{Q}_{3,3}^2 \Big)$$

see Appendix C. Hence, $\boldsymbol{\mathcal{W}}(\rho)$ for $i = 1, 2, 3$ is

$$\boldsymbol{\mathcal{W}}(\rho) = \frac{1}{4} \left(\mathbf{I}_3 + [\rho]_\times + \rho\rho^\top \right) \mathcal{Q}^2 \rho \tag{4.52}$$

see Appendix C. Manipulating equations (4.51) and (4.52), the stochastic dynamics of the Rodriguez vector can be expressed as

$$d\rho = \mathcal{F}(\rho, b) \, dt + g(\rho) \mathcal{Q} d\beta \tag{4.53}$$

where $g(\rho) := -\frac{1}{2} \left(\mathbf{I}_3 + [\rho]_\times + \rho\rho^\top \right)$ and $\mathcal{F}(\rho, b) := -g(\rho)(\Omega_m - b) + \boldsymbol{\mathcal{W}}(\rho)$. Define the error in attitude estimate similar to (4.16). Also, assume that the elements of covariance matrix $\mathcal{Q}^2$ are upper bounded by σ as given in (4.10) such that the bound

of σ is unknown with nonnegative elements.

Consider the following nonlinear stochastic filter design

$$\dot{\hat{R}} = \hat{R}\left[\Omega_m - \hat{b} - \frac{1}{2}\frac{\operatorname{diag}\left(\boldsymbol{\Upsilon}_a(\tilde{R})\right)}{1-||\tilde{R}||_I}\hat{\sigma} - W\right]_\times \tag{4.54}$$

$$\dot{\hat{b}} = \gamma_1||\tilde{R}||_I\boldsymbol{\Upsilon}_a(\tilde{R}) - \gamma_1 k_b\hat{b}, \quad \hat{b}(0) = \hat{b}_0 \tag{4.55}$$

$$\dot{\hat{\sigma}} = \gamma_2||\tilde{R}||_I\left(k_1\mathcal{D}_\Upsilon^\top + \frac{1}{2}\frac{\operatorname{diag}\left(\boldsymbol{\Upsilon}_a(\tilde{R})\right)}{1-||\tilde{R}||_I}\right)\boldsymbol{\Upsilon}_a(\tilde{R}) - \gamma_2 k_\sigma\hat{\sigma}, \quad \hat{\sigma}(0) = \hat{\sigma}_0 \tag{4.56}$$

$$W = \frac{k_1}{\varepsilon}\frac{2-||\tilde{R}||_I}{1-||\tilde{R}||_I}\boldsymbol{\Upsilon}_a(\tilde{R}) + k_2\mathcal{D}_\Upsilon\hat{\sigma} \tag{4.57}$$

where $\hat{R}(0) = \hat{R}_0$, Ω_m is the angular velocity measurement as defined in (4.3), $\hat{b}$ and $\hat{\sigma}$ are estimates of the unknown parameters b and σ, respectively, $\tilde{R} = R_y^\top\hat{R}$ with R_y being the reconstructed attitude, $\boldsymbol{\Upsilon}_a(\tilde{R}) = \mathbf{vex}\left(\boldsymbol{\mathcal{P}}_a(\tilde{R})\right)$ was given in (A.4), $||\tilde{R}||_I$ is the Euclidean distance of $\tilde{R}$, and $\mathcal{D}_\Upsilon = \left[\boldsymbol{\Upsilon}_a(\tilde{R}), \boldsymbol{\Upsilon}_a(\tilde{R}), \boldsymbol{\Upsilon}_a(\tilde{R})\right]$. γ_1 and γ_2 are positive adaptation gains, $\varepsilon > 0$ is a small constant, while k_b, k_σ, k_1 and k_2 are positive constants.

Theorem 4.2 *Consider the rotation kinematics in (4.9) with angular velocity measurements and given vector measurements in (4.3) and (4.2), respectively, being coupled with the observer in (4.54), (4.55), (4.56) and (4.57). Assume that two or more body-frame non-collinear vectors are available for measurements. Then, for angular velocity measurements contaminated with noise ($\omega \neq \underline{\mathbf{0}}_3$), $\left[\tilde{\rho}^\top, \tilde{b}^\top, \tilde{\sigma}^\top\right]^\top$ is semi-globally uniformly ultimately bounded in mean square. Moreover, the observer errors can be made sufficiently small by choosing the appropriate design parameters.*

Proof: Let the error in vector b and σ be defined as in (4.17) and (4.18), respectively. Hence, the derivative of (4.16) in incremental form can be obtained from (4.8) and (4.54) by

$$d\tilde{R} = \tilde{R}\left[\Omega - \tilde{R}^\top\Omega + \tilde{b} - \frac{1}{2}\operatorname{diag}(\tilde{\rho})\hat{\sigma} - W\right]_\times dt + \tilde{R}\left[\mathcal{Q}d\beta\right]_\times \tag{4.58}$$

Assume that the Rodriguez error vector dynamic of (4.58) is defined in the sense

of Stratonovich. The extraction of Rodriguez error vector dynamics in view of the transformation of (4.4) into (4.53) can be expressed from (4.58) to (4.59) in Ito's representation (Stratonovich (1967)) as

$$d\tilde{\rho} = \tilde{\mathcal{F}}dt + \tilde{g}\mathcal{Q}d\beta \tag{4.59}$$

where $\tilde{\rho}$ is Rodriguez error vector associated with $\tilde{R}$ with

$$\begin{aligned}
\tilde{g} &= \frac{1}{2}\left(\mathbf{I}_3 + [\tilde{\rho}]_\times + \tilde{\rho}\tilde{\rho}^\top\right) \\
\tilde{\mathcal{F}} &= \tilde{g}\left(\Omega - \tilde{R}^\top\Omega + \tilde{b} - \frac{1}{2}\mathrm{diag}\left(\tilde{\rho}\right)\hat{\sigma} - W\right) + \boldsymbol{\mathcal{W}}\left(\tilde{\rho}\right) \\
\boldsymbol{\mathcal{W}}\left(\tilde{\rho}\right) &= \frac{1}{4}\left(\mathbf{I}_3 + [\tilde{\rho}]_\times + \tilde{\rho}\tilde{\rho}^\top\right)\mathcal{Q}^2\tilde{\rho}
\end{aligned}$$

Consider the following potential function

$$V\left(\tilde{\rho}, \tilde{b}, \tilde{\sigma}\right) = \left(\frac{\|\tilde{\rho}\|^2}{1 + \|\tilde{\rho}\|^2}\right)^2 + \frac{1}{2\gamma_1}\tilde{b}^\top\tilde{b} + \frac{1}{2\gamma_2}\tilde{\sigma}^\top\tilde{\sigma} \tag{4.60}$$

For $V := V\left(\tilde{\rho}, \tilde{b}, \tilde{\sigma}\right)$, the differential operator $\mathcal{L}V$ in Definition 4.1 for the dynamic system in (4.59) can be written as

$$\mathcal{L}V = V_{\tilde{\rho}}^\top\tilde{\mathcal{F}} + \frac{1}{2}\mathrm{Tr}\left\{\tilde{g}^\top V_{\tilde{\rho}\tilde{\rho}}\tilde{g}\mathcal{Q}^2\right\} - \frac{1}{\gamma_1}\tilde{b}^\top\dot{\tilde{b}} - \frac{1}{\gamma_2}\tilde{\sigma}^\top\dot{\tilde{\sigma}} \tag{4.61}$$

The first and the second partial derivatives of (4.60) with respect to $\tilde{\rho}$ are similar to (4.35) and (4.36), respectively. The first part of differential operator $\mathcal{L}V$ in (4.61) can be evaluated by

$$\begin{aligned}
V_{\tilde{\rho}}^\top\tilde{\mathcal{F}} =& 2\frac{\|\tilde{\rho}\|^2}{\left(1 + \|\tilde{\rho}\|^2\right)^2}\tilde{\rho}^\top\left(\tilde{b} - \frac{1}{2}\mathrm{diag}\left(\tilde{\rho}\right)\hat{\sigma} + \frac{1}{2}\mathcal{Q}^2\tilde{\rho} - W\right) \\
\leq& 2\frac{\|\tilde{\rho}\|^2}{\left(1 + \|\tilde{\rho}\|^2\right)^2}\tilde{\rho}^\top\left(\tilde{b} + \frac{1}{2}\mathrm{diag}\left(\tilde{\rho}\right)\tilde{\sigma} - W\right)
\end{aligned} \tag{4.62}$$

where $\frac{1}{2}V_{\tilde{\rho}}^{\top}\left(\mathbf{I}_3+[\tilde{\rho}]_{\times}+\tilde{\rho}\tilde{\rho}^{\top}\right)\left(\Omega-\tilde{R}^{\top}\Omega\right)=0$, see Appendix C. The component $\mathrm{Tr}\left\{\tilde{g}^{\top}V_{\tilde{\rho}\tilde{\rho}}\tilde{g}\mathcal{Q}^2\right\}$ is similar to (4.38). Let $\bar{q}=\left[\mathcal{Q}_{1,1},\mathcal{Q}_{2,2},\mathcal{Q}_{3,3}\right]^{\top}$ and σ be similar to (4.10). The operator $\mathcal{L}V$ in (4.60) becomes

$$\begin{aligned}\mathcal{L}V \leq & 2\frac{\|\tilde{\rho}\|^2\,\tilde{\rho}^{\top}\left(\tilde{b}-W+\frac{1}{2}\mathrm{diag}\left(\tilde{\rho}\right)\tilde{\sigma}\right)}{\left(1+\|\tilde{\rho}\|^2\right)^2}+\frac{\mathrm{Tr}\left\{\|\tilde{\rho}\|^2\,\mathcal{Q}^2\right\}}{2\left(1+\|\tilde{\rho}\|^2\right)^2}\\ & +\frac{\mathrm{Tr}\left\{\left(2-\|\tilde{\rho}\|^2-3\,\|\tilde{\rho}\|^4\right)\tilde{\rho}\tilde{\rho}^{\top}\mathcal{Q}^2\right\}}{2\left(1+\|\tilde{\rho}\|^2\right)^3}-\frac{1}{\gamma_1}\tilde{b}^{\top}\dot{\tilde{b}}-\frac{1}{\gamma_2}\tilde{\sigma}^{\top}\dot{\tilde{\sigma}}\end{aligned}$$

Since $\|\bar{q}\|^2=\mathrm{Tr}\left\{\mathcal{Q}^2\right\}$ and $\mathrm{Tr}\left\{\tilde{\rho}\tilde{\rho}^{\top}\mathcal{Q}^2\right\}\leq\|\tilde{\rho}\|^2\,\|\bar{q}\|^2$, we obtain

$$\begin{aligned}\mathcal{L}V \leq & 2\frac{\|\tilde{\rho}\|^2\,\tilde{\rho}^{\top}\left(\tilde{b}-W+\frac{1}{2}\mathrm{diag}\left(\tilde{\rho}\right)\tilde{\sigma}\right)}{\left(1+\|\tilde{\rho}\|^2\right)^2}+\frac{\|\tilde{\rho}\|^4\,\mathrm{Tr}\left\{\mathcal{Q}^2\right\}+3\,\|\tilde{\rho}\|^2\,\|\bar{q}\|^2}{2\left(1+\|\tilde{\rho}\|^2\right)^3}\\ & -\frac{1}{\gamma_1}\tilde{b}^{\top}\dot{\tilde{b}}-\frac{1}{\gamma_2}\tilde{\sigma}^{\top}\dot{\tilde{\sigma}}-\frac{\|\tilde{\rho}\|^2\left(1+3\,\|\tilde{\rho}\|^2\right)\tilde{\rho}^{\top}\mathcal{Q}^2\tilde{\rho}}{2\left(1+\|\tilde{\rho}\|^2\right)^3}\end{aligned}\tag{4.63}$$

From the last result and taking into consideration the inequality in (4.41), according to Lemma 4.2, and (4.10), equation (4.63) becomes

$$\begin{aligned}\mathcal{L}V \leq & 2\frac{\|\tilde{\rho}\|^2\,\tilde{\rho}^{\top}\left(\tilde{b}-W+\frac{1}{2}\mathrm{diag}\left(\tilde{\rho}\right)\tilde{\sigma}\right)}{\left(1+\|\tilde{\rho}\|^2\right)^2}+2\frac{\|\tilde{\rho}\|^2\,\tilde{\rho}^{\top}\left(\frac{1}{4}\mathcal{D}_{\tilde{\rho}}\sigma+\frac{9}{16\varepsilon}\tilde{\rho}\right)}{\left(1+\|\tilde{\rho}\|^2\right)^3}\\ & -\frac{1}{\gamma_1}\tilde{b}^{\top}\dot{\tilde{b}}-\frac{1}{\gamma_2}\tilde{\sigma}^{\top}\dot{\tilde{\sigma}}-\frac{\|\tilde{\rho}\|^2\left(1+3\,\|\tilde{\rho}\|^2\right)\tilde{\rho}^{\top}\mathcal{Q}^2\tilde{\rho}}{2\left(1+\|\tilde{\rho}\|^2\right)^3}+\frac{\varepsilon}{2}\left(\sum_{i=1}^{3}\sigma_i\right)^2\end{aligned}\tag{4.64}$$

with $\mathcal{D}_{\tilde{\rho}}=[\tilde{\rho},\tilde{\rho},\tilde{\rho}]$. From (4.64), we have $\tilde{\rho}^{\top}\mathcal{D}_{\tilde{\rho}}\sigma=\left(\sum_{i=1}^{3}\sigma_i\right)\|\tilde{\rho}\|^2$. Let us define $\bar{\sigma}=\sum_{i=1}^{3}\sigma_i$. Substitute for the differential operators $\dot{\tilde{b}}$, $\dot{\tilde{\sigma}}$ and the correction factor W from (4.55), (4.56) and (4.57), respectively, with $||\tilde{R}||_I=\|\tilde{\rho}\|^2/\left(1+\|\tilde{\rho}\|^2\right)$ and

$\boldsymbol{\Upsilon}_a(\tilde{R}) = 2\tilde{\rho}/\left(1+\|\tilde{\rho}\|^2\right)$. Hence, the result in (4.64) is equivalent to

$$\begin{aligned}\mathcal{L}V \leq &-4\left(\frac{8k_2-1}{8}\bar{\sigma}+\frac{32k_1-9}{32\varepsilon}\right)\frac{\|\tilde{\rho}\|^4}{\left(1+\|\tilde{\rho}\|^2\right)^3}-\frac{\left(1+3\|\tilde{\rho}\|^2\right)\|\tilde{\rho}\|^2\,\tilde{\rho}^\top\mathcal{Q}^2\tilde{\rho}}{2\left(1+\|\tilde{\rho}\|^2\right)^3}\\ &-\frac{4k_1}{\varepsilon}\frac{\|\tilde{\rho}\|^4}{\left(1+\|\tilde{\rho}\|^2\right)^2}-k_b||\tilde{b}||^2-k_\sigma\|\tilde{\sigma}\|^2+k_b\tilde{b}^\top b+k_\sigma\tilde{\sigma}^\top\sigma+\frac{\varepsilon}{2}\bar{\sigma}^2 \qquad (4.65)\end{aligned}$$

applying Young's inequality, one has

$$\begin{aligned}k_b\tilde{b}^\top b &\leq \frac{k_b}{2}||\tilde{b}||^2+\frac{k_b}{2}\|b\|^2\\ k_\sigma\tilde{\sigma}^\top\sigma &\leq \frac{k_\sigma}{2}\|\tilde{\sigma}\|^2+\frac{k_\sigma}{2}\bar{\sigma}^2\end{aligned}$$

Consequently, (4.65) becomes

$$\begin{aligned}\mathcal{L}V \leq &-4\left(\frac{8k_2-1}{8}\bar{\sigma}+\frac{32k_1-9}{32\varepsilon}\right)\frac{\|\tilde{\rho}\|^4}{\left(1+\|\tilde{\rho}\|^2\right)^3}-\frac{\left(1+3\|\tilde{\rho}\|^2\right)\|\tilde{\rho}\|^2\,\tilde{\rho}^\top\mathcal{Q}^2\tilde{\rho}}{2\left(1+\|\tilde{\rho}\|^2\right)^3}\\ &-\frac{4k_1}{\varepsilon}\frac{\|\tilde{\rho}\|^4}{\left(1+\|\tilde{\rho}\|^2\right)^2}-\frac{k_b}{2}||\tilde{b}||^2-\frac{k_\sigma}{2}\|\tilde{\sigma}\|^2+\frac{k_b}{2}\|b\|^2+\frac{1}{2}\left(k_\sigma+\varepsilon\right)\bar{\sigma}^2 \qquad (4.66)\end{aligned}$$

In other words, (4.66) in $\mathbb{SO}(3)$ form is equivalent to

$$\begin{aligned}\mathcal{L}V \leq &-\left(\frac{1}{8}+\frac{3}{8}\frac{||\tilde{R}||_I}{1-||\tilde{R}||_I}\right)||\tilde{R}||_I\boldsymbol{\Upsilon}_a(\tilde{R})^\top\mathcal{Q}^2\boldsymbol{\Upsilon}_a(\tilde{R})\\ &-\left(\frac{8k_2-1}{8}\bar{\sigma}+\frac{32k_1-9}{32\varepsilon}\right)||\tilde{R}||_I\left\|\boldsymbol{\Upsilon}_a(\tilde{R})\right\|^2-\frac{4k_1}{\varepsilon}||\tilde{R}||_I^2\\ &-\frac{k_b}{2}||\tilde{b}||^2-\frac{k_\sigma}{2}\|\tilde{\sigma}\|^2+\frac{k_b}{2}\|b\|^2+\frac{1}{2}\left(k_\sigma+\varepsilon\right)\bar{\sigma}^2 \qquad (4.67)\end{aligned}$$

Setting $\gamma_1 \geq 1$, $\gamma_2 \geq 1$, $k_1 \geq \frac{9}{32}$, $k_2 \geq \frac{1}{8}$, $k_b > 0$, $k_\sigma > 0$, and the positive constant ε being sufficiently small, and defining $c_2 = \frac{k_b}{2}\|b\|^2 + \frac{1}{2}\left(k_\sigma+\varepsilon\right)\bar{\sigma}^2$, the operator $\mathcal{L}V$ in (4.66) becomes similar to (4.16) in Deng et al. (2001) which is in turn similar to

(4.12) in Lemma 4.1. Define

$$\tilde{X} = \left[\frac{\|\tilde{\rho}\|^2}{1+\|\tilde{\rho}\|^2}, \frac{1}{\sqrt{2\gamma_1}}\tilde{b}^\top, \frac{1}{\sqrt{2\gamma_2}}\tilde{\sigma}^\top \right]^\top \in \mathbb{R}^7,$$

$$\mathcal{H} = \begin{bmatrix} 4k_1/\varepsilon & \underline{\mathbf{0}}_3^\top & \underline{\mathbf{0}}_3^\top \\ \underline{\mathbf{0}}_3 & \gamma_1 k_b \mathbf{I}_3 & \mathbf{0}_{3\times 3} \\ \underline{\mathbf{0}}_3 & \mathbf{0}_{3\times 3} & \gamma_2 k_\sigma \mathbf{I}_3 \end{bmatrix} \in \mathbb{R}^{7\times 7}$$

Thereby, the differential operator in (4.66) is

$$\begin{aligned} \mathcal{L}V \leq & -\left(\frac{8k_2-1}{2}\bar{\sigma} + \frac{32k_1-9}{8\varepsilon}\right)\frac{\|\tilde{\rho}\|^4}{\left(1+\|\tilde{\rho}\|^2\right)^3} \\ & - \frac{\left(1+3\|\tilde{\rho}\|^2\right)\|\tilde{\rho}\|^2\,\tilde{\rho}^\top\mathcal{Q}^2\tilde{\rho}}{2\left(1+\|\tilde{\rho}\|^2\right)^3} - \tilde{X}^\top\mathcal{H}\tilde{X} + c_2 \\ \leq & -h\left(\|\tilde{\rho}\|\right) - \underline{\lambda}\left(\mathcal{H}\right)V + c_2 \end{aligned} \tag{4.68}$$

such that $h(\cdot)$ is a class $\mathcal{K}$ function which includes the first two components in (4.68). Based on (4.68), one easily obtains

$$\frac{d\left(\mathbb{E}\left[V\right]\right)}{dt} = \mathbb{E}\left[\mathcal{L}V\right] \leq -\underline{\lambda}\left(\mathcal{H}\right)\mathbb{E}\left[V\right] + c_2 \tag{4.69}$$

Let $\mathrm{K} = \mathbb{E}\left[V(t)\right]$; then $\frac{d(\mathbb{E}[V])}{dt} \leq 0$ for $\underline{\lambda}(\mathcal{H}) > \frac{c_2}{\mathrm{K}}$. Thereby, $V(t) \leq \mathrm{K}$ is an invariant set and for $\mathbb{E}\left[V(0)\right] \leq \mathrm{K}$ it follows that $\mathbb{E}\left[V(t)\right] \leq \mathrm{K}\forall t > 0$. Accordingly, the inequality in (4.69) holds for $V(0) \leq \mathrm{K}$ and for all $t > 0$ which means that

$$0 \leq \mathbb{E}\left[V(t)\right] \leq V(0)\exp\left(-\underline{\lambda}\left(\mathcal{H}\right)t\right) + \frac{c_2}{\underline{\lambda}\left(\mathcal{H}\right)}, \forall t \geq 0 \tag{4.70}$$

The above inequality entails that $\mathbb{E}\left[V(t)\right]$ is eventually bounded by $c_2/\underline{\lambda}(\mathcal{H})$ which implies that $\tilde{X}$ is SGUUB in the mean square. For a rotation matrix $R \in \mathbb{SO}(3)$, define $\mathcal{U}_0 \subseteq \mathbb{SO}(3)\times\mathbb{R}^3\times\mathbb{R}^3$ as $\mathcal{U}_0 = \left\{\left(\tilde{R}_0, \tilde{b}_0, \tilde{\sigma}_0\right) \middle| \operatorname{Tr}\left\{\tilde{R}_0\right\} = -1, \tilde{b}_0 = \underline{\mathbf{0}}_3, \tilde{\sigma}_0 = \underline{\mathbf{0}}_3\right\}$. The set $\mathcal{U}_0$ is forward invariant and unstable for the dynamic system in (4.4). Therefore, for almost any initial condition such that $\tilde{R}_0 \notin \mathcal{U}_0$ or, equivalently, for any $\tilde{\rho}_0 \in \mathbb{R}^3$, $\tilde{X}$ is SGUUB in the mean square as in Definition 4.2.

Since, $\mathcal{Q}^2 : \mathbb{R}_+ \to \mathbb{R}^{3\times 3}$ is bounded, we have $d\left(\mathbb{E}\left[V\right]\right)/dt < 0$ for $V > c_2/\underline{\lambda}\left(\mathcal{H}\right)$. Considering Lemma 4.1 and the design parameters of the stochastic observer in Theorem 4.1 or 4.2 and combining them with prior knowledge about the covariance upper bound, allows to make the error signal smaller if the design parameters are chosen appropriately.

4.3.4 Stochastic Attitude Filters: Ito vs Stratonovich

In this work, the selection of potential functions in (4.33) and (4.60) contributes to attenuating and controlling the noise level associated with angular velocity measurements. Also, the selection of potential functions in (4.33) and (4.60) produced results analogous to those (4.47) and (4.68), respectively. This similarity in potential function selection and final results is critical as it guarantees fair comparison between the two proposed stochastic filters. The proposed stochastic filters are able to correct the attitude allowing the user to reduce the noise level associated with angular velocity measurements through $\underline{\lambda}\left(\mathcal{H}\right)$ by setting the values of ε, k_1, k_b, k_σ, γ_1 and γ_2 appropriately. Nonlinear deterministic attitude filters lack this advantage.
The main features of the nonlinear stochastic attitude filter in the sense of Ito can be listed as

1) The filter requires less computational power in comparison with the Stratonovich's filter.

2) No prior information about the covariance matrix $\mathcal{Q}^2$ is required.

3) This filter is applicable to white noise.

Whereas, the main characteristics of the nonlinear stochastic attitude filter in the sense of Stratonovich are

1) The filter demands more computational power in comparison with the Ito's filter.

2) No prior information about the covariance matrix $\mathcal{Q}^2$ is required.

3) The filter is applicable for white as well as colored noise.

4.4 Simulations

This section presents the performance and comparison among the two proposed nonlinear stochastic filters on $\mathbb{SO}(3)$. The first nonlinear stochastic filter is driven in the sense of Ito and the second one considers Stratonovich. Consider the orientation matrix R obtained from attitude dynamics in equation (4.4) with the following angular velocity input signal

$$\Omega = \begin{bmatrix} \sin(0.7t) \\ 0.7\sin(0.5t+\pi) \\ 0.5\sin\left(0.3t+\frac{\pi}{3}\right) \end{bmatrix} (\text{rad/sec})$$

while the initial attitude is $R(0) = \mathbf{I}_3$. Let the true angular velocity (Ω) be contaminated with a wide-band of random noise process with zero mean and standard deviation (STD) be equal to $0.5\,(\text{rad/sec})$ such that $\Omega_m = \Omega + b + \omega$ with $b = 0.1\,[1,-1,1]^\top$, $\omega = 0.5n(t)$, where t denotes real time, $n(t) = \text{randn}(3,1)$ where $\text{randn}(3,1)$ is a MATLAB® command, which refers to a normally distributed random vector at each time instant. Let non-collinear inertial-frame vectors be given as $\mathrm{v}_1^{\mathcal{I}(\mathrm{R})} = \frac{1}{\sqrt{3}}[1,-1,1]^\top$ and $\mathrm{v}_2^{\mathcal{I}(\mathrm{R})} = [0,0,1]^\top$, while body-frame vectors $\mathrm{v}_1^{\mathcal{B}(\mathrm{R})}$ and $\mathrm{v}_2^{\mathcal{B}(\mathrm{R})}$ are obtained by $\mathrm{v}_i^{\mathcal{B}(\mathrm{R})} = R^\top \mathrm{v}_i^{\mathcal{I}(\mathrm{R})} + \mathrm{b}_i^{\mathcal{B}(\mathrm{R})} + \omega_i^{\mathcal{B}(\mathrm{R})}$ for $i = 1,2$. Also, suppose that an additional noise vector $\omega_i^{\mathcal{B}(\mathrm{R})}$ with zero mean and STD of 0.15 corrupted the body-frame vector measurements and bias components $\mathrm{b}_1^{\mathcal{B}(\mathrm{R})} = 0.1\,[-1,1,0.5]^\top$ and $\mathrm{b}_2^{\mathcal{B}(\mathrm{R})} = 0.1\,[0,0,1]^\top$. The third vector of inertial-frame and body-frame is extracted by $\mathrm{v}_3^{\mathcal{I}(\mathrm{R})} = \mathrm{v}_1^{\mathcal{I}(\mathrm{R})} \times \mathrm{v}_2^{\mathcal{I}(\mathrm{R})}$ and $\mathrm{v}_3^{\mathcal{B}(\mathrm{R})} = \mathrm{v}_1^{\mathcal{B}(\mathrm{R})} \times \mathrm{v}_2^{\mathcal{B}(\mathrm{R})}$ and followed by normalization of the three vectors at each time instant according to (4.2). From vectorial measurements, the corrupted reconstructed attitude R_y is obtained by SVD (Markley (1988)) with $\tilde{R} = R_y^\top \hat{R}$, see Appendix B. The total simulation time is 15 seconds.

For a very large initial attitude error, the initial rotation of attitude estimate is given according to angle-axis parameterization in (2.7) by $\hat{R}(0) = \mathcal{R}_\alpha(\alpha, u/\|u\|)$ with $\alpha = 179.9\,(\text{deg})$ and $u = [1,5,3]^\top$ being very close to the unstable equilibria

such that $||\tilde{R}(0)||_I \approx 0.99999$. The initial conditions are

$$R(0) = \begin{bmatrix} 1 & 0 & 0 \\ 0 & 1 & 0 \\ 0 & 0 & 1 \end{bmatrix}, \quad \hat{R}(0) = \begin{bmatrix} -0.9429 & 0.2848 & 0.1729 \\ 0.2866 & 0.4286 & 0.8568 \\ 0.1700 & 0.8574 & -0.4857 \end{bmatrix}$$

Initial estimates for both filters are $\hat{b}(0) = [0,0,0]^\top$ and $\hat{\sigma}(0) = [0,0,0]^\top$. The same notation is used in derivations of both nonlinear stochastic filters. The design parameters were chosen as $\gamma_1 = 1$, $\gamma_2 = 1$, $k_b = 0.5$, $k_\sigma = 0.5$, $k_1 = 0.5$, $k_2 = 0.5$ and $\varepsilon = 0.5$. Additionally, the following color notation is used: green color demonstrates the true value, red illustrates the performance of Ito's filter and blue represents the performance of Stratonovich stochastic filter. Also, magenta refers to a measured value.

The true angular velocity (Ω) and the high values of noise and bias components introduced through the measurement process of Ω_m plotted against time are depicted in Figure 4.2. Also, Figure 4.3 presents the true body-frame vectors and their uncertain measurements. Figure 4.4 shows the tracked Euler angles (ϕ, θ, ψ) of Ito and Stratonovich stochastic attitude filters relative to true angles plotted against time. Figure 4.4 presents impressive tracking performance of the proposed stochastic filters. The mapping from $\mathbb{SO}(3)$ implies that $\tilde{\rho} \to \infty$ as $||\tilde{R}||_I \to 1$. Accordingly, Figure 4.5 demonstrates the convergence of the square error of Rodriguez vector $\tilde{\rho}^2$ from large error initialization to a very small value close to zero. Figure 4.6 confirms all the previous discussion using normalized Euclidean distance $||\tilde{R}||_I = \frac{1}{4}\mathrm{Tr}\left\{\mathbf{I}_3 - R^\top \hat{R}\right\}$ which shows remarkable stable and fast convergence to very small neighborhood of the origin. However, Ito stochastic filter is characterized by higher oscillatory performance compared to Stratonovich stochastic filter.

To further compare the steady-state performance of the proposed filters in terms of normalized Euclidean distance of the error ($||\tilde{R}||_I$), Table 4.1 summarizes statistical details of the mean and the STD of $||\tilde{R}||_I$. Both filters showed very small mean error of $||\tilde{R}||_I$ with $||\tilde{R}||_I$ being regulated to close neighborhood of the origin however, Stratonovich's filter showed a remarkable less mean errors and STD in comparison with Ito's filter. Numerical results included in Table 4.1 proves that the proposed nonlinear stochastic filters are robust as illustrated in Figure 4.4, 4.5, and 4.6.

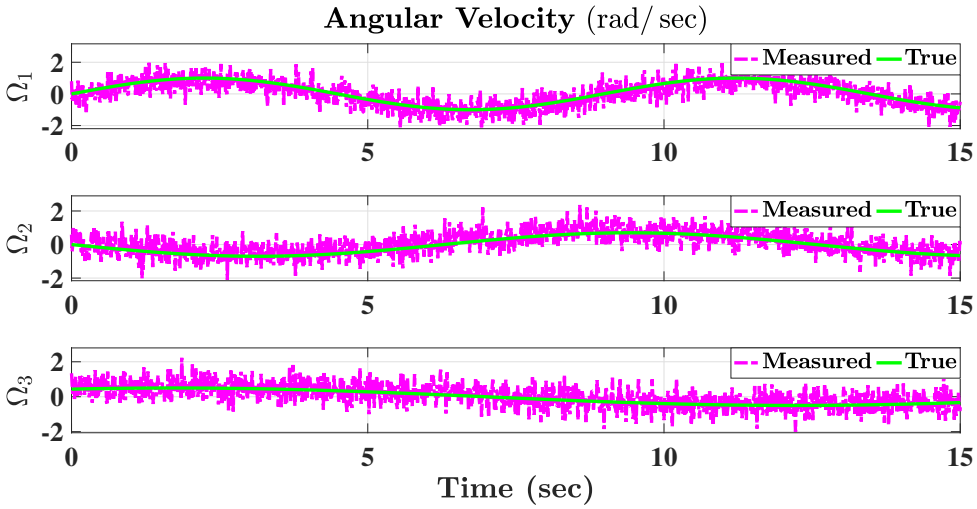

Figure 4.2: True and measured angular velocities.

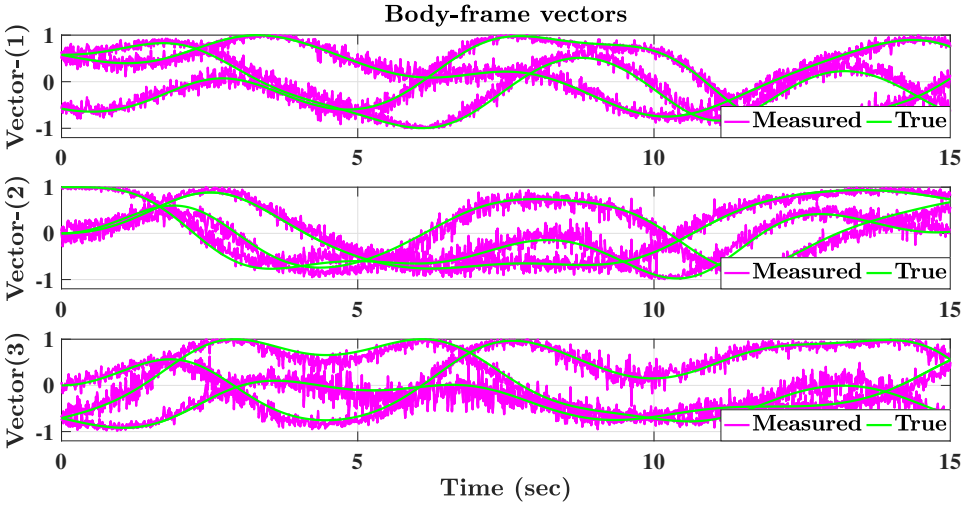

Figure 4.3: True and measured body-frame vectorial measurements.

Table 4.1: Statistical analysis of $||\tilde{R}||_I$ of the two proposed filter.

Output data of $||\tilde{R}||_I$ over the period (1-15 sec)		
Filter	Ito	Stratonovich
Mean	4.1×10^{-3}	2.8×10^{-3}
STD	3×10^{-3}	1.6×10^{-3}

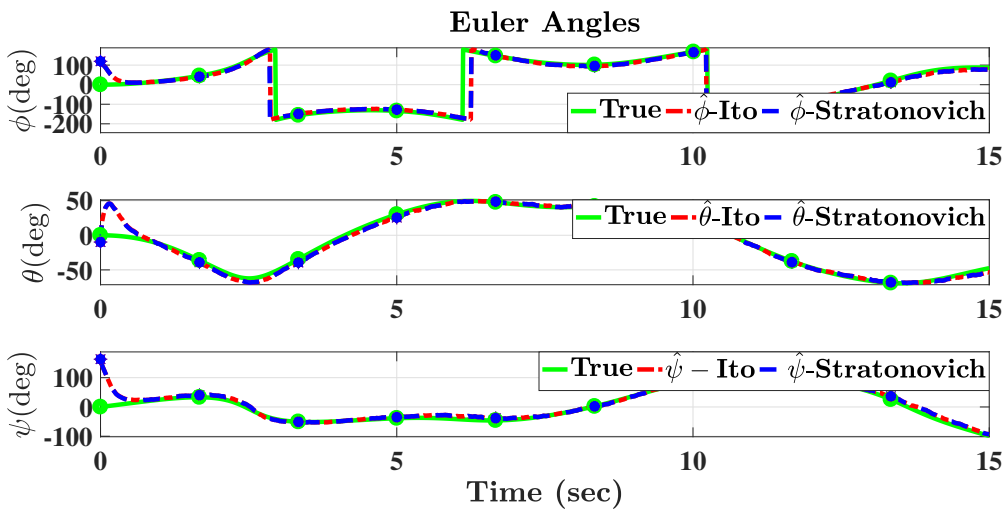

Figure 4.4: Tracking performance of Euler angles.

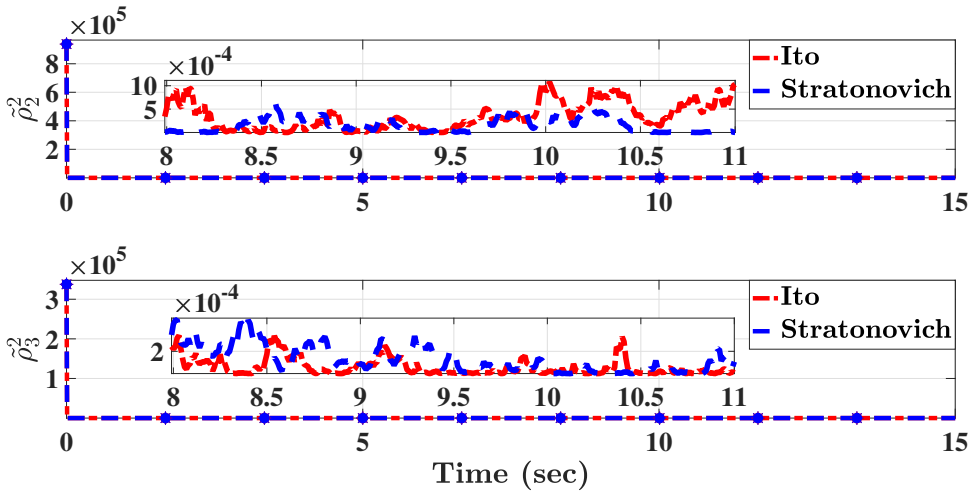

Figure 4.5: Rodriguez vector square error $\tilde{\rho}^2$.

Finally, Figure 4.7 and 4.8 illustrate the estimates of the stochastic filters plotted against time. It can be concluded from Figure 4.7 and 4.8 that the estimates of the proposed filter are stable and smooth.

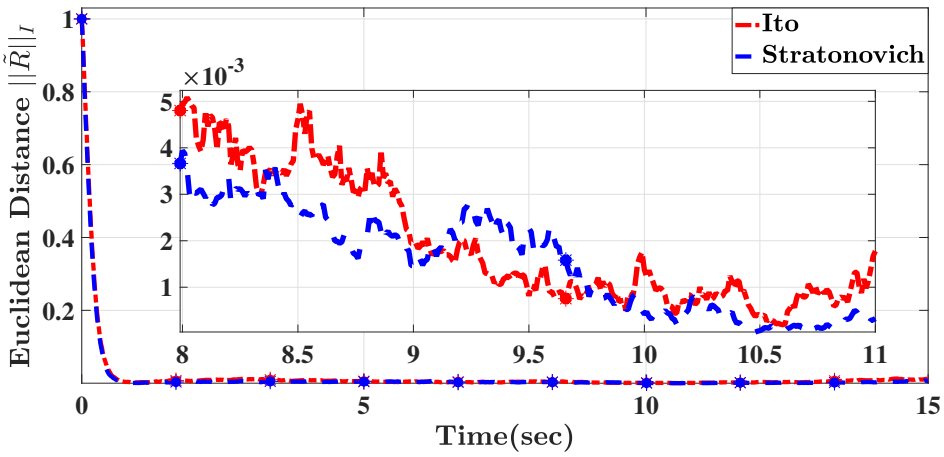

Figure 4.6: Tracking performance of normalized Euclidean distance error $||\tilde{R}||_I$.

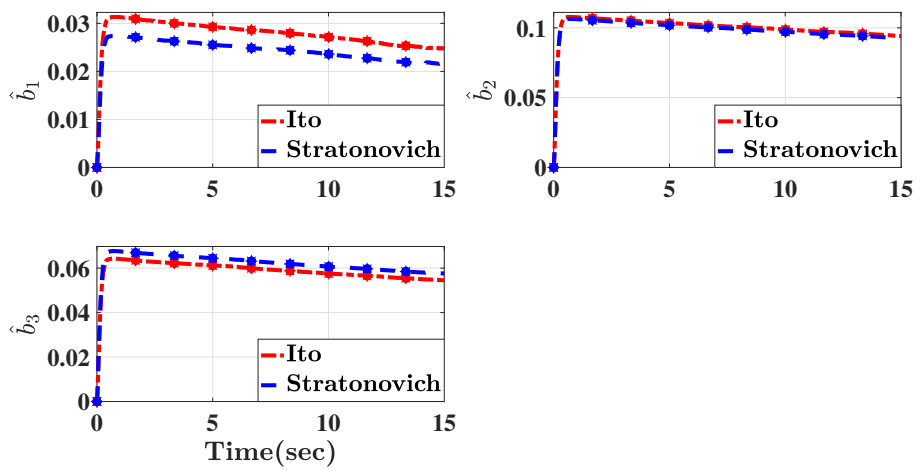

Figure 4.7: Estimates of stochastic attitude filters ($\hat{b}$).

Results show effectiveness and robustness of the two stochastic filters against bias and noise components contaminating angular velocity measurements, as well as uncertainty in vectorial measurements and large initial error. Stochastic filters have proven to be able to correct their attitude in a small amount of time requiring no prior information about the covariance matrix $\mathcal{Q}^2$ in order to obtain impressive estimation performance. The main advantage of Stratonovich stochastic filter, as mentioned in Subsection 4.3.4, is that the filter is applicable to white as well as colored noise. In addition, it had smaller mean square error and STD to Ito's filter as given in Table 4.1. Nonetheless, Ito stochastic filter requires less computational power.

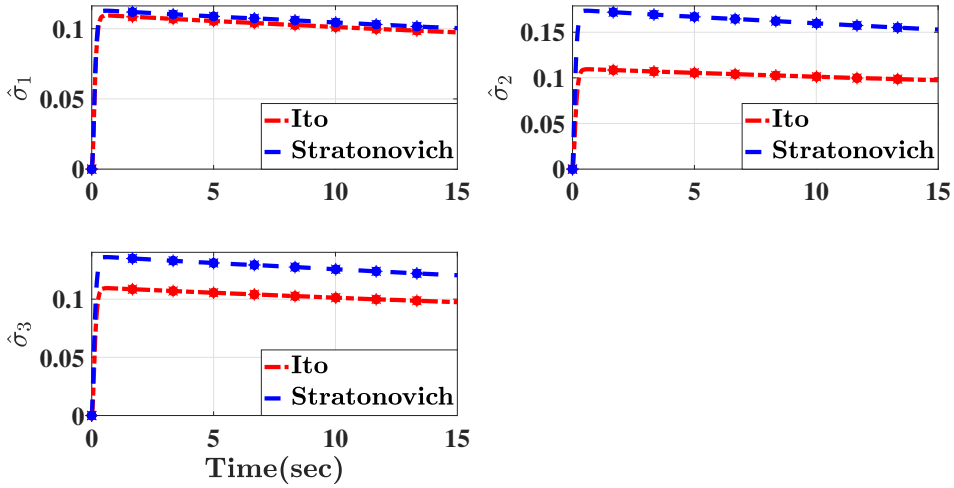

Figure 4.8: Estimates of stochastic attitude filters ($\hat{\sigma}$).

4.5 Conclusion

Deterministic filters neglect the noise associated with the angular velocity measurements in filter derivation. This can be clearly noticed in the selection of the potential function. However, an alternate potential function which has not been considered in the literature is able to significantly attenuate the effects of noise in angular velocities to lower levels. As such, this chapter reformulated the attitude problem to stochastic sense through Rodriguez vector parameterization. Two different nonlinear stochastic attitude filters on the Special Orthogonal Group $\mathbb{SO}(3)$ have been proposed. The first filter is developed in the sense of Ito and the second filter is driven in the sense of Stratonovich. The resulting estimators have proven to have fast convergence properties in the presence of high levels of noise in angular velocity and vectorial measurements.

Chapter 5
Nonlinear Explicit Stochastic Attitude Filter on $\mathbb{SO}(3)$

5.1 Introduction

This chapter proposes a nonlinear stochastic filter evolved on the Special Orthogonal Group $\mathbb{SO}(3)$ as a solution to the attitude filtering problem. One of the most common potential functions for nonlinear deterministic attitude observers is studied and reformulated to address the noise attached to the attitude dynamics. The resultant estimator and correction factor demonstrate convergence properties and remarkable ability to attenuate the noise. The stochastic dynamics of the attitude problem are mapped from $\mathbb{SO}(3)$ to Rodriguez vector. The proposed stochastic filter evolved on $\mathbb{SO}(3)$ guarantees that errors in the Rodriguez vector and estimates steer very close to the neighborhood of the origin and that the errors are semi-globally uniformly ultimately bounded in mean square. Simulation results illustrate the robustness of the proposed filter in the presence of high uncertainties in measurements. The results of this chapter were first published in Hashim et al. (2018a).

The rest of the chapter is organized as follows: gives an overview of mathematical notation and preliminaries. The problem is formulated in stochastic sense in Section 5.2. The nonlinear stochastic filter on $\mathbb{SO}(3)$ is proposed and the stability analysis is presented in Section 5.3. Section 5.4 demonstrates the numerical results. Finally, closing notes are provided in Section 5.5.

5.2 Problem Formulation

The attitude can be extracted from n-known non-collinear inertial vectors measured in a coordinate system fixed to the rigid body. Consider that the superscripts $\mathcal{I}$ and $\mathcal{B}$ refer to the vectors associated with the inertial-frame and body-frame, respectively. Let $\mathrm{v}_i^{\mathcal{B}(\mathrm{R})} \in \mathbb{R}^3$ be the ith measurement vector in the body-fixed frame for $i = 1, 2, \ldots, n$. Let $R \in \mathbb{SO}(3)$ denote the rotation matrix from body-fixed frame to a given inertial-fixed frame such that the body-fixed frame vector is defined by

$$\mathrm{v}_i^{\mathcal{B}(\mathrm{R})} = R^\top \mathrm{v}_i^{\mathcal{I}(\mathrm{R})} + \mathrm{b}_i^{\mathcal{B}(\mathrm{R})} + \omega_i^{\mathcal{B}(\mathrm{R})} \tag{5.1}$$

where $\mathrm{v}_i^{\mathcal{I}(\mathrm{R})} \in \mathbb{R}^3$ denotes the inertial-fixed frame vector while $\mathrm{b}_i^{\mathcal{B}(\mathrm{R})}$ and $\omega_i^{\mathcal{B}(\mathrm{R})}$ denote the additive bias and noise components of the associated body-frame vector, respectively, for all $\mathrm{b}_i^{\mathcal{B}(\mathrm{R})}, \omega_i^{\mathcal{B}(\mathrm{R})} \in \mathbb{R}^3$ and $i = 1, 2, \ldots, n$. The assumption that $n \geq 2$ is necessary for instantaneous three-dimensional attitude determination. It is common to employ the normalized values of reference and body-frame vectors in the process of attitude estimation such as

$$\upsilon_i^{\mathcal{I}(\mathrm{R})} = \frac{\mathrm{v}_i^{\mathcal{I}(\mathrm{R})}}{\left\| \mathrm{v}_i^{\mathcal{I}(\mathrm{R})} \right\|}, \quad \upsilon_i^{\mathcal{B}(\mathrm{R})} = \frac{\mathrm{v}_i^{\mathcal{B}(\mathrm{R})}}{\left\| \mathrm{v}_i^{\mathcal{B}(\mathrm{R})} \right\|} \tag{5.2}$$

and the attitude can be defined knowing $\upsilon_i^{\mathcal{I}(\mathrm{R})}$ and $\upsilon_i^{\mathcal{B}(\mathrm{R})}$. For the sake of simplicity, the body frame vector ($\mathrm{v}_i^{\mathcal{B}(\mathrm{R})}$) is considered to be noise and bias free in the stability analysis. In the Simulation Section, on the contrary, noise and bias are present in the measurements. The true attitude dynamics and the associated Rodriguez vector dynamics are given in (5.3) and (5.4), respectively, as

$$\dot{R} = R\,[\omega]_\times \tag{5.3}$$

$$\dot{\rho} = \frac{1}{2}\left(\mathbf{I}_3 + [\rho]_\times + \rho\rho^\top\right)\Omega \tag{5.4}$$

where $\Omega \in \mathbb{R}^3$ denotes the true value of angular velocity. Gyroscope or the rate gyros measures the angular velocity vector in the body-frame relative to the inertial-frame.

The measurement vector of angular velocity is

$$\Omega_m = \Omega + b + \omega \tag{5.5}$$

where b and ω denote the additive bias and noise components, respectively, for all $b, \omega \in \mathbb{R}^3$. The noise vector ω is assumed to be a Gaussian noise vector such that $\mathbb{E}[\omega] = 0$. The measurement of angular velocity vector is subject to additive noise and bias, which are characterized by randomness and unknown behavior, impairing the estimation process of the true attitude dynamics in (5.3) or (5.4). As such, (5.5) is assumed to be excited by a wide-band of random Gaussian noise process. Derivative of any Gaussian process yields a Gaussian process allowing the stochastic attitude dynamics to be written as a function of Brownian motion process vector (Khasminskii (1980))

$$\omega = \mathcal{Q}\frac{d\beta}{dt}$$

where $\mathcal{Q} \in \mathbb{R}^{3\times 3}$ is a non-negative unknown time-variant diagonal matrix. In addition, each parameter of $\mathcal{Q}$ in the diagonal is bounded with an unknown bound. The properties of Brownian motion process can be found in Deng et al. (2001); Hashim et al. (2018b); Ito and Rao (1984). The covariance component associated with noise ω can be defined by a diagonal matrix $\mathcal{Q}^2 = \mathcal{Q}\mathcal{Q}^\top$. Considering the attitude dynamics in (5.4) and replacing ω by $\mathcal{Q}d\beta/dt$, the stochastic differential equation in (5.4) can be expressed by

$$d\rho = f(\rho, b)\, dt + g(\rho)\, \mathcal{Q}d\beta \tag{5.6}$$

Similarly, the stochastic dynamics of (5.3) are

$$dR = R\left[\Omega_m - b\right]_\times dt - R\left[\mathcal{Q}d\beta\right]_\times \tag{5.7}$$

where $g(\rho) = -\frac{1}{2}\left(\mathbf{I}_3 + [\rho]_\times + \rho\rho^\top\right)$ and $f(\rho, b) = -g(\rho)(\Omega_m - b)$ with $g : \mathbb{R}^3 \to \mathbb{R}^{3\times 3}$ and $f : \mathbb{R}^3 \times \mathbb{R}^3 \to \mathbb{R}^3$. g is locally Lipschitz in ρ and f is locally Lipschitz in ρ and b. Accordingly, the dynamic system in (5.6) has a solution on $t \in [t_0, T]\, \forall t_0 \leq T < \infty$ in the mean square sense for any $\rho(t)$ such that $t \neq t_0$, $\rho - \rho_0$ is independent of $\{\beta(\tau), \tau \geq t\}, \forall t \in [t_0, T]$ (Deng et al. (2001); Hashim et al. (2018b)). Aiming to achieve adaptive stabilization of the unknown time-variant covariance matrix, let us

introduce the following unknown constant

$$\sigma = \left[\max\left\{\mathcal{Q}_{1,1}^2\right\}, \max\left\{\mathcal{Q}_{2,2}^2\right\}, \max\left\{\mathcal{Q}_{3,3}^2\right\}\right]^\top \tag{5.8}$$

where $\max\{\cdot\}$ is the maximum value of the associated element. From (5.5), and (5.8), it can be noticed that b and σ are bounded. It is important to introduce the following Lemma which will be useful in the subsequent filter derivation.

Lemma 5.1 *Let $R \in \mathbb{SO}(3)$, $\mathbf{M}_\mathrm{R} = (\mathbf{M}_\mathrm{R})^\top \in \mathbb{R}^{3\times 3}$, $\mathbf{M}_\mathrm{R}$ be positive-definite, and $\mathrm{Tr}\{\mathbf{M}_\mathrm{R}\} = 3$. Define $\bar{\mathbf{M}}_\mathrm{R} = \mathrm{Tr}\{\mathbf{M}_\mathrm{R}\}\mathbf{I}_3 - \mathbf{M}_\mathrm{R}$ and let the minimum singular values of $\bar{\mathbf{M}}_\mathrm{R}$ be $\underline{\lambda} := \underline{\lambda}\left(\bar{\mathbf{M}}_\mathrm{R}\right)$. Then, the following holds:*

$$\|\mathbf{M}_\mathrm{R} R\|_I = \frac{1}{2}\frac{\rho^\top \bar{\mathbf{M}}_\mathrm{R}\rho}{1+\|\rho\|^2} \tag{5.9}$$

$$\mathbf{vex}\left(\boldsymbol{\mathcal{P}}_a\left(\mathbf{M}_\mathrm{R} R\right)\right) = \frac{\left(\mathbf{I}_3 + [\rho]_\times\right)^\top \bar{\mathbf{M}}_\mathrm{R}}{1+\|\rho\|^2}\rho \tag{5.10}$$

$$\|\mathbf{M}_\mathrm{R} R\|_I \leq \frac{2}{\underline{\lambda}}\frac{||\mathbf{vex}\left(\boldsymbol{\mathcal{P}}_a\left(\mathbf{M}_\mathrm{R} R\right)\right)||^2}{1+\mathrm{Tr}\left\{\left(\mathbf{M}_\mathrm{R}\right)^{-1}\mathbf{M}_\mathrm{R} R\right\}} \tag{5.11}$$

Proof. See Appendix A.

Definition 5.1 *Ji and Xi (2006) The Rodriguez vector ρ of the stochastic dynamics in (5.6) is known to be semi-globally uniformly ultimately bounded (SGUUB) if for a compact set $\Lambda \in \mathbb{R}^3$ and any $\rho_0 = \rho(t_0)$, there exists a constant $\kappa > 0$, and a time constant $T = T(\kappa, \rho_0)$ such that $\mathbb{E}[\|\rho\|] < \kappa, \forall t > t_0 + T$.*

Definition 5.2 *Consider the stochastic dynamics in (5.6). For a given function $V(\rho) \in \mathcal{C}^2$, the differential operator $\mathcal{L}V$ is defined by*

$$\mathcal{L}V(\rho) = V_\rho^\top f(\rho, b) + \frac{1}{2}\mathrm{Tr}\left\{g(\rho)\mathcal{Q}^2 g^\top(\rho) V_{\rho\rho}\right\}$$

such that $V_\rho = \partial V/\partial\rho$, and $V_{\rho\rho} = \partial^2 V/\partial\rho^2$.

Lemma 5.2 *Deng et al. (2001) Let the stochastic dynamics in (5.6) be given a potential function $V \in \mathcal{C}^2$ such that $V : \mathbb{R}^3 \to \mathbb{R}^+$, class $\mathcal{K}_\infty$ functions $\varphi_1(\cdot)$ and $\varphi_2(\cdot)$,*

constants $c_1 > 0$ *and* $c_2 \geq 0$*, and a non-negative function* $\boldsymbol{Z}(\|\rho\|)$ *such that*

$$\varphi_1(\|\rho\|) \leq V(\rho) \leq \varphi_2(\|\rho\|) \tag{5.12}$$

$$\begin{aligned}\mathcal{L}V(\rho) =& V_\rho^\top f(\rho, b) + \frac{1}{2}\mathrm{Tr}\left\{g(\rho)\mathcal{Q}^2 g^\top(\rho) V_{\rho\rho}\right\} \\ \leq& -c_1 \boldsymbol{Z}(\|\rho\|) + c_2\end{aligned} \tag{5.13}$$

then for $\rho_0 \in \mathbb{R}^3$*, there exists almost a unique strong solution on* $[0, \infty)$ *for the dynamic system in* (5.6)*. The solution* ρ *is bounded in probability such that*

$$\mathbb{E}[V(\rho)] \leq V(\rho_0)\exp(-c_1 t) + \frac{c_2}{c_1} \tag{5.14}$$

Furthermore, if the inequality in (5.14) *holds, then* ρ *in* (5.6) *is SGUUB in the mean square.*

The proof of Lemma 5.2 can be found in Deng et al. (2001); Ji and Xi (2006). Consider the attitude $R \in \mathbb{SO}(3)$ and define the unstable set $\mathcal{U} \subseteq \mathbb{SO}(3)$ by $\mathcal{U} := \{R | \mathrm{Tr}\{R\} = -1, \boldsymbol{\mathcal{P}}_a(R) = 0\}$ such that the unstable set $\mathcal{U}$ is forward invariant for the stochastic dynamics in (5.3) which implies that $\rho = \infty$. As such, for almost any initial condition such that $R_0 \notin \mathcal{U}$ or $\rho_0 \in \mathbb{R}^3$, one has $-1 < \mathrm{Tr}\{R_0\} \leq 3$ and the trajectory of ρ converges to the neighborhood of the equilibrium point.

Lemma 5.3 *(Young's inequality) Let* y *and* x *be real values such that* $y, x \in \mathbb{R}^n$*. Then, for any* $c > 0$ *and* $d > 0$ *satisfying* $\frac{1}{c} + \frac{1}{d} = 1$ *with appropriately small positive constant* ε*, the following inequality is satisfied*

$$y^\top x \leq (1/c)\,\varepsilon^c \|y\|^c + (1/d)\,\varepsilon^{-d}\|x\|^d \tag{5.15}$$

5.3 Nonlinear Stochastic Filter on $\mathbb{SO}(3)$

A set of vectorial measurements $\upsilon_i^{\mathcal{I}}$ and $\upsilon_i^{\mathcal{B}}$ in (5.2) can be employed to reconstruct the uncertain attitude matrix R_y, however, obtaining R_y might be very computationally complex. Therefore, the objective is to propose a nonlinear stochastic attitude filter

which uses a set of vectorial measurements directly without the need of attitude reconstruction. Consider the error from body-frame to estimator-frame defined as

$$\tilde{R} = R\hat{R}^\top \tag{5.16}$$

Also, let the error in b and σ be given by

$$\tilde{b} = b - \hat{b} \tag{5.17}$$

$$\tilde{\sigma} = \sigma - \hat{\sigma} \tag{5.18}$$

Recall $\upsilon_i^{\mathcal{I}(\mathrm{R})}$ and $\upsilon_i^{\mathcal{B}(\mathrm{R})}$ from (5.2) for $i = 1, \ldots, n$. Define

$$\begin{aligned} \mathbf{M}_\mathrm{R} = (\mathbf{M}_\mathrm{R})^\top &= \sum_{i=1}^{n} s_i \upsilon_i^{\mathcal{I}(\mathrm{R})} \left(\upsilon_i^{\mathcal{I}(\mathrm{R})}\right)^\top \\ M^{\mathcal{B}} = \left(M^{\mathcal{B}}\right)^\top &= \sum_{i=1}^{n} s_i \upsilon_i^{\mathcal{B}(\mathrm{R})} \left(\upsilon_i^{\mathcal{B}(\mathrm{R})}\right)^\top = R^\top \mathbf{M}_\mathrm{R} R \end{aligned} \tag{5.19}$$

with $s_i > 0$ being the confidence level of the ith sensor measurement. Each of $\mathbf{M}_\mathrm{R}$ and $M^{\mathcal{B}}$ are symmetric matrices. Consider $\upsilon_i^{\mathcal{I}(\mathrm{R})}$ and $\upsilon_i^{\mathcal{B}(\mathrm{R})}$ from (5.2) for $i = 1, \ldots, n$ and at least two non-collinear vectors available ($n \geq 2$). If $n = 2$, the third vector is obtained by $\upsilon_3^{\mathcal{I}(\mathrm{R})} = \upsilon_1^{\mathcal{I}(\mathrm{R})} \times \upsilon_2^{\mathcal{I}(\mathrm{R})}$ and $\upsilon_3^{\mathcal{B}(\mathrm{R})} = \upsilon_1^{\mathcal{B}(\mathrm{R})} \times \upsilon_2^{\mathcal{B}(\mathrm{R})}$ which is non-collinear with the other two vectors such that $\mathrm{rank}\,(\mathbf{M}_\mathrm{R}) = \mathrm{rank}\left(M^{\mathcal{B}}\right) = 3$ full rank. Consequently, the three eigenvalues of $\mathbf{M}_\mathrm{R}$ and $M^{\mathcal{B}}$ are greater than zero. Let $\bar{\mathbf{M}}_\mathrm{R} = \mathrm{Tr}\,\{\mathbf{M}_\mathrm{R}\}\,\mathbf{I}_3 - \mathbf{M}_\mathrm{R} \in \mathbb{R}^{3\times 3}$, provided that $\mathrm{rank}\,(\mathbf{M}_\mathrm{R}) = 3$, the following statements hold (Bullo and Lewis (2004) page. 553):

i. $\bar{\mathbf{M}}_\mathrm{R}$ is a symmetric positive-definite matrix.

ii. Define the three eigenvalues of $\mathbf{M}_\mathrm{R}$ by $\lambda\,(\mathbf{M}_\mathrm{R}) = \{\lambda_1, \lambda_2, \lambda_3\}$, then $\lambda\left(\bar{\mathbf{M}}_\mathrm{R}\right) = \{\lambda_3 + \lambda_2, \lambda_3 + \lambda_1, \lambda_2 + \lambda_1\}$ such that the minimum singular value $\underline{\lambda}\left(\bar{\mathbf{M}}_\mathrm{R}\right) > 0$.

In all the discussion that follows it is assumed that the above statements hold. Consider $\sum_{i=1}^{n} s_i = 3$ and define

$$\hat{\upsilon}_i^{\mathcal{B}(\mathrm{R})} = \hat{R}^\top \upsilon_i^{\mathcal{I}(\mathrm{R})} \tag{5.20}$$

From the identity in (2.11), one can find

$$\begin{aligned}
&\sum_{i=1}^{n} \frac{s_i}{2} \left[\upsilon_i^{\mathcal{B}(\mathrm{R})} \times \hat{\upsilon}_i^{\mathcal{B}(\mathrm{R})} \right]_\times \\
&= \sum_{i=1}^{n} \frac{s_i}{2} \left(\hat{\upsilon}_i^{\mathcal{B}(\mathrm{R})} \left(\upsilon_i^{\mathcal{B}(\mathrm{R})} \right)^\top - \upsilon_i^{\mathcal{B}(\mathrm{R})} \left(\hat{\upsilon}_i^{\mathcal{B}(\mathrm{R})} \right)^\top \right) \\
&= \frac{1}{2} \sum_{i=1}^{n} k_i \left(\hat{R}^\top \upsilon_i^{\mathcal{I}(\mathrm{R})} \left(\upsilon_i^{\mathcal{I}(\mathrm{R})} \right)^\top R - R^\top \upsilon_i^{\mathcal{I}(\mathrm{R})} \left(\upsilon_i^{\mathcal{I}(\mathrm{R})} \right)^\top \hat{R} \right) \\
&= \frac{1}{2} \hat{R}^\top \left(\mathbf{M}_\mathrm{R} \tilde{R} - \tilde{R}^\top \mathbf{M}_\mathrm{R} \right) \hat{R} = \hat{R}^\top \boldsymbol{\mathcal{P}}_a \left(\mathbf{M}_\mathrm{R} \tilde{R} \right) \hat{R}
\end{aligned}$$

Hence, the following components can be obtained in terms of vector measurements which will be used in the proposed filter design

$$\mathbf{vex}\left(\boldsymbol{\mathcal{P}}_a\left(\mathbf{M}_\mathrm{R}\tilde{R}\right)\right) = \mathbf{vex}\left(\boldsymbol{\mathcal{P}}_a\left(\mathbf{M}_\mathrm{R}\tilde{R}\right)\right) = \hat{R}\sum_{i=1}^{n}\frac{s_i}{2}\upsilon_i^{\mathcal{B}(\mathrm{R})} \times \hat{\upsilon}_i^{\mathcal{B}(\mathrm{R})} \tag{5.21}$$

$$\begin{aligned}
||\mathbf{M}_\mathrm{R}\tilde{R}||_I &= \frac{1}{4}\mathrm{Tr}\left\{\mathbf{M}_\mathrm{R}\left(\mathbf{I}_3 - \tilde{R}\right)\right\} \\
&= \frac{3}{4} - \frac{1}{4}\mathrm{Tr}\left\{\hat{R}\sum_{i=1}^{n}\left(s_i\hat{\upsilon}_i^{\mathcal{B}(\mathrm{R})}\left(\upsilon_i^{\mathcal{B}(\mathrm{R})}\right)^\top\right)\hat{R}^\top\right\}
\end{aligned} \tag{5.22}$$

$$\begin{aligned}
\Upsilon\left(\mathbf{M}_\mathrm{R}, \tilde{R}\right) = &\mathrm{Tr}\left\{\left(\sum_{i=1}^{n} s_i \upsilon_i^{\mathcal{I}(\mathrm{R})}\left(\upsilon_i^{\mathcal{I}(\mathrm{R})}\right)^\top\right)^{-1}\right. \\
&\left.\times \hat{R}\sum_{i=1}^{n}\left(s_i\hat{\upsilon}_i^{\mathcal{B}(\mathrm{R})}\left(\upsilon_i^{\mathcal{B}(\mathrm{R})}\right)^\top\right)\hat{R}^\top\right\}
\end{aligned} \tag{5.23}$$

where $\left[\hat{R}\sum_{i=1}^{n}\frac{s_i}{2}\upsilon_i^{\mathcal{B}(\mathrm{R})} \times \hat{\upsilon}_i^{\mathcal{B}(\mathrm{R})}\right]_\times = \hat{R}\sum_{i=1}^{n}\frac{s_i}{2}\left[\upsilon_i^{\mathcal{B}(\mathrm{R})} \times \hat{\upsilon}_i^{\mathcal{B}(\mathrm{R})}\right]_\times \hat{R}^\top$ as in (2.12). Define $\underline{\lambda} := \underline{\lambda}\left(\bar{\mathbf{M}}_\mathrm{R}\right)$, $\Upsilon := \Upsilon\left(\mathbf{M}_\mathrm{R}, \tilde{R}\right)$, and $\mathbf{vex}\left(\boldsymbol{\mathcal{P}}_a\left(\mathbf{M}_\mathrm{R}\tilde{R}\right)\right) := \mathbf{vex}\left(\boldsymbol{\mathcal{P}}_a\left(\mathbf{M}_\mathrm{R}\tilde{R}\right)\right)$,

and consider the following nonlinear filter design on $\mathbb{SO}(3)$

$$\dot{\hat{R}} = \hat{R}\left[\Omega_m - \hat{b}\right]_\times + [W]_\times \hat{R} \tag{5.24}$$

$$\dot{\hat{b}} = -\gamma ||\mathbf{M}_\mathrm{R}\tilde{R}||_I \hat{R}^\top \mathbf{vex}\left(\boldsymbol{\mathcal{P}}_a\left(\mathbf{M}_\mathrm{R}\tilde{R}\right)\right) - \gamma k_b \hat{b} \tag{5.25}$$

$$\dot{\hat{\sigma}} = \frac{\gamma ||\mathbf{M}_\mathrm{R}\tilde{R}||_I}{\underline{\lambda}} \frac{\mathrm{diag}\left(\hat{R}^\top \mathbf{vex}\left(\boldsymbol{\mathcal{P}}_a\left(\mathbf{M}_\mathrm{R}\tilde{R}\right)\right)\right)}{1+\Upsilon} \hat{R}^\top \mathbf{vex}\left(\boldsymbol{\mathcal{P}}_a\left(\mathbf{M}_\mathrm{R}\tilde{R}\right)\right) - \gamma k_\sigma \hat{\sigma} \tag{5.26}$$

$$W = \frac{k_w}{\varepsilon\underline{\lambda}} \frac{(1+\Upsilon)^2 \underline{\lambda}^2 + 1}{1+\Upsilon} \mathbf{vex}\left(\boldsymbol{\mathcal{P}}_a\left(\mathbf{M}_\mathrm{R}\tilde{R}\right)\right) + \frac{1}{\underline{\lambda}} \frac{\hat{R}\mathrm{diag}\left(\hat{R}^\top \mathbf{vex}\left(\boldsymbol{\mathcal{P}}_a\left(\mathbf{M}_\mathrm{R}\tilde{R}\right)\right)\right)}{1+\Upsilon} \hat{\sigma} \tag{5.27}$$

where $\mathbf{vex}\left(\boldsymbol{\mathcal{P}}_a\left(\mathbf{M}_\mathrm{R}\tilde{R}\right)\right)$, $\left\|\mathbf{M}_\mathrm{R}\tilde{R}\right\|_I$, and $\Upsilon\left(\mathbf{M}_\mathrm{R}, \tilde{R}\right)$ are defined in (5.21), (5.22), and (5.23) in terms of vectorial measurements, respectively, $\mathrm{diag}(\cdot)$ is a diagonal of the associated component, k_w, k_b, k_σ, and γ are positive constants, and $\hat{b}$ and $\hat{\sigma}$ are the estimate of b and σ, respectively.

Theorem 5.1 *Consider the observer in (5.24), (5.25), (5.26) and (5.27) coupled with angular velocity measurements in (5.5) and the normalized vectors in (5.2). Assume that two or more body-frame non-collinear vectors are available for measurements such that* $\mathbf{M}_\mathrm{R}$ *in (5.19) is nonsingular. Then, for angular velocity measurements contaminated with noise and* $\tilde{\rho} \in \mathbb{R}^3$, $\tilde{\rho}$, $\tilde{b}$ *and* $\tilde{\sigma}$ *are regulated to an arbitrarily small neighborhood of the origin in probability; and* $\left[\tilde{\rho}^\top, \tilde{b}^\top, \tilde{\sigma}^\top\right]^\top$ *is SGUUB in mean square.*

Proof: Let the error in attitude be $\tilde{R} = R\hat{R}^\top$ as given in (5.16) and consider (5.17) and (5.18). In view of (5.3) and (5.24), the derivative of attitude error in incremental form becomes

$$\begin{aligned} d\tilde{R} =& -R\left[\Omega_m - \hat{b}\right]_\times \hat{R}^\top dt - R\hat{R}^\top [W]_\times dt \\ &+ R\left[\Omega_m - b - \mathcal{Q}\frac{d\beta}{dt}\right]_\times \hat{R}^\top dt \\ =& -R[\tilde{\sigma}]_\times \hat{R}^\top dt - R\hat{R}^\top [W]_\times dt - R[\mathcal{Q}d\beta]_\times \hat{R}^\top \\ =& -\tilde{R}\left[\hat{R}\tilde{b} + W\right]_\times dt - \tilde{R}\left[\hat{R}\mathcal{Q}d\beta\right]_\times \end{aligned} \tag{5.28}$$

where $\left[\hat{R}\tilde{\sigma}\right]_\times = \hat{R}\left[\tilde{\sigma}\right]_\times \hat{R}^\top$ as in (2.12). Recalling the extraction of Rodriguez vector dynamics from (5.7) to (5.6), the Rodriguez error vector dynamic in (5.28) can be expressed as

$$d\tilde{\rho} = \tilde{f}dt + \tilde{g}\hat{R}\mathcal{Q}d\beta \tag{5.29}$$

where $\tilde{\rho}$ is a Rodriguez error vector associated with $\tilde{R}$, $\tilde{g} = -\frac{1}{2}\left(\mathbf{I}_3 + [\tilde{\rho}]_\times + \tilde{\rho}\tilde{\rho}^\top\right)$, and $\tilde{f} = \tilde{g}\left(\hat{R}\tilde{b} + W\right)$.

Remark 5.1 *From literature, one of the traditional potential functions of the adaptive filter is similar to Crassidis et al. (2007); Mahony et al. (2008); Zlotnik and Forbes (2017)*

$$V\left(\tilde{R}, \tilde{b}\right) = \frac{1}{4}\mathrm{Tr}\left\{\mathbf{M}_\mathrm{R}\left(\mathbf{I}_3 - \tilde{R}\right)\right\} + \frac{1}{2\gamma}\tilde{b}^\top\tilde{b} \tag{5.30}$$

Given (5.9), the expression in (5.30) is equivalent to (5.31) in Rodriquez vector form

$$V\left(\tilde{\rho}, \tilde{b}\right) = \frac{1}{2}\frac{\tilde{\rho}^\top\bar{\mathbf{M}}_\mathrm{R}\tilde{\rho}}{1 + \|\tilde{\rho}\|^2} + \frac{1}{2\gamma}\tilde{b}^\top\tilde{b} \tag{5.31}$$

The weakness of the potential function in (5.31) is that the trace component of the operator $\mathcal{L}V$ in Definition 5.2 for the dynamic system in (5.6) at $\tilde{\rho} = 0$ can be evaluated by

$$\frac{1}{2}\mathrm{Tr}\left\{\hat{R}^\top\tilde{g}^\top V_{\tilde{\rho}\tilde{\rho}}\tilde{g}\hat{R}\mathcal{Q}^2\right\}\Big|_{\tilde{\rho}=0} = \frac{1}{8}\mathrm{Tr}\left\{\hat{R}^\top\bar{\mathbf{M}}_\mathrm{R}\hat{R}\mathcal{Q}^2\right\}$$

such that the significant impact of $\mathcal{Q}^2$ cannot be lessened.

Therefore, consider the following smooth attitude potential function

$$V\left(\tilde{\rho}, \tilde{b}, \tilde{\sigma}\right) = \frac{1}{4}\left(\frac{\tilde{\rho}^\top\bar{\mathbf{M}}_\mathrm{R}\tilde{\rho}}{1 + \|\tilde{\rho}\|^2}\right)^2 + \frac{1}{2\gamma}\tilde{b}^\top\tilde{b} + \frac{1}{2\gamma}\tilde{\sigma}^\top\tilde{\sigma} \tag{5.32}$$

For $V := V\left(\tilde{\rho}, \tilde{b}, \tilde{\sigma}\right)$, the differential operator $\mathcal{L}V$ in Definition 5.2 can be written as

$$\mathcal{L}V = V_{\tilde{\rho}}^\top\tilde{f} + \frac{1}{2}\mathrm{Tr}\left\{\hat{R}^\top\tilde{g}^\top V_{\tilde{\rho}\tilde{\rho}}\tilde{g}\hat{R}\mathcal{Q}^2\right\} - \frac{1}{\gamma}\tilde{b}^\top\dot{\tilde{b}} - \frac{1}{\gamma}\tilde{\sigma}^\top\dot{\tilde{\sigma}} \tag{5.33}$$

Hence, the first and second partial derivatives of (5.32) can be defined respectively, as follows

$$V_{\tilde{\rho}} = \frac{\tilde{\rho}^\top \bar{\mathbf{M}}_{\mathrm{R}} \tilde{\rho}}{\left(1+\|\tilde{\rho}\|^2\right)^3} \left(\left(1+\|\tilde{\rho}\|^2\right)\mathbf{I}_3 - \tilde{\rho}\tilde{\rho}^\top\right)\bar{\mathbf{M}}_{\mathrm{R}}\tilde{\rho} \tag{5.34}$$

$$\begin{aligned} V_{\tilde{\rho}\tilde{\rho}} =& \frac{\tilde{\rho}^\top \bar{\mathbf{M}}_{\mathrm{R}} \tilde{\rho}}{\left(1+\|\tilde{\rho}\|^2\right)^2}\bar{\mathbf{M}}_{\mathrm{R}} + 2\frac{\bar{\mathbf{M}}_{\mathrm{R}}\tilde{\rho}\tilde{\rho}^\top\bar{\mathbf{M}}_{\mathrm{R}}}{\left(1+\|\tilde{\rho}\|^2\right)^2} \\ &- 4\frac{\tilde{\rho}^\top \bar{\mathbf{M}}_{\mathrm{R}} \tilde{\rho}}{\left(1+\|\tilde{\rho}\|^2\right)^3}\left(\bar{\mathbf{M}}_{\mathrm{R}}\tilde{\rho}\tilde{\rho}^\top + \tilde{\rho}\tilde{\rho}^\top\bar{\mathbf{M}}_{\mathrm{R}}\right) \\ &+ \frac{\left(\tilde{\rho}^\top \bar{\mathbf{M}}_{\mathrm{R}} \tilde{\rho}\right)^2}{\left(1+\|\tilde{\rho}\|^2\right)^4}\left(6\tilde{\rho}\tilde{\rho}^\top - \left(1+\|\tilde{\rho}\|^2\right)\mathbf{I}_3\right) \end{aligned} \tag{5.35}$$

from (5.29) and (5.34), the first part of (5.33) can be defined by

$$\begin{aligned} V_{\tilde{\rho}}^\top \tilde{f} &= -\frac{1}{2}\frac{\tilde{\rho}^\top \bar{\mathbf{M}}_{\mathrm{R}}\tilde{\rho}\tilde{\rho}^\top\bar{\mathbf{M}}_{\mathrm{R}}}{\left(1+\|\tilde{\rho}\|^2\right)^2}\left(\mathbf{I}_3 + [\tilde{\rho}]_\times\right)\left(\hat{R}\tilde{b} + W\right)dt \\ &= -||\mathbf{M}_{\mathrm{R}}\tilde{R}||_I \mathbf{vex}\left(\boldsymbol{\mathcal{P}}_a\left(\mathbf{M}_{\mathrm{R}}\tilde{R}\right)\right)^\top\left(\hat{R}\tilde{b} + W\right)dt \end{aligned} \tag{5.36}$$

where $||\mathbf{M}_{\mathrm{R}}\tilde{R}||_I$ and $\mathbf{vex}\left(\boldsymbol{\mathcal{P}}_a\left(\mathbf{M}_{\mathrm{R}}\tilde{R}\right)\right)$ are defined in (5.9) and (5.10), respectively. From (5.29) and (5.35), the second part of (5.33) can be obtained by

$$\begin{aligned} \frac{1}{2}\mathrm{Tr}\left\{\hat{R}^\top\tilde{g}^\top V_{\tilde{\rho}\tilde{\rho}}\tilde{g}\hat{R}\mathcal{Q}^2\right\} =& -\frac{1}{4}\mathrm{Tr}\left\{\frac{1}{4}\left(\frac{\tilde{\rho}^\top\bar{\mathbf{M}}_{\mathrm{R}}\tilde{\rho}}{1+\|\tilde{\rho}\|^2}\right)^2\hat{R}\mathcal{Q}^2\hat{R}^\top\right\} \\ &+ \frac{1}{8}\frac{\tilde{\rho}^\top\bar{\mathbf{M}}_{\mathrm{R}}\tilde{\rho}}{\left(1+\|\tilde{\rho}\|^2\right)^2}\mathrm{Tr}\left\{\left(\mathbf{I}_3+[\tilde{\rho}]_\times\right)^\top\bar{\mathbf{M}}_{\mathrm{R}}\left(\mathbf{I}_3+[\tilde{\rho}]_\times\right)\hat{R}\mathcal{Q}^2\hat{R}^\top\right. \\ &\left. - \left(\tilde{\rho}\tilde{\rho}^\top\bar{\mathbf{M}}_{\mathrm{R}}\left(\mathbf{I}_3+[\tilde{\rho}]_\times\right) + \left(\mathbf{I}_3+[\tilde{\rho}]_\times\right)^\top\bar{\mathbf{M}}_{\mathrm{R}}\tilde{\rho}\tilde{\rho}^\top\right)\hat{R}\mathcal{Q}^2\hat{R}^\top\right\} \\ &+ \mathrm{Tr}\left\{\frac{\left(\mathbf{I}_3+[\tilde{\rho}]_\times\right)^\top\bar{\mathbf{M}}_{\mathrm{R}}\tilde{\rho}\tilde{\rho}^\top\bar{\mathbf{M}}_{\mathrm{R}}\left(\mathbf{I}_3+[\tilde{\rho}]_\times\right)}{4\left(1+\|\tilde{\rho}\|^2\right)^2}\hat{R}\mathcal{Q}^2\hat{R}^\top\right\} \end{aligned} \tag{5.37}$$

from (5.9) and (5.10), one has

$$\begin{aligned}
&\frac{1}{2}\mathrm{Tr}\left\{\hat{R}^\top \tilde{g}^\top V_{\tilde{\rho}\tilde{\rho}} \tilde{g}\hat{R}\mathcal{Q}^2\right\} = \\
&-\frac{1}{4}\mathrm{Tr}\left\{||\mathbf{M}_{\mathrm{R}}\tilde{R}||_I \left(\frac{\left(\mathbf{I}_3 + [\tilde{\rho}]_\times\right)^\top \mathbf{M}_{\mathrm{R}}\left(\mathbf{I}_3 + [\tilde{\rho}]_\times\right)}{1+\|\tilde{\rho}\|^2}\right.\right. \\
&\qquad\qquad \left.\left. +||\mathbf{M}_{\mathrm{R}}\tilde{R}||_I \mathbf{I}_3\right)\hat{R}\mathcal{Q}^2\hat{R}^\top\right\} \\
&+\frac{1}{4}\mathrm{Tr}\left\{\left(\mathbf{vex}\left(\boldsymbol{\mathcal{P}}_a\left(\mathbf{M}_{\mathrm{R}}\tilde{R}\right)\right)\mathbf{vex}\left(\boldsymbol{\mathcal{P}}_a\left(\mathbf{M}_{\mathrm{R}}\tilde{R}\right)\right)^\top\right.\right. \\
&\qquad \left.\left. +||\mathbf{M}_{\mathrm{R}}\tilde{R}||_I\left(3\mathbf{I}_3 - 2\mathbf{vex}\left(\boldsymbol{\mathcal{P}}_a\left(\mathbf{M}_{\mathrm{R}}\tilde{R}\right)\right)\tilde{\rho}^\top\right)\right)\right\}\hat{R}\mathcal{Q}^2\hat{R}^\top
\end{aligned} \tag{5.38}$$

where the first part of (5.38) is negative for all $\tilde{\rho} \neq 0$ and $\mathcal{Q}^2 \neq 0$. From **Appendix A**, one can easily find that for $\Upsilon := \Upsilon\left(\mathbf{M}_{\mathrm{R}}, \tilde{R}\right)$

$$1 + ||\tilde{\rho}||^2 = \frac{1}{1 - ||\tilde{R}||_I} = \frac{4}{1+\Upsilon} \tag{5.39}$$

Accordingly, from **Appendix A**, $\mathbf{vex}\left(\boldsymbol{\mathcal{P}}_a\left(\tilde{R}\right)\right) = 2\tilde{\rho}/\left(1 + ||\tilde{\rho}||^2\right)$, and from (5.10)

$$\mathbf{vex}\left(\boldsymbol{\mathcal{P}}_a\left(\mathbf{M}_{\mathrm{R}}\tilde{R}\right)\right) = \frac{\left(\mathbf{I}_3 + [\tilde{\rho}]_\times\right)^\top \bar{\mathbf{M}}_{\mathrm{R}}\tilde{\rho}}{\left(1 + ||\tilde{\rho}||^2\right)} \tag{5.40}$$

In addition to the result in (5.39), one has

$$\begin{aligned}
&\underline{\lambda}\mathbf{vex}\left(\boldsymbol{\mathcal{P}}_a\left(\mathbf{M}_{\mathrm{R}}\tilde{R}\right)\right)^\top \hat{R}\mathcal{Q}^2\hat{R}^\top\tilde{\rho} \\
&\qquad \leq 2\frac{\mathbf{vex}\left(\boldsymbol{\mathcal{P}}_a\left(\mathbf{M}_{\mathrm{R}}\tilde{R}\right)\right)^\top \hat{R}\mathrm{diag}\left(\hat{R}^\top\mathbf{vex}\left(\boldsymbol{\mathcal{P}}_a\left(\mathbf{M}_{\mathrm{R}}\tilde{R}\right)\right)\right)}{1+\Upsilon}\sigma
\end{aligned} \tag{5.41}$$

Define $q = \left[\mathcal{Q}_{1,1}, \mathcal{Q}_{2,2}, \mathcal{Q}_{3,3}\right]^\top$, as $\mathrm{Tr}\left\{\hat{R}\mathcal{Q}^2\hat{R}^\top\right\} = \mathrm{Tr}\left\{\mathcal{Q}^2\right\}$, thereby, the following inequality holds

$$\begin{aligned}
&\mathrm{Tr}\left\{\mathbf{vex}\left(\boldsymbol{\mathcal{P}}_a\left(\mathbf{M}_{\mathrm{R}}\tilde{R}\right)\right)\mathbf{vex}\left(\boldsymbol{\mathcal{P}}_a\left(\mathbf{M}_{\mathrm{R}}\tilde{R}\right)\right)^\top\hat{R}\mathcal{Q}^2\hat{R}^\top\right\} \\
&\qquad \leq \|q\|^2\left\|\mathbf{vex}\left(\boldsymbol{\mathcal{P}}_a\left(\mathbf{M}_{\mathrm{R}}\tilde{R}\right)\right)\right\|^2
\end{aligned} \tag{5.42}$$

Let us combine the results in (5.41) and (5.42) with (5.38). Next, we express the differential operator in (5.33) in its complete form

$$\begin{aligned}\mathcal{L}V \leq &- ||\mathbf{M}_{\mathrm{R}}\tilde{R}||_I \mathbf{vex}\left(\boldsymbol{\mathcal{P}}_a\left(\mathbf{M}_{\mathrm{R}}\tilde{R}\right)\right)^\top\left(\hat{R}\tilde{b}+W\right)\\ &- \frac{1}{4}\mathrm{Tr}\left\{||\mathbf{M}_{\mathrm{R}}\tilde{R}||_I\left(\frac{\left(\mathbf{I}_3+[\tilde{\rho}]_\times\right)^\top\mathbf{M}_{\mathrm{R}}\left(\mathbf{I}_3+[\tilde{\rho}]_\times\right)}{1+\|\tilde{\rho}\|^2}+||\mathbf{M}_{\mathrm{R}}\tilde{R}||_I\mathbf{I}_3\right)\hat{R}\mathcal{Q}^2\hat{R}^\top\right\}\\ &+ \frac{1}{4}\mathrm{Tr}\left\{\left(\left\|\mathbf{vex}\left(\boldsymbol{\mathcal{P}}_a\left(\mathbf{M}_{\mathrm{R}}\tilde{R}\right)\right)\right\|^2+3||\mathbf{M}_{\mathrm{R}}\tilde{R}||_I\right)\|q\|^2\right\}\\ &+ \frac{||\mathbf{M}_{\mathrm{R}}\tilde{R}||_I}{\underline{\lambda}}\mathbf{vex}\left(\boldsymbol{\mathcal{P}}_a\left(\mathbf{M}_{\mathrm{R}}\tilde{R}\right)\right)^\top\hat{R}\frac{\mathrm{diag}\left(\hat{R}^\top\mathbf{vex}\left(\boldsymbol{\mathcal{P}}_a\left(\mathbf{M}_{\mathrm{R}}\tilde{R}\right)\right)\right)}{1+\Upsilon}\sigma\\ &- \frac{1}{\gamma}\tilde{b}^\top\dot{\hat{b}}-\frac{1}{\gamma}\tilde{\sigma}^\top\dot{\hat{\sigma}}\end{aligned} \tag{5.43}$$

Considering (5.15) in Lemma 5.3, one obtains

$$\begin{aligned}\|q\|^2\left\|\mathbf{vex}\left(\boldsymbol{\mathcal{P}}_a\left(\mathbf{M}_{\mathrm{R}}\tilde{R}\right)\right)\right\|^2 &\leq \frac{\varepsilon}{2}\|q\|^4+\frac{1}{2\varepsilon}\left\|\mathbf{vex}\left(\boldsymbol{\mathcal{P}}_a\left(\mathbf{M}_{\mathrm{R}}\tilde{R}\right)\right)\right\|^4\\ \|q\|^2||\mathbf{M}_{\mathrm{R}}\tilde{R}||_I &\leq \frac{\varepsilon}{2}\|q\|^4+\frac{1}{2\varepsilon}||\mathbf{M}_{\mathrm{R}}\tilde{R}||_I^2\end{aligned} \tag{5.44}$$

since the second term in (5.43) is negative semi-definite, we combine (5.44) with (5.43). Disregarding the second term in (5.43) and consider the inequality in (5.11) such that

$$\begin{aligned}\mathcal{L}V \leq &- ||\mathbf{M}_{\mathrm{R}}\tilde{R}||_I \mathbf{vex}\left(\boldsymbol{\mathcal{P}}_a\left(\mathbf{M}_{\mathrm{R}}\tilde{R}\right)\right)^\top\left(\hat{R}\tilde{b}+W\right)\\ &+ \frac{1}{\underline{\lambda}}||\mathbf{M}_{\mathrm{R}}\tilde{R}||_I\mathbf{vex}\left(\boldsymbol{\mathcal{P}}_a\left(\mathbf{M}_{\mathrm{R}}\tilde{R}\right)\right)^\top\left(\frac{1}{2\varepsilon}\frac{(1+\Upsilon)^2\,\underline{\lambda}^2+1}{1+\Upsilon}\mathbf{vex}\left(\boldsymbol{\mathcal{P}}_a\left(\mathbf{M}_{\mathrm{R}}\tilde{R}\right)\right)\right.\\ &\qquad\left.+\frac{\hat{R}\mathrm{diag}\left(\hat{R}^\top\mathbf{vex}\left(\boldsymbol{\mathcal{P}}_a\left(\mathbf{M}_{\mathrm{R}}\tilde{R}\right)\right)\right)}{1+\Upsilon}\sigma\right)\\ &- \frac{1}{\gamma}\tilde{b}^\top\dot{\hat{b}}-\frac{1}{\gamma}\tilde{\sigma}^\top\dot{\hat{\sigma}}+\frac{\varepsilon}{2}\bar{\sigma}^2\end{aligned} \tag{5.45}$$

where $\bar{\sigma} = \sum_{i=1}^{3} \sigma_i \geq \|q\|^2$. With direct substitution of $\dot{\hat{b}}$, $\dot{\hat{\sigma}}$ and W from (5.25), (5.26), and (5.27), respectively, one finds

$$\begin{aligned}\mathcal{L}V \leq & -\frac{2k_w - 1}{2\varepsilon}\left(\underline{\lambda}^2 (1+\Upsilon)^2 + 1\right) ||\mathbf{M}_{\mathrm{R}}\tilde{R}||_I^2 - k_b||\tilde{b}||^2 \\ & - k_\sigma \|\tilde{\sigma}\|^2 + k_b\tilde{b}^\top b + k_\sigma\tilde{\sigma}^\top\sigma + \frac{\varepsilon}{2}\bar{\sigma}^2\end{aligned} \tag{5.46}$$

According to (5.15) in Lemma 5.3, one has

$$\begin{aligned}\tilde{b}^\top b &\leq \frac{1}{2}||\tilde{b}||^2 + \frac{1}{2}\|b\|^2 \\ \tilde{\sigma}^\top\sigma &\leq \frac{1}{2}\|\tilde{\sigma}\|^2 + \frac{1}{2}\|\sigma\|^2\end{aligned}$$

Thus, the differential operator in (5.46) becomes

$$\begin{aligned}\mathcal{L}V \leq & -\frac{2k_w - 1}{2\varepsilon}||\mathbf{M}_{\mathrm{R}}\tilde{R}||_I^2 - \frac{k_b}{2}||\tilde{b}||^2 - \frac{k_\sigma}{2}\|\tilde{\sigma}\|^2 \\ & + \frac{1}{2}(k_\sigma + \varepsilon)\bar{\sigma}^2 + \frac{1}{2}k_b\|b\|^2\end{aligned} \tag{5.47}$$

Define

$$\begin{aligned}c_2 &= \frac{1}{2}(k_\sigma + \varepsilon)\bar{\sigma}^2 + \frac{1}{2}k_b\|b\|^2 \in \mathbb{R} \\ \tilde{X} &= \left[\frac{1}{2}\frac{\tilde{\rho}^\top\bar{\mathbf{M}}_{\mathrm{R}}\tilde{\rho}}{1+\|\tilde{\rho}\|^2}, \frac{1}{\sqrt{2\gamma}}\tilde{b}^\top, \frac{1}{\sqrt{2\gamma}}\tilde{\sigma}^\top\right]^\top \in \mathbb{R}^7 \\ \mathcal{H} &= \begin{bmatrix} \frac{2k_w-1}{2\varepsilon} & \underline{\mathbf{0}}_3^\top & \underline{\mathbf{0}}_3^\top \\ \underline{\mathbf{0}}_3 & \gamma k_b\mathbf{I}_3 & \mathbf{0}_{3\times3} \\ \underline{\mathbf{0}}_3 & \mathbf{0}_{3\times3} & \gamma k_\sigma\mathbf{I}_3 \end{bmatrix} \in \mathbb{R}^{7\times7}\end{aligned}$$

as such, the differential operator in (5.47) becomes

$$\mathcal{L}V \leq -\tilde{X}^\top\mathcal{H}\tilde{X} + c_2 \leq -\underline{\lambda}(\mathcal{H})V + c_2 \tag{5.48}$$

where $\underline{\lambda}(\cdot)$ is the minimum singular value of a matrix. Hence, from (5.48), one has

$$d(\mathbb{E}[V])/dt = \mathbb{E}[\mathcal{L}V] \leq -\underline{\lambda}(\mathcal{H})V + c_2 \tag{5.49}$$

According to Lemma (5.2), the inequality in (5.49) means

$$0 \leq \mathbb{E}\left[V\left(t\right)\right] \leq V\left(0\right)\exp\left(-\underline{\lambda}\left(\mathcal{H}\right)t\right) + \frac{c_2}{\underline{\lambda}\left(\mathcal{H}\right)}, \forall t \geq 0 \tag{5.50}$$

The inequality in (5.50) means that $\mathbb{E}\left[V\left(t\right)\right]$ is ultimately bounded by $c_2/\underline{\lambda}\left(\mathcal{H}\right)$. Let $\tilde{Y} = [\tilde{\rho}^\top, \tilde{b}^\top, \tilde{\sigma}^\top]^\top$, hence, $\tilde{Y}$ is SGUUB in the mean square. For $\tilde{Y}_0 \in \mathbb{R}^9$, the trajectory of $\tilde{Y}$ steers to the neighborhood of the origin and $c_2/\underline{\lambda}\left(\mathcal{H}\right)$ being the ultimate upper bound of the neighborhood.

5.4 Simulation

Let R be expressed by the dynamics in (5.3) with

$$\Omega = \left[\sin\left(0.7t\right), 0.7\sin\left(0.5t+\pi\right), 0.5\sin\left(0.3t+\frac{\pi}{3}\right)\right]^\top \text{rad/sec}$$

and initial attitude $R\left(0\right) = \mathbf{I}_3$. The true angular velocity is considered to be corrupted by a wide-band of random noise process ω with standard deviation (STD) being $0.2\,(\text{rad/sec})$ and zero mean, and bias $b = 0.2\left[1, -1, 1\right]^\top$. Consider two non-collinear inertial-frame measurements being given by $\mathrm{v}_1^{\mathcal{I}(\mathrm{R})} = \frac{1}{\sqrt{3}}\left[1, -1, 1\right]^\top$ and $\mathrm{v}_2^{\mathcal{I}(\mathrm{R})} = \left[0, 0, 1\right]^\top$ and their body-frame measurements being given by $\mathrm{v}_i^{\mathcal{B}(\mathrm{R})} = R^\top \mathrm{v}_i^{\mathcal{I}(\mathrm{R})} + \mathrm{b}_i^{\mathcal{B}(\mathrm{R})} + \omega_i^{\mathcal{B}(\mathrm{R})}$ where $\omega_1^{\mathcal{B}(\mathrm{R})}$ and $\omega_2^{\mathcal{B}(\mathrm{R})}$ are Gaussian noise process vectors with STD $=$ 0.2 and zero mean and the associated bias components $\mathrm{b}_1^{\mathcal{B}(\mathrm{R})} = 0.1\left[-1, 1, 0.5\right]^\top$ and $\mathrm{b}_2^{\mathcal{B}(\mathrm{R})} = 0.1\left[0, 0, 1\right]^\top$. The third vector is obtained by the cross product.

$\hat{R}\left(0\right)$ is given by angle-axis parameterization in (2.7) as $\hat{R}\left(0\right) = \mathcal{R}_\alpha\left(\alpha, u/\left\|u\right\|\right)$ with $\alpha = 179\,(\text{deg})$ and $u = \left[1, 5, 3\right]^\top$ such that $\tilde{R}$ approaches the unstable equilibria $||\tilde{R}||_I \approx 0.9999$

$$R\left(0\right) = \mathbf{I}_3, \quad \hat{R}\left(0\right) = \begin{bmatrix} -0.9427 & 0.2768 & 0.1862 \\ 0.2945 & 0.4286 & 0.8541 \\ 0.1567 & 0.8600 & -0.4856 \end{bmatrix}$$

Initial estimates are selected as $\hat{b}\left(0\right) = \underline{\mathbf{0}}_3$, $\hat{\sigma}\left(0\right) = \underline{\mathbf{0}}_3$, and design parameters are as follows: $\gamma = 1$, $k_b = 0.5$, $k_\sigma = 0.5$, $k_w = 5$, and $\varepsilon = 0.5$.

Figure 5.1 presents the true angular velocity (Ω) and true body-frame vectors as black centerlines and the associated high values of noise and bias components are represented by colored solid lines. The robustness of the filter against large initialization error and high values of noise and bias components is demonstrated in Figure 5.2. The normalized Euclidean distance error $||\tilde{R}||_I$ was initiated very close to the unstable equilibria (+1), eventually reduced to the neighborhood of the origin in probability as illustrated in Figure 5.2. Figure 5.3 shows an impressive tracking performance of Euler angles of the proposed filter plotted against the true angles.

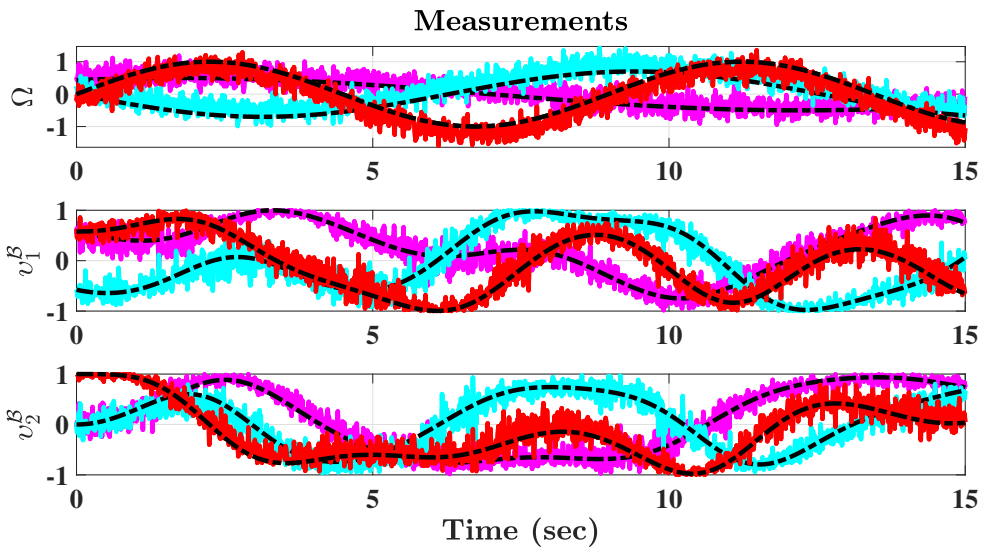

Figure 5.1: True values and measurements of Ω, $v_1^{\mathcal{B}(R)}$, and $v_2^{\mathcal{B}(R)}$.

5.5 Conclusion

An explicit stochastic nonlinear attitude filter is proposed on $\mathbb{SO}(3)$. The proposed filter shares its structure with previously developed deterministic filters, but in stochastic sense. An alternate attitude potential function which has not been considered in literature, is introduced in this work. The resulting stochastic filter ensures that the errors in Rodriguez vector and estimates are semi-globally uniformly ultimately bounded in mean square. Numerical results show high convergence capabilities when large error is initialized in the attitude and high levels of noise and bias are observed in the vector measurements.

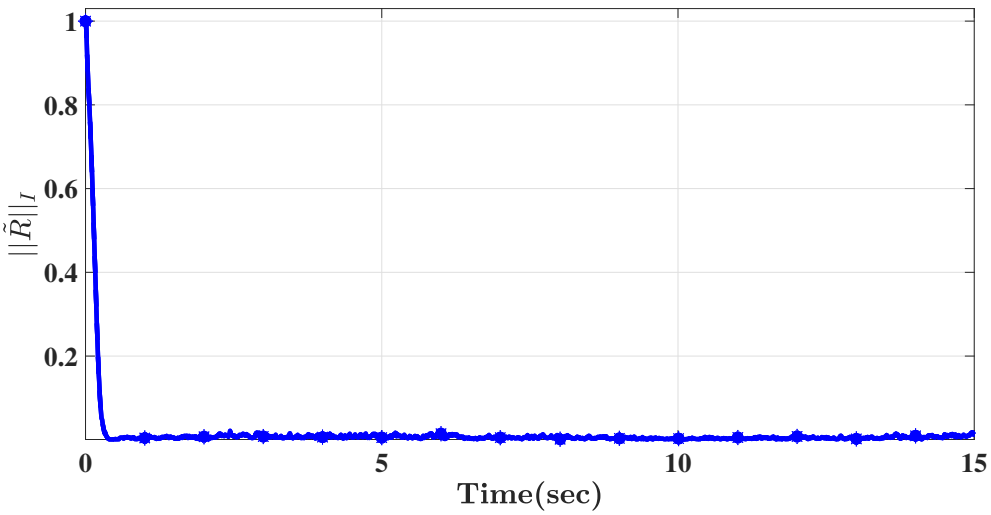

Figure 5.2: Tracking performance of normalized Euclidean distance error.

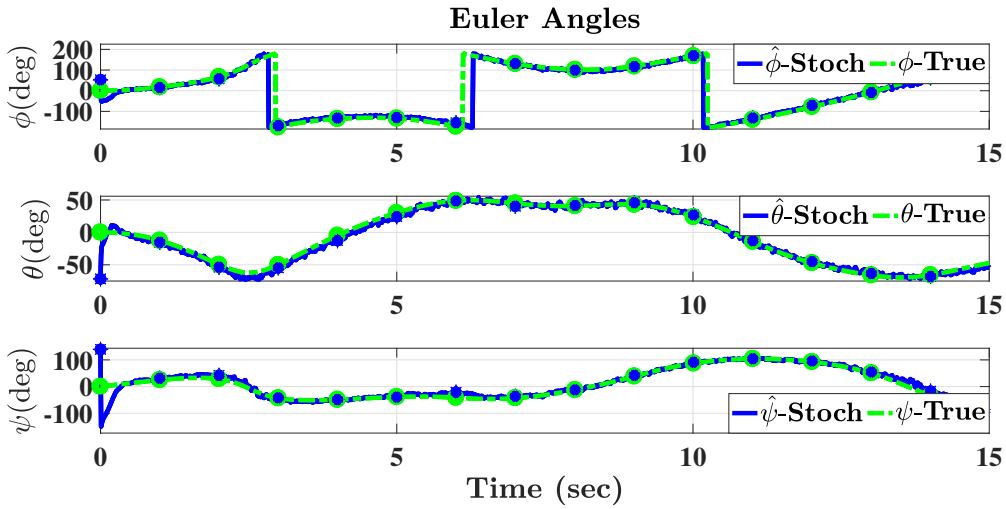

Figure 5.3: Tracking performance of Euler angles, proposed filter performance vs true trajectories.

Chapter 6
Nonlinear Pose Filters on $\mathbb{SE}(3)$ with Prescribed Performance

6.1 Introduction

Two novel nonlinear pose filters developed directly on the Special Euclidean Group $\mathbb{SE}(3)$ able to guarantee prescribed characteristics of transient and steady-state performance are proposed. The position error and normalized Euclidean distance of attitude error are trapped to arbitrarily start within a given large set and converge systematically and asymptotically to the origin from almost any initial condition. The transient error is guaranteed not to exceed a prescribed value while the steady-state error is bounded by a predefined small value. The first pose filter operates based on a set of vectorial measurements coupled with a group of velocity vectors and requires preliminary pose reconstruction. The second filter, on the contrary, is able to perform its function using a set of vectorial measurements and a group of velocity vectors directly. Both proposed filters provide reasonable pose estimates with superior convergence properties while being able to use measurements obtained from low-cost inertial measurement, landmark measurement, and velocity measurement units. Simulation results demonstrate effectiveness and robustness of the proposed filters considering large error in initialization and high level of uncertainties in velocity vectors as well as in the set of vector measurements. The results of this chapter were first published in Hashim, Brown, and McIsaac (2019b, 2019c).

The remainder of the chapter is organized as follows: The pose problem is formulated, vector measurements are demonstrated and prescribed performance is introduced in Section 6.2. The two proposed filters and the related stability analysis are presented in Section 6.3. Section 6.4 elaborates on the effectiveness and robustness of the proposed filters. Finally, Section 6.5 draws a conclusion of this work.

6.2 Problem Formulation with Prescribed Performance

Pose estimator relies on a set of vectorial measurements made on inertial-frame and body-frame. This section aims to define the pose problem and present the associated measurements. Next, the pose error and its reformulation are geared towards attaining desired characteristics of transient and steady-state performance.

6.2.1 Pose Kinematics and Measurements

The pose of any rigid-body in 3D space consists of two elements: attitude and position, and this work aims to estimate both elements. The attitude of a rigid-body is commonly represented by a rotational matrix $R \in \mathbb{SO}(3)$ defined relative to the body-frame such that $R \in \{\mathcal{B}\}$. Position of a rigid-body is, on the contrary, defined by $P \in \mathbb{R}^3$ with respect to the inertial-frame $P \in \{\mathcal{I}\}$. The pose problem can be characterized by the homogeneous transformation matrix $\boldsymbol{T} \in \mathbb{SE}(3)$ as

$$\boldsymbol{T} = \begin{bmatrix} R & P \\ \underline{\mathbf{0}}_3^\top & 1 \end{bmatrix} \tag{6.1}$$

The pose estimation problem of a rigid-body in 3D space is depicted in Fig. 6.1.

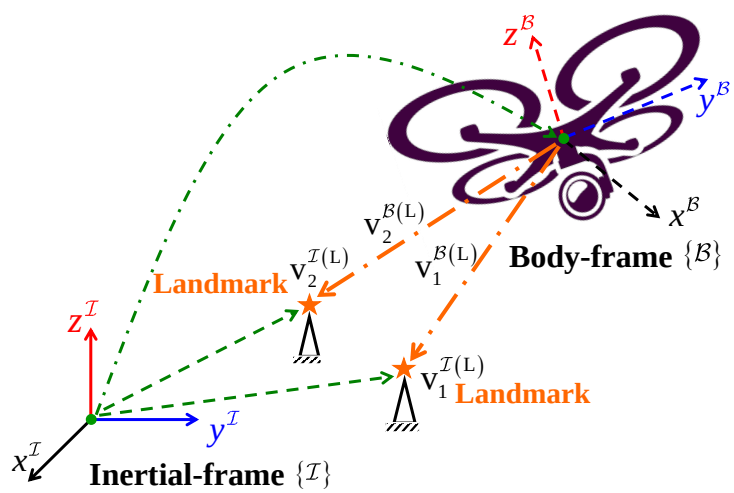

Figure 6.1: Pose estimation problem of a rigid-body in 3D space.

Let the components associated with body-frame and inertial-frame be assigned superscripts $\mathcal{B}$ and $\mathcal{I}$, respectively. The attitude can be obtained given N_{R} known non-collinear inertial vectors, available for measurements at a coordinate fixed to the moving body. IMU exemplify sensors, which could provide those measurements. The ith body-frame vector measurement is given by

$$\begin{bmatrix} \mathrm{v}_i^{\mathcal{B}(\mathrm{R})} \\ 0 \end{bmatrix} = \boldsymbol{T}^{-1} \begin{bmatrix} \mathrm{v}_i^{\mathcal{I}(\mathrm{R})} \\ 0 \end{bmatrix} + \begin{bmatrix} \mathrm{b}_i^{\mathcal{B}(\mathrm{R})} \\ 0 \end{bmatrix} + \begin{bmatrix} \omega_i^{\mathcal{B}(\mathrm{R})} \\ 0 \end{bmatrix}$$

such that

$$\mathrm{v}_i^{\mathcal{B}(\mathrm{R})} = R^\top \mathrm{v}_i^{\mathcal{I}(\mathrm{R})} + \mathrm{b}_i^{\mathcal{B}(\mathrm{R})} + \omega_i^{\mathcal{B}(\mathrm{R})} \tag{6.2}$$

with $\mathrm{v}_i^{\mathcal{I}(\mathrm{R})}$ being the ith known vector in the inertial-frame, and $\mathrm{b}_i^{\mathcal{B}(\mathrm{R})}$ and $\omega_i^{\mathcal{B}(\mathrm{R})}$ being unknown bias and noise components added to the ith measurement, respectively, for all $\mathrm{v}_i^{\mathcal{B}(\mathrm{R})}, \mathrm{v}_i^{\mathcal{I}(\mathrm{R})}, \mathrm{b}_i^{\mathcal{B}(\mathrm{R})}, \omega_i^{\mathcal{B}(\mathrm{R})} \in \mathbb{R}^3$ and $i = 1, 2, \ldots, N_{\mathrm{R}}$. The known inertial vector $\mathrm{v}_i^{\mathcal{I}(\mathrm{R})}$ and the available body-frame measurement $\mathrm{v}_i^{\mathcal{B}(\mathrm{R})}$ in (6.2) can be normalized such that

$$\upsilon_i^{\mathcal{I}(\mathrm{R})} = \frac{\mathrm{v}_i^{\mathcal{I}(\mathrm{R})}}{\left\|\mathrm{v}_i^{\mathcal{I}(\mathrm{R})}\right\|}, \quad \upsilon_i^{\mathcal{B}(\mathrm{R})} = \frac{\mathrm{v}_i^{\mathcal{B}(\mathrm{R})}}{\left\|\mathrm{v}_i^{\mathcal{B}(\mathrm{R})}\right\|} \tag{6.3}$$

Thus, the attitude of a rigid-body can be extracted using $\upsilon_i^{\mathcal{I}(\mathrm{R})}$ and $\upsilon_i^{\mathcal{B}(\mathrm{R})}$ in (6.3) rather than $\mathrm{v}_i^{\mathcal{I}(\mathrm{R})}$ and $\mathrm{v}_i^{\mathcal{B}(\mathrm{R})}$. Let us introduce the following two sets

$$\begin{aligned} \upsilon^{\mathcal{I}(\mathrm{R})} &= \left[\upsilon_1^{\mathcal{I}(\mathrm{R})}, \ldots, \upsilon_{N_{\mathrm{R}}}^{\mathcal{I}(\mathrm{R})}\right] \in \{\mathcal{I}\} \\ \upsilon^{\mathcal{B}(\mathrm{R})} &= \left[\upsilon_1^{\mathcal{B}(\mathrm{R})}, \ldots, \upsilon_{N_{\mathrm{R}}}^{\mathcal{B}(\mathrm{R})}\right] \in \{\mathcal{B}\} \end{aligned} \tag{6.4}$$

where the two sets in (6.4) include the normalized vectors in (6.3) for all $\upsilon^{\mathcal{I}(\mathrm{R})}, \upsilon^{\mathcal{B}(\mathrm{R})} \in \mathbb{R}^{3\times N_{\mathrm{R}}}$. The position of the moving body can be extracted if its attitude R has already been determined and there exist N_{L} known landmarks (feature points) obtained, for example, by a vision system. The ith body-frame landmark measurement is given by

$$\begin{bmatrix} \mathrm{v}_i^{\mathcal{B}(\mathrm{L})} \\ 1 \end{bmatrix} = \boldsymbol{T}^{-1} \begin{bmatrix} \mathrm{v}_i^{\mathcal{I}(\mathrm{L})} \\ 1 \end{bmatrix} + \begin{bmatrix} \mathrm{b}_i^{\mathcal{B}(\mathrm{L})} \\ 0 \end{bmatrix} + \begin{bmatrix} \omega_i^{\mathcal{B}(\mathrm{L})} \\ 0 \end{bmatrix}$$

such that

$$\mathrm{v}_i^{\mathcal{B}(\mathrm{L})} = R^\top \left(\mathrm{v}_i^{\mathcal{I}(\mathrm{L})} - P\right) + \mathrm{b}_i^{\mathcal{B}(\mathrm{L})} + \omega_i^{\mathcal{B}(\mathrm{L})} \tag{6.5}$$

where $\mathrm{v}_i^{\mathcal{I}(\mathrm{L})}$ is the ith known fixed landmark located in the inertial-frame, $\mathrm{b}_i^{\mathcal{B}(\mathrm{L})}$ and $\omega_i^{\mathcal{B}(\mathrm{L})}$ are the additive unknown bias and noise vectors of the ith measurement, respectively, for all $\mathrm{v}_i^{\mathcal{B}(\mathrm{L})}, \mathrm{v}_i^{\mathcal{I}(\mathrm{L})}, \mathrm{b}_i^{\mathcal{B}(\mathrm{L})}, \omega_i^{\mathcal{B}(\mathrm{L})} \in \mathbb{R}^3$ and $i = 1, 2, \ldots, N_\mathrm{L}$. Define the set of inertial-frame and body-frame vectors associated with landmarks by

$$\begin{aligned} \mathrm{v}^{\mathcal{B}(\mathrm{L})} &= \left[\mathrm{v}_1^{\mathcal{B}(\mathrm{L})}, \ldots, \mathrm{v}_{N_\mathrm{L}}^{\mathcal{B}(\mathrm{L})}\right] \in \{\mathcal{B}\} \\ \mathrm{v}^{\mathcal{I}(\mathrm{L})} &= \left[\mathrm{v}_1^{\mathcal{I}(\mathrm{L})}, \ldots, \mathrm{v}_{N_\mathrm{L}}^{\mathcal{I}(\mathrm{L})}\right] \in \{\mathcal{I}\} \end{aligned} \tag{6.6}$$

In case when more than one landmark is available for measurement, it is common to obtain a weighted geometric center of all the landmarks, which can be calculated as follows:

$$\mathcal{G}_c^{\mathcal{I}} = \frac{1}{\sum_{i=1}^{N_\mathrm{L}} k_i^\mathrm{L}} \sum_{i=1}^{N_\mathrm{L}} k_i^\mathrm{L} \mathrm{v}_i^{\mathcal{I}(\mathrm{L})} \tag{6.7}$$

$$\mathcal{G}_c^{\mathcal{B}} = \frac{1}{\sum_{i=1}^{N_\mathrm{L}} k_i^\mathrm{L}} \sum_{i=1}^{N_\mathrm{L}} k_i^\mathrm{L} \mathrm{v}_i^{\mathcal{B}(\mathrm{L})} \tag{6.8}$$

such that k_i^L is the confidence level of the ith measurement.

Assumption 6.1 *(Rigid-body pose observability) The pose of a rigid-body in 3D space can be extracted given the availability of at least two non-collinear vectors from the sets in (6.4) ($N_\mathrm{R} \geq 2$) and at least one feature point from the sets in (6.6) with $N_\mathrm{L} \geq 1$. In the case when $N_\mathrm{R} = 2$, the third vector can be obtained by the means of cross multiplication: $\upsilon_3^{\mathcal{I}(\mathrm{R})} = \upsilon_1^{\mathcal{I}(\mathrm{R})} \times \upsilon_2^{\mathcal{I}(\mathrm{R})}$ and $\upsilon_3^{\mathcal{B}(\mathrm{R})} = \upsilon_1^{\mathcal{B}(\mathrm{R})} \times \upsilon_2^{\mathcal{B}(\mathrm{R})}$.*

According to Assumption 6.2 a set of vectorial measurement described in (6.4) is sufficient to have rank 3. Accordingly, the homogeneous transformation matrix $\boldsymbol{T}$ can be extracted if Assumption 6.2 is met. For simplicity, the body-frame vectors $\mathrm{v}_i^{\mathcal{B}(\mathrm{R})}$ and $\mathrm{v}_i^{\mathcal{B}(\mathrm{L})}$ are considered to be noise and bias free in the stability analysis. In the Simulation Section, on the contrary, the noise and bias corrupting the measurements of $\mathrm{v}_i^{\mathcal{B}(\mathrm{R})}$ and $\mathrm{v}_i^{\mathcal{B}(\mathrm{L})}$ are taken into consideration. The pose kinematics of the

homogeneous transformation matrix $\boldsymbol{T}$ in (6.1) are given by

$$\begin{bmatrix} \dot{R} & \dot{P} \\ \underline{\mathbf{0}}_3^\top & 0 \end{bmatrix} = \begin{bmatrix} R & P \\ \underline{\mathbf{0}}_3^\top & 1 \end{bmatrix} \begin{bmatrix} [\Omega]_\times & V \\ \underline{\mathbf{0}}_3^\top & 0 \end{bmatrix}$$

such that

$$\dot{P} = RV$$

$$\dot{R} = R\,[\Omega]_\times \tag{6.9}$$

$$\dot{\boldsymbol{T}} = \boldsymbol{T}\,[\mathcal{Y}]_\wedge \tag{6.10}$$

with $\Omega \in \mathbb{R}^3$ and $V \in \mathbb{R}^3$ being the true angular and translational velocity of the moving body, respectively, and $\mathcal{Y} = \left[\Omega^\top, V^\top\right]^\top \in \mathbb{R}^6$ being the group velocity vector. The angular velocity can be measured by a gyroscope, for example, and expressed as follows:

$$\Omega_m = \Omega + b_\Omega + \omega_\Omega \in \{\mathcal{B}\} \tag{6.11}$$

where b_Ω is an unknown constant or slowly time-varying bias, and ω_Ω is an unknown random noise attached to the measurement, for all $b_\Omega, \omega_\Omega \in \mathbb{R}^3$. Likewise, the translational velocity measurement of a moving body can be obtained using a GPS, for instance, and defined by

$$V_m = V + b_V + \omega_V \in \{\mathcal{B}\} \tag{6.12}$$

with $b_V \in \mathbb{R}^3$ denoting an unknown constant or slowly time-varying bias, and $\omega_V \in \mathbb{R}^3$ being random noise attached to the translational velocity measurements. The group of velocity measurements and bias associated with it can be defined by $\mathcal{Y}_m = \left[\Omega_m^\top, V_m^\top\right]^\top \in \mathbb{R}^6$ and $b = \left[b_\Omega^\top, b_V^\top\right]^\top \in \mathbb{R}^6$, respectively. For the sake of simplicity, we consider $\omega_\Omega = \omega_V = \underline{\mathbf{0}}_3$ in the analysis. However, in the implementation it is used $\omega_\Omega \neq \underline{\mathbf{0}}_3$ and $\omega_V \neq \underline{\mathbf{0}}_3$. Considering the normalized Euclidean distance of the rotational matrix R in (2.6) and the identity in (2.16), the true attitude kinematics

in (6.9) can be expressed in view of (2.6) as

$$\begin{aligned} ||\dot{R}||_I &= -\frac{1}{4}\mathrm{Tr}\{\dot{R}\} \\ &= -\frac{1}{4}\mathrm{Tr}\{\boldsymbol{\mathcal{P}}_a(R)[\Omega]_\times\} \\ &= \frac{1}{2}\mathbf{vex}(\boldsymbol{\mathcal{P}}_a(R))^\top\Omega \end{aligned} \tag{6.13}$$

Accordingly, the problem of pose dynamics in (6.10) can be reformulated and expressed in vector form as

$$\begin{bmatrix} ||\dot{R}||_I \\ \dot{P} \end{bmatrix} = \begin{bmatrix} \frac{1}{2}\mathbf{vex}(\boldsymbol{\mathcal{P}}_a(R))^\top & \underline{\mathbf{0}}_3^\top \\ \mathbf{0}_{3\times 3} & R \end{bmatrix} \begin{bmatrix} \Omega_m - b_\Omega \\ V_m - b_V \end{bmatrix} \tag{6.14}$$

with $\mathbf{0}_{3\times 3}$ being a zero matrix and $\omega_\Omega = \omega_V = \underline{\mathbf{0}}_3$. Let the estimate of the homogeneous transformation matrix in (6.1), denoted by $\hat{\boldsymbol{T}}$, be given by

$$\hat{\boldsymbol{T}} = \begin{bmatrix} \hat{R} & \hat{P} \\ \underline{\mathbf{0}}_3^\top & 1 \end{bmatrix} \tag{6.15}$$

with $\hat{R}$ and $\hat{P}$ being the estimates of R and P, respectively. Let us define the error in the homogeneous transformation matrix from body-frame to estimator-frame by

$$\tilde{\boldsymbol{T}} = \hat{\boldsymbol{T}}\boldsymbol{T}^{-1} = \begin{bmatrix} \tilde{R} & \hat{P} - \tilde{R}P \\ \underline{\mathbf{0}}_3^\top & 1 \end{bmatrix} = \begin{bmatrix} \tilde{R} & \tilde{P} \\ \underline{\mathbf{0}}_3^\top & 1 \end{bmatrix} \tag{6.16}$$

where $\tilde{R} = \hat{R}R^\top$ and $\tilde{P}$ are the errors associated with attitude and position, respectively. The aim of this work is to drive $\hat{\boldsymbol{T}} \to \boldsymbol{T}$ which in turn guarantees driving $\tilde{P} \to \underline{\mathbf{0}}_3$, $\tilde{R} \to \mathbf{I}_3$, and $\tilde{\boldsymbol{T}} \to \mathbf{I}_4$. Lemma 6.1 presented below will prove useful in the subsequent filter derivation.

Lemma 6.1 *Let $R \in \mathbb{SO}(3)$, $M = M^\top \in \mathbb{R}^{3\times 3}$, M have rank 3, $\mathrm{Tr}\{M\} = 3$, and $\bar{\mathbf{M}} = \mathrm{Tr}\{M\}\mathbf{I}_3 - M$, while the minimum singular value of $\bar{\mathbf{M}}$ is $\underline{\lambda} := \underline{\lambda}(\bar{\mathbf{M}})$. Then,*

the following holds:

$$||\mathbf{vex}(\boldsymbol{\mathcal{P}}_a(R))||^2 = 4(1 - ||R||_I)||R||_I \tag{6.17}$$

$$\frac{2}{\underline{\lambda}} \frac{||\mathbf{vex}(\boldsymbol{\mathcal{P}}_a(RM))||^2}{1 + \mathrm{Tr}\{RMM^{-1}\}} \geq \|RM\|_I \tag{6.18}$$

Proof. See Appendix A.

6.2.2 Prescribed Performance

Considering the error in the homogeneous transformation matrix as in (6.16) and in view of the pose dynamics in (6.14), let us define the error in vector form by

$$\boldsymbol{e} = [\boldsymbol{e}_1, \boldsymbol{e}_2, \boldsymbol{e}_3, \boldsymbol{e}_4]^\top = \left[||\tilde{R}||_I, \tilde{P}^\top\right]^\top \in \mathbb{R}^4 \tag{6.19}$$

The objective of this subsection is to reformulate the problem such that the error in (6.19) satisfies transient as well as steady-state measures predefined by the user. This can be achieved by selecting a large known set which is guaranteed to contain the initial error vector $\boldsymbol{e}$ and after decaying smoothly and systematically settle within a predefined small set using prescribed performance function (PPF) Bechlioulis and Rovithakis (2008); Hashim, El-Ferik, and Lewis (2017, 2019). The PPF is defined by $\xi_i(t)$ which is a positive smooth time-decreasing function which satisfies $\xi_i : \mathbb{R}_+ \to \mathbb{R}_+$ and $\lim_{t\to\infty} \xi_i(t) = \xi_i^\infty > 0$ and can be expressed by Bechlioulis and Rovithakis (2008)

$$\xi_i(t) = \left(\xi_i^0 - \xi_i^\infty\right) \exp(-\ell_i t) + \xi_i^\infty \tag{6.20}$$

with $\xi_i(0) = \xi_i^0$ being the initial value of the PPF and the upper bound of the known large set, ξ_i^∞ being the upper bound of the narrow set, and ℓ_i being a positive constant controlling the convergence rate of $\xi(t)$ from ξ_i^0 to ξ_i^∞ for all $i = 1, \ldots, 4$. The error $\boldsymbol{e}_i(t)$ is guaranteed to follow the predefined transient and steady-state boundaries, if the conditions below are met:

$$-\delta\xi_i(t) < \boldsymbol{e}_i(t) < \xi_i(t), \text{ if } \boldsymbol{e}_i(0) > 0 \tag{6.21}$$

$$-\xi_i(t) < \boldsymbol{e}_i(t) < \delta\xi_i(t), \text{ if } \boldsymbol{e}_i(0) < 0 \tag{6.22}$$

with $\delta \in [0,1]$. For clarity, define $\boldsymbol{e}_i := \boldsymbol{e}_i(t)$ and $\xi_i := \xi_i(t)$. Also, let us define $\xi = [\xi_1, \xi_2, \xi_3, \xi_4]^\top$, $\ell = [\ell_1, \ell_2, \ell_3, \ell_4]^\top$, $\xi^0 = \left[\xi_1^0, \xi_2^0, \xi_3^0, \xi_4^0\right]^\top$, and $\xi^\infty = \left[\xi_1^\infty, \xi_2^\infty, \xi_3^\infty, \xi_4^\infty\right]^\top$ for all $\xi, \ell, \xi^0, \xi^\infty \in \mathbb{R}^4$. The systematic convergence of the tracking error $\boldsymbol{e}_i$, from a given large set to a given narrow set in accordance with (6.21) and (6.22) is depicted in Fig. 6.2.

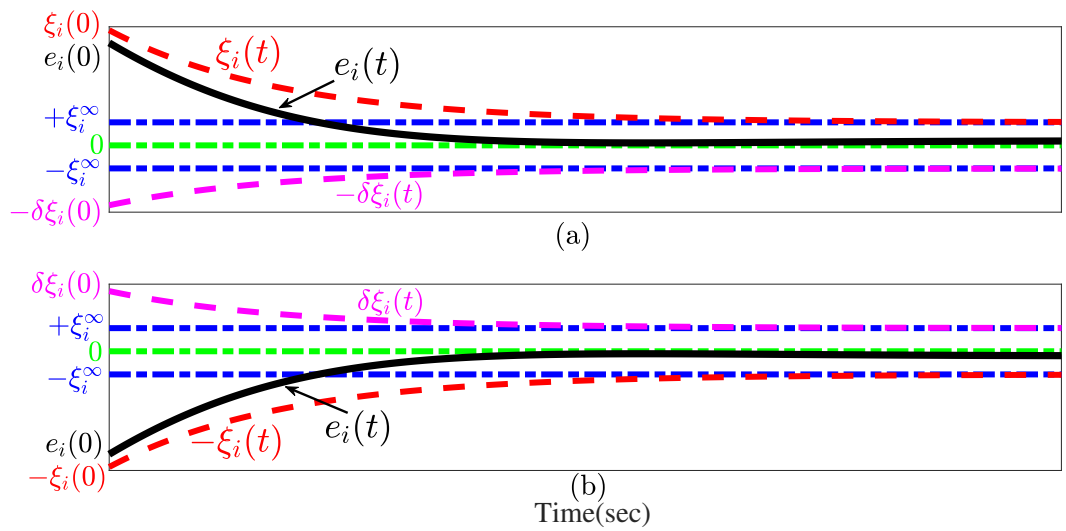

Figure 6.2: Graphical representation of the systematic convergence of tracking error $\boldsymbol{e}_i$ with PPF satisfying (a) Eq. (6.21); (b) Eq. (6.22).

Remark 6.1 *In accordance with the discussion in Bechlioulis and Rovithakis (2008); Hashim, El-Ferik, and Lewis (2017, 2019), knowing the upper bound and the sign of $\boldsymbol{e}_i(0)$ is sufficient to force the error to satisfy the performance constraints and maintain the error regulation within predefined dynamically reducing boundaries for all $t > 0$. If the condition in (6.21) or (6.22) is met, the maximum overshoot is sufficient to be bounded by $\pm\delta\xi_i$, the steady-state error is bounded by $\pm\xi_i^\infty$, and $|\boldsymbol{e}_i|$ is trapped between ξ_i and $\delta\xi_i$ as presented in Fig. 6.2.*

Define the error $\boldsymbol{e}_i$ by

$$\boldsymbol{e}_i = \xi_i \mathcal{Z}(\mathcal{E}_i) \tag{6.23}$$

where $\xi_i \in \mathbb{R}$ is defined in (6.20), $\mathcal{E}_i \in \mathbb{R}$ is a relaxed form of the constrained error referred to as transformed error, and $\mathcal{Z}(\mathcal{E}_i)$ is a smooth function that behaves according to Assumption 6.2:

Assumption 6.2 *The smooth function $\mathcal{Z}(\mathcal{E}_i)$ has the following properties Bechlioulis and Rovithakis (2008):*

1. *$\mathcal{Z}(\mathcal{E}_i)$ is smooth and strictly increasing.*

2. *$\mathcal{Z}(\mathcal{E}_i)$ is constrained by the following two bounds*
   $-\underline{\delta}_i < \mathcal{Z}(\mathcal{E}_i) < \bar{\delta}_i,$ *if* $\boldsymbol{e}_i(0) \geq 0$
   $-\bar{\delta}_i < \mathcal{Z}(\mathcal{E}_i) < \underline{\delta}_i,$ *if* $\boldsymbol{e}_i(0) < 0$
   with $\bar{\delta}_i$ and $\underline{\delta}_i$ being positive constants satisfy $\underline{\delta}_i \leq \bar{\delta}_i$.

3. $$\left.\begin{array}{l}\lim\limits_{\mathcal{E}_i\to-\infty}\mathcal{Z}(\mathcal{E}_i) = -\underline{\delta}_i \\ \lim\limits_{\mathcal{E}_i\to+\infty}\mathcal{Z}(\mathcal{E}_i) = \bar{\delta}_i\end{array}\right\} \text{ if } \boldsymbol{e}_i \geq 0$$
   $$\left.\begin{array}{l}\lim\limits_{\mathcal{E}_i\to-\infty}\mathcal{Z}(\mathcal{E}_i) = -\bar{\delta}_i \\ \lim\limits_{\mathcal{E}_i\to+\infty}\mathcal{Z}(\mathcal{E}_i) = \underline{\delta}_i\end{array}\right\} \text{ if } \boldsymbol{e}_i < 0$$
   such that

$$\mathcal{Z}(\mathcal{E}_i) = \begin{cases} \frac{\bar{\delta}_i \exp(\mathcal{E}_i) - \underline{\delta}_i \exp(-\mathcal{E}_i)}{\exp(\mathcal{E}_i)+\exp(-\mathcal{E}_i)}, & \bar{\delta}_i \geq \underline{\delta}_i \text{ if } \boldsymbol{e}_i \geq 0 \\ \frac{\bar{\delta}_i \exp(\mathcal{E}_i) - \underline{\delta}_i \exp(-\mathcal{E}_i)}{\exp(\mathcal{E}_i)+\exp(-\mathcal{E}_i)}, & \underline{\delta}_i \geq \bar{\delta}_i \text{ if } \boldsymbol{e}_i < 0 \end{cases} \tag{6.24}$$

The transformed error could be extracted through the inverse transformation of (6.24)

$$\mathcal{E}_i(\boldsymbol{e}_i, \xi_i) = \mathcal{Z}^{-1}(\boldsymbol{e}_i/\xi_i) \tag{6.25}$$

with $\mathcal{E}_i \in \mathbb{R}$, $\mathcal{Z} \in \mathbb{R}$ and $\mathcal{Z}^{-1} \in \mathbb{R}$ being smooth functions. For simplicity, let $\mathcal{E}_i := \mathcal{E}_i(\cdot,\cdot)$, $\bar{\delta} = [\bar{\delta}_1, \bar{\delta}_2, \bar{\delta}_3, \bar{\delta}_4]^\top$, $\underline{\delta} = [\underline{\delta}_1, \underline{\delta}_2, \underline{\delta}_3, \underline{\delta}_4]^\top$, $\mathcal{E} = \left[\mathcal{E}_R, \mathcal{E}_P^\top\right]^\top$ for all $\bar{\delta}, \underline{\delta}, \mathcal{E} \in \mathbb{R}^4$ with $\mathcal{E}_R = \mathcal{E}_1 \in \mathbb{R}$ and $\mathcal{E}_P = [\mathcal{E}_2, \mathcal{E}_3, \mathcal{E}_4]^\top \in \mathbb{R}^3$. In fact, the transformed error $\mathcal{E}_i$ translates $\boldsymbol{e}_i$ from the given constrained form in (6.21) or (6.22) to its unconstrained form as in (6.25). From (6.24), the inverse transformation can be expressed as

$$\mathcal{E}_i = \frac{1}{2}\begin{cases} \ln\frac{\underline{\delta}_i + \boldsymbol{e}_i/\xi_i}{\bar{\delta}_i - \boldsymbol{e}_i/\xi_i}, & \bar{\delta}_i \geq \underline{\delta}_i \text{ if } \boldsymbol{e}_i \geq 0 \\ \ln\frac{\underline{\delta}_i + \boldsymbol{e}_i/\xi_i}{\bar{\delta}_i - \boldsymbol{e}_i/\xi_i}, & \underline{\delta}_i \geq \bar{\delta}_i \text{ if } \boldsymbol{e}_i < 0 \end{cases} \tag{6.26}$$

Remark 6.2 *Consider the transformed error in (6.26). The transient and steady-state performance of the tracking error ($\boldsymbol{e}_i$) is bounded by the performance function ξ_i, and therefore, the prescribed performance is achieved if and only if $\mathcal{E}_i$ is guaranteed to be bounded for all $t \geq 0$.*

Proposition 6.1 *Consider the error vector in (6.19) with the normalized Euclidean distance error $||\tilde{R}||_I$ being given by (2.6). From (6.23), (6.24), and (6.25) let the transformed error be expressed as in (6.26) provided that $\underline{\delta} = \bar{\delta}$. Then the following statements are true.*

(i) The only possible representation of $\mathcal{E}_1$ is as follows:

$$\mathcal{E}_1 = \frac{1}{2} ln \frac{\underline{\delta}_1 + \boldsymbol{e}_1/\xi_1}{\bar{\delta}_1 - \boldsymbol{e}_1/\xi_1} = \frac{1}{2} ln \frac{\underline{\delta}_1 + ||\tilde{R}||_I/\xi_1}{\bar{\delta}_1 - ||\tilde{R}||_I/\xi_1} \tag{6.27}$$

(ii) The transformed error $\mathcal{E}_1 > 0 \forall ||\tilde{R}||_I \neq 0$.

(iii) $\mathcal{E} = \underline{\mathbf{0}}_4$ only at $\boldsymbol{e} = \underline{\mathbf{0}}_4$ and the critical point of $\mathcal{E}$ satisfies $\boldsymbol{e} = \underline{\mathbf{0}}_4$.

(iv) The only critical point of $\mathcal{E}$ is $\tilde{\boldsymbol{T}} = \mathbf{I}_4$.

Proof. Given that $0 \leq ||\tilde{R}(t)||_I \leq 1, \forall t \geq 0$ as defined in (2.6), one can find that the upper part of (6.26) holds $\forall t \geq 0$ which proves (i). Since $\underline{\delta} = \bar{\delta}$ with the constraint $||\tilde{R}||_I \leq \xi_1$, the expression in (6.27) is $(\underline{\delta}_1 + ||\tilde{R}||_I/\xi_1)/(\bar{\delta}_1 - ||\tilde{R}||_I/\xi_1) \geq 1 \forall ||\tilde{R}||_I \neq 0$. Thus, $\mathcal{E}_1 > 0 \forall ||\tilde{R}||_I \neq 0$ which confirms (ii). Considering $\underline{\delta} = \bar{\delta}$ with the constraint $\boldsymbol{e}_i \leq \xi_i$, it is clear that $(\underline{\delta}_i + \boldsymbol{e}_i/\xi_i)/(\bar{\delta}_i - \boldsymbol{e}_i/\xi_i) = 1$ if and only if $\boldsymbol{e}_i = 0$. Accordingly, $\mathcal{E}_i \neq 0 \forall \boldsymbol{e}_i \neq 0$ and $\mathcal{E}_i = 0$ only at $\boldsymbol{e}_i = 0$ which proves (iii). For (iv), from (2.6) and (6.16), $||\tilde{R}||_I = 0$ and $\tilde{P} = 0$ if and only if $\tilde{\boldsymbol{T}} = \mathbf{I}_4$. Thus, the critical point of $\mathcal{E}$ satisfies $||\tilde{R}||_I = 0$ and $\tilde{P} = 0$ which in turn satisfies $\tilde{\boldsymbol{T}} = \mathbf{I}_4$ and proves (iv). Define $\mu_i := \mu_i(\boldsymbol{e}_i, \xi_i)$ such that

$$\mu_i = \frac{1}{2\xi_i} \frac{\partial \mathcal{Z}^{-1}(\boldsymbol{e}_i/\xi_i)}{\partial(\boldsymbol{e}_i/\xi_i)} = \frac{1}{2\xi_i} \left(\frac{1}{\underline{\delta}_i + \boldsymbol{e}_i/\xi_i} + \frac{1}{\bar{\delta}_i - \boldsymbol{e}_i/\xi_i} \right) \tag{6.28}$$

Hence, one can find that the derivative of $\dot{\mathcal{E}}_i$ is as follows:

$$\dot{\mathcal{E}}_i = \mu_i \left(\dot{\boldsymbol{e}}_i - \frac{\dot{\xi}_i}{\xi_i} \boldsymbol{e}_i \right) \tag{6.29}$$

More simply, the expression in (6.29) is

$$\dot{\mathcal{E}} = \begin{bmatrix} \boldsymbol{\Psi}_R & \underline{\mathbf{0}}_3^\top \\ \underline{\mathbf{0}}_3 & \boldsymbol{\Psi}_P \end{bmatrix} \left(\dot{\boldsymbol{e}} - \begin{bmatrix} \boldsymbol{\Lambda}_R & \underline{\mathbf{0}}_3^\top \\ \underline{\mathbf{0}}_3 & \boldsymbol{\Lambda}_P \end{bmatrix} \boldsymbol{e} \right) \tag{6.30}$$

with $\boldsymbol{\Lambda}_R = \frac{\dot{\xi}_1}{\xi_1}$, $\boldsymbol{\Lambda}_P = \operatorname{diag}\left(\frac{\dot{\xi}_2}{\xi_2}, \frac{\dot{\xi}_3}{\xi_3}, \frac{\dot{\xi}_4}{\xi_4}\right)$, $\boldsymbol{\Psi}_R = \mu_1$, and $\boldsymbol{\Psi}_P = \operatorname{diag}(\mu_2, \mu_3, \mu_4)$ for all $\boldsymbol{\Lambda}_R, \boldsymbol{\Psi}_R \in \mathbb{R}$ and $\boldsymbol{\Lambda}_P, \boldsymbol{\Psi}_P \in \mathbb{R}^{3\times 3}$. The following section introduces two nonlinear pose filters on $\mathbb{SE}(3)$ with prescribed performance characteristics which for $0 \leq |\boldsymbol{e}_i(0)| < \xi_i(0)$ guarantee $\mathcal{E}_i \in \mathcal{L}_\infty, \forall t \geq 0$ and, therefore, satisfy (6.21) or (6.22).

6.3 Nonlinear Complementary Pose Filters On $\mathbb{SE}(3)$ with Prescribed Performance

This section aims to provide a comprehensive description of the two nonlinear complementary pose filters evolved on $\mathbb{SE}(3)$ with the error vector, introduced in (6.19), behaving in accordance with the predefined transient as well as steady-state measures specified by the user. The first proposed filter is named a semi-direct pose filter with prescribed performance and the second one is termed a direct pose filter with prescribed performance. The difference between the two lies in the fact that while the semi-direct filter requires both attitude and position to be reconstructed through a set of vectorial measurements given in (6.4) and (6.6) combined with the measurement of the group velocity vector as described in (6.11) and (6.12), the direct filter only utilizes the above-mentioned measurements in the filter design. The structure of the proposed pose filters described in the two subsequent subsections is nonlinear on the Lie group of $\mathbb{SE}(3)$ and is given by

$$\dot{\hat{\boldsymbol{T}}} = \hat{\boldsymbol{T}}[\hat{\mathcal{Y}}]_\wedge$$

with $\hat{\mathcal{Y}} = [\hat{\Omega}^\top, \hat{V}^\top] \in \mathbb{R}^6$ such that $\dot{\hat{R}} = \hat{R}[\hat{\Omega}]_\times$ and $\dot{\hat{P}} = \hat{R}\hat{V}$.

6.3.1 Semi-direct Pose Filter with Prescribed Performance

Recall the error in (6.19) $\boldsymbol{e} = \left[||\tilde{R}||_I, \tilde{P}^\top\right]^\top$. Define $\boldsymbol{T}_y = \begin{bmatrix} R_y & P_y \\ \underline{\mathbf{0}}_3^\top & 1 \end{bmatrix}$ as a reconstructed homogeneous transformation matrix of the true $\boldsymbol{T}$. R_y corrupted by uncertain measurements can be reconstructed as in Markley (1988); Shuster and Oh (1981) or for simplicity visit the Appendix in Hashim et al. (2018b); Hashim, Brown, and McIsaac (2019d). From (6.7) and (6.8) P_y is reconstructed in the following manner

$$P_y = \frac{1}{\sum_{i=1}^{N_{\mathrm{L}}} k_i^{\mathrm{L}}} \sum_{i=1}^{N_{\mathrm{L}}} k_i^{\mathrm{L}} \left(\mathrm{v}_i^{\mathcal{I}(\mathrm{L})} - R_y \mathrm{v}_i^{\mathcal{B}(\mathrm{L})} \right) = \mathcal{G}_c^{\mathcal{I}} - R_y \mathcal{G}_c^{\mathcal{B}} \tag{6.31}$$

Consider the following pose filter design

$$\dot{\hat{R}} = \hat{R}\left[\Omega_m - \hat{b}_\Omega - \hat{R}^\top W_\Omega\right]_\times \tag{6.32}$$

$$\dot{\hat{P}} = \hat{R}(V_m - \hat{b}_V - W_V) \tag{6.33}$$

$$\dot{\hat{b}}_\Omega = \frac{\gamma}{2}\boldsymbol{\Psi}_R \mathcal{E}_R \hat{R}^\top \mathbf{vex}(\boldsymbol{\mathcal{P}}_a(\tilde{R})) + \gamma \hat{R}^\top \left[\tilde{P} - \hat{P}\right]_\times \boldsymbol{\Psi}_P \mathcal{E}_P \tag{6.34}$$

$$\dot{\hat{b}}_V = \gamma \hat{R}^\top \boldsymbol{\Psi}_P \mathcal{E}_P \tag{6.35}$$

$$W_\Omega = 2\frac{k_w \boldsymbol{\Psi}_R \mathcal{E}_R - \boldsymbol{\Lambda}_R/4}{1 - ||\tilde{R}||_I} \mathbf{vex}(\boldsymbol{\mathcal{P}}_a(\tilde{R})) \tag{6.36}$$

$$W_V = \hat{R}^\top \left(k_w \boldsymbol{\Psi}_P \mathcal{E}_P + \left[\tilde{P} - \hat{P}\right]_\times W_\Omega - \boldsymbol{\Lambda}_P \tilde{P} \right) \tag{6.37}$$

with $\tilde{R} = \hat{R}R_y^\top$, $\tilde{P} = \hat{P} - \tilde{R}P_y$, $\mathcal{E}_R$, $\mathcal{E}_P$, $\boldsymbol{\Psi}_R$ and $\boldsymbol{\Psi}_P$ being defined in (6.28), and (6.29), respectively, k_w and γ being positive constants, and each of $\hat{b}_\Omega$ and $\hat{b}_V$ being the estimates of b_Ω and b_V, respectively.

Define the error between the true and the estimated bias by

$$\tilde{b}_\Omega = b_\Omega - \hat{b}_\Omega \tag{6.38}$$

$$\tilde{b}_V = b_V - \hat{b}_V \tag{6.39}$$

where $\tilde{b} = \left[\tilde{b}_\Omega^\top, \tilde{b}_V^\top\right]^\top \in \mathbb{R}^6$ is the group error bias vector.

Theorem 6.1 *Consider the pose dynamics in (6.10), the group of noise-free velocity measurements in (6.11) and (6.12) such that $\Omega_m = \Omega + b_\Omega$ and $V_m = V + b_V$, in addition to other vector measurements given in (6.4) and (6.6) coupled with the filter kinematics in (6.32), (6.33), (6.34), (6.35), (6.36), and (6.37). Let Assumption 6.2 hold. Define $\mathcal{U} \subseteq \mathbb{SE}(3) \times \mathbb{R}^6$ by*

$$\mathcal{U} := \left\{ \left(\tilde{\boldsymbol{T}}(0), \tilde{b}(0)\right) \middle| \operatorname{Tr}\{\tilde{R}(0)\} = -1, \tilde{P}(0) = \underline{\mathbf{0}}_3, \tilde{b}(0) = \underline{\mathbf{0}}_6 \right\}$$

From almost any initial condition such that $\operatorname{Tr}\{\tilde{R}(0)\} \notin \mathcal{U}$ and $\mathcal{E}(0) \in \mathcal{L}_\infty$, all signals in the closed loop are bounded, $\lim_{t\to\infty} \mathcal{E}(t) = 0$, and $\tilde{\boldsymbol{T}}$ asymptotically approaches $\mathbf{I}_4$.

Theorem 6.1 guarantees that the pose error dynamics in (6.32), (6.33), (6.34), (6.35), (6.36), and (6.37) are stable with $\mathcal{E}(t)$ asymptotically approaching the origin. Since $\mathcal{E}(t)$ is bounded, the error vector $\boldsymbol{e}$ in (6.19) is constrained by the transient and steady-state boundaries introduced in (6.20).

Proof. Consider the error in the homogeneous transformation matrix from body-frame to estimator-frame defined as (6.16). From (6.9) and (6.32) the error dynamics are

$$\dot{\tilde{R}} = \hat{R}\left[\tilde{b}_\Omega - \hat{R}^\top W_\Omega\right]_\times R^\top = \left[\hat{R}\tilde{b}_\Omega - W_\Omega\right]_\times \tilde{R} \tag{6.40}$$

where $\left[\hat{R}\tilde{b}_\Omega\right]_\times = \hat{R}\left[\tilde{b}_\Omega\right]_\times \hat{R}^\top$ as given in identity (2.12). In view of (6.9) and (6.13), one can express the error dynamics in (6.40) in terms of normalized Euclidean distance as

$$\begin{aligned}
\frac{d}{dt}||\tilde{R}||_I &= \frac{d}{dt}\frac{1}{4}\operatorname{Tr}\{\mathbf{I}_3 - \tilde{R}\} \\
&= -\frac{1}{4}\operatorname{Tr}\left\{\left[\hat{R}\tilde{b}_\Omega - W_\Omega\right]_\times \boldsymbol{\mathcal{P}}_a(\tilde{R})\right\} \\
&= \frac{1}{2}\mathbf{vex}(\boldsymbol{\mathcal{P}}_a(\tilde{R}))^\top(\hat{R}\tilde{b}_\Omega - W_\Omega)
\end{aligned} \tag{6.41}$$

with $\mathrm{Tr}\left\{\tilde{R}\left[\tilde{b}-W\right]_\times\right\} = -2\mathbf{vex}(\boldsymbol{\mathcal{P}}_a(\tilde{R}))^\top(\tilde{b}-W)$ being defined in (2.16). Since the position error is given by $\tilde{P}=\hat{P}-\tilde{R}P$ in (6.16), one can find the derivative of $\tilde{P}$ to be

$$\begin{aligned}\dot{\tilde{P}} &= \dot{\hat{P}} - \dot{\tilde{R}}P - \tilde{R}\dot{P}\\ &= \dot{\hat{P}} - \left[\hat{R}\tilde{b}_\Omega - W_\Omega\right]_\times \tilde{R}P - \tilde{R}R(V_m - b_V)\\ &= \hat{R}(\tilde{b}_V - W_V) + \left[\hat{P}-\tilde{P}\right]_\times(\hat{R}\tilde{b}_\Omega - W_\Omega)\end{aligned} \tag{6.42}$$

with $\left[\hat{R}\tilde{b}_\Omega\right]_\times \hat{P} = -\left[\hat{P}\right]_\times \hat{R}\tilde{b}_\Omega$. From (6.41) and (6.42), and in view of (6.14), the dynamics of the error vector in (6.19) become

$$\begin{bmatrix} ||\dot{\tilde{R}}||_I \\ \dot{\tilde{P}} \end{bmatrix} = \begin{bmatrix} \frac{1}{2}\mathbf{vex}(\boldsymbol{\mathcal{P}}_a(\tilde{R}))^\top & \underline{\mathbf{0}}_3^\top \\ \left[\hat{P}-\tilde{P}\right]_\times & \hat{R} \end{bmatrix} \begin{bmatrix} \hat{R}\tilde{b}_\Omega - W_\Omega \\ \tilde{b}_V - W_V \end{bmatrix} \tag{6.43}$$

Accordingly, the derivative of the transformed error in (6.30) can be represented with direct substitution of $\boldsymbol{e} = \left[||\tilde{R}||_I, \tilde{P}^\top\right]^\top$ in addition to the result in (6.43). Now, consider the following candidate Lyapunov function

$$V(\mathcal{E},\tilde{b}_\Omega,\tilde{b}_V) = \frac{1}{2}||\mathcal{E}||^2 + \frac{1}{2\gamma}||\tilde{b}_\Omega||^2 + \frac{1}{2\gamma}||\tilde{b}_V||^2 \tag{6.44}$$

Differentiating $V := V(\mathcal{E},\tilde{b}_\Omega,\tilde{b}_V)$ in (6.44) results in

$$\begin{aligned}\dot{V} =& \mathcal{E}^\top\dot{\mathcal{E}} - \frac{1}{\gamma}\tilde{b}_\Omega^\top\dot{\tilde{b}}_\Omega - \frac{1}{\gamma}\tilde{b}_V^\top\dot{\tilde{b}}_V\\ =& \mathcal{E}_R\boldsymbol{\Psi}_R\left(\frac{1}{2}\mathbf{vex}(\boldsymbol{\mathcal{P}}_a(\tilde{R}))^\top(\hat{R}\tilde{b}_\Omega - W_\Omega) - \boldsymbol{\Lambda}_R||\tilde{R}||_I\right)\\ &+ \mathcal{E}_P^\top\boldsymbol{\Psi}_P\left(\hat{R}(\tilde{b}_V - W_V) + \left[\hat{P}-\tilde{P}\right]_\times(\hat{R}\tilde{b}_\Omega - W_\Omega)\right)\\ &- \mathcal{E}_P^\top\boldsymbol{\Psi}_P\boldsymbol{\Lambda}_P\tilde{P} - \frac{1}{\gamma}\tilde{b}_\Omega^\top\dot{\tilde{b}}_\Omega - \frac{1}{\gamma}\tilde{b}_V^\top\dot{\tilde{b}}_V\end{aligned} \tag{6.45}$$

Consider $||\tilde{R}||_I = \frac{1}{4}\frac{||\mathbf{vex}(\boldsymbol{\mathcal{P}}_a(\tilde{R}))||^2}{1-||\tilde{R}||_I}$ as defined in (6.17). Using the result in (6.45)

and directly substituting $\dot{\tilde{b}}_\Omega$, $\dot{\tilde{b}}_V$, W_Ω and W_V with their definitions in (6.34), (6.35), (6.36), and (6.37), respectively, one obtains

$$\begin{aligned}\dot{V} &= -\frac{1}{4}k_w\mathcal{E}_R^2\mathbf{\Psi}_R^2\frac{||\mathbf{vex}(\boldsymbol{\mathcal{P}}_a(\tilde{R}))||^2}{1-||\tilde{R}||_I} - k_w\mathcal{E}_P^\top\mathbf{\Psi}_P^2\mathcal{E}_P \\ &= -k_w\mathcal{E}_R^2\mathbf{\Psi}_R^2||\tilde{R}||_I - k_w\mathcal{E}_P^\top\mathbf{\Psi}_P^2\mathcal{E}_P \end{aligned} \tag{6.46}$$

The result obtained in (6.46) indicates that $V(t) \leq V(0), \forall t \geq 0$. Given that $V(t) \leq V(0), \forall t \geq 0$, $\tilde{R}(0) \notin \mathcal{U}$ and $\mathcal{E}(0) \in \mathbb{R}^4$, $\tilde{b}$ remains bounded, and $\mathcal{E}$ is bounded and well defined for all $t \geq 0$. Consequently, $\tilde{P}$, $||\tilde{R}||_I$ and $\mathbf{vex}(\boldsymbol{\mathcal{P}}_a(\tilde{R}))$ are bounded, which in turn signifies that $\dot{\tilde{P}}$, $||\dot{\tilde{R}}||_I$, $\dot{\mathcal{E}}_R$ and $\dot{\mathcal{E}}_P$ are bounded as well. From the result in (6.46) it follows that

$$\begin{aligned}\ddot{V} =& -k_w\left(2\mathcal{E}_R\mathbf{\Psi}_R(\dot{\mathcal{E}}_R\mathbf{\Psi}_R + \mathcal{E}_R\dot{\mathbf{\Psi}}_R)||\tilde{R}||_I + \mathcal{E}_R^2\mathbf{\Psi}_R^2||\dot{\tilde{R}}||_I\right) \\ &- 2k_w\mathcal{E}_P^\top\mathbf{\Psi}_P^2\dot{\mathcal{E}}_P - 2k_w\mathcal{E}_P^\top\mathbf{\Psi}_P\dot{\mathbf{\Psi}}_P\mathcal{E}_P \end{aligned} \tag{6.47}$$

Since $\mathbf{\Psi}_R = \mu_1$ and $\mathbf{\Psi}_P = \mathrm{diag}(\mu_2, \mu_3, \mu_4)$ defined in (6.28), $\dot{\mu}_i$ can be expressed as follows for all $i = 1, 2, \ldots, 4$

$$\dot{\mu}_i = -\frac{1}{2}\frac{\underline{\delta}_i\dot{\xi}_i + \dot{\boldsymbol{e}}_i}{(\underline{\delta}_i\xi_i + \boldsymbol{e}_i)^2} - \frac{1}{2}\frac{\bar{\delta}_i\dot{\xi}_i - \dot{\boldsymbol{e}}_i}{(\bar{\delta}_i\xi_i - \boldsymbol{e}_i)^2} \tag{6.48}$$

with $\dot{\xi}_i = -\ell_i(\xi_i^0 - \xi_i^\infty)\exp(-\ell_i t)$. Due to the fact that $\dot{\boldsymbol{e}}_i$ is bounded for all $i = 1, 2, \ldots, 4$, $\dot{\mu}_i$ is bounded and $\ddot{V}$ in (6.47) is uniformly bounded for all $t \geq 0$. It should be remarked that $\mathcal{E}_1 > 0$ for all $||\tilde{R}||_I > 0$, and $\mathcal{E}_1 \to 0$ as $||\tilde{R}||_I \to 0$ and vice versa as stated in property (ii) of Proposition 6.1. In addition, $\mathcal{E}_i \neq 0 \forall \boldsymbol{e}_i \neq 0$ and $\mathcal{E}_i = 0$ if and only if $\boldsymbol{e}_i = 0$ as indicated in property (iii) of Proposition 6.1. Therefore, $\dot{V}$ is uniformly continuous, and in consistence with Barbalat Lemma, $\dot{V} \to 0$ as $t \to \infty$ signifies that $\mathcal{E}_i \to 0$ and $\boldsymbol{e}_i \to 0$. As mentioned by property (iv) of Proposition 6.1, $\mathcal{E} \to 0$ implies that $\tilde{\boldsymbol{T}}$ asymptotically approaches $\mathbf{I}_4$ which completes the proof.

6.3.2 Direct Pose Filter with Prescribed Performance

The reconstructed homogeneous transformation matrix $\boldsymbol{T}_y$ defined in Subsection 6.3.1 consists of two elements: R_y and P_y. Although, R_y can be statically reconstructed

applying, for example, QUEST Shuster and Oh (1981), or SVD Markley (1988), the aforementioned methods of static reconstruction could significantly increase processing cost Hashim et al. (2018a); Hashim, Brown, and McIsaac (2019a, 2019d); Mahony et al. (2008). Thus, the pose filter proposed in this Subsection avoids the necessity of attitude reconstruction and instead uses measurements from the inertial and body-frame units directly. Let us define

$$\boldsymbol{\mathcal{M}}_{\mathrm{T}} = \begin{bmatrix} \mathbf{M}_{\mathrm{T}} & \mathbf{m}_{\mathrm{v}} \\ \mathbf{m}_{\mathrm{v}}^{\top} & \mathbf{m}_{\mathrm{c}} \end{bmatrix} = \sum_{i=1}^{N_{\mathrm{R}}} k_i^{\mathrm{R}} \begin{bmatrix} \upsilon_i^{\mathcal{I}(\mathrm{R})} \\ 0 \end{bmatrix} \begin{bmatrix} \upsilon_i^{\mathcal{I}(\mathrm{R})} \\ 0 \end{bmatrix}^{\top} + \sum_{j=1}^{N_{\mathrm{L}}} k_j^{\mathrm{L}} \begin{bmatrix} \mathrm{v}_j^{\mathcal{I}(\mathrm{L})} \\ 1 \end{bmatrix} \begin{bmatrix} \mathrm{v}_j^{\mathcal{I}(\mathrm{L})} \\ 1 \end{bmatrix}^{\top} \tag{6.49}$$

such that $\mathbf{M}_{\mathrm{T}} = \mathbf{M}_{\mathrm{R}} + \mathbf{M}_{\mathrm{L}}$ with

$$\begin{aligned} \mathbf{M}_{\mathrm{R}} &= \sum_{i=1}^{N_{\mathrm{R}}} k_i^{\mathrm{R}} \upsilon_i^{\mathcal{I}(\mathrm{R})} \left(\upsilon_i^{\mathcal{I}(\mathrm{R})}\right)^{\top} \\ \mathbf{M}_{\mathrm{L}} &= \sum_{j=1}^{N_{\mathrm{L}}} k_j^{\mathrm{L}} \mathrm{v}_j^{\mathcal{I}(\mathrm{L})} \left(\mathrm{v}_j^{\mathcal{I}(\mathrm{L})}\right)^{\top} \\ \mathbf{m}_{\mathrm{v}} &= \sum_{j=1}^{N_{\mathrm{L}}} k_j^{\mathrm{L}} \mathrm{v}_j^{\mathcal{I}(\mathrm{L})} \\ \mathbf{m}_{\mathrm{c}} &= \sum_{j=1}^{N_{\mathrm{L}}} k_j^{\mathrm{L}} \end{aligned} \tag{6.50}$$

where k_i^{R} and k_j^{L} are constant gains of the confidence level of ith and jth sensor measurements, respectively. Define

$$\boldsymbol{\mathcal{K}}_{\mathrm{T}} = \begin{bmatrix} \mathbf{K}_{\mathrm{T}} & \mathbf{k}_{\mathrm{v}} \\ \mathbf{m}_{\mathrm{v}}^{\top} & \mathbf{m}_{\mathrm{c}} \end{bmatrix} = \sum_{i=1}^{N_{\mathrm{R}}} k_i^{\mathrm{R}} \begin{bmatrix} \upsilon_i^{\mathcal{B}(\mathrm{R})} \\ 0 \end{bmatrix} \begin{bmatrix} \upsilon_i^{\mathcal{I}(\mathrm{R})} \\ 0 \end{bmatrix}^{\top} + \sum_{j=1}^{N_{\mathrm{L}}} k_j^{\mathrm{L}} \begin{bmatrix} \mathrm{v}_j^{\mathcal{B}(\mathrm{L})} \\ 1 \end{bmatrix} \begin{bmatrix} \mathrm{v}_j^{\mathcal{I}(\mathrm{L})} \\ 1 \end{bmatrix}^{\top} \tag{6.51}$$

such that $\mathbf{m}_{\mathrm{v}} = \sum_{j=1}^{N_{\mathrm{L}}} k_j^{\mathrm{L}} \mathrm{v}_j^{\mathcal{I}(\mathrm{L})}$ and $\mathbf{m}_{\mathrm{c}} = \sum_{j=1}^{N_{\mathrm{L}}} k_j^{\mathrm{L}}$ as defined in (6.50), and

$$\begin{aligned}
\mathbf{K}_{\mathrm{T}} &= \sum_{i=1}^{N_{\mathrm{R}}} k_i^{\mathrm{R}} \upsilon_i^{\mathcal{B}(\mathrm{R})} \left(\upsilon_i^{\mathcal{I}(\mathrm{R})}\right)^{\top} + \sum_{j=1}^{N_{\mathrm{L}}} k_i^{\mathrm{L}} \mathrm{v}_j^{\mathcal{B}(\mathrm{L})} \left(\mathrm{v}_j^{\mathcal{I}(\mathrm{L})}\right)^{\top} \\
\mathbf{k}_{\mathrm{v}} &= \sum_{j=1}^{N_{\mathrm{L}}} k_j^{\mathrm{L}} \mathrm{v}_j^{\mathcal{B}(\mathrm{L})}
\end{aligned} \tag{6.52}$$

In this work k_i^{R} is selected such that $\sum_{i=1}^{N_{\mathrm{R}}} k_i^{\mathrm{R}} = 3$. It can be easily deduced that $\mathbf{M}_{\mathrm{R}}$ is symmetric. Assuming that Assumption 6.2 holds, $\mathbf{M}_{\mathrm{R}}$ is nonsingular with $\mathrm{rank}(\mathbf{M}_{\mathrm{R}}) = 3$. Accordingly, the three eigenvalues of $\mathbf{M}_{\mathrm{R}}$ are greater than zero. Define $\bar{\mathbf{M}}_{\mathrm{R}} = \mathrm{Tr}\{\mathbf{M}_{\mathrm{R}}\}\mathbf{I}_3 - \mathbf{M}_{\mathrm{R}} \in \mathbb{R}^{3\times 3}$, provided that $\mathrm{rank}(\mathbf{M}_{\mathrm{R}}) = 3$, then, the following three statements hold (Bullo and Lewis (2004) page. 553):

1. $\mathbf{M}_{\mathrm{R}}$ is a positive-definite matrix.
2. The eigenvectors of $\mathbf{M}_{\mathrm{R}}$ coincide with the eigenvectors of $\bar{\mathbf{M}}_{\mathrm{R}}$.
3. Assuming that the three eigenvalues of $\mathbf{M}_{\mathrm{R}}$ are $\lambda(\mathbf{M}_{\mathrm{R}}) = \{\lambda_1, \lambda_2, \lambda_3\}$, then $\lambda(\bar{\mathbf{M}}_{\mathrm{R}}) = \{\lambda_3+\lambda_2, \lambda_3+\lambda_1, \lambda_2+\lambda_1\}$ with the minimum singular value $\underline{\lambda}(\bar{\mathbf{M}}_{\mathrm{R}}) > 0$.

In the remainder of this Subsection, it is considered that $\mathrm{rank}(\mathbf{M}_{\mathrm{R}}) = 3$ in order to ensure that the above-mentioned statements are true. Define

$$\hat{\upsilon}_i^{\mathcal{B}(\mathrm{R})} = \hat{R}^{\top} \upsilon_i^{\mathcal{I}(\mathrm{R})} \tag{6.53}$$

Defining the error in the homogeneous transformation matrix as in (6.16), the attitude error can be expressed as $\tilde{R} = \hat{R}R^{\top}$ and the position error is defined by $\tilde{P} = \hat{P} - \tilde{R}P$. Also, let the bias error be as in (6.38) and (6.39). In order to derive the direct pose filter, it is necessary to introduce the following series of equations written in terms of

vectorial measurements. According to identity (2.11) and (2.12), one has

$$\begin{aligned}
\left[\hat{R}\sum_{i=1}^{N_{\mathrm{R}}}\frac{k_i^{\mathrm{R}}}{2}\hat{\upsilon}_i^{\mathcal{B}(\mathrm{R})}\times\upsilon_i^{\mathcal{B}(\mathrm{R})}\right]_\times &= \hat{R}\left[\sum_{i=1}^{N_{\mathrm{R}}}\frac{k_i^{\mathrm{R}}}{2}\hat{\upsilon}_i^{\mathcal{B}(\mathrm{R})}\times\upsilon_i^{\mathcal{B}(\mathrm{R})}\right]_\times\hat{R}^\top \\
&= \hat{R}\sum_{i=1}^{N_{\mathrm{R}}}\frac{k_i^{\mathrm{R}}}{2}\left(\upsilon_i^{\mathcal{B}(\mathrm{R})}\left(\hat{\upsilon}_i^{\mathcal{B}(\mathrm{R})}\right)^\top-\hat{\upsilon}_i^{\mathcal{B}(\mathrm{R})}\left(\upsilon_i^{\mathcal{B}(\mathrm{R})}\right)^\top\right)\hat{R}^\top \\
&= \frac{1}{2}\hat{R}R^\top\mathbf{M}_{\mathrm{R}}-\frac{1}{2}\mathbf{M}_{\mathrm{R}}R\hat{R}^\top \\
&= \boldsymbol{\mathcal{P}}_a(\tilde{R}\mathbf{M}_{\mathrm{R}})
\end{aligned}$$

such that

$$\mathbf{vex}(\boldsymbol{\mathcal{P}}_a(\tilde{R}\mathbf{M}_{\mathrm{R}}))=\hat{R}\sum_{i=1}^{N_{\mathrm{R}}}\left(\frac{k_i^{\mathrm{R}}}{2}\hat{\upsilon}_i^{\mathcal{B}(\mathrm{R})}\times\upsilon_i^{\mathcal{B}(\mathrm{R})}\right) \tag{6.54}$$

Thus, $\tilde{R}\mathbf{M}_{\mathrm{R}}$ is defined in terms of vectorial measurements by

$$\tilde{R}\mathbf{M}_{\mathrm{R}}=\hat{R}\sum_{i=1}^{N_{\mathrm{R}}}\left(k_i^{\mathrm{R}}\upsilon_i^{\mathcal{B}(\mathrm{R})}\left(\upsilon_i^{\mathcal{I}(\mathrm{R})}\right)^\top\right) \tag{6.55}$$

The normalized Euclidean distance of $\tilde{R}\mathbf{M}_{\mathrm{R}}$ is found to be

$$\begin{aligned}
||\tilde{R}\mathbf{M}_{\mathrm{R}}||_I &= \frac{1}{4}\mathrm{Tr}\{(\mathbf{I}_3-\tilde{R})\mathbf{M}_{\mathrm{R}}\} \\
&= \frac{1}{4}\mathrm{Tr}\left\{\mathbf{I}_3-\hat{R}\sum_{i=1}^{N_{\mathrm{R}}}\left(k_i^{\mathrm{R}}\upsilon_i^{\mathcal{B}(\mathrm{R})}\left(\upsilon_i^{\mathcal{I}(\mathrm{R})}\right)^\top\right)\right\} \\
&= \frac{1}{4}\sum_{i=1}^{N_{\mathrm{R}}}\left(1-\left(\hat{\upsilon}_i^{\mathcal{B}(\mathrm{R})}\right)^\top\upsilon_i^{\mathcal{B}(\mathrm{R})}\right)
\end{aligned} \tag{6.56}$$

Let us introduce the following variable

$$\begin{aligned}\boldsymbol{\Upsilon}(\mathbf{M}_{\mathrm{R}}, \tilde{R}) =& \mathrm{Tr}\left\{\tilde{R}\mathbf{M}_{\mathrm{R}}\mathbf{M}_{\mathrm{R}}^{-1}\right\} \\ =& \mathrm{Tr}\left\{\left(\sum_{i=1}^{N_{\mathrm{R}}} k_i^{\mathrm{R}} \upsilon_i^{\mathcal{B}(\mathrm{R})}\left(\upsilon_i^{\mathcal{I}(\mathrm{R})}\right)^{\top}\right)\left(\sum_{i=1}^{N_{\mathrm{R}}} k_i^{\mathrm{R}} \hat{\upsilon}_i^{\mathcal{B}(\mathrm{R})}\left(\upsilon_i^{\mathcal{I}(\mathrm{R})}\right)^{\top}\right)^{-1}\right\}\end{aligned} \tag{6.57}$$

From (6.49) and (6.50), one obtains

$$\tilde{\boldsymbol{T}}\boldsymbol{\mathcal{M}}^{\mathcal{I}} = \begin{bmatrix} \tilde{R}\mathbf{M}_{\mathrm{T}} + \tilde{P}\mathbf{m}_{\mathrm{v}}^{\top} & \tilde{R}\mathbf{m}_{\mathrm{v}} + \mathbf{m}_{\mathrm{c}}\tilde{P} \\ \mathbf{m}_{\mathrm{v}}^{\top} & \mathbf{m}_{\mathrm{c}} \end{bmatrix} \tag{6.58}$$

The above-mentioned result can be additionally expressed as

$$\tilde{\boldsymbol{T}}\boldsymbol{\mathcal{M}}^{\mathcal{I}} = \begin{bmatrix} \hat{R} & \hat{P} \\ \underline{\mathbf{0}}_3^{\top} & 1 \end{bmatrix}\begin{bmatrix} \mathbf{K}_{\mathrm{T}} & \mathbf{k}_{\mathrm{v}} \\ \mathbf{m}_{\mathrm{v}}^{\top} & \mathbf{m}_{\mathrm{c}} \end{bmatrix} = \begin{bmatrix} \hat{R}\mathbf{K}_{\mathrm{T}} + \hat{P}\mathbf{m}_{\mathrm{v}}^{\top} & \hat{R}\mathbf{k}_{\mathrm{v}} + \mathbf{m}_{\mathrm{c}}\hat{P} \\ \mathbf{m}_{\mathrm{v}}^{\top} & \mathbf{m}_{\mathrm{c}} \end{bmatrix} \tag{6.59}$$

As such, from (6.58) and (6.59), the position error can be reformulated with respect to vectorial measurements as

$$\tilde{P} = \hat{P} + \frac{1}{\mathbf{m}_{\mathrm{c}}}\left(\hat{R}\mathbf{k}_{\mathrm{v}} - \tilde{R}\mathbf{M}_{\mathrm{R}}\mathbf{M}_{\mathrm{R}}^{-1}\mathbf{m}_{\mathrm{v}}\right) \tag{6.60}$$

with $\tilde{R}\mathbf{M}_{\mathrm{R}}$ being calculated as in (6.55). Consequently, $\mathbf{vex}(\boldsymbol{\mathcal{P}}_a(\tilde{R}\mathbf{M}_{\mathrm{R}}))$, $\tilde{R}\mathbf{M}_{\mathrm{R}}$, $||\tilde{R}\mathbf{M}_{\mathrm{R}}||_I$, $\boldsymbol{\Upsilon}(\mathbf{M}_{\mathrm{R}}, \tilde{R})$, and $\tilde{P}$ will be obtained through a set of vectorial measurements as defined in (6.54), (6.55), (6.56), (6.57), and (6.60), respectively, in all the subsequent derivations and calculations. Let us modify the vector error in (6.19) to be

$$\boldsymbol{e} = [\boldsymbol{e}_1, \boldsymbol{e}_2, \boldsymbol{e}_3, \boldsymbol{e}_4]^{\top} = \left[||\tilde{R}\mathbf{M}_{\mathrm{R}}||_I, \tilde{P}^{\top}\right]^{\top} \tag{6.61}$$

with $||\tilde{R}\mathbf{M}_{\mathrm{R}}||_I$ and $\tilde{P}$ being defined in (6.56) and (6.60), respectively. Thus, all the discussion in Subsection 6.2.2 is to be reformulated using the error vector in (6.61) instead of (6.19). Define the minimum eigenvalue of $\bar{\mathbf{M}}_{\mathrm{R}}$ as $\underline{\lambda} := \underline{\lambda}(\bar{\mathbf{M}}_{\mathrm{R}})$, and consider

the following filter design

$$\dot{\hat{R}} = \hat{R}\left[\Omega_m - \hat{b}_\Omega - \hat{R}^\top W_\Omega\right]_\times \tag{6.62}$$

$$\dot{\hat{P}} = \hat{R}(V_m - \hat{b}_V - W_V) \tag{6.63}$$

$$\dot{\hat{b}}_\Omega = \frac{\gamma}{2}\mathbf{\Psi}_R \mathcal{E}_R \hat{R}^\top \mathbf{vex}(\boldsymbol{\mathcal{P}}_a(\tilde{R}\mathbf{M}_\mathrm{R})) + \gamma \hat{R}^\top \left[\tilde{P} - \hat{P}\right]_\times \mathbf{\Psi}_P \mathcal{E}_P \tag{6.64}$$

$$\dot{\hat{b}}_V = \gamma \hat{R}^\top \mathbf{\Psi}_P \mathcal{E}_P \tag{6.65}$$

$$W_\Omega = \frac{4}{\underline{\lambda}} \frac{k_w \mathbf{\Psi}_R \mathcal{E}_R - \mathbf{\Lambda}_R}{1 + \mathbf{\Upsilon}(\mathbf{M}_\mathrm{R}, \tilde{R})} \mathbf{vex}(\boldsymbol{\mathcal{P}}_a(\tilde{R}\mathbf{M}_\mathrm{R})) \tag{6.66}$$

$$W_V = \hat{R}^\top \left(k_w \mathbf{\Psi}_P \mathcal{E}_P + \left[\tilde{P} - \hat{P}\right]_\times W_\Omega - \mathbf{\Lambda}_P \tilde{P}\right) \tag{6.67}$$

with $\mathbf{\Upsilon}(\mathbf{M}_\mathrm{R}, \tilde{R})$ and $\mathbf{vex}(\boldsymbol{\mathcal{P}}_a(\tilde{R}\mathbf{M}_\mathrm{R}))$ being specified in (6.57) and (6.54), respectively, $\mathcal{E} = [\mathcal{E}_R, \mathcal{E}_P^\top]^\top = [\mathcal{E}_1, \ldots, \mathcal{E}_4]^\top$, $\mathcal{E}_i := \mathcal{E}_i(\boldsymbol{e}_i, \xi_i)$ and $\mu_i := \mu_i(\boldsymbol{e}_i, \xi_i)$ being defined in (6.27) and (6.28), respectively, while $\boldsymbol{e}$ is as in (6.61), k_w and γ are positive constants, and $\hat{b}_\Omega$ and $\hat{b}_V$ are the estimates of b_Ω and b_V, respectively.

Theorem 6.2 *Consider coupling the pose filter in (6.62), (6.63), (6.64), (6.65), (6.66), and (6.67) with the set of vector measurements in (6.4) and (6.6), and the velocity measurements in (6.11) and (6.12) where $\Omega_m = \Omega + b_\Omega$ and $V_m = V + b_V$. Let Assumption 6.2 hold. Define $\mathcal{U} \subseteq \mathbb{SE}(3) \times \mathbb{R}^6$ by*

$$\mathcal{U} := \left\{ (\tilde{\boldsymbol{T}}(0), \tilde{b}(0)) \middle| \mathrm{Tr}\{\tilde{R}(0)\} = -1, \tilde{P}(0) = \underline{\mathbf{0}}_3, \tilde{b}(0) = \underline{\mathbf{0}}_6 \right\}$$

If $\tilde{R}(0) \notin \mathcal{U}$ and $\mathcal{E}(0) \in \mathcal{L}_\infty$, then, all error signals are bounded, $\mathcal{E}(t)$ asymptotically approaches 0, and $\tilde{\boldsymbol{T}}$ asymptotically approaches $\mathbf{I}_4$.

Theorem 6.2 guarantees the observer dynamics in (6.62), (6.63), (6.64), (6.65), (6.66), and (6.67) to be stable. In consistence with Remark 6.2 boundedness of $\mathcal{E}(t)$ indicates that $\boldsymbol{e}$ follows the dynamic decreasing boundaries in (6.20).

Proof. Consider the error in the homogeneous transformation matrix and bias defined as in (6.16), (6.38) and (6.39), respectively. From (6.9) and (6.62), the error dynamics of $\tilde{R}$ can be found to be analogous to (6.40). The ith inertial measurements $\mathrm{v}_i^{\mathcal{I}(\mathrm{R})}$ and $\mathrm{v}_i^{\mathcal{I}(\mathrm{L})}$ are constant, thus, $\dot{\mathbf{M}}_\mathrm{R} = \mathbf{0}_{3\times 3}$. Consequently, from (6.40), the

derivative of $||\tilde{R}\mathbf{M}_{\mathrm{R}}||_I$ is equivalent to

$$\begin{aligned}\frac{d}{dt}||\tilde{R}\mathbf{M}_{\mathrm{R}}||_I =& -\frac{1}{4}\mathrm{Tr}\left\{\left[\hat{R}\tilde{b}_\Omega - W_\Omega\right]_\times \tilde{R}\mathbf{M}_{\mathrm{R}}\right\}\\ =& -\frac{1}{4}\mathrm{Tr}\left\{\left[\hat{R}\tilde{b}_\Omega - W_\Omega\right]_\times \boldsymbol{\mathcal{P}}_a(\tilde{R}\mathbf{M}_{\mathrm{R}})\right\}\\ =&\frac{1}{2}\mathbf{vex}(\boldsymbol{\mathcal{P}}_a(\tilde{R}\mathbf{M}_{\mathrm{R}}))^\top(\hat{R}\tilde{b}_\Omega - W_\Omega)\end{aligned} \tag{6.68}$$

where $\mathrm{Tr}\left\{[W_\Omega]_\times \tilde{R}\mathbf{M}_{\mathrm{R}}\right\} = -2\mathbf{vex}(\boldsymbol{\mathcal{P}}_a(\tilde{R}\mathbf{M}_{\mathrm{R}}))^\top W_\Omega$ as given in (2.16). One could find that the derivative of $\tilde{P}$ is equivalent to (6.42). From (6.68) and (6.42), and in view of (6.14), the derivative of $\boldsymbol{e}$ given in (6.61), becomes

$$\dot{\boldsymbol{e}} = \begin{bmatrix} \frac{1}{2}\mathbf{vex}(\boldsymbol{\mathcal{P}}_a(\tilde{R}\mathbf{M}_{\mathrm{R}}))^\top & 0_{1\times 3} \\ \left[\hat{P} - \tilde{P}\right]_\times & \hat{R} \end{bmatrix} \begin{bmatrix} \hat{R}\tilde{b}_\Omega - W_\Omega \\ \tilde{b}_V - W_V \end{bmatrix} \tag{6.69}$$

The derivative of the transformed error in (6.30) be acquired by direct substitution of $\boldsymbol{e}$ as in (6.61), in addition to the result in (6.69). Consider the candidate Lyapunov function

$$V(\mathcal{E}, \tilde{b}_\Omega, \tilde{b}_V) = \frac{1}{2}||\mathcal{E}||^2 + \frac{1}{2\gamma}||\tilde{b}_\Omega||^2 + \frac{1}{2\gamma}||\tilde{b}_V||^2 \tag{6.70}$$

The derivative of $V := V(\mathcal{E}, \tilde{b}_\Omega, \tilde{b}_V)$ is as follows

$$\begin{aligned}\dot{V} =& \mathcal{E}^\top\dot{\mathcal{E}} - \frac{1}{\gamma}\tilde{b}_\Omega^\top\dot{\hat{b}}_\Omega - \frac{1}{\gamma}\tilde{b}_V^\top\dot{\hat{b}}_V\\ =&\frac{1}{2}\mathcal{E}_R\boldsymbol{\Psi}_R\mathbf{vex}(\boldsymbol{\mathcal{P}}_a(\tilde{R}\mathbf{M}_{\mathrm{R}}))^\top(\hat{R}\tilde{b}_\Omega - W_\Omega)\\ &+ \mathcal{E}_P^\top\boldsymbol{\Psi}_P\left(\hat{R}(\tilde{b}_V - W_V) + \left[\hat{P} - \tilde{P}\right]_\times(\hat{R}\tilde{b}_\Omega - W_\Omega)\right)\\ &- \mathcal{E}_R\boldsymbol{\Psi}_R\boldsymbol{\Lambda}_R||\tilde{R}\mathbf{M}_{\mathrm{R}}||_I - \mathcal{E}_P^\top\boldsymbol{\Psi}_P\boldsymbol{\Lambda}_P\tilde{P} - \frac{1}{\gamma}\tilde{b}_\Omega^\top\dot{\hat{b}}_\Omega - \frac{1}{\gamma}\tilde{b}_V^\top\dot{\hat{b}}_V\end{aligned} \tag{6.71}$$

Directly substituting for $\dot{\hat{b}}_\Omega$, $\dot{\hat{b}}_V$, W_Ω and W_V in (6.64), (6.65), (6.66), and (6.67),

respectively, results in

$$\begin{aligned}\dot{V} \leq & \boldsymbol{\Lambda}_R \left(\frac{2}{\underline{\lambda}} \frac{||\mathbf{vex}(\boldsymbol{\mathcal{P}}_a(\tilde{R}\mathbf{M}_\mathrm{R}))||^2}{1+\boldsymbol{\Upsilon}(\mathbf{M}_\mathrm{R}, \tilde{R})} - ||\tilde{R}\mathbf{M}_\mathrm{R}||_I \right) \mathcal{E}_R \boldsymbol{\Psi}_R \\ & - \frac{2}{\underline{\lambda}} \frac{k_w \mathcal{E}_R^2 \boldsymbol{\Psi}_R^2}{1+\boldsymbol{\Upsilon}(\mathbf{M}_\mathrm{R}, \tilde{R})} \left\| \mathbf{vex}(\boldsymbol{\mathcal{P}}_a(\tilde{R}\mathbf{M}_\mathrm{R})) \right\|^2 - k_w \mathcal{E}_P^\top \boldsymbol{\Psi}_P^2 \mathcal{E}_P \end{aligned} \tag{6.72}$$

It can be easily found that

$$\boldsymbol{\Lambda}_R \left(\frac{2}{\underline{\lambda}} \frac{\left\| \mathbf{vex}(\boldsymbol{\mathcal{P}}_a(\tilde{R}\mathbf{M}_\mathrm{R})) \right\|^2}{1+\boldsymbol{\Upsilon}(\mathbf{M}_\mathrm{R}, \tilde{R})} - ||\tilde{R}\mathbf{M}_\mathrm{R}||_I \right) \mathcal{E}_R \boldsymbol{\Psi}_R \leq 0 \tag{6.73}$$

where $\mathcal{E}_R > 0 \forall ||\tilde{R}\mathbf{M}_\mathrm{R}||_I \neq 0$ and $\mathcal{E}_R = 0$ at $||\tilde{R}\mathbf{M}_\mathrm{R}||_I = 0$ as presented in (ii) Proposition 6.1, and $\boldsymbol{\Psi}_R > 0 \forall t \geq 0$ as given in (6.28). Also, $\dot{\xi}_i$ is negative and strictly increasing that satisfies $\dot{\xi}_i \to 0$ as $t \to \infty$, and $\xi_i : \mathbb{R}_+ \to \mathbb{R}_+$ such that $\xi_i \to \xi_i^\infty$ as $t \to \infty$. Thus, $\dot{\xi}_i / \xi_i \leq 0$ which means that $\boldsymbol{\Lambda}_R \leq 0$. Considering (6.18) in Lemma 6.1, thus, the expression in (6.73) is negative semi-definite. As such, the inequality in (6.72) can be expressed as

$$\dot{V} \leq - k_w \mathcal{E}_R^2 \boldsymbol{\Psi}_R^2 ||\tilde{R}\mathbf{M}_\mathrm{R}||_I - k_w \mathcal{E}_P^\top \boldsymbol{\Psi}_P^2 \mathcal{E}_P \tag{6.74}$$

This signifies that $V(t) \leq V(0), \forall t \geq 0$. From almost any initial conditions such that $\mathrm{Tr}\left\{\tilde{R}(0)\right\} \neq -1$ and $\mathcal{E}(0) \in \mathbb{R}^4$, $\mathcal{E}$ and $\tilde{b}$ are bounded for all $t \geq 0$. Thereby, $\mathcal{E}$ is bounded and well-defined for all $t \geq 0$. $\tilde{P}$, $||\tilde{R}\mathbf{M}_\mathrm{R}||_I$, and $\mathbf{vex}(\boldsymbol{\mathcal{P}}_a(\tilde{R}\mathbf{M}_\mathrm{R}))$ are also bounded which indicates that $\dot{\tilde{P}}$, $||\dot{\tilde{R}}\mathbf{M}_\mathrm{R}||_I$, $\dot{\mathcal{E}}_R$ and $\dot{\mathcal{E}}_P$ are bounded as well. In order to prove asymptotic convergence of $\mathcal{E}$ to the origin and $\tilde{\boldsymbol{T}}$ to the identity, it is necessary to show that the second derivative of (6.70) is

$$\begin{aligned}\ddot{V} \leq & - 2k_w \mathcal{E}_R \boldsymbol{\Psi}_R (\dot{\mathcal{E}}_R \boldsymbol{\Psi}_R + \mathcal{E}_R \dot{\boldsymbol{\Psi}}_R) ||\tilde{R}\mathbf{M}_\mathrm{R}||_I - k_w \mathcal{E}_R^2 \boldsymbol{\Psi}_R^2 ||\dot{\tilde{R}}\mathbf{M}_\mathrm{R}||_I \\ & - 2k_w \mathcal{E}_P^\top \boldsymbol{\Psi}_P (\boldsymbol{\Psi}_P \dot{\mathcal{E}}_P + \dot{\boldsymbol{\Psi}}_P \mathcal{E}_P) \end{aligned} \tag{6.75}$$

Recall that $\boldsymbol{\Psi}_R = \mu_1$ and $\boldsymbol{\Psi}_P = \mathrm{diag}(\mu_2, \mu_3, \mu_4)$, where $\dot{\mu}_i$ was defined in (6.48) for all $i = 1, 2, \ldots, 4$. Since $\dot{\boldsymbol{e}}_i$ is bounded, $\dot{\mu}_i$ is bounded as well and $\ddot{V}$ in (6.75) is bounded for all $t \geq 0$. From property (ii) of Proposition 6.1, $||\mathcal{E}_1|| \to 0$ indicates that $||\tilde{R}\mathbf{M}_\mathrm{R}||_I \to 0$, while $\mathcal{E}_1 \neq 0 \forall ||\tilde{R}\mathbf{M}_\mathrm{R}||_I \neq 0$ and according to property (iii) of

Proposition 6.1, $\mathcal{E}_i \neq 0 \forall \boldsymbol{e}_i \neq 0$ and $\mathcal{E}_i = 0$ if and only if $\boldsymbol{e}_i = 0$ for all $i = 1, \ldots, 4$. Therefore, $\dot{V}$ is uniformly continuous, and on the basis of Barbalat Lemma, $\dot{V} \to 0$ implies that $||\mathcal{E}|| \to 0$ and $\|\boldsymbol{e}\| \to 0$ as $t \to \infty$. This means that $\tilde{\boldsymbol{T}}$ approaches $\mathbf{I}_4$ asymptotically in accordance with (iv) of Proposition 6.1, which completes the proof.

The estimates $\dot{\hat{b}}_\Omega$ and $\dot{\hat{b}}_V$ and the correction factors W_Ω and W_V are functions of the transformed error $\mathcal{E}$ and the auxiliary component μ. $\mathcal{E}$ and μ rely on the error $\boldsymbol{e}$ such that their values become increasingly aggressive as $||\tilde{R}||_I$ approaches the unstable equilibria $||\tilde{R}||_I \to +1$ and $\tilde{P} \to \infty$. Their dynamic behavior is essential for forcing the proposed filters to obey the prescribed performance constraints. On the other side $\mathcal{E} \to 0$ as $\boldsymbol{e} \to 0$. This significant advantage was not offered in literature, such as Baldwin et al. (2009, 2007); Hashim, Brown, and McIsaac (2019d); Hua et al. (2011); Rehbinder and Ghosh (2003); Vasconcelos et al. (2010).

Remark 6.3 ***(Design parameters)*** *The dynamic boundaries of $\boldsymbol{e}$ are described by $\bar{\delta}$, $\underline{\delta}$, ξ_∞, and ξ_0 where ξ_0 and ξ_∞ define the large and small sets, respectively. The rate of convergence from the given large set to the small set is controlled by ℓ. The initial value of $\boldsymbol{e}(0)$ in (6.19) or (6.61) can be easily obtained. When applying semi-direct pose filter, $R_y(0)$ can be reconstructed, for example, using Markley (1988); Shuster and Oh (1981), $P_y(0)$ can be evaluated by $P_y(0) = \mathcal{G}_c^{\mathcal{I}} - R_y(0)\,\mathcal{G}_c^{\mathcal{B}}$ as in (6.31), and finally $||\tilde{R}(0)||_I = \frac{1}{4}\mathrm{Tr}\{\mathbf{I}_3 - \hat{R}(0)\,R_y^\top(0)\}$ and $\tilde{P}(0) = \hat{P}(0) - \tilde{R}(0)\,P_y(0)$. In case when the direct pose filter is used, $||\tilde{R}(0)\,\mathbf{M}_\mathrm{R}||_I$ can be defined from (6.56) and $\tilde{P}(0)$ can be easily obtained in the form of a vectorial measurement based on (6.60). Next, the user can select $\bar{\delta}$, $\underline{\delta}$, and ξ_0 to be greater than $\boldsymbol{e}(0)$.*

6.3.3 Simplified steps of the proposed pose filters

The implementation of the proposed nonlinear pose filters on $\mathbb{SE}(3)$ with prescribed performance given in Subsections 6.3.1 and 6.3.2 can be summarized in the following 7 simplified steps:

Step 1*: Select $\gamma, k_w > 0$, $\bar{\delta} = \underline{\delta} > \boldsymbol{e}(0)$, the desired speed of the convergence rate ℓ, and the upper bound of the small set ξ_∞.*

Step 2*: For the case of the semi-direct pose filter, define $\boldsymbol{e} = \left[||\tilde{R}||_I, \tilde{P}^\top\right]^\top$ with $\tilde{R} = \hat{R}R_y^\top$ and $\tilde{P} = \hat{P} - \tilde{R}P_y$ where P_y is given in (6.31) and R_y is reconstructed*

(for example Markley (1988); Shuster and Oh (1981)). For the case of the direct pose filter, define $\boldsymbol{e} = \left[||\tilde{R}\mathbf{M}_{\mathrm{R}}||_I, \tilde{P}^\top\right]^\top$ *with* $||\tilde{R}\mathbf{M}_{\mathrm{R}}||_I$ *and* $\tilde{P}$ *being specified as in* (6.56) *and* (6.60)*, respectively.*

Step 3*: For the case of the semi-direct pose filter, evaluate* $\mathbf{vex}(\boldsymbol{\mathcal{P}}_a(\tilde{R}))$*, whereas, for the case of the direct pose filter, define* $\mathbf{vex}(\boldsymbol{\mathcal{P}}_a(M^{\mathcal{B}}\tilde{R}))$ *and* $\boldsymbol{\Upsilon}(\mathbf{M}_{\mathrm{R}}, \tilde{R})$ *from* (6.54)*, and* (6.57)*, respectively.*

Step 4*: Find the PPF* ξ *from* (6.20)*.*

Step 5*: Evaluate the transformed error* $\mathcal{E}$*,* $\boldsymbol{\Lambda}_R$*,* $\boldsymbol{\Psi}_R$*,* $\boldsymbol{\Lambda}_P$*, and* $\boldsymbol{\Psi}_P$ *from* (6.27) *and* (6.28)*, respectively.*

Step 6*: Obtain the filter kinematics* $\dot{\hat{R}}$*,* $\dot{\hat{P}}$*,* $\dot{\hat{b}}_\Omega$*,* $\dot{\hat{b}}_V$*,* W_Ω*, and* W_V *from* (6.32)*,* (6.33)*,* (6.34)*,* (6.35)*,* (6.36)*, and* (6.37)*, respectively, for the semi-direct pose filter, or from* (6.62)*,* (6.63)*,* (6.64)*,* (6.65)*,* (6.66)*, and* (6.67)*, respectively, for the direct pose filter.*

Step 7*: Go to* ***Step 2****.*

6.4 Simulations

This section illustrates the robustness of the proposed pose filters on $\mathbb{SE}(3)$ with prescribed performance against large error in initialization of $\tilde{\boldsymbol{T}}(0)$ and high levels of bias and noise inherent to the measurement process. Let the dynamics of the homogeneous transformation matrix $\boldsymbol{T}$ follow (6.10). Define the true angular velocity (rad/sec) by

$$\Omega = \left[\sin(0.5t), 0.7\sin(0.4t+\pi), 0.5\sin\left(0.35t+\frac{\pi}{3}\right)\right]^\top$$

with $R(0) = \mathbf{I}_3$. Consider the following true translational velocity (m/sec)

$$V = \left[0.3\sin(0.6t), 0.18\sin\left(0.4t+\frac{\pi}{2}\right), 0.3\sin\left(0.1t+\frac{\pi}{4}\right)\right]^\top$$

and the initial position $P(0) = \underline{\mathbf{0}}_3$. Let the measurements of angular and translational velocities be $\Omega_m = \Omega + b_\Omega + \omega_\Omega$ and $V_m = V + b_V + \omega_V$, respectively, with

$b_\Omega = 0.1\,[1,-1,1]^\top$ and $b_V = 0.1\,[2,5,1]^\top$. ω_Ω and ω_V represent random noise process at each time instant with zero mean and standard deviation (STD) equal to $0.15\,(\text{rad/sec})$ and $0.3\,(\text{m/sec})$, respectively. Assume that one landmark is available for measurement ($N_{\mathrm{L}} = 1$)

$$\mathrm{v}_1^{\mathcal{I}(\mathrm{L})} = \left[\frac{1}{2}, \sqrt{2}, 1\right]^\top$$

where the body-frame measurements are defined as (6.5) $\mathrm{v}_1^{\mathcal{B}(\mathrm{L})} = R^\top\left(\mathrm{v}_1^{\mathcal{I}(\mathrm{L})} - P\right) + \mathrm{b}_1^{\mathcal{B}(\mathrm{L})} + \omega_1^{\mathcal{B}(\mathrm{L})}$. The bias vector is $\mathrm{b}_1^{\mathcal{B}(\mathrm{L})} = 0.1\,[0.3, 0.2, -0.2]^\top$ while $\omega_1^{\mathcal{B}(\mathrm{L})}$ is a Gaussian noise vector with zero mean and STD $= 0.1$. Assume that two non-collinear inertial-frame vectors ($N_{\mathrm{R}} = 2$) are available with

$$\mathrm{v}_1^{\mathcal{I}(\mathrm{R})} = \frac{1}{\sqrt{3}}\,[1,-1,1]^\top, \quad \mathrm{v}_2^{\mathcal{I}(\mathrm{R})} = [0,0,1]^\top$$

while the two body-frame vectors are defined as in (6.2) $\mathrm{v}_i^{\mathcal{B}(\mathrm{R})} = R^\top \mathrm{v}_i^{\mathcal{I}(\mathrm{R})} + \mathrm{b}_i^{\mathcal{B}(\mathrm{R})} + \omega_i^{\mathcal{B}(\mathrm{R})}$ for $i = 1, 2$ such that $\mathrm{b}_1^{\mathcal{B}(\mathrm{R})} = 0.1\,[-1, 1, 0.5]^\top$ and $\mathrm{b}_2^{\mathcal{B}(\mathrm{R})} = 0.1\,[0, 0, 1]^\top$. In addition, $\omega_1^{\mathcal{B}(\mathrm{R})}$ and $\omega_2^{\mathcal{B}(\mathrm{R})}$ are Gaussian noise vectors with zero mean and STD $= 0.1$. The third vector is obtained using $\mathrm{v}_3^{\mathcal{I}(\mathrm{R})} = \mathrm{v}_1^{\mathcal{I}(\mathrm{R})} \times \mathrm{v}_2^{\mathcal{I}(\mathrm{R})}$ and $\mathrm{v}_3^{\mathcal{B}(\mathrm{R})} = \mathrm{v}_1^{\mathcal{B}(\mathrm{R})} \times \mathrm{v}_2^{\mathcal{B}(\mathrm{R})}$. This step is followed by the normalization of $\mathrm{v}_i^{\mathcal{B}(\mathrm{R})}$ and $\mathrm{v}_i^{\mathcal{I}(\mathrm{R})}$ to $\upsilon_i^{\mathcal{B}(\mathrm{R})}$ and $\upsilon_i^{\mathcal{I}(\mathrm{R})}$, respectively, for $i = 1, 2, 3$ as given in (6.3). Thus, Assumption 6.2 holds. For the semi-direct pose filter with prescribed performance, R_y is obtained by SVD Markley (1988), or for simplicity visit the Appendix in Hashim et al. (2018b) with $\tilde{R} = \hat{R}R_y^\top$. The total simulation time is 30 seconds.

Initial attitude error is set to be considerably large. Initial attitude estimate is given by $\hat{R}(0) = \mathcal{R}_\alpha(\alpha, u/||u||)$ according to angle-axis parameterization as in (2.7) with $\alpha = 175\,(\text{deg})$ and $u = [3, 10, 8]^\top$. It is worth noting that the value of $||\tilde{R}||_I \approx 0.999$ is fairly close to the unstable equilibria $(+1)$ and the initial position is $\hat{P}(0) = [4, -3, 5]^\top$. In brief, we have

$$\boldsymbol{T}(0) = \mathbf{I}_4, \quad \hat{\boldsymbol{T}}(0) = \begin{bmatrix} -0.8923 & 0.2932 & 0.3432 & 4 \\ 0.3992 & 0.1577 & 0.9032 & -3 \\ 0.2107 & 0.9430 & -0.2577 & 5 \\ 0 & 0 & 0 & 1 \end{bmatrix}$$

The design parameters of the proposed filters are chosen as $\gamma = 1$, $k_w = 5$, $\bar{\delta} = \underline{\delta} =$

$[1.3, 5, 4, 6]^\top$, $\xi^0 = [1.3, 5, -4, 6]^\top$, $\xi^\infty = [0.07, 0.3, 0.3, 0.3]^\top$, and $\ell = [4, 4, 4, 4]^\top$. The initial bias estimates are $\hat{b}_\Omega(0) = [0, 0, 0]^\top$ and $\hat{b}_V(0) = [0, 0, 0]^\top$.

Color notation used in the plots is: black center-lines and green solid-lines refer to the true values, red illustrates the performance of the nonlinear semi-direct pose filter (S-DIR) on $\mathbb{SE}(3)$ proposed in Subsection 6.3.1, and blue demonstrates the performance of the direct filter (DIR) on $\mathbb{SE}(3)$ presented in Subsection 6.3.2. Also, magenta depicts a measured value while orange and black dashed lines refer to the prescribed performance response.

Fig. 6.3, 6.4 and 6.5 depict high values of noise and bias components attached to velocity and body-frame vector measurements plotted against the true values. Fig. 6.6 and 6.7 show the output performance of the proposed filters described in terms of Euler angles (ϕ, θ, ψ) and the true position in 3D space, respectively. Fig. 6.6 and 6.7 present remarkable tracking performance with fast convergence to the true Euler angles and xyz-positions 3D space. The systematic and smooth convergence of the error vector $\boldsymbol{e}$ is depicted in Fig. 6.8. It can be clearly observed how $||\tilde{R}||_I$ in Fig. 6.8 started very near to the unstable equilibria while $\tilde{P}_1$, $\tilde{P}_2$, and $\tilde{P}_3$ started remarkably far from the origin within the predefined large set and decayed smoothly and systematically to the predefined small set guided by the dynamic boundaries of the PPF such that $\tilde{R} = \hat{R}R^\top$ and $\tilde{P} = \hat{P} - \tilde{R}P$. Finally, the estimated bias $\hat{b}$ is bounded as depicted in Fig. 6.9.

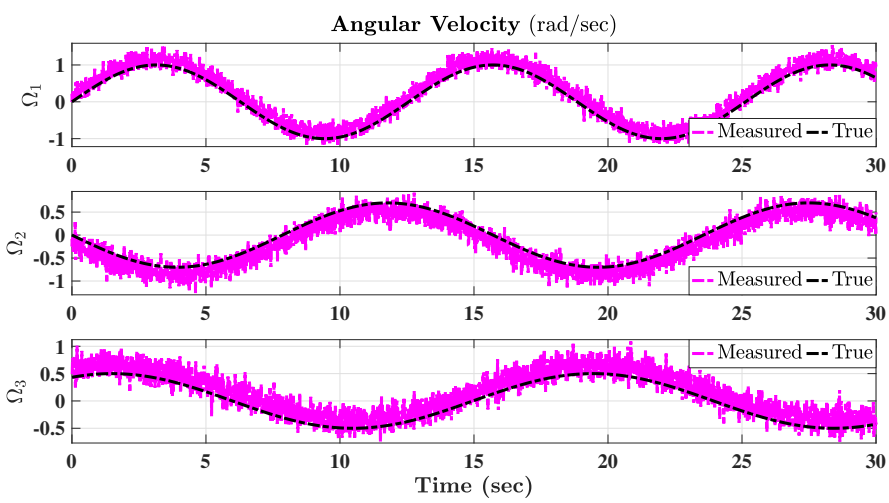

Figure 6.3: Measured and true values of angular velocities.

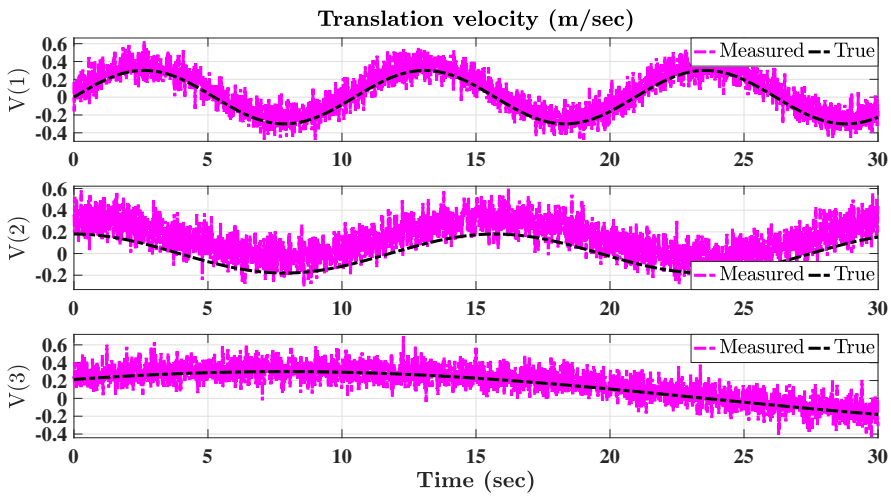

Figure 6.4: Measured and true values of translational velocities.

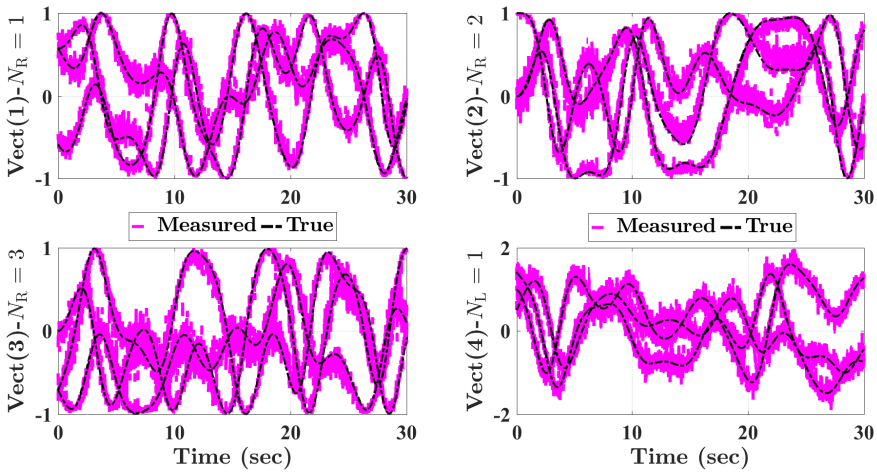

Figure 6.5: True and measured body-frame vectorial measurements.

The simulation results establish the strong filtering capability of the two proposed pose filters and their robustness against uncertain measurements and large initialized errors making them perfectly fit for the measurements obtained from low quality sensors such as IMU. The two filters conform to the dynamic constraints imposed by the user referring guaranteed prescribed performance measures in transient as well as steady-state performance. The pose filters previously proposed in the literature Baldwin et al. (2009, 2007); Hua et al. (2011); Rehbinder and Ghosh (2003); Vasconcelos et al. (2010) lack this remarkable quality. Semi-direct pose filter with prescribed performance demands pose reconstruction, in this case attitude has been

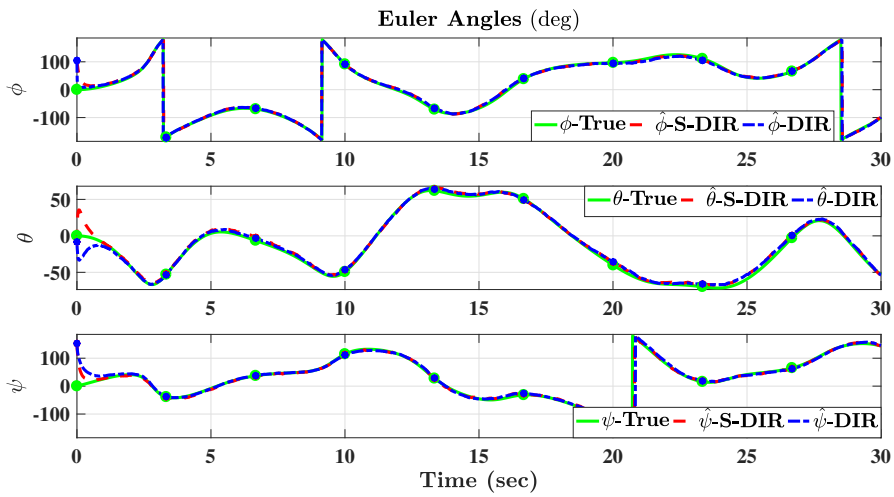

Figure 6.6: True and estimated Euler angles of the rigid-body.

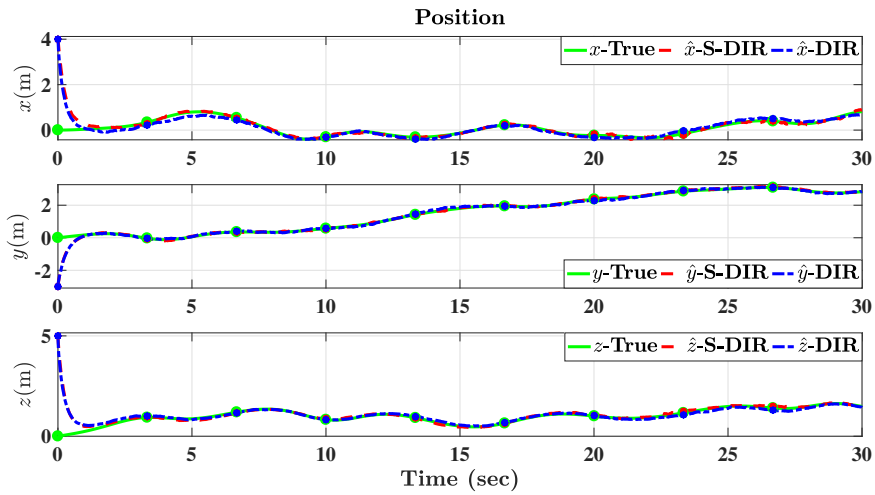

Figure 6.7: True and estimated rigid-body positions in 3D space.

extracted using SVD Hashim et al. (2018b); Markley (1988). This adds complexity, and therefore the semi-direct pose filter requires more computational power in comparison with the direct pose filter with prescribed performance. Nevertheless, the two proposed pose filters are robust and demonstrate impressive convergence capabilities.

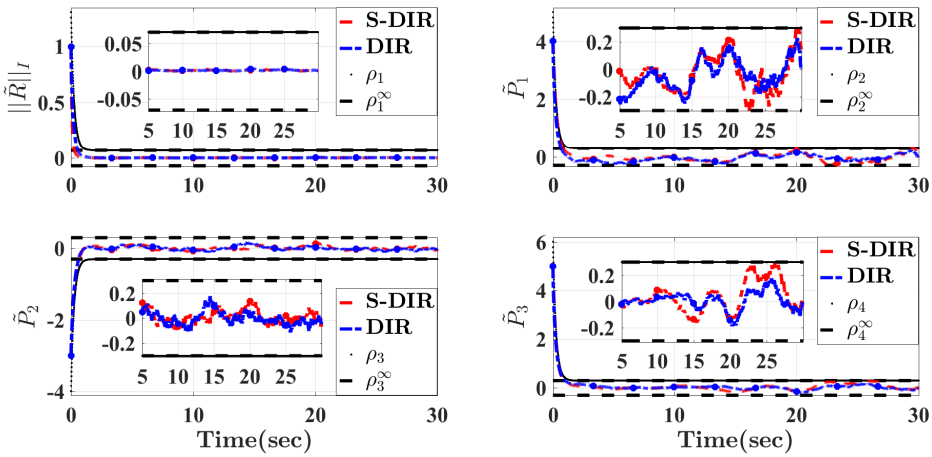

Figure 6.8: Systematic convergence of the error trajectories within the prescribed performance boundaries.

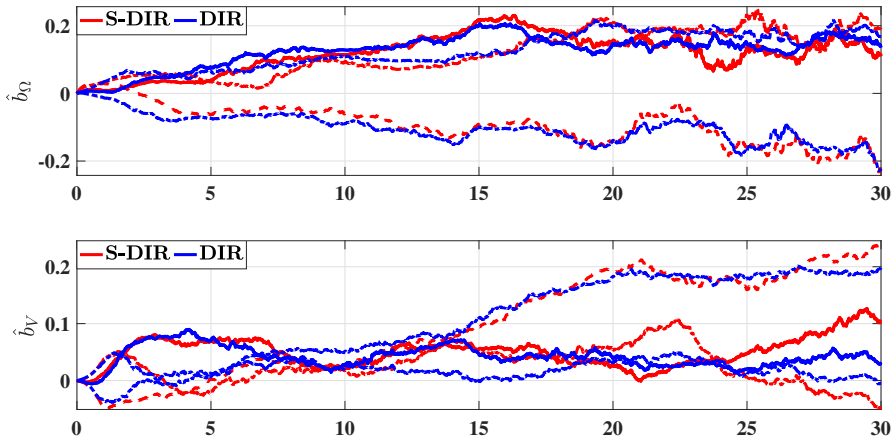

Figure 6.9: The estimated bias of the proposed filters.

6.5 Conclusion

Two nonlinear pose filters evolved directly on $\mathbb{SE}(3)$ with prescribed performance characteristics have been considered. Pose error has been defined in terms of position error and normalized Euclidean distance error, and the innovation term has been selected to guarantee predefined measures of transient and steady-state performance. As a result, the proposed filters exhibit superior convergence properties with transient error being bounded by a predefined dynamically decreasing constrained function

and steady-state error being less than a predefined lower bound. The proposed pose filters are deterministic and the stability analysis ensure boundedness of all closed loop signals with asymptotic convergence of the homogeneous transformation matrix to the origin. Simulation results established the strong ability of the proposed filters to impose the predefined constraints on the pose error considering large initial pose error and high level of uncertainties in the measurements.

Chapter 7
Nonlinear Stochastic Pose Filter on $\mathbb{SE}(3)$

7.1 Introduction

This chapter formulates the pose (attitude and position) estimation problem as nonlinear stochastic filter kinematics evolved directly on the Special Euclidean Group $\mathbb{SE}(3)$. This work proposes an alternate way of potential function selection and handles the problem as a stochastic filtering problem. The problem is mapped from $\mathbb{SE}(3)$ to vector form, using the Rodriguez vector and the position vector, and then followed by the definition of the pose problem in the sense of Stratonovich. The proposed filter guarantees that the errors present in position and Rodriguez vector estimates are semi-globally uniformly ultimately bounded (SGUUB) in mean square, and that they converge to small neighborhood of the origin in probability. Simulation results show the robustness and effectiveness of the proposed filter in presence of high levels of noise and bias associated with the velocity vector as well as body-frame measurements. The results of this chapter were first published in Hashim, Brown, and McIsaac (2019d).

The rest of the chapter is organized as follows: Pose estimation dynamic problem in the stochastic sense is presented in Section 7.2. The nonlinear stochastic filter on $\mathbb{SE}(3)$ and the stability analysis are presented in Section 7.3. Section 7.4 demonstrates numerical results and shows the output performance of the proposed stochastic filter. Finally, Section 7.5 draws a conclusion of this work.

7.2 Problem Formulation in Stochastic Sense

The orientation of a rigid-body rotating in 3D space $R \in \mathbb{SO}(3)$ is normally defined in terms of the body-frame $R \in \{\mathcal{B}\}$ relative to the inertial-frame $\{\mathcal{I}\}$. Let $P \in \mathbb{R}^3$

be the position of the rigid-body measured on the inertial-frame $P \in \{\mathcal{I}\}$. Thereby, this work concerns position as well as attitude estimation of a rigid-body moving and rotating in 3D space. Consider the homogeneous transformation matrix given by

$$\boldsymbol{T} = \begin{bmatrix} R & P \\ \underline{\mathbf{0}}_3^\top & 1 \end{bmatrix} \in \mathbb{SE}(3) \tag{7.1}$$

Let $\Omega \in \mathbb{R}^3$ and $V \in \mathbb{R}^3$ be angular and translational velocity of a moving rigid-body attached to the body-frame, respectively, for all $\Omega, V \in \{\mathcal{B}\}$. Hence, the dynamics of the homogeneous transformation matrix $\boldsymbol{T}$ are expressed by

$$\dot{P} = RV$$

$$\dot{R} = R\left[\Omega\right]_\times \tag{7.2}$$

$$\dot{\boldsymbol{T}} = \boldsymbol{T}\left[\mathcal{Y}\right]_\wedge \tag{7.3}$$

where $\mathcal{Y} = \left[\Omega^\top, V^\top\right]^\top \in \mathbb{R}^6$ is the group velocity vector expressed relative to the body-frame. The homogeneous transformation matrix $\boldsymbol{T}$ can be reconstructed through a set of known vectors in the inertial-frame and their measurements in the body-frame. Let the superscript $\mathcal{B}$ and $\mathcal{I}$ denote the associated body-frame and inertial-frame of the component, respectively. The pose estimation problem is illustrated in Figure 7.1.

Assume that there exists a number of feature points or landmarks denoted by N_{L} such that

$$\mathrm{v}_i^{\mathcal{B}(\mathrm{L})} = R^\top\left(\mathrm{v}_i^{\mathcal{I}(\mathrm{L})} - P\right) + \mathrm{b}_i^{\mathcal{B}(\mathrm{L})} + \omega_i^{\mathcal{B}(\mathrm{L})} \tag{7.4}$$

with $\mathrm{v}_i^{\mathcal{B}(\mathrm{L})} \in \mathbb{R}^3$ being the landmark measurement in the body-frame and $\mathrm{v}_i^{\mathcal{I}(\mathrm{L})} \in \mathbb{R}^3$ being a known constant feature in the inertial-frame for all $i = 1, \ldots, N_{\mathrm{L}}$. Also, $\mathrm{b}_i^{\mathcal{B}(\mathrm{L})} \in \mathbb{R}^3$ and $\omega_i^{\mathcal{B}(\mathrm{L})} \in \mathbb{R}^3$ are unknown bias and noise vectors attached to the ith measurement for all $i = 1, \ldots, N_{\mathrm{L}}$. The position P can be simply constructed if the attitude matrix R is available. Let us denote the set of vectors associated with

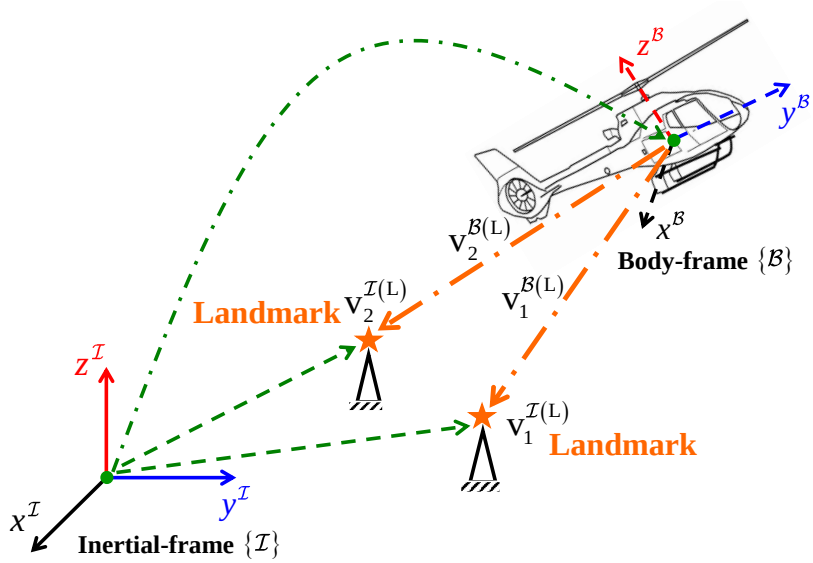

Figure 7.1: Pose estimation problem of a rigid-body moving in 3D space.

landmarks by

$$\begin{aligned}\mathrm{v}^{\mathcal{B}(\mathrm{L})} &= \left[\mathrm{v}_1^{\mathcal{B}(\mathrm{L})}, \ldots, \mathrm{v}_{N_\mathrm{L}}^{\mathcal{B}(\mathrm{L})}\right] \in \{\mathcal{B}\} \\ \mathrm{v}^{\mathcal{I}(\mathrm{L})} &= \left[\mathrm{v}_1^{\mathcal{I}(\mathrm{L})}, \ldots, \mathrm{v}_{N_\mathrm{L}}^{\mathcal{I}(\mathrm{L})}\right] \in \{\mathcal{I}\}\end{aligned} \tag{7.5}$$

A weighted geometric center is considered for the case of more than one landmark is available for measurement. The center is given by

$$P_c^{\mathcal{I}} = \frac{1}{\sum_{i=1}^{N_\mathrm{L}} k_i^\mathrm{L}} \sum_{i=1}^{N_\mathrm{L}} k_i^\mathrm{L} \mathrm{v}_i^{\mathcal{I}(\mathrm{L})} \tag{7.6}$$

$$P_c^{\mathcal{B}} = \frac{1}{\sum_{i=1}^{N_\mathrm{L}} k_i^\mathrm{L}} \sum_{i=1}^{N_\mathrm{L}} k_i^\mathrm{L} \mathrm{v}_i^{\mathcal{B}(\mathrm{L})} \tag{7.7}$$

with k_i^L refers to the confidence level of the ith measurement. On the other side, the attitude matrix R can be obtained through a set of N_R-known non-collinear vectors. The N_R vectors are measured in the moving frame $\{\mathcal{B}\}$. Let $\mathrm{v}_i^{\mathcal{B}(\mathrm{R})} \in \mathbb{R}^3$ be a measured vector in the body-frame such that the ith body-frame vector is given by

$$\mathrm{v}_i^{\mathcal{B}(\mathrm{R})} = R^\top \mathrm{v}_i^{\mathcal{I}(\mathrm{R})} + \mathrm{b}_i^{\mathcal{B}(\mathrm{R})} + \omega_i^{\mathcal{B}(\mathrm{R})} \tag{7.8}$$

where $\mathrm{v}_i^{\mathcal{I}(\mathrm{R})}$ refers to the known vector i in the inertial-frame for $i = 1, 2, \ldots, N_{\mathrm{R}}$. $\mathrm{b}_i^{\mathcal{B}(\mathrm{R})}$ and $\omega_i^{\mathcal{B}(\mathrm{R})}$ represent the unknown bias and noise components attached to the ith measurement, respectively, for all $\mathrm{b}_i^{\mathcal{B}(\mathrm{R})}, \omega_i^{\mathcal{B}(\mathrm{R})} \in \mathbb{R}^3$. Let us denote the set of vectors associated with attitude reconstruction by

$$\begin{aligned} \mathrm{v}^{\mathcal{B}(\mathrm{R})} &= \left[\mathrm{v}_1^{\mathcal{B}(\mathrm{R})}, \ldots, \mathrm{v}_{N_{\mathrm{R}}}^{\mathcal{B}(\mathrm{R})}\right] \in \{\mathcal{B}\} \\ \mathrm{v}^{\mathcal{I}(\mathrm{R})} &= \left[\mathrm{v}_1^{\mathcal{I}(\mathrm{R})}, \ldots, \mathrm{v}_{N_{\mathrm{R}}}^{\mathcal{I}(\mathrm{R})}\right] \in \{\mathcal{I}\} \end{aligned} \tag{7.9}$$

Assumption 7.1 *At least one feature point is available for measurements* (7.4) *with* $N_{\mathrm{L}} \geq 1$*, and three non-collinear vectors are available for measurements* (7.8) *with* $N_{\mathrm{R}} \geq 2$*. In case when* $N_{\mathrm{R}} = 2$*, the third vector can be obtained by* $\mathrm{v}_3^{\mathcal{I}(\mathrm{R})} = \mathrm{v}_1^{\mathcal{I}(\mathrm{R})} \times \mathrm{v}_2^{\mathcal{I}(\mathrm{R})}$ *and* $\mathrm{v}_3^{\mathcal{B}(\mathrm{R})} = \mathrm{v}_1^{\mathcal{B}(\mathrm{R})} \times \mathrm{v}_2^{\mathcal{B}(\mathrm{R})}$.

According to Assumption 7.1, $N_{\mathrm{R}} \geq 2$ means that the set of vectorial measurements in (7.9) is sufficient to have rank 3. The homogeneous transformation matrix $\boldsymbol{T}$ can be reconstructed if Assumption 7.1 is satisfied. It is common to obtain the normalized values of inertial and body-frame measurements in (7.8) such that

$$\upsilon_i^{\mathcal{I}(\mathrm{R})} = \frac{\mathrm{v}_i^{\mathcal{I}(\mathrm{R})}}{\left\|\mathrm{v}_i^{\mathcal{I}(\mathrm{R})}\right\|}, \quad \upsilon_i^{\mathcal{B}(\mathrm{R})} = \frac{\mathrm{v}_i^{\mathcal{B}(\mathrm{R})}}{\left\|\mathrm{v}_i^{\mathcal{B}(\mathrm{R})}\right\|} \tag{7.10}$$

and the normalized set of (7.10) is

$$\begin{aligned} \upsilon^{\mathcal{B}(\mathrm{R})} &= \left[\upsilon_1^{\mathcal{B}(\mathrm{R})}, \ldots, \upsilon_{N_{\mathrm{R}}}^{\mathcal{B}(\mathrm{R})}\right] \in \{\mathcal{B}\} \\ \upsilon^{\mathcal{I}(\mathrm{R})} &= \left[\upsilon_1^{\mathcal{I}(\mathrm{R})}, \ldots, \upsilon_{N_{\mathrm{R}}}^{\mathcal{I}(\mathrm{R})}\right] \in \{\mathcal{I}\} \end{aligned} \tag{7.11}$$

In that case, the attitude can be extracted knowing $\upsilon_i^{\mathcal{I}(\mathrm{R})}$ and $\upsilon_i^{\mathcal{B}(\mathrm{R})}$ instead of $\mathrm{v}_i^{\mathcal{I}(\mathrm{R})}$ and $\mathrm{v}_i^{\mathcal{B}(\mathrm{R})}$. Gyroscope obtains the measurements of angular velocity in the body-frame $\{\mathcal{B}\}$ and the measurement vector is defined by

$$\Omega_m = \Omega + b_\Omega + \omega_\Omega \in \{\mathcal{B}\} \tag{7.12}$$

with Ω denoting the true value of angular velocity, $b_\Omega \in \mathbb{R}^3$ denoting the bias component which is unknown constant or slowly time-varying vector, and $\omega_\Omega \in \mathbb{R}^3$ being the unknown noise component attached to angular velocity measurements. Also, the translational velocity is expressed in the body-frame and its measurement is defined by

$$V_m = V + b_V + \omega_V \in \{\mathcal{B}\} \tag{7.13}$$

where V denotes the true value of the translational velocity, $b_V \in \mathbb{R}^3$ denotes the unknown bias component, and $\omega_V \in \mathbb{R}^3$ is the unknown noise component attached to translational velocity measurements. Let the group of velocity measurements, bias and noise vectors be defined by $\mathcal{Y}_m = \left[\Omega_m^\top, V_m^\top\right]^\top$, $b = \left[b_\Omega^\top, b_V^\top\right]^\top$ and $\omega = \left[\omega_\Omega^\top, \omega_V^\top\right]^\top$, respectively, for all $\mathcal{Y}_m, b, \omega \in \mathbb{R}^6$. The noise vector ω is assumed to be Gaussian with zero mean. The dynamics of (7.2) can be mapped to Rodriguez vector and expressed as follows (Shuster (1993))

$$\dot{\rho} = \frac{1}{2}\left(\mathbf{I}_3 + [\rho]_\times + \rho\rho^\top\right)\Omega \tag{7.14}$$

Therefore, the dynamics of the homogeneous transformation matrix in (7.3) can be mapped to vector form in the sense of Rodriguez parameters from (7.14) and (A.1) as

$$\begin{bmatrix} \dot{\rho} \\ \dot{P} \end{bmatrix} = \begin{bmatrix} \frac{\mathbf{I}_3 + [\rho]_\times + \rho\rho^\top}{2} & \mathbf{0}_{3\times 3} \\ \mathbf{0}_{3\times 3} & \mathcal{R}_\rho(\rho) \end{bmatrix} \begin{bmatrix} \Omega \\ V \end{bmatrix} \tag{7.15}$$

where $\mathcal{R}_\rho(\rho) = R \in \mathbb{SO}(3)$ as given in (A.1). According to (7.12) and (7.13), the measurements of angular and translational velocities are subject to noise and bias components. These components are characterized by randomness and uncertainty. As such, the randomness in measurements could lead to unknown behavior (Hashim, El-Ferik, Ayinde, and Abido (2017); Hashim, El-Ferik, and Lewis (2017, 2019)) and impair the whole estimation process. The dynamics of the homogeneous transformation matrix in (7.3) become

$$\dot{\boldsymbol{T}} = \boldsymbol{T}\left[\ \mathcal{Y}_m - b - \omega\ \right]_\wedge \tag{7.16}$$

In view of (7.3) and (7.15), the dynamics in (7.16) can be mapped in the same sense

and represented as

$$\begin{bmatrix} \dot{\rho} \\ \dot{P} \end{bmatrix} = \begin{bmatrix} \frac{\mathbf{I}_3 + [\rho]_\times + \rho\rho^\top}{2} & \mathbf{0}_{3\times 3} \\ \mathbf{0}_{3\times 3} & \mathcal{R}_\rho(\rho) \end{bmatrix} (\mathcal{Y}_m - b - \omega) \tag{7.17}$$

where ω is a continuous Gaussian random noise vector with zero mean which is bounded. The derivative of any Gaussian process yields a Gaussian process (Jazwinski (2007); Khasminskii (1980)). Hence, the vector ω can be written as a function of Brownian motion process vector $d\beta/dt$ with $\beta \in \mathbb{R}^6$ such that

$$\omega = \mathcal{Q}\frac{d\beta}{dt}$$

where $\beta = \left[\beta_\Omega^\top, \beta_V^\top\right]^\top$ and $\mathcal{Q} \in \mathbb{R}^{6\times 6}$ is a diagonal matrix whose diagonal has unknown time-variant nonnegative components defined by

$$\mathcal{Q} = \begin{bmatrix} \mathcal{Q}_\Omega & \mathbf{0}_{3\times 3} \\ \mathbf{0}_{3\times 3} & \mathcal{Q}_V \end{bmatrix}$$

where $\mathcal{Q}_\Omega \in \mathbb{R}^{3\times 3}$ is associated with ω_Ω and $\mathcal{Q}_V \in \mathbb{R}^{3\times 3}$ is associated with ω_V. In addition, $\mathcal{Q}^2 = \mathcal{Q}\mathcal{Q}^\top$ is a covariance component associated with the noise vector ω. The properties of Brownian motion process are defined by (Deng et al. (2001); Ito and Rao (1984); Jazwinski (2007))

$$\mathbb{P}\{\beta(0) = 0\} = 1, \quad \mathbb{E}[d\beta/dt] = 0, \quad \mathbb{E}[\beta] = 0$$

Let the dynamics of the homogeneous transformation in (7.3) be defined in the sense of Stratonovich (Stratonovich (1967)) and substitute ω by $\mathcal{Q}d\beta/dt$. Accordingly, the stochastic differential equation of (7.3) can be expressed as

$$d\boldsymbol{T} = \boldsymbol{T}[\mathcal{Y}_m - b]_\wedge dt - \boldsymbol{T}[\mathcal{Q}d\beta]_\wedge \tag{7.18}$$

in view of (7.16) and (7.17), the stochastic differential equation in (7.18) is given by

$$\begin{bmatrix} d\rho \\ dP \end{bmatrix} = \begin{bmatrix} \frac{\mathbf{I}_3+[\rho]_\times+\rho\rho^\top}{2} & \mathbf{0}_{3\times3} \\ \mathbf{0}_{3\times3} & \mathcal{R}_\rho(\rho) \end{bmatrix} ((\mathcal{Y}_m - b)\,dt - \mathcal{Q}d\beta) \tag{7.19}$$

Let us define

$$\begin{aligned} dX &= f(\rho, b)\,dt - \mathcal{G}(\rho)\,\mathcal{Q}d\beta \\ \mathcal{G}(\rho) &= \begin{bmatrix} g_\rho & \mathbf{0}_{3\times3} \\ \mathbf{0}_{3\times3} & g_P \end{bmatrix} = \begin{bmatrix} \frac{\mathbf{I}_3+[\rho]_\times+\rho\rho^\top}{2} & \mathbf{0}_{3\times3} \\ \mathbf{0}_{3\times3} & \mathcal{R}_\rho(\rho) \end{bmatrix} \\ f(\rho, b) &= \mathcal{G}(\rho)(\mathcal{Y}_m - b) \end{aligned} \tag{7.20}$$

with $X = \left[\rho^\top, P^\top\right]^\top \in \mathbb{R}^6$, $\mathcal{G} : \mathbb{R}^3 \to \mathbb{R}^{6\times6}$ and $f : \mathbb{R}^3 \times \mathbb{R}^6 \to \mathbb{R}^6$. $\mathcal{G}(\rho)$ is locally Lipschitz in ρ and $f(\rho, b)$ is locally Lipschitz in ρ and b. Consequently, the dynamic system in (7.19) has a solution on $t \in [t(0), T]\,\forall t(0) \leq T < \infty$ in the mean square sense and for any $\rho(t)$ and $P(t)$ such that $t \neq t(0)$, $X - X(0)$ is independent of $\{\beta(\tau), \tau \geq t\}, \forall t \in [t(0), T]$ (Theorem 4.5 Jazwinski (2007)). The aim is to achieve adaptive stabilization of an unknown constant bias and unknown time-variant covariance matrix. Let $\sigma = \left[\sigma_\Omega^\top, \sigma_V^\top\right]^\top \in \mathbb{R}^6$ with $\sigma_\Omega, \sigma_V \in \mathbb{R}^3$ being the upper bound of $\mathcal{Q}^2$ such that

$$\sigma = \left[\max\left\{\mathcal{Q}^2_{(1,1)}\right\}, \max\left\{\mathcal{Q}^2_{(2,2)}\right\}, \ldots, \max\left\{\mathcal{Q}^2_{(6,6)}\right\}\right]^\top \tag{7.21}$$

where $\max\{\cdot\}$ is the maximum value of the associated covariance element.

Assumption 7.2 *Both b and σ belong to a given compact set Δ and are upper bounded by a scalar Γ such that $\|\Delta\| \leq \Gamma < \infty$.*

Definition 7.1 *(Ji and Xi (2006)) The trajectory $X = \left[\rho^\top, P^\top\right]^\top$ of the stochastic differential system in (7.19) is said to be semi-globally uniformly ultimately bounded (SGUUB) if for some compact set $\Xi \in \mathbb{R}^6$ and any $X(0) = X(t(0))$, there exists a constant $\vartheta > 0$, and a time constant $T = T(\vartheta, X(0))$ such that $\mathbb{E}[\|X\|] < \vartheta, \forall t > t(0) + T$.*

Definition 7.2 *Consider the stochastic differential system in (7.19). For a given function $V(X) \in \mathcal{C}^2$ with $X = \left[\rho^\top, P^\top\right]^\top$ the differential operator $\mathcal{L}V$ is given by*

$$\mathcal{L}V(X) = V_X^\top f(\rho, b) + \frac{1}{2}\mathrm{Tr}\left\{\mathcal{G}(\rho)\mathcal{Q}^2\mathcal{G}^\top(\rho)V_{XX}\right\}$$

such that $V_X = \partial V/\partial X$, and $V_{XX} = \partial^2 V/\partial X^2$.

Lemma 7.1 *(Deng and Krsti (1997); Deng et al. (2001); Ji and Xi (2006)) Consider the dynamic system in (7.19) with potential function $V \in \mathcal{C}^2$, such that $V : \mathbb{R}^6 \to \mathbb{R}_+$, class $\mathcal{K}_\infty$ function $\bar{\alpha}_1(\cdot)$ and $\bar{\alpha}_2(\cdot)$, constants $c_1 > 0$ and $c_2 \geq 0$ and a nonnegative function $\mathbf{Z}(\|X\|)$ such that*

$$\bar{\alpha}_1(\|X\|) \leq V \leq \bar{\alpha}_2(\|X\|) \tag{7.22}$$

$$\begin{aligned}\mathcal{L}V(X) =& V_X^\top f(\rho, b) + \frac{1}{2}\mathrm{Tr}\left\{\mathcal{G}(\rho)\mathcal{Q}^2\mathcal{G}^\top(\rho)V_{XX}\right\} \\ \leq& -c_1\mathbf{Z}(\|X\|) + c_2\end{aligned} \tag{7.23}$$

then for $X(0) \in \mathbb{R}^6$, there exists almost a unique strong solution on $[0, \infty)$ for the dynamic system in (7.19). The solution X is bounded in probability such that

$$\mathbb{E}[V(X)] \leq V(X(0))\exp(-c_1 t) + \frac{c_2}{c_1} \tag{7.24}$$

Moreover, if the inequality in (7.24) holds, then X in (7.19) is SGUUB in the mean square. Also, when $c_2 = 0$, $f(0, b) = 0$, $\mathcal{G}(0) = 0$, and $\mathbf{Z}(\|X\|)$ is continuous, the equilibrium point $X = 0$ is globally asymptotically stable in probability and the solution of X satisfies

$$\mathbb{P}\left\{\lim_{t\to\infty}\mathbf{Z}(\|X\|) = 0\right\} = 1, \quad \forall X(0) \in \mathbb{R}^6 \tag{7.25}$$

The proof of this lemma and the existence of a unique solution can be found in Deng et al. (2001). For a rotation matrix $R \in \mathbb{SO}(3)$, let us define $\mathcal{U}_0 \subseteq \mathbb{SO}(3) \times \mathbb{R}^3$ by $\mathcal{U}_0 = \{(R(0), P(0)) | \mathrm{Tr}\{R(0)\} = -1, P(0) = \underline{\mathbf{0}}_3\}$. The set $\mathcal{U}_0$ is forward invariant and unstable for the dynamic system (7.2) and (7.3), as $\mathrm{Tr}\{R(0)\} = -1$ implies $\rho(0) = \infty$ (Hashim et al. (2018b); Shuster (1993)). From almost any initial condition

such that $R(0) \notin \mathcal{U}_0$ or equivalently $\rho(0) \in \mathbb{R}^3$, we have $-1 < \mathrm{Tr}\{R(0)\} \leq 3$ and the trajectory of $X = \left[\rho^\top, P^\top\right]^\top$ converges to the neighborhood of the equilibrium point conditioned on the value of c_2 in (7.23).

Lemma 7.2 *(Young's inequality) Let x and y be real values such that $x, y \in \mathbb{R}^3$. Then, for any positive real numbers c and d satisfying $\frac{1}{c} + \frac{1}{d} = 1$ with appropriately small positive constant ε, the following inequality holds*

$$x^\top y \leq (1/c)\,\varepsilon^c \|x\|^c + (1/d)\,\varepsilon^{-d} \|y\|^d \tag{7.26}$$

7.3 Nonlinear Stochastic Complementary Filter on $\mathbb{SE}(3)$

Let $\hat{\boldsymbol{T}}$ be the estimator of the homogeneous transformation matrix $\boldsymbol{T}$ such that

$$\hat{\boldsymbol{T}} = \begin{bmatrix} \hat{R} & \hat{P} \\ \underline{\mathbf{0}}_3^\top & 1 \end{bmatrix} \in \mathbb{SE}(3)$$

The main purpose of this section is to design a pose estimator to drive $\hat{\boldsymbol{T}} \to \boldsymbol{T}$. Let us define the error in the estimation of the homogeneous transformation matrix by

$$\tilde{\boldsymbol{T}} = \boldsymbol{T}\hat{\boldsymbol{T}}^{-1} = \begin{bmatrix} R\hat{R}^\top & P - R\hat{R}^\top\hat{P} \\ \underline{\mathbf{0}}_3^\top & 1 \end{bmatrix} = \begin{bmatrix} \tilde{R} & \tilde{P} \\ \underline{\mathbf{0}}_3^\top & 1 \end{bmatrix} \tag{7.27}$$

with $\tilde{R} = R\hat{R}^\top$ and $\tilde{P} = P - \tilde{R}\hat{P}$. Driving $\hat{\boldsymbol{T}} \to \boldsymbol{T}$ guarantees that $\tilde{P} \to 0$ and $\tilde{\rho} \to 0$, where $\tilde{P}$ is the position error associated with $\tilde{\boldsymbol{T}}$ and $\tilde{\rho}$ is the error of Rodriguez vector associated with $\tilde{R}$ which is in turn associated with $\tilde{\boldsymbol{T}}$. In this Section, a nonlinear deterministic filter on $\mathbb{SE}(3)$ is presented. This filter is subsequently modified into a nonlinear stochastic filter evolved directly on $\mathbb{SE}(3)$. The nonlinear stochastic filter is driven in the sense of Stratonovich. For $\tilde{X} = \left[\tilde{\rho}^\top, \tilde{P}^\top\right]^\top \in \mathbb{R}^6$, the error vector $\tilde{X}$ is regulated to an arbitrarily small neighborhood of the origin in the case where velocity vector measurements $\mathcal{Y}_m$ are contaminated with constant bias and random noise at each time instant. Let $\hat{b}$ and $\hat{\sigma}$ denote estimates of unknown parameters b,

and σ, respectively. Let the error in vector b and σ be defined by

$$\tilde{b} = b - \hat{b} \tag{7.28}$$

$$\tilde{\sigma} = \sigma - \hat{\sigma} \tag{7.29}$$

7.3.1 Nonlinear Deterministic Pose Filter

The aim of this subsection is to study the behavior of nonlinear deterministic pose filter evolved directly on $\mathbb{SE}(3)$ in presence of noise in the velocity vector measurements $\mathcal{Y}_m$. The attitude can be constructed algebraically given a set of measurements in (7.9) to form R_y, for example (Markley (1988); Wahba (1965)). However, R_y is uncertain and significantly far from the true R. The given set of measurements in (7.11) helps in finding R_y and for a given landmark(s) we have $P_y = \frac{1}{\sum_{i=1}^{N_{\mathrm{L}}} k_i^{\mathrm{L}}} \sum_{i=1}^{N_{\mathrm{L}}} k_i^{\mathrm{L}} \left(\mathrm{v}_i^{\mathcal{I}(\mathrm{L})} - R_y \mathrm{v}_i^{\mathcal{B}(\mathrm{L})} \right)$ and $\boldsymbol{T}_y = \begin{bmatrix} R_y & P_y \\ \underline{\mathbf{0}}_3^\top & 1 \end{bmatrix}$. Hence, the filter design aims to use the given measured $\boldsymbol{T}_y$, and the velocity measurements in (7.12), and (7.13) to obtain a good estimate of the true $\boldsymbol{T}$. Consider the nonlinear deterministic pose filter design

$$\dot{\hat{\boldsymbol{T}}} = \hat{\boldsymbol{T}} \left[\mathcal{Y}_m - \hat{b} + k_w W \right]_\wedge, \quad \hat{\boldsymbol{T}}(0) \in \mathbb{SE}(3) \tag{7.30}$$

$$\dot{\hat{b}} = -\Gamma \overline{\breve{\mathbf{Ad}}}_{\hat{\boldsymbol{T}}}^\top \begin{bmatrix} \left\| \tilde{R} \right\|_I \mathbf{I}_3 & \mathbf{0}_{3\times 3} \\ \mathbf{0}_{3\times 3} & 4\tilde{R}^\top \end{bmatrix} \boldsymbol{\Upsilon}\left(\tilde{\boldsymbol{T}} \right) - k_b \Gamma \hat{b} \tag{7.31}$$

$$W = k_p \overline{\breve{\mathbf{Ad}}}_{\hat{\boldsymbol{T}}}^{-1} \begin{bmatrix} \frac{2 - \left\| \tilde{R} \right\|_I}{1 - \left\| \tilde{R} \right\|_I} \mathbf{I}_3 & \mathbf{0}_{3\times 3} \\ \mathbf{0}_{3\times 3} & \tilde{R}^\top \end{bmatrix} \boldsymbol{\Upsilon}\left(\tilde{\boldsymbol{T}} \right) \tag{7.32}$$

where $\mathcal{Y}_m = \left[\Omega_m^\top, V_m^\top \right]^\top$ is a measured vector of angular and translational velocity defined in (7.12) and (7.13), respectively, with no noise attached to measurements ($\omega = 0$). $\hat{b} = \left[\hat{b}_\Omega^\top, \hat{b}_V^\top \right]^\top \in \mathbb{R}^6$ is the estimate of the unknown bias vector b, $\tilde{\boldsymbol{T}} = \boldsymbol{T}_y \hat{\boldsymbol{T}}^{-1}$, $\boldsymbol{\Upsilon}\left(\tilde{\boldsymbol{T}} \right) = \left[\boldsymbol{\Upsilon}_a^\top \left(\tilde{R} \right), \tilde{P}^\top \right]^\top$ as in (2.5), $\boldsymbol{\Upsilon}_a \left(\tilde{R} \right) = \mathbf{vex}\left(\boldsymbol{\mathcal{P}}_a \left(\tilde{R} \right) \right)$, and $\left\| \tilde{R} \right\|_I = \frac{1}{4} \mathrm{Tr} \left\{ \mathbf{I}_3 - \tilde{R} \right\}$. Also, $\overline{\breve{\mathbf{Ad}}}_{\hat{\boldsymbol{T}}} = \begin{bmatrix} \hat{R} & \mathbf{0}_{3\times 3} \\ \left[\hat{P} \right]_\times \hat{R} & \hat{R} \end{bmatrix}$, $\Gamma = \begin{bmatrix} \Gamma_\Omega & \mathbf{0}_{3\times 3} \\ \mathbf{0}_{3\times 3} & \Gamma_V \end{bmatrix} =$

$\gamma\mathbf{I}_6$, is an adaptation gain with $\Gamma_\Omega, \Gamma_V \in \mathbb{R}^{3\times 3}$, $\gamma > 0$, and k_b, k_p and k_w are positive constants.

Theorem 7.1 *Consider the homogeneous transformation matrix dynamics in* (7.3) *with velocity measurements* $\mathcal{Y}_m$ *in* (7.12) *and* (7.13)*. Let Assumption 7.1 hold and assume that the vector measurements in* (7.8) *are normalized to* (7.10)*. Let* $\boldsymbol{T}_y$ *be reconstructed using the vector measurement in* (7.4) *and* (7.10) *, and be coupled with the observer in* (7.30)*,* (7.31) *and* (7.32)*. In case when velocity vector measurements* $\mathcal{Y}_m$ *are subject to constant bias, no noise is introduced to the system* $(\omega = 0)$*,* $\tilde{X}(0) = \left[\tilde{\rho}(0)^\top, \tilde{P}(0)^\top\right]^\top \in \mathbb{R}^6$*, and* $\tilde{X}(0) \neq \underline{\mathbf{0}}_6$*, 1) the error vector* $\tilde{X}$ *is uniformly ultimately bounded for all* $t \geq t(0)$*; and 2) consequently* $\left(\tilde{\boldsymbol{T}}, \tilde{b}\right)$ *steers to the neighborhood of the equilibrium set* $\mathcal{S} = \left\{\left(\tilde{\boldsymbol{T}}, \tilde{b}\right) \in \mathbb{SE}(3) \times \mathbb{R}^6 : \tilde{\boldsymbol{T}} = \mathbf{I}_4, \tilde{b} = \underline{\mathbf{0}}_6\right\}$.

Proof. Let the error in b and $\tilde{\boldsymbol{T}}$ be defined as in (7.28), and (7.27), respectively. Therefore, the derivative of homogeneous transformation matrix error in (7.27) can be expressed from (7.16) and (7.30) as

$$\begin{aligned}
\dot{\tilde{\boldsymbol{T}}} &= \dot{\boldsymbol{T}}\hat{\boldsymbol{T}}^{-1} + \boldsymbol{T}\dot{\hat{\boldsymbol{T}}}^{-1} \\
&= \boldsymbol{T}\left[\mathcal{Y}_m - b\right]_\wedge \hat{\boldsymbol{T}}^{-1} - \boldsymbol{T}\left[\mathcal{Y}_m - \hat{b} + k_w W\right]_\wedge \hat{\boldsymbol{T}}^{-1} \\
&= \boldsymbol{T}\hat{\boldsymbol{T}}^{-1}\hat{\boldsymbol{T}}\left[-\tilde{b} - k_w W\right]_\wedge \hat{\boldsymbol{T}}^{-1} \\
&= -\tilde{\boldsymbol{T}}\left[\overline{\breve{\mathbf{Ad}}}_{\hat{\boldsymbol{T}}}\left(\tilde{b} + k_w W\right)\right]_\wedge
\end{aligned} \tag{7.33}$$

where $\dot{\hat{\boldsymbol{T}}}^{-1} = -\hat{\boldsymbol{T}}^{-1}\dot{\hat{\boldsymbol{T}}}\hat{\boldsymbol{T}}^{-1}$, and $\tilde{b} = \left[\tilde{b}_\Omega^\top, \tilde{b}_V^\top\right]^\top$. Considering the math identity in (2.10), we have $\hat{\boldsymbol{T}}\left[\tilde{b}\right]_\wedge \hat{\boldsymbol{T}}^{-1} = \left[\overline{\breve{\mathbf{Ad}}}_{\hat{\boldsymbol{T}}}\tilde{b}\right]_\wedge$. For $\tilde{X} = \left[\tilde{\rho}^\top, \tilde{P}^\top\right]^\top$, and in view of the transformation of (7.16) into (7.17), one may write (7.33) as

$$\dot{\tilde{X}} = -\mathcal{G}(\tilde{\rho})\,\overline{\breve{\mathbf{Ad}}}_{\hat{\boldsymbol{T}}}\left(\tilde{b} + k_w W\right) \tag{7.34}$$

with

$$\mathcal{G}(\tilde{\rho}) = \begin{bmatrix} \frac{\mathbf{I}_3 + [\tilde{\rho}]_\times + \tilde{\rho}\tilde{\rho}^\top}{2} & \mathbf{0}_{3\times 3} \\ \mathbf{0}_{3\times 3} & \mathcal{R}_{\tilde{\rho}}(\tilde{\rho}) \end{bmatrix}$$

and $\mathcal{R}_{\tilde{\rho}}(\tilde{\rho}) = \tilde{R} \in \mathbb{SO}(3)$ as given in (A.1). Consider the following potential function

$$V\left(\tilde{\rho}, \tilde{P}, \tilde{b}\right) = \left(\frac{\|\tilde{\rho}\|^2}{1+\|\tilde{\rho}\|^2}\right)^2 + 2\left\|\tilde{P}\right\|^2 + \frac{1}{2}\tilde{b}^\top \Gamma^{-1}\tilde{b} \tag{7.35}$$

for $V := V\left(\tilde{\rho}, \tilde{P}, \tilde{b}\right)$ the derivative of (7.35) is defined by

$$\begin{aligned}
\dot{V} &= -4\tilde{X}^\top \begin{bmatrix} \frac{\|\tilde{\rho}\|^2}{\left(1+\|\tilde{\rho}\|^2\right)^3}\mathbf{I}_3 & \mathbf{0}_{3\times 3} \\ \mathbf{0}_{3\times 3} & \mathbf{I}_3 \end{bmatrix} \mathcal{G}(\tilde{\rho})\, \overline{\breve{\mathbf{Ad}}}_{\hat{\boldsymbol{T}}}\left(\tilde{b} + k_w W\right) - \tilde{b}^\top \Gamma^{-1}\dot{\hat{b}} \\
&= -\tilde{X}^\top \begin{bmatrix} \frac{2\|\tilde{\rho}\|^2}{\left(1+\|\tilde{\rho}\|^2\right)^2}\mathbf{I}_3 & \mathbf{0}_{3\times 3} \\ \mathbf{0}_{3\times 3} & 4\tilde{R} \end{bmatrix} \overline{\breve{\mathbf{Ad}}}_{\hat{\boldsymbol{T}}}\left(\tilde{b} + k_w W\right) - \tilde{b}^\top \Gamma^{-1}\dot{\hat{b}}
\end{aligned} \tag{7.36}$$

substitute for $\left\|\tilde{R}\right\|_I = \|\tilde{\rho}\|^2 / \left(1+\|\tilde{\rho}\|^2\right)$ and $\boldsymbol{\Upsilon}_a\left(\tilde{R}\right) = 2\tilde{\rho}/\left(1+\|\tilde{\rho}\|^2\right)$ from (A.2) and (A.4), respectively, the result in (7.36) becomes

$$\dot{V} = -\boldsymbol{\Upsilon}\left(\tilde{\boldsymbol{T}}\right)^\top \begin{bmatrix} \left\|\tilde{R}\right\|_I \mathbf{I}_3 & \mathbf{0}_{3\times 3} \\ \mathbf{0}_{3\times 3} & 4\tilde{R} \end{bmatrix} \overline{\breve{\mathbf{Ad}}}_{\hat{\boldsymbol{T}}}\left(\tilde{b} + k_w W\right) - \tilde{b}^\top \Gamma^{-1}\dot{\hat{b}} \tag{7.37}$$

such that $\boldsymbol{\Upsilon}\left(\tilde{\boldsymbol{T}}\right) = \left[\boldsymbol{\Upsilon}_a^\top\left(\tilde{R}\right), \tilde{P}^\top\right]^\top$, substituting for $\dot{\hat{b}}$ and W from (7.31) and (7.32), respectively, with $\left\|\boldsymbol{\Upsilon}_a\left(\tilde{R}\right)\right\|^2 = 4\left(1 - \left\|\tilde{R}\right\|_I\right)\left\|\tilde{R}\right\|_I = 4\frac{\|\tilde{\rho}\|^2}{\left(1+\|\tilde{\rho}\|^2\right)^2}$ as in (A.6) yields

$$\begin{aligned}
\dot{V} &= -k_w k_p \left\|\tilde{R}\right\|_I \left\|\boldsymbol{\Upsilon}_a\left(\tilde{\boldsymbol{T}}\right)\right\|^2 - 4k_w k_p\left(\left\|\tilde{R}\right\|_I^2 + \left\|\tilde{P}\right\|^2\right) - k_b\left\|\tilde{b}\right\|^2 + k_b\tilde{b}^\top b \\
&= -4k_w k_p \frac{\|\tilde{\rho}\|^4}{\left(1+\|\tilde{\rho}\|^2\right)^3} - 4k_w k_p\left(\frac{\|\tilde{\rho}\|^4}{\left(1+\|\tilde{\rho}\|^2\right)^2} + \left\|\tilde{P}\right\|^2\right) - k_b\left\|\tilde{b}\right\|^2 + k_b\tilde{b}^\top b
\end{aligned} \tag{7.38}$$

applying Young's inequality to $k_b\tilde{b}^\top b$, one obtains $k_b\tilde{b}^\top b \leq \frac{k_b}{2}\left\|\tilde{b}\right\|^2 + \frac{k_b}{2}\|b\|^2$. Define

$$\tilde{Y} = \left[\frac{\|\tilde{\rho}\|^2}{1+\|\tilde{\rho}\|^2}, \left\|\tilde{P}\right\|^2, \frac{1}{\sqrt{2\gamma}}\tilde{b}^\top\right]^\top \in \mathbb{R}^8,$$
$$\mathcal{H} = \operatorname{diag}\left(4k_pk_w, 4k_pk_w, \gamma k_b\mathbf{1}_6^\top\right) \in \mathbb{R}^{8\times 8}$$

therefore, equation (7.38) becomes

$$\begin{aligned}\dot{V} &\leq -4k_wk_p\frac{\|\tilde{\rho}\|^4}{\left(1+\|\tilde{\rho}\|^2\right)^3} - \tilde{Y}^\top\mathcal{H}\tilde{Y} + \frac{k_b}{2}\|b\|^2 \\ &\leq -\underline{\lambda}(\mathcal{H})V + \frac{k_b}{2}\|b\|^2 \end{aligned} \tag{7.39}$$

Let $c_1 = \underline{\lambda}(\mathcal{H})$ and $c_2 = \frac{k_b}{2}\|b\|^2$, thus, the result in (7.39) implies that $\hat{X}$ and $\hat{b}$ will eventually converge to the compact set

$$\Xi_s = \left\{\hat{X}(t), \hat{b}(t) \middle| \lim_{t\to\infty}\left\|\tilde{X}(t)\right\| = \mu_X, \lim_{t\to\infty}\left\|\tilde{b}(t)\right\| = \mu_b\right\}$$

with

$$\mu_X = \sqrt{\frac{c_2}{c_1}}, \quad \mu_b = \sqrt{\frac{2c_2}{c_1\gamma}}$$

and

$$\left\|\tilde{X}(t)\right\| \leq \sqrt{\left(V(0) - \frac{c_2}{c_1}\right)\exp(-c_1t) + \frac{c_2}{c_1}}$$
$$\left\|\tilde{b}(t)\right\| \leq \frac{1}{\gamma}\sqrt{\left(V(0) - \frac{c_2}{c_1}\right)\exp(-c_1t) + \frac{c_2}{c_1}}$$

The result obtained in (7.39) is similar to Lemma 1.2 in Ge and Wang (2004) which confirms the result in Theorem 7.1. Theorem 7.1 is developed for deterministic observers, assuming absence of noises in the system dynamics. Hence, Lyapunov's direct method guarantees that for $\operatorname{Tr}\left\{\tilde{R}(0)\right\} \neq -1$, $\boldsymbol{\Upsilon}\left(\tilde{\boldsymbol{T}}\right)$ converges to a small neighborhood of the origin. However, if the velocity vector $\mathcal{Y}_m$ is contaminated with noise

such that ($\omega \neq 0$), it would no longer be convenient to express the derivative of (7.35) similar to (7.36). Therefore, the derivative of (7.35) should be expressed analogously to the differential operator in Definition 7.2 and consequently, the covariance matrix $\mathcal{Q}^2$ appears there. As a result, one solution is to reformulate the potential function in (7.35) such that $\tilde{\rho}$ and $\tilde{P}$ are of order higher than two (Deng and Krsti (1997); Deng et al. (2001)). Clearly, this is not the case in Theorem 7.1 as well as in previous studies such as Baldwin et al. (2009, 2007); Hua et al. (2011); Rehbinder and Ghosh (2003); Vasconcelos et al. (2010).

7.3.2 Nonlinear Stochastic Pose Filter in Stratonovich Sense

Generally, nonlinear deterministic attitude or attitude-position filters assume that velocity measurements are subject only to constant bias (for example Baldwin et al. (2009, 2007); Crassidis et al. (2007); Hua et al. (2011); Mahony et al. (2008); Rehbinder and Ghosh (2003)). In contrast, the velocity vector $\mathcal{Y}_m$ is contaminated not only with bias but also noise components. The added components could impair the estimation process of the true position and attitude. As such, the aim is to design a nonlinear stochastic filter evolved directly on $\mathbb{SE}(3)$ in the sense of Stratonovich (Stratonovich (1967)) considering that measurement in the velocity vector $\mathcal{Y}_m$ is contaminated with constant bias and a wide-band of Gaussian random noise with zero mean. Stochastic differential equations can be defined and solved in the sense of Ito's integral (Ito and Rao (1984)). Alternatively, Stratonovich's integral (Stratonovich (1967)) can be employed for solving stochastic differential equations. The common feature between Stratonovich and Ito integral is that if the associated function multiplied by $d\beta$ is continuous and Lipschitz, the mean square limit exists. The Ito integral is defined for functional on $\{\beta(\tau), \tau \leq t\}$ which is more natural but it does not obey the chain rule. Conversely, Stratonovich is a well-defined Riemann integral for the sampled function, it has a continuous partial derivative with respect to β, it obeys the chain rule, and it is more convenient for colored noise (Jazwinski (2007); Stratonovich (1967)). Hence, the Stratonovich integral is defined for explicit functions of β. In case of a wide-band of random colored noise process being attached to the velocity measurements, for $X = \left[\rho^\top, P^\top\right]^\top$ with $X(t_0) = 0$, the solution of (7.19) is defined

by

$$X(t) = \int_{t_0}^{t} f(\rho(\tau), b(\tau))\, d\tau + \int_{t_0}^{t} \mathcal{G}(\rho(\tau))\, \mathcal{Q} d\beta \tag{7.40}$$

if the problem has been considered and solved directly in the sense of Ito, the expected value of (7.40) is

$$\mathbb{E}[X] \neq \int_{t_0}^{t} \mathbb{E}[f(\rho(\tau), b(\tau))]\, d\tau$$

Hence, Stratonovich came up with the Wong-Zakai correction factor to balance any colored noise that may be introduced to the system dynamics and to end with $\mathbb{E}[X] = \int_{t_0}^{t} \mathbb{E}[f(\rho, b)]\, d\tau$. A remarkable advantage of Stratonovich is its applicability to white noise as well as colored noise which makes the filter more robust for real time applications (Jazwinski (2007); Khasminskii (1980); Stratonovich (1967)). Let us assume that the attitude dynamics in (7.19) were defined in the sense of Stratonovich Stratonovich (1967). Therefore, the equivalent Ito (Ito and Rao (1984); Jazwinski (2007); Khasminskii (1980)) can be expressed as

$$[dX]_i = [f(\rho, b)]_i\, dt + \sum_{k=1}^{6} \sum_{j=1}^{6} \frac{\mathcal{Q}_{j,j}^2}{2} \mathcal{G}_{kj}(\rho) \frac{\partial \mathcal{G}_{ij}(\rho)}{\partial X_k} dt + [\mathcal{G}(\rho)\, \mathcal{Q} d\beta]_i \tag{7.41}$$

where both $f(\rho, b)$ and $\mathcal{G}(\rho)$ are defined in (7.19). $\sum_{k=1}^{6} \sum_{j=1}^{6} \frac{\mathcal{Q}_{j,j}^2}{2} \mathcal{G}_{kj}(\rho) \frac{\partial \mathcal{G}_{ij}(\rho)}{\partial \rho_k}$ is termed the Wong-Zakai correction factor of stochastic differential equations (SDEs) in the sense of Ito (Wong and Zakai (1965)), and $i, j, k = 1, \ldots, 6$ denote ith, jth and/or kth elements of the associated vector or matrix. Assume that $\boldsymbol{\mathcal{W}}(\rho) = \left[\boldsymbol{\mathcal{W}}_\rho^\top, \boldsymbol{\mathcal{W}}_P^\top\right]^\top \in \mathbb{R}^6$. Let $\boldsymbol{\mathcal{W}}_{\rho i} = \sum_{k=1}^{3} \sum_{j=1}^{3} \frac{\mathcal{Q}_{j,j}^2}{2} \mathcal{G}_{kj}(\rho) \frac{\partial \mathcal{G}_{ij}(\rho)}{\partial \rho_k}$, therefore, for $i = 1$

$$\boldsymbol{\mathcal{W}}_{\rho i} = \frac{1}{4} \left(\left(1 + \rho_1^2\right) \rho_1 \mathcal{Q}_{1,1}^2 + (\rho_1 \rho_2 - \rho_3)\, \rho_2 \mathcal{Q}_{2,2}^2 + (\rho_2 + \rho_1 \rho_3)\, \rho_3 \mathcal{Q}_{3,3}^2 \right)$$

see Appendix C. Thus, one can find that for $i = 1, 2, 3$, $\boldsymbol{\mathcal{W}}_\rho \in \mathbb{R}^3$ can be defined after some steps of calculations as follows

$$\boldsymbol{\mathcal{W}}_\rho = \frac{1}{4} \left(\mathbf{I}_3 + [\rho]_\times + \rho \rho^\top \right) \mathcal{Q}_\Omega^2 \rho \tag{7.42}$$

see Appendix C. And $\boldsymbol{\mathcal{W}}_{Pi} = \sum_{k=4}^{6}\sum_{j=4}^{6}\frac{\mathcal{Q}_{j,j}^2}{2}\mathcal{G}_{kj}(\rho)\frac{\partial \mathcal{G}_{ij}(\rho)}{\partial P_k} = 0$, for $i = 4,5,6$, visit Appendix C. This implies that

$$\boldsymbol{\mathcal{W}}_P = \underline{\mathbf{0}}_3 \in \mathbb{R}^3 \tag{7.43}$$

Manipulating equations (7.41), (7.42) and (7.43), the stochastic dynamics of the Rodriguez vector can be expressed as

$$dX = \left(f(\rho,b)\left(\mathcal{Y}_m - b\right) + \boldsymbol{\mathcal{W}}(\rho)\right)dt - \mathcal{G}(\rho)\,\mathcal{Q}d\beta \tag{7.44}$$

Assume that the elements of covariance matrix $\mathcal{Q}^2$ are upper bounded by σ as given in (7.21) such that the bound of σ is unknown for nonnegative elements. Consider the nonlinear stochastic pose filter design

$$\begin{aligned}
\dot{\hat{\boldsymbol{T}}} =& \hat{\boldsymbol{T}}\left[\mathcal{Y}_m - \hat{b} + k_w W + \overline{\breve{\mathbf{Ad}}}_{\hat{\boldsymbol{T}}^{-1}}\begin{bmatrix} \frac{1}{2}\frac{1}{1-\left\|\tilde{R}\right\|_I}\mathbf{I}_3 & \mathbf{0}_{3\times3} \\ \mathbf{0}_{3\times3} & \mathbf{0}_{3\times3}\end{bmatrix}\operatorname{diag}\left(\boldsymbol{\Upsilon}\left(\tilde{\boldsymbol{T}}\right)\right)\hat{\sigma}\right]_{\wedge}, \\
&\hat{\boldsymbol{T}}(0) \in \mathbb{SE}(3)
\end{aligned} \tag{7.45}$$

$$\dot{\hat{b}} = -\Gamma\overline{\breve{\mathbf{Ad}}}_{\hat{\boldsymbol{T}}}^{\top}\begin{bmatrix} \left\|\tilde{R}\right\|_I\mathbf{I}_3 & \mathbf{0}_{3\times3} \\ \mathbf{0}_{3\times3} & 4\left\|\tilde{P}\right\|^2\tilde{R}^{\top}\end{bmatrix}\boldsymbol{\Upsilon}\left(\tilde{\boldsymbol{T}}\right) - k_b\Gamma\hat{b} \tag{7.46}$$

$$\begin{aligned}
\dot{\hat{\sigma}} =& \Pi\left(\frac{1}{4}\frac{\left\|\tilde{R}\right\|_I}{1-\left\|\tilde{R}\right\|_I}\operatorname{diag}\left(\begin{bmatrix}\boldsymbol{\Upsilon}_a\left(\tilde{R}\right) \\ \underline{\mathbf{0}}_3\end{bmatrix}\right) + k_w k_p\begin{bmatrix}\left\|\tilde{R}\right\|_I\mathcal{D}_{\Upsilon}^{\top} & \mathbf{0}_{3\times3} \\ \mathbf{0}_{3\times3} & \mathbf{0}_{3\times3}\end{bmatrix}\right)\boldsymbol{\Upsilon}\left(\tilde{\boldsymbol{T}}\right) \\
&- k_\sigma\Pi\hat{\sigma}
\end{aligned} \tag{7.47}$$

$$W = k_p\overline{\breve{\mathbf{Ad}}}_{\hat{\boldsymbol{T}}^{-1}}\left(\frac{1}{\varepsilon}\begin{bmatrix}\frac{2-\left\|\tilde{R}\right\|_I}{1-\left\|\tilde{R}\right\|_I}\mathbf{I}_3 & \mathbf{0}_{3\times3} \\ \mathbf{0}_{3\times3} & \tilde{R}^{\top}\end{bmatrix}\boldsymbol{\Upsilon}\left(\tilde{\boldsymbol{T}}\right) + \begin{bmatrix}\mathcal{D}_{\Upsilon} & \mathbf{0}_{3\times3} \\ \mathbf{0}_{3\times3} & \mathbf{0}_{3\times3}\end{bmatrix}\hat{\sigma}\right) \tag{7.48}$$

where $\mathcal{Y}_m = \left[\Omega_m^{\top}, V_m^{\top}\right]^{\top}$ denotes the measured vector of angular and translational velocity defined in (7.12) and (7.13), respectively. $\hat{b} = \left[\hat{b}_{\Omega}^{\top}, \hat{b}_V^{\top}\right]^{\top} \in \mathbb{R}^6$ and $\hat{\sigma} = \left[\hat{\sigma}_{\Omega}^{\top}, \hat{\sigma}_V^{\top}\right]^{\top} \in \mathbb{R}^6$ are estimates of the unknown parameter b and σ, respectively, $\tilde{\boldsymbol{T}} = \boldsymbol{T}_y\hat{\boldsymbol{T}}^{-1}$, $\boldsymbol{\Upsilon}\left(\tilde{\boldsymbol{T}}\right) = \left[\boldsymbol{\Upsilon}_a^{\top}\left(\tilde{R}\right), \tilde{P}^{\top}\right]^{\top}$ as in (2.5), $\boldsymbol{\Upsilon}_a\left(\tilde{R}\right) = \mathbf{vex}\left(\boldsymbol{\mathcal{P}}_a\left(\tilde{R}\right)\right)$ as

given in (A.4), $\left\|\tilde{R}\right\|_I = \frac{1}{4}\mathrm{Tr}\left\{\mathbf{I}_3 - \tilde{R}\right\}$ is the Euclidean distance of $\tilde{R}$ as defined in (A.2), and $\mathcal{D}_\Upsilon = \left[\boldsymbol{\Upsilon}_a\left(\tilde{R}\right), \boldsymbol{\Upsilon}_a\left(\tilde{R}\right), \boldsymbol{\Upsilon}_a\left(\tilde{R}\right)\right]$. Also, $\overline{\breve{\mathbf{Ad}}}_{\hat{\boldsymbol{T}}} = \begin{bmatrix} \hat{R} & \mathbf{0}_{3\times3} \\ \left[\hat{P}\right]_\times \hat{R} & \hat{R} \end{bmatrix}$, $\Gamma = \begin{bmatrix} \Gamma_\Omega & \mathbf{0}_{3\times3} \\ \mathbf{0}_{3\times3} & \Gamma_V \end{bmatrix} = \gamma\mathbf{I}_6$, and $\Pi = \begin{bmatrix} \Pi_\Omega & \mathbf{0}_{3\times3} \\ \mathbf{0}_{3\times3} & \Pi_V \end{bmatrix} = \bar{\pi}\mathbf{I}_6$ are adaptation gains with $\Gamma_\Omega, \Gamma_V, \Pi_\Omega, \Pi_V \in \mathbb{R}^{3\times3}$ where $\gamma, \bar{\pi} > 0$, $\varepsilon > 0$ is a small constant, and k_b, k_σ, k_p and k_w are positive constants.

Theorem 7.2 *Consider the homogeneous transformation matrix dynamics in* (7.3) *with velocity measurements* $\mathcal{Y}_m = \left[\Omega_m^\top, V_m^\top\right]^\top$ *in* (7.12) *and* (7.13)*. Let Assumption 7.1 hold and assume that the vector measurements in* (7.8) *are normalized to* (7.10)*. Let* $\boldsymbol{T}_y$ *be reconstructed using the vector measurements in* (7.4) *and* (7.10)*, and be coupled with the observer in* (7.45)*,* (7.46)*,* (7.47) *and* (7.48)*. Assume the design parameters* Γ*,* Π*,* ε*,* k_b*,* k_σ*,* k_p *and* k_w *are chosen appropriately with* ε *being selected sufficiently small. When velocity measurements* $\mathcal{Y}_m$ *are contaminated with bias and noise* $(\omega \neq 0)$*,* $\tilde{X}(0) = \left[\tilde{\rho}(0)^\top, \tilde{P}(0)^\top\right]^\top \in \mathbb{R}^6$*, and* $\tilde{X}(0) \neq \underline{\mathbf{0}}_6$*, then 1) the errors* $\left(\tilde{\boldsymbol{T}}, \tilde{b}, \tilde{\sigma}\right)$ *are regulated to the neighborhood of the equilibrium set* $\mathcal{S} = \left\{\left(\tilde{\boldsymbol{T}}, \tilde{b}, \tilde{\sigma}\right) \in \mathbb{SE}(3) \times \mathbb{R}^6 \times \mathbb{R}^6 : \tilde{\boldsymbol{T}} = \mathbf{I}_4, \tilde{b} = \underline{\mathbf{0}}_6, \tilde{\sigma} = \underline{\mathbf{0}}_6\right\}$*; and 2)* $\left[\tilde{X}^\top, \tilde{b}^\top, \tilde{\sigma}^\top\right]^\top$ *is semi-globally uniformly ultimately bounded in mean square.*

Proof: Let the error in the homogeneous transformation matrix $\boldsymbol{T}$ be given as in (7.27) and the error in vector b be defined as in (7.28). Therefore, the derivative of homogeneous transformation matrix error $\tilde{\boldsymbol{T}}$ in (7.27) in incremental form can be

obtained from (7.16) and (7.45) by

$$
\begin{aligned}
d\tilde{\boldsymbol{T}} =& d\boldsymbol{T}\hat{\boldsymbol{T}}^{-1} + \boldsymbol{T}d\hat{\boldsymbol{T}}^{-1} \\
=& \boldsymbol{T}\left[\mathcal{Y}_m - b\right]_\wedge \hat{\boldsymbol{T}}^{-1}dt - \boldsymbol{T}\left[\mathcal{Q}d\beta\right]_\wedge \hat{\boldsymbol{T}}^{-1} \\
& - \boldsymbol{T}\left[\mathcal{Y}_m - \hat{b} + k_w W + \overline{\mathbf{Ad}}_{\hat{\boldsymbol{T}}^{-1}} \begin{bmatrix} \frac{1}{2}\frac{1}{1-\left\|\tilde{R}\right\|_I}\mathbf{I}_3 & \mathbf{0}_{3\times3} \\ \mathbf{0}_{3\times3} & \mathbf{0}_{3\times3} \end{bmatrix} \operatorname{diag}\left(\boldsymbol{\Upsilon}\left(\tilde{\boldsymbol{T}}\right)\right)\hat{\sigma}\right]_\wedge \hat{\boldsymbol{T}}^{-1}dt \\
=& -\tilde{\boldsymbol{T}}\hat{\boldsymbol{T}}\left[\tilde{b} + k_w W + \overline{\mathbf{Ad}}_{\hat{\boldsymbol{T}}^{-1}} \begin{bmatrix} \frac{1}{2}\frac{1}{1-\left\|\tilde{R}\right\|_I}\mathbf{I}_3 & \mathbf{0}_{3\times3} \\ \mathbf{0}_{3\times3} & \mathbf{0}_{3\times3} \end{bmatrix} \operatorname{diag}\left(\boldsymbol{\Upsilon}\left(\tilde{\boldsymbol{T}}\right)\right)\hat{\sigma}\right]_\wedge \hat{\boldsymbol{T}}^{-1}dt \\
& - \tilde{\boldsymbol{T}}\hat{\boldsymbol{T}}\left[\mathcal{Q}d\beta\right]_\wedge \hat{\boldsymbol{T}}^{-1} \\
=& -\tilde{\boldsymbol{T}}\left[\overline{\mathbf{Ad}}_{\hat{\boldsymbol{T}}}\left(\tilde{b} + k_w W\right) + \begin{bmatrix} \frac{1}{2}\frac{1}{1-\left\|\tilde{R}\right\|_I}\mathbf{I}_3 & \mathbf{0}_{3\times3} \\ \mathbf{0}_{3\times3} & \mathbf{0}_{3\times3} \end{bmatrix} \operatorname{diag}\left(\boldsymbol{\Upsilon}\left(\tilde{\boldsymbol{T}}\right)\right)\hat{\sigma}\right]_\wedge dt \\
& - \tilde{\boldsymbol{T}}\left[\overline{\mathbf{Ad}}_{\hat{\boldsymbol{T}}}\mathcal{Q}d\beta\right]_\wedge
\end{aligned}
\tag{7.49}
$$

where $\dot{\hat{\boldsymbol{T}}}^{-1} = -\hat{\boldsymbol{T}}^{-1}\dot{\hat{\boldsymbol{T}}}\hat{\boldsymbol{T}}^{-1}$, and $\tilde{b} = \left[\tilde{b}_\Omega^\top, \tilde{b}_V^\top\right]^\top$. Considering the math identity in (2.10) we have $\hat{\boldsymbol{T}}\left[\tilde{b}\right]_\wedge \hat{\boldsymbol{T}}^{-1} = \left[\overline{\mathbf{Ad}}_{\hat{\boldsymbol{T}}}\tilde{b}\right]_\wedge$, and from the math identity in (2.17) and (2.18), we have $\overline{\mathbf{Ad}}_{\hat{\boldsymbol{T}}}\overline{\mathbf{Ad}}_{\hat{\boldsymbol{T}}^{-1}} = \mathbf{I}_6$. Similarly to transition from (7.18) to (7.19), extraction of vector dynamics in (7.49) can be expressed as (7.50) and (7.51) in Stratonovich's representation (Stratonovich (1967)) as follows

$$
\begin{aligned}
d\tilde{X} = -& \begin{bmatrix} \frac{\mathbf{I}_3 + [\tilde{\rho}]_\times + \tilde{\rho}\tilde{\rho}^\top}{2} & \mathbf{0}_{3\times3} \\ \mathbf{0}_{3\times3} & \mathcal{R}_{\tilde{\rho}}\left(\tilde{\rho}\right) \end{bmatrix} \Bigg(\begin{bmatrix} \frac{1}{2}\frac{1}{1-\left\|\tilde{R}\right\|_I}\mathbf{I}_3 & \mathbf{0}_{3\times3} \\ \mathbf{0}_{3\times3} & \mathbf{0}_{3\times3} \end{bmatrix} \operatorname{diag}\left(\boldsymbol{\Upsilon}\left(\tilde{\boldsymbol{T}}\right)\right)\hat{\sigma} \\
& + \overline{\mathbf{Ad}}_{\hat{\boldsymbol{T}}}\left(\tilde{b} + k_w W\right)\Bigg)dt - \begin{bmatrix} \frac{\mathbf{I}_3 + [\tilde{\rho}]_\times + \tilde{\rho}\tilde{\rho}^\top}{2} & \mathbf{0}_{3\times3} \\ \mathbf{0}_{3\times3} & \mathcal{R}_{\tilde{\rho}}\left(\tilde{\rho}\right) \end{bmatrix} \overline{\mathbf{Ad}}_{\hat{\boldsymbol{T}}}\mathcal{Q}d\beta
\end{aligned}
\tag{7.50}
$$

Or more simply as

$$
d\tilde{X} = -f_{\tilde{X}}dt - \mathcal{G}\left(\tilde{\rho}\right)\overline{\mathbf{Ad}}_{\hat{\boldsymbol{T}}}\mathcal{Q}d\beta \tag{7.51}
$$

where

$$\mathcal{G}(\tilde{\rho}) = \begin{bmatrix} g_{\tilde{\rho}}(\tilde{\rho}) & \mathbf{0}_{3\times3} \\ \mathbf{0}_{3\times3} & g_{\tilde{P}}(\tilde{\rho}) \end{bmatrix}$$
$$g_{\tilde{\rho}}(\tilde{\rho}) = \frac{\mathbf{I}_3 + [\tilde{\rho}]_\times + \tilde{\rho}\tilde{\rho}^\top}{2}$$
$$g_{\tilde{P}}(\tilde{\rho}) = \mathcal{R}_{\tilde{\rho}}(\tilde{\rho})$$

and

$$f_{\tilde{X}} = -\mathcal{G}(\tilde{\rho}) \left(\overline{\breve{\mathbf{Ad}}}_{\hat{\boldsymbol{T}}} \left(\tilde{b} + k_w W \right) + \begin{bmatrix} \frac{1}{2}\frac{1}{1-\left\|\tilde{R}\right\|_I}\mathbf{I}_3 & \mathbf{0}_{3\times3} \\ \mathbf{0}_{3\times3} & \mathbf{0}_{3\times3} \end{bmatrix} \operatorname{diag}\left(\boldsymbol{\Upsilon}\left(\tilde{\boldsymbol{T}}\right)\right) \hat{\sigma} \right)$$

One can re-define

$$\bar{\omega}_\Omega = \hat{R}\omega_\Omega$$
$$\bar{\omega}_V = \left[\hat{P}\right]_\times \hat{R}\omega_\Omega + \hat{R}\omega_V$$

for all $\bar{\omega}_\Omega, \bar{\omega}_V \in \mathbb{R}^3$ such that

$$\bar{\omega}_\Omega = \bar{\mathcal{Q}}_\Omega \frac{d\bar{\beta}_\Omega}{dt}, \quad \bar{\omega}_V = \bar{\mathcal{Q}}_V \frac{d\bar{\beta}_V}{dt}$$

with

$$\bar{\beta} = \left[\bar{\beta}_\Omega^\top, \bar{\beta}_V^\top\right]^\top \in \mathbb{R}^6$$
$$\bar{\mathcal{Q}} = \begin{bmatrix} \bar{\mathcal{Q}}_\Omega & \mathbf{0}_{3\times3} \\ \mathbf{0}_{3\times3} & \bar{\mathcal{Q}}_V \end{bmatrix} \in \mathbb{R}^{6\times6}$$

Thus, the dynamics in (7.49) and (7.51) can be re-expressed, respectively, as

$$d\tilde{\boldsymbol{T}} = -\tilde{\boldsymbol{T}} \left[\overline{\breve{\mathbf{Ad}}}_{\hat{\boldsymbol{T}}} \left(\tilde{b} + k_w W \right) + \begin{bmatrix} \frac{1}{2}\frac{1}{1-\left\|\tilde{R}\right\|_I}\mathbf{I}_3 & \mathbf{0}_{3\times3} \\ \mathbf{0}_{3\times3} & \mathbf{0}_{3\times3} \end{bmatrix} \operatorname{diag}\left(\boldsymbol{\Upsilon}\left(\tilde{\boldsymbol{T}}\right)\right) \hat{\sigma} \right]_\wedge dt$$
$$- \tilde{\boldsymbol{T}} \left[\bar{\mathcal{Q}} d\bar{\beta}\right]_\wedge \tag{7.52}$$

$$d\tilde{X} = -f_{\tilde{X}}dt - \mathcal{G}(\tilde{\rho})\,\bar{\mathcal{Q}}d\bar{\beta} \tag{7.53}$$

Hence, in view of (7.41) and (7.44), the error dynamics in (7.53) can be re-expressed in the sense of Ito (Ito and Rao (1984)) as

$$\begin{aligned} d\tilde{X} = &-\mathcal{G}(\tilde{\rho})\left(\overline{\breve{\mathbf{Ad}}}_{\hat{\boldsymbol{T}}}\left(\tilde{b}+k_w W\right) + \begin{bmatrix} \frac{1}{2}\frac{1}{1-\left\|\tilde{R}\right\|_I}\mathbf{I}_3 & \mathbf{0}_{3\times3} \\ \mathbf{0}_{3\times3} & \mathbf{0}_{3\times3} \end{bmatrix} \operatorname{diag}\left(\boldsymbol{\Upsilon}\left(\tilde{\boldsymbol{T}}\right)\right)\hat{\sigma}\right)dt \\ &+ \begin{bmatrix} \boldsymbol{\mathcal{W}}_{\tilde{\rho}} \\ \boldsymbol{\mathcal{W}}_{\tilde{P}} \end{bmatrix} dt - \mathcal{G}(\tilde{\rho})\,\bar{\mathcal{Q}}d\bar{\beta} \end{aligned} \tag{7.54}$$

with $\boldsymbol{\mathcal{W}}_{\tilde{\rho}} = \frac{1}{4}\left(\mathbf{I}_3 + [\tilde{\rho}]_\times + \tilde{\rho}\tilde{\rho}^\top\right)\bar{\mathcal{Q}}_\Omega^2\tilde{\rho}$ and $\boldsymbol{\mathcal{W}}_{\tilde{P}} = \underline{\mathbf{0}}_3$ as defined in (7.42) and (7.43), respectively, which can be further simplified as shown below

$$\begin{aligned} d\tilde{X} &= \left(-f_{\tilde{X}} + \boldsymbol{\mathcal{W}}(\tilde{\rho})\right)dt - \mathcal{G}(\tilde{\rho})\,\bar{\mathcal{Q}}d\bar{\beta} \\ &= \mathcal{F}dt - \mathcal{G}(\tilde{\rho})\,\bar{\mathcal{Q}}d\bar{\beta} \end{aligned} \tag{7.55}$$

where $\mathcal{F} = \left[\mathcal{F}_{\tilde{\rho}}^\top, \mathcal{F}_{\tilde{P}}^\top\right]^\top = -f_{\tilde{X}} + \boldsymbol{\mathcal{W}}(\tilde{\rho})$. Let us re-define σ as the upper bound of $\bar{\mathcal{Q}}^2$ with $\sigma = \left[\sigma_\Omega^\top, \sigma_V^\top\right]^\top \in \mathbb{R}^6$ and $\sigma_\Omega, \sigma_V \in \mathbb{R}^3$ such that

$$\sigma = \left[\max\left\{\bar{\mathcal{Q}}_{(1,1)}^2\right\}, \max\left\{\bar{\mathcal{Q}}_{(2,2)}^2\right\}, \ldots, \max\left\{\bar{\mathcal{Q}}_{(6,6)}^2\right\}\right]^\top \tag{7.56}$$

Let the error in σ be defined similar to (7.29) with $\tilde{\sigma} = \sigma - \hat{\sigma}$. Consider the following potential function

$$V\left(\tilde{\rho}, \tilde{P}, \tilde{b}, \tilde{\sigma}\right) = \left(\frac{\|\tilde{\rho}\|^2}{1+\|\tilde{\rho}\|^2}\right)^2 + \left\|\tilde{P}\right\|^4 + \frac{1}{2}\tilde{b}^\top\Gamma^{-1}\tilde{b} + \frac{1}{2}\tilde{\sigma}^\top\Pi^{-1}\tilde{\sigma} \tag{7.57}$$

For $V := V\left(\tilde{\rho}, \tilde{P}, \tilde{b}, \tilde{\sigma}\right)$, the differential operator $\mathcal{L}V$ in Definition 7.2 can be written as

$$\begin{aligned} \mathcal{L}V = &V_{\tilde{\rho}}^\top\mathcal{F}_{\tilde{\rho}} + \frac{1}{2}\operatorname{Tr}\left\{g_{\tilde{\rho}}^\top V_{\tilde{\rho}\tilde{\rho}}g_{\tilde{\rho}}\bar{\mathcal{Q}}_\Omega^2\right\} + V_{\tilde{P}}^\top\mathcal{F}_{\tilde{P}} + \frac{1}{2}\operatorname{Tr}\left\{g_{\tilde{P}}^\top V_{\tilde{P}\tilde{P}}g_{\tilde{P}}\bar{\mathcal{Q}_V}^2\right\} \\ &- \tilde{b}^\top\Gamma^{-1}\dot{\hat{b}} - \tilde{\sigma}^\top\Pi^{-1}\dot{\hat{\sigma}} \end{aligned} \tag{7.58}$$

One can easily show that the first and second partial derivatives of (7.57) in terms of $\tilde{\rho}$ can be obtained as follows

$$V_{\tilde{\rho}} = 4\frac{\|\tilde{\rho}\|^2}{\left(1+\|\tilde{\rho}\|^2\right)^3}\tilde{\rho} \tag{7.59}$$

$$V_{\tilde{\rho}\tilde{\rho}} = 4\frac{\left(1+\|\tilde{\rho}\|^2\right)\|\tilde{\rho}\|^2\mathbf{I}_3 + \left(2-4\|\tilde{\rho}\|^2\right)\tilde{\rho}\tilde{\rho}^\top}{\left(1+\|\tilde{\rho}\|^2\right)^4} \tag{7.60}$$

Similarly, the first and second partial derivatives of (7.57) in terms of $\tilde{P}$ can be obtained as follows

$$V_{\tilde{P}} = 4\left\|\tilde{P}\right\|^2\tilde{P} \tag{7.61}$$

$$V_{\tilde{P}\tilde{P}} = 4\left\|\tilde{P}\right\|^2\mathbf{I}_3 + 8\tilde{P}\tilde{P}^\top \tag{7.62}$$

The first part of the differential operator $\mathcal{L}V$ in (7.58) can be evaluated by

$$\begin{aligned} V_{\tilde{\rho}}^\top\mathcal{F}_{\tilde{\rho}} =& -2\frac{\|\tilde{\rho}\|^2}{\left(1+\|\tilde{\rho}\|^2\right)^2}\tilde{\rho}^\top\hat{R}\left(\tilde{b}_\Omega + k_w W_\Omega + \hat{R}^\top\mathrm{diag}\left(\left[\frac{1}{2}\frac{\boldsymbol{\Upsilon}_a\left(\tilde{R}\right)}{1-\left\|\tilde{R}\right\|_I}\right]\right)\hat{\sigma}_\Omega\right) \\ &+ \frac{\|\tilde{\rho}\|^2}{\left(1+\|\tilde{\rho}\|^2\right)^2}\tilde{\rho}^\top\bar{\mathcal{Q}}_\Omega^2\tilde{\rho} \\ \leq& -2\frac{\|\tilde{\rho}\|^2}{\left(1+\|\tilde{\rho}\|^2\right)^2}\tilde{\rho}^\top\hat{R}\left(\tilde{b}_\Omega + k_w W_\Omega - \hat{R}^\top\mathrm{diag}\left(\left[\frac{1}{2}\frac{\boldsymbol{\Upsilon}_a\left(\tilde{R}\right)}{1-\left\|\tilde{R}\right\|_I}\right]\right)\tilde{\sigma}_\Omega\right) \end{aligned} \tag{7.63}$$

Hence, the differential operator $\mathcal{L}V$ in (7.58) can be described by

$$\begin{aligned}\mathcal{L}V \leq & -4\tilde{X}^\top \begin{bmatrix} \frac{\|\tilde{\rho}\|^2}{\left(1+\|\tilde{\rho}\|^2\right)^3}\mathbf{I}_3 & \mathbf{0}_{3\times3} \\ \mathbf{0}_{3\times3} & \left\|\tilde{P}\right\|^2\mathbf{I}_3 \end{bmatrix} \mathcal{G}(\tilde{\rho}) \left(\breve{\overline{\mathbf{Ad}}}_{\hat{\boldsymbol{T}}} \left(\tilde{b} + k_w W\right) \right. \\ & \left. - \begin{bmatrix} \frac{1}{2}\mathbf{I}_3 & \mathbf{0}_{3\times3} \\ \mathbf{0}_{3\times3} & \mathbf{0}_{3\times3} \end{bmatrix} \operatorname{diag}\left(\tilde{X}\right)\tilde{\sigma} \right) \\ & + \operatorname{Tr}\left\{ \frac{\|\tilde{\rho}\|^4\mathbf{I}_3 + \left(\|\tilde{\rho}\|^2\mathbf{I}_3 + 2\tilde{\rho}\tilde{\rho}^\top\right)}{2\left(1+\|\tilde{\rho}\|^2\right)^3}\bar{\mathcal{Q}}_\Omega^2 + 2\left(\left\|\tilde{P}\right\|^2\mathbf{I}_3 + 2\tilde{R}^\top\tilde{P}\tilde{P}^\top\tilde{R}\right)\bar{\mathcal{Q}}_V^2 \right\} \\ & - \tilde{b}^\top\Gamma^{-1}\dot{\hat{b}} - \tilde{\sigma}^\top\Pi^{-1}\dot{\hat{\sigma}} - \frac{\|\tilde{\rho}\|^2\left(1+3\|\tilde{\rho}\|^2\right)\tilde{\rho}^\top\bar{\mathcal{Q}}_\Omega^2\tilde{\rho}}{2\left(1+\|\tilde{\rho}\|^2\right)^3} \end{aligned} \tag{7.64}$$

where $\frac{1}{4}\frac{\boldsymbol{\Upsilon}_a\left(\tilde{R}\right)}{1-\left\|\tilde{R}\right\|_I} = \frac{1}{2}\tilde{\rho}$ as given in (A.2) and (A.4). Now, let us simplify the trace bracket in (7.64). To simplify the result in (7.64), one has

$$\operatorname{Tr}\left\{\left(\|\tilde{\rho}\|^2\mathbf{I}_3 + 2\tilde{\rho}\tilde{\rho}^\top\right)\bar{\mathcal{Q}}_\Omega^2\right\} \leq 3\|\tilde{\rho}\|^2\operatorname{Tr}\left\{\bar{\mathcal{Q}}_\Omega^2\right\}$$

and for

$$\bar{q}_\Omega = \left[\bar{\mathcal{Q}}_{\Omega(1,1)}, \bar{\mathcal{Q}}_{\Omega(2,2)}, \bar{\mathcal{Q}}_{\Omega(3,3)}\right]^\top$$

we have

$$\|\tilde{\rho}\|^2\operatorname{Tr}\left\{\bar{\mathcal{Q}}_\Omega^2\right\} = 3\|\tilde{\rho}\|^2\|\bar{q}_\Omega\|^2$$

Similarly, one can find

$$\operatorname{Tr}\left\{\left(4\left\|\tilde{P}\right\|^2\mathbf{I}_3 + 8\tilde{R}^\top\tilde{P}\tilde{P}^\top\tilde{R}\right)\bar{\mathcal{Q}}_V^2\right\} \leq 12\left\|\tilde{P}\right\|^2\operatorname{Tr}\left\{\bar{\mathcal{Q}}_V^2\right\}$$

and for

$$\bar{q}_V = \left[\bar{\mathcal{Q}}_{V(1,1)}, \bar{\mathcal{Q}}_{V(2,2)}, \bar{\mathcal{Q}}_{V(3,3)}\right]^\top$$

we have

$$12\left\|\tilde{P}\right\|^2\operatorname{Tr}\left\{\bar{\mathcal{Q}}_V^2\right\} = 12\left\|\tilde{P}\right\|^2\|\bar{q}_V\|^2$$

Hence, the operator in (7.64) becomes

$$\begin{aligned}\mathcal{L}V \leq & -4\tilde{X}^\top \begin{bmatrix} \frac{\|\tilde{\rho}\|^2}{\left(1+\|\tilde{\rho}\|^2\right)^3}\mathbf{I}_3 & \mathbf{0}_{3\times 3} \\ \mathbf{0}_{3\times 3} & \left\|\tilde{P}\right\|^2 \mathbf{I}_3 \end{bmatrix} \mathcal{G}(\tilde{\rho}) \left(\breve{\overline{\mathbf{Ad}}}_{\hat{\boldsymbol{T}}} \left(\tilde{b} + k_w W\right) \right. \\ & \left. - \begin{bmatrix} \frac{1}{2}\mathbf{I}_3 & \mathbf{0}_{3\times 3} \\ \mathbf{0}_{3\times 3} & \mathbf{0}_{3\times 3} \end{bmatrix} \operatorname{diag}\left(\tilde{X}\right) \tilde{\sigma} \right) + \frac{\|\tilde{\rho}\|^4 \operatorname{Tr}\left\{\bar{\mathcal{Q}}_\Omega^2\right\} + 3\|\tilde{\rho}\|^2 \|\bar{q}_\Omega\|^2}{2\left(1+\|\tilde{\rho}\|^2\right)^3} \\ & + 6\left\|\tilde{P}\right\|^2 \|\bar{q}_V\|^2 - \tilde{b}^\top \Gamma^{-1}\dot{\hat{b}} - \tilde{\sigma}^\top \Pi^{-1}\dot{\hat{\sigma}} - \frac{\|\tilde{\rho}\|^2\left(1+3\|\tilde{\rho}\|^2\right)\tilde{\rho}^\top \bar{\mathcal{Q}}_\Omega^2 \tilde{\rho}}{2\left(1+\|\tilde{\rho}\|^2\right)^3} \end{aligned} \tag{7.65}$$

According to Lemma 7.2, the following two equations hold

$$\begin{aligned}\frac{3\|\tilde{\rho}\|^2 \|\overline{q}_\Omega\|^2}{2\left(1+\|\tilde{\rho}\|^2\right)^3} &\leq \frac{1}{2\varepsilon}\frac{9}{4\left(1+\|\tilde{\rho}\|^2\right)^6}\|\tilde{\rho}\|^4 + \frac{\varepsilon}{2}\|\bar{q}_\Omega\|^4 \\ &\leq \frac{9}{8\left(1+\|\tilde{\rho}\|^2\right)^3\varepsilon}\|\tilde{\rho}\|^4 + \frac{\varepsilon}{2}\left(\sum_{i=1}^{3}\sigma_i\right)^2 \end{aligned} \tag{7.66}$$

$$\begin{aligned} 6\left\|\tilde{P}\right\|^2 \|\overline{q}_V\|^2 &\leq \frac{36}{2\varepsilon}\left\|\tilde{P}\right\|^4 + \frac{\varepsilon}{2}\|\bar{q}_V\|^4 \\ &\leq \frac{18}{\varepsilon}\left\|\tilde{P}\right\|^4 + \frac{\varepsilon}{2}\left(\sum_{i=4}^{6}\sigma_i\right)^2 \end{aligned} \tag{7.67}$$

Considering the results in (7.66) and (7.67), in addition, $\left(\sum_{i=1}^{6}\sigma_i\right)^2 \geq \left(\sum_{i=1}^{3}\sigma_i\right)^2 + \left(\sum_{i=4}^{6}\sigma_i\right)^2$, hence, the operator in (7.65) can be expressed as

$$\begin{aligned}\mathcal{L}V \leq &-4\tilde{X}^\top \begin{bmatrix} \frac{\|\tilde{\rho}\|^2}{\left(1+\|\tilde{\rho}\|^2\right)^3}\mathbf{I}_3 & \mathbf{0}_{3\times3} \\ \mathbf{0}_{3\times3} & \left\|\tilde{P}\right\|^2\mathbf{I}_3 \end{bmatrix} \mathcal{G}(\tilde{\rho}) \Bigg(\breve{\overline{\mathbf{Ad}}}_{\hat{\boldsymbol{T}}} \left(\tilde{b} + k_w W\right) \\ &- \begin{bmatrix} \frac{1}{2}\mathbf{I}_3 & \mathbf{0}_{3\times3} \\ \mathbf{0}_{3\times3} & \mathbf{0}_{3\times3} \end{bmatrix} \operatorname{diag}\left(\tilde{X}\right)\tilde{\sigma}\Bigg) + \frac{\|\tilde{\rho}\|^4 \operatorname{Tr}\left\{\bar{\mathcal{Q}}_\Omega^2\right\}}{2\left(1+\|\tilde{\rho}\|^2\right)^3} + \frac{9\|\tilde{\rho}\|^4}{8\left(1+\|\tilde{\rho}\|^2\right)^3}\varepsilon \\ &+ \frac{18}{\varepsilon}\left\|\tilde{P}\right\|^4 + \frac{\varepsilon}{2}\left(\sum_{i=1}^{6}\sigma_i\right)^2 - \tilde{b}^\top\Gamma^{-1}\dot{\hat{b}} - \tilde{\sigma}^\top\Pi^{-1}\dot{\hat{\sigma}} - \frac{\|\tilde{\rho}\|^2\left(1+3\|\tilde{\rho}\|^2\right)\tilde{\rho}^\top\bar{\mathcal{Q}}_\Omega^2\tilde{\rho}}{2\left(1+\|\tilde{\rho}\|^2\right)^3}\end{aligned} \tag{7.68}$$

The result in (7.68) can be written as

$$\begin{aligned}\mathcal{L}V \leq &-4\tilde{X}^\top \begin{bmatrix} \frac{\|\tilde{\rho}\|^2}{\left(1+\|\tilde{\rho}\|^2\right)^3}\mathbf{I}_3 & \mathbf{0}_{3\times3} \\ \mathbf{0}_{3\times3} & \left\|\tilde{P}\right\|^2\mathbf{I}_3 \end{bmatrix} \mathcal{G}(\tilde{\rho}) \Bigg(\breve{\overline{\mathbf{Ad}}}_{\hat{\boldsymbol{T}}} \left(\tilde{b} + k_w W\right) \\ &- \begin{bmatrix} \frac{1}{2}\mathbf{I}_3 & \mathbf{0}_{3\times3} \\ \mathbf{0}_{3\times3} & \mathbf{0}_{3\times3} \end{bmatrix} \operatorname{diag}\left(\tilde{X}\right)\tilde{\sigma}\Bigg) \\ &+ \tilde{X}^\top \begin{bmatrix} 2\frac{\|\tilde{\rho}\|^2}{\left(1+\|\tilde{\rho}\|^2\right)^2}\mathbf{I}_3 & \mathbf{0}_{3\times3} \\ \mathbf{0}_{3\times3} & 4\left\|\tilde{P}\right\|^2\mathbf{I}_3 \end{bmatrix} \Bigg(\begin{bmatrix} \frac{1}{4}\frac{\mathcal{D}_{\tilde{\rho}}}{1+\|\tilde{\rho}\|^2} & \mathbf{0}_{3\times3} \\ \mathbf{0}_{3\times3} & \mathbf{0}_{3\times3} \end{bmatrix}\sigma \\ &+ \frac{1}{\varepsilon}\begin{bmatrix} \frac{9}{16}\frac{1}{1+\|\tilde{\rho}\|^2}\mathbf{I}_3 & \mathbf{0}_{3\times3} \\ \mathbf{0}_{3\times3} & 4.5\mathbf{I}_3 \end{bmatrix}\tilde{X}\Bigg) \\ &+ \frac{\varepsilon}{2}\left(\sum_{i=1}^{6}\sigma_i\right)^2 - \tilde{b}^\top\Gamma^{-1}\dot{\hat{b}} - \tilde{\sigma}^\top\Pi^{-1}\dot{\hat{\sigma}} - \frac{\|\tilde{\rho}\|^2\left(1+3\|\tilde{\rho}\|^2\right)\tilde{\rho}^\top\bar{\mathcal{Q}}_\Omega^2\tilde{\rho}}{2\left(1+\|\tilde{\rho}\|^2\right)^3}\end{aligned} \tag{7.69}$$

According to (A.2) and (A.4), we have $\left\|\tilde{R}\right\|_I = \|\tilde{\rho}\|^2 / \left(1 + \|\tilde{\rho}\|^2\right)$ and $\boldsymbol{\Upsilon}_a\left(\tilde{R}\right) = 2\tilde{\rho}/\left(1 + \|\tilde{\rho}\|^2\right)$, while $\left\|\boldsymbol{\Upsilon}_a\left(\tilde{R}\right)\right\|^2 = 4\left(1 - \left\|\tilde{R}\right\|_I\right)\left\|\tilde{R}\right\|_I = 4\frac{\|\tilde{\rho}\|^2}{\left(1+\|\tilde{\rho}\|^2\right)^2}$ as in (A.6). Substituting for the differential operators $\dot{\hat{b}}$ and $\dot{\hat{\sigma}}$ and the correction factor W from (7.46), (7.47) and (7.48), respectively, yields

$$\begin{aligned}\mathcal{L}V \leq &-4\left(\left(k_p k_w - \frac{1}{8}\right)\left(\sum_{i=1}^{3}\sigma_i\right) + \frac{1}{\varepsilon}\left(k_p k_w - \frac{9}{32}\right)\right)\frac{\|\tilde{\rho}\|^4}{\left(1+\|\tilde{\rho}\|^2\right)^3} \\ &- \frac{\|\tilde{\rho}\|^2\left(1+3\|\tilde{\rho}\|^2\right)\tilde{\rho}^\top\bar{\mathcal{Q}}_\Omega^2\tilde{\rho}}{2\left(1+\|\tilde{\rho}\|^2\right)^3} - \frac{4k_p k_w}{\varepsilon}\left(\frac{\|\tilde{\rho}\|^2}{1+\|\tilde{\rho}\|^2}\right)^2 - 4\left(k_p k_w - 4.5\right)\left\|\tilde{P}\right\|^4 \\ &- k_b\left\|\tilde{b}\right\|^2 - k_\sigma\|\tilde{\sigma}\|^2 + k_b\tilde{b}^\top b + k_\sigma\tilde{\sigma}^\top\sigma + \frac{\varepsilon}{2}\left(\sum_{i=1}^{6}\sigma_i\right)^2 \end{aligned} \tag{7.70}$$

applying Young's inequality to $k_b\tilde{b}^\top b$ and $k_\sigma\tilde{\sigma}^\top\sigma$, respectively, one has

$$\begin{aligned} k_b\tilde{b}^\top b &\leq \frac{k_b}{2}\left\|\tilde{b}\right\|^2 + \frac{k_b}{2}\|b\|^2 \\ k_\sigma\tilde{\sigma}^\top\sigma &\leq \frac{k_\sigma}{2}\|\tilde{\sigma}\|^2 + \frac{k_\sigma}{2}\left(\sum_{i=1}^{6}\sigma_i\right)^2 \end{aligned}$$

consequently, (7.70) becomes

$$\begin{aligned}\mathcal{L}V \leq &-4\left(\left(k_p k_w - \frac{1}{8}\right)\left(\sum_{i=1}^{3}\sigma_i\right) + \frac{1}{\varepsilon}\left(k_p k_w - \frac{9}{32}\right)\right)\frac{\|\tilde{\rho}\|^4}{\left(1+\|\tilde{\rho}\|^2\right)^3} \\ &- \frac{\|\tilde{\rho}\|^2\left(1+3\|\tilde{\rho}\|^2\right)\tilde{\rho}^\top\bar{\mathcal{Q}}_\Omega^2\tilde{\rho}}{2\left(1+\|\tilde{\rho}\|^2\right)^3} - \frac{4k_p k_w}{\varepsilon}\left(\frac{\|\tilde{\rho}\|^2}{1+\|\tilde{\rho}\|^2}\right)^2 - 4\left(k_p k_w - 4.5\right)\left\|\tilde{P}\right\|^4 \\ &- \frac{k_b}{2}\left\|\tilde{b}\right\|^2 - \frac{k_\sigma}{2}\|\tilde{\sigma}\|^2 + \frac{k_b}{2}\|b\|^2 + \frac{1}{2}\left(k_\sigma + \varepsilon\right)\left(\sum_{i=1}^{6}\sigma_i\right)^2 \end{aligned} \tag{7.71}$$

Setting $\gamma > 0$, $\bar{\pi} > 0$, $k_p k_w > 4.5$, $k_b > 0$, $k_\sigma > 0$, and the positive constant ε is sufficiently small, the operator $\mathcal{L}V$ in (7.70) becomes similar to (4.16) in Deng et al.

(2001) which is in turn similar to (7.23) in Lemma 7.1. In that case, the constant component c_2 in Lemma 7.1 is $c_2 = \frac{k_b}{2}\|b\|^2 + \frac{1}{2}(k_\sigma + \varepsilon)\left(\sum_{i=1}^{6}\sigma_i\right)^2$. Let us define

$$
\begin{aligned}
c_2 =& \frac{k_b}{2}\|b\|^2 + \frac{1}{2}(k_\sigma + \varepsilon)\left(\sum_{i=1}^{6}\sigma_i\right)^2 \\
\tilde{Y} =& \left[\frac{\|\tilde{\rho}\|^2}{1+\|\tilde{\rho}\|^2}, \left\|\tilde{P}\right\|^2, \frac{1}{\sqrt{2\gamma}}\tilde{b}^\top, \frac{1}{\sqrt{2\bar{\pi}}}\tilde{\sigma}^\top\right]^\top \in \mathbb{R}^{14}, \\
\mathcal{H} =& \operatorname{diag}\left(\frac{4k_pk_w}{\varepsilon}, 4\left(k_pk_w - 4.5\right), \gamma k_b \underline{\mathbf{1}}_6^\top, \bar{\pi}k_\sigma \underline{\mathbf{1}}_6^\top\right) \in \mathbb{R}^{14\times 14}
\end{aligned}
$$

The differential operator in (7.71) is

$$
\begin{aligned}
\mathcal{L}V \leq& -4\left(\left(k_pk_w - \frac{1}{8}\right)\left(\sum_{i=1}^{3}\sigma_i\right) + \frac{1}{\varepsilon}\left(k_pk_w - \frac{9}{32}\right)\right)\frac{\|\tilde{\rho}\|^4}{\left(1+\|\tilde{\rho}\|^2\right)^3} \\
&- \frac{\|\tilde{\rho}\|^2\left(1+3\|\tilde{\rho}\|^2\right)\tilde{\rho}^\top\bar{\mathcal{Q}}_\Omega^2\tilde{\rho}}{2\left(1+\|\tilde{\rho}\|^2\right)^3} - \tilde{Y}^\top\mathcal{H}\tilde{Y} + c_2
\end{aligned} \tag{7.72}
$$

and more simply

$$
\mathcal{L}V \leq -h\left(\|\tilde{\rho}\|\right) - \underline{\lambda}\left(\mathcal{H}\right)V + c_2 \tag{7.73}
$$

such that $h(\cdot)$ is a class $\mathcal{K}$ function that includes the first two components in (7.72), and $\underline{\lambda}(\cdot)$ denotes the minimum eigenvalue of a matrix. Based on (7.73), one easily obtains

$$
\frac{d\left(\mathbb{E}\left[V\right]\right)}{dt} = \mathbb{E}\left[\mathcal{L}V\right] \leq -\underline{\lambda}\left(\mathcal{H}\right)V + c_2 \tag{7.74}
$$

as such, (7.74) means that

$$
0 \leq \mathbb{E}\left[V(t)\right] \leq V(0)\exp\left(-\underline{\lambda}\left(\mathcal{H}\right)t\right) + \frac{c_2}{\underline{\lambda}\left(\mathcal{H}\right)}, \forall t \geq 0 \tag{7.75}
$$

The inequality in (7.75) implies that $\mathbb{E}\left[V(t)\right]$ is eventually bounded by $c_2/\underline{\lambda}\left(\mathcal{H}\right)$. Since, $\mathcal{Q}^2 : \mathbb{R}_+ \to \mathbb{R}^{6\times 6}$ is bounded, the operator in (7.74) is $\mathcal{L}V \leq c_2/\underline{\lambda}\left(\mathcal{H}\right)$. Define $\tilde{Z} = \left[\tilde{\rho}^\top, \tilde{P}^\top, \tilde{b}^\top, \tilde{\sigma}^\top\right]^\top \in \mathbb{R}^{18}$, $\tilde{Z}$ is SGUUB in mean square as in Definition 7.1.

Define $\mathcal{U}_0 \subseteq \mathbb{SO}(3) \times \mathbb{R}^3 \times \mathbb{R}^6 \times \mathbb{R}^6$ by

$$\mathcal{U}_0 = \left\{ \left(\tilde{R}(0), \tilde{P}(0), \tilde{b}(0), \tilde{\sigma}(0)\right) \middle| \operatorname{Tr}\left\{\tilde{R}(0)\right\} = -1, \tilde{P}(0) = \underline{\mathbf{0}}_3, \tilde{b}(0) = \underline{\mathbf{0}}_6, \tilde{\sigma}(0) = \underline{\mathbf{0}}_6 \right\}$$

The set $\mathcal{U}_0$ is forward invariant and unstable. Therefore, from almost any initial condition such that $\tilde{R}(0) \notin \mathcal{U}_0$ or equivalently for any $\tilde{\rho}(0) \in \mathbb{R}^3$, the trajectory of $\tilde{Z}$ converges to the neighborhood of the origin which depends on the value of $c_2/\underline{\lambda}(\mathcal{H})$ in (7.75). From Lemma 7.1 and design parameters of the stochastic observer in Theorem 7.2 in addition if we have prior knowledge about the covariance upper bound σ, $c_2/\underline{\lambda}(\mathcal{H})$ can be made smaller if we choose the design parameters appropriately. Clearly, the minimum singular value of $\underline{\lambda}(\mathcal{H})$ can be controlled by k_p, k_w, γ and $\bar{\pi}$. To conclude our discussion, it should be remarked that solving the problem in the sense of Stratonovich with the proper selection of potential function as in (7.57) helps to attenuate or control the noise level associated with the velocity measurements vector $\mathcal{Y}_m$. The proposed nonlinear stochastic filter is able to correct the position as well as the attitude and reduce the noise level associated with velocity measurements $\mathcal{Y}_m$ through the setting of parameters in presence of high level of noise and bias components. This advantage is not given in nonlinear deterministic $\mathbb{SE}(3)$ filters. The main benefit of the nonlinear stochastic filter in the sense of Stratonovich is that no prior information about the covariance matrix $\mathcal{Q}^2$ is required. Also, the filter is applicable for white as well as colored noise which offers flexibility in the design process.

Remark 7.1 *Notice that, as* $k_p, k_w, \gamma, \bar{\pi} \to \infty$ *and* $\varepsilon \to 0$, $\mathbb{P}\left\{\lim_{t\to\infty} \left\|\tilde{X}\right\| = 0\right\} \to 1, \forall t \geq 0$ *with perfect cancellation of undesirable time-variant components and uncertainties.*

7.4 Simulations

This section presents the performance of the proposed nonlinear stochastic filter on $\mathbb{SE}(3)$ considering high levels of bias and noise introduced in the measurement process combined with the large initial error in the homogeneous transformation matrix $\tilde{\boldsymbol{T}}(0)$. The performance of the proposed stochastic filter is compared to Hua et al. (2011). Let us define the dynamics of the homogeneous transformation matrix $\boldsymbol{T}$ as in (7.3).

Let the angular velocity input signal be

$$\Omega = \begin{bmatrix} \sin(0.3t) \\ 0.7\sin(0.25t+\pi) \\ 0.5\sin\left(0.2t+\frac{\pi}{3}\right) \end{bmatrix} \text{(rad/sec)}$$

with initial attitude being $R(0) = \mathbf{I}_3$. Let the translational velocity be

$$V = \begin{bmatrix} \sin(0.2t) \\ 0.6\sin\left(0.15t+\frac{\pi}{2}\right) \\ \sin\left(0.25t+\frac{\pi}{4}\right) \end{bmatrix} \text{(m/sec)}$$

and the initial position $P(0) = \underline{\mathbf{0}}_3$. Let the angular velocity measurement $\Omega_m = \Omega + b_\Omega + \omega_\Omega$ be corrupted with a wide-band of random noise process with zero mean ω_Ω and standard deviation (STD) equal to $0.15\,(\text{rad/sec})$ and $b_\Omega = 0.1\,[1,-1,1]^\top$. Similarly, let the translational velocity measurement $V_m = V + b_V + \omega_V$ be subject to a wide-band of random noise process ω_V with zero mean and STD $= 0.15\,(\text{m/sec})$, and $b_V = 0.1\,[2,5,1]^\top$.

Consider one landmark feature available for measurement ($N_\text{L} = 1$)

$$\mathrm{v}_1^{\mathcal{I}(\mathrm{L})} = \left[\frac{1}{2}, \sqrt{2}, 1\right]^\top$$

and body-frame measurements obtained by (7.4) such that

$$\mathrm{v}_i^{\mathcal{B}(\mathrm{L})} = R^\top\left(\mathrm{v}_i^{\mathcal{I}(\mathrm{L})} - P\right) + \mathrm{b}_i^{\mathcal{B}(\mathrm{L})} + \omega_i^{\mathcal{B}(\mathrm{L})}$$

where the bias vector is defined as $\mathrm{b}_1^{\mathcal{B}(\mathrm{L})} = 0.1\,[1.5,1,-1]^\top$ and a Gaussian noise vector $\omega_1^{\mathcal{B}(\mathrm{L})}$ with zero mean and STD $= 0.1$ corrupts the body-frame vector measurements associated with the feature point.

Consider that two non-collinear inertial-frame vectors ($N_\text{R} = 2$) are given by

$$\mathrm{v}_1^{\mathcal{I}(\mathrm{R})} = \frac{1}{\sqrt{3}}\,[1,-1,1]^\top$$
$$\mathrm{v}_2^{\mathcal{I}(\mathrm{R})} = [0,0,1]^\top$$

while body-frame vectors $\mathrm{v}_1^{\mathcal{B}(\mathrm{R})}$ and $\mathrm{v}_2^{\mathcal{B}(\mathrm{R})}$ are obtained by (7.8)

$$\mathrm{v}_i^{\mathcal{B}(\mathrm{R})} = R^\top \mathrm{v}_i^{\mathcal{I}(\mathrm{R})} + \mathrm{b}_i^{\mathcal{B}(\mathrm{R})} + \omega_i^{\mathcal{B}(\mathrm{R})}$$

for $i = 1, 2$. The body-frame vector measurements are subject to bias components $\mathrm{b}_1^{\mathcal{B}(\mathrm{R})} = 0.1\,[-1, 1, 0.5]^\top$ and $\mathrm{b}_2^{\mathcal{B}(\mathrm{R})} = 0.1\,[0, 0, 1]^\top$. In addition to bias, Gaussian noise vectors $\omega_1^{\mathcal{B}(\mathrm{R})}$ and $\omega_2^{\mathcal{B}(\mathrm{R})}$ with zero mean and of STD $= 0.1$ corrupt the measurements. The third inertial and body-frame vector measurements are obtained by $\mathrm{v}_3^{\mathcal{I}(\mathrm{R})} = \mathrm{v}_1^{\mathcal{I}(\mathrm{R})} \times \mathrm{v}_2^{\mathcal{I}(\mathrm{R})}$ and $\mathrm{v}_3^{\mathcal{B}(\mathrm{R})} = \mathrm{v}_1^{\mathcal{B}(\mathrm{R})} \times \mathrm{v}_2^{\mathcal{B}(\mathrm{R})}$. Next, both body-frame and inertial-frame vectors are normalized, such that $\mathrm{v}_i^{\mathcal{B}(\mathrm{R})}$ and $\mathrm{v}_i^{\mathcal{I}(\mathrm{R})}$ are normalized to $\upsilon_i^{\mathcal{B}(\mathrm{R})}$ and $\upsilon_i^{\mathcal{I}(\mathrm{R})}$, respectively, for $i = 1, 2, 3$ as given in (7.10). Therefore, Assumption 7.1 holds. From vectorial measurements, the corrupted reconstructed attitude R_y is obtained by SVD Hashim et al. (2018b); Markley (1988) with $\tilde{R} = R_y \hat{R}^\top$, Appendix B. The total simulation time is 30 seconds.

For large initial attitude error, the initial rotation of attitude estimate is given according to the mapping of angle-axis parameterization in (2.7) by $\hat{R}(0) = \mathcal{R}_\alpha(\alpha, u/\|u\|)$ with $\alpha = 170\,(\mathrm{deg})$ and $u = [3, 10, 8]^\top$ such that $\left\|\tilde{R}(0)\right\|_I$ approaches the unstable equilibria $+1$. Also, the initial position of the estimator is selected to be $\hat{P}(0) = [2, 3, 1]^\top$. The matrices below summarize the initial conditions:

$$\boldsymbol{T}(0) = \begin{bmatrix} 1 & 0 & 0 & 0 \\ 0 & 1 & 0 & 0 \\ 0 & 0 & 1 & 0 \\ 0 & 0 & 0 & 1 \end{bmatrix}, \quad \hat{\boldsymbol{T}}(0) = \begin{bmatrix} -0.8816 & 0.2386 & 0.4074 & 2 \\ 0.4498 & 0.1625 & 0.8782 & 3 \\ 0.1433 & 0.9574 & -0.2505 & 1 \\ 0 & 0 & 0 & 1 \end{bmatrix}$$

The initial estimates of $\hat{b}$ and $\hat{\sigma}$ are $\hat{b}(0) = \underline{\mathbf{0}}_6$ and $\hat{\sigma}(0) = \underline{\mathbf{0}}_6$. Design parameters used in the derivation of the nonlinear stochastic filter are selected as $\Gamma = \mathbf{I}_6$, $\Pi = \mathbf{I}_6$, $k_b = 0.1$, $k_\sigma = 0.1$, $k_p = 2$, $k_w = 3$, and $\varepsilon = 0.5$. Additionally, the following color notation is used: green color refers to the true value, blue represents the performance of the proposed nonlinear stochastic filter, and red illustrates the performance of the filter previously proposed in literature. Finally, magenta demonstrates measured values.

The first three figures present the true values of the velocity vectors and body-

frame vectors plotted against their measured values. The true angular velocity (Ω) and the high values of noise and bias components introduced through the measurement process of Ω_m plotted against time are depicted in Figure 7.2. Similarly, the true translational velocity (V) and the high values of noise and bias components associated with the measurement process of V_m plotted against time are illustrated in Figure 7.3. In addition, Figure 7.4 presents the true body-frame vectors and their uncertain measurements corrupted with noise. High levels of noise and bias inherent to the measurements can be noticed in all the above-mentioned graphs (Figure 7.2, 7.3 and 7.4).

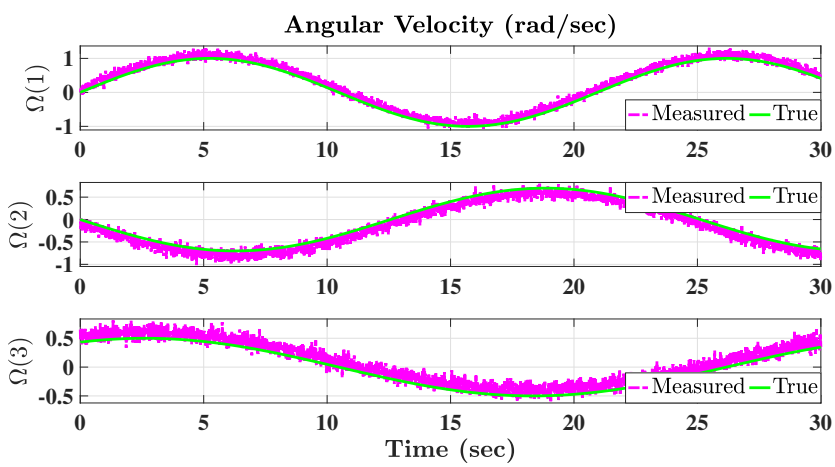

Figure 7.2: True and measured angular velocities.

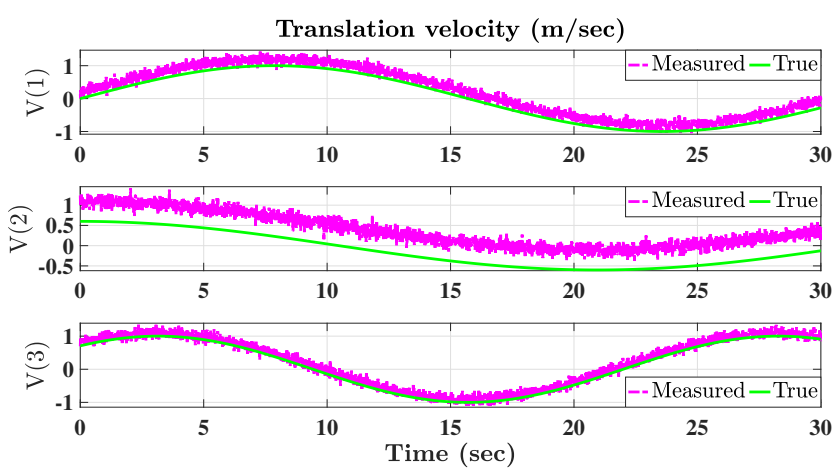

Figure 7.3: True and measured translational velocities.

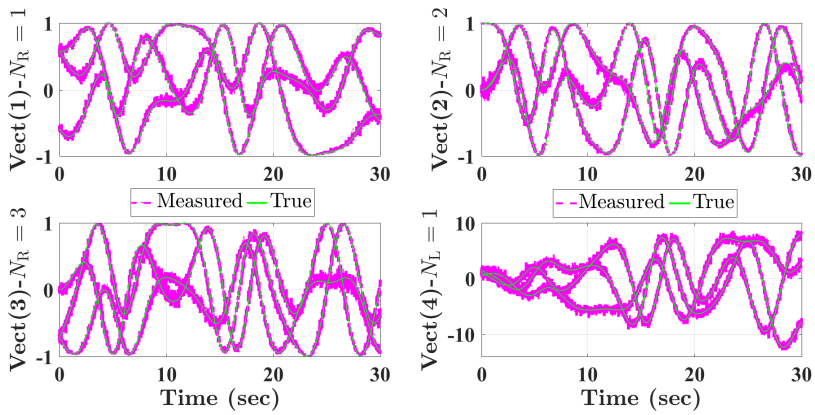

Figure 7.4: True values and vectorial measurements of the body-frame.

The position and attitude tracking performance of the proposed stochastic filter is demonstrated in Figure 7.5 and 7.6. Figure 7.5 depicts the estimated Euler angles $\left(\text{Roll}(\hat{\phi}), \text{Pitch}(\hat{\theta}), \text{Yaw}(\hat{\psi})\right)$ versus the true values (ϕ, θ, ψ). Also, Figure 7.6 illustrates the high value of the attitude initial error. The tracking position $(\hat{x}, \hat{y}, \hat{z})$ of the stochastic estimator in 3D space is compared to the true position (x, y, z) over time in Figure 7.6. Figure 7.5 and 7.6 show impressive tracking performance of the proposed stochastic observer in terms of position and attitude in presence of large initial error between the true and the estimated pose. Also, Figure 7.5 and 7.6 demonstrate remarkable tracking performance in case when high values of bias and noise corrupt the measurements.

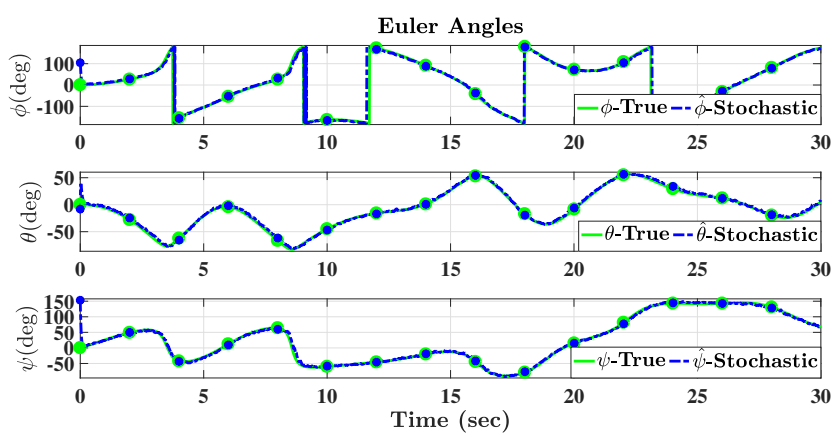

Figure 7.5: Tracking performance of Euler angles of the stochastic filter.

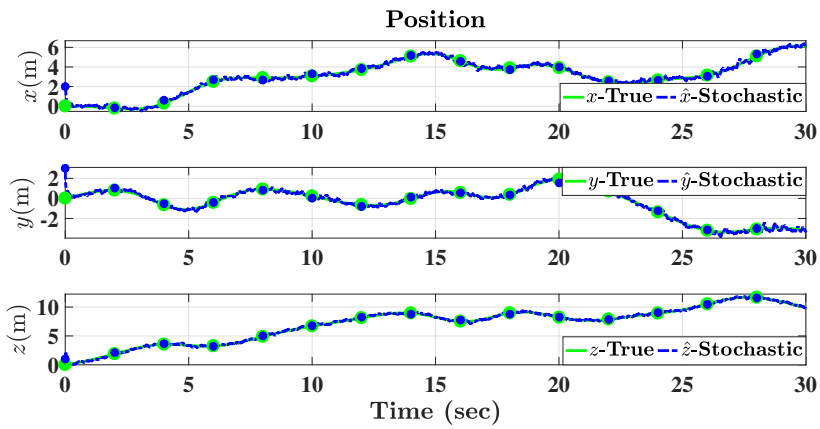

Figure 7.6: Tracking performance of x, y and z trajectory of the stochastic filter in 3D space.

A comparison between the proposed stochastic observer in Theorem 7.2 and the deterministic pose observer in Hua et al. (2011) is presented in Figure 7.7. The upper portion of Figure 7.7 illustrates the normalized Euclidean distance $||\tilde{R}||_I$, while the lower portion presents the Euclidean distance $||P - \hat{P}||$ for both observers such that $\tilde{R} = \hat{R}R^\top$. Figure 7.7 shows stable output performance of the stochastic observer with $||\tilde{R}||_I$ and $||P - \hat{P}||$ being regulated very close to the neighborhood of the origin confirming the results shown in Figure 7.5 and 7.6. On the other side, the deterministic filter shows high oscillatory performance before it goes out of stability.

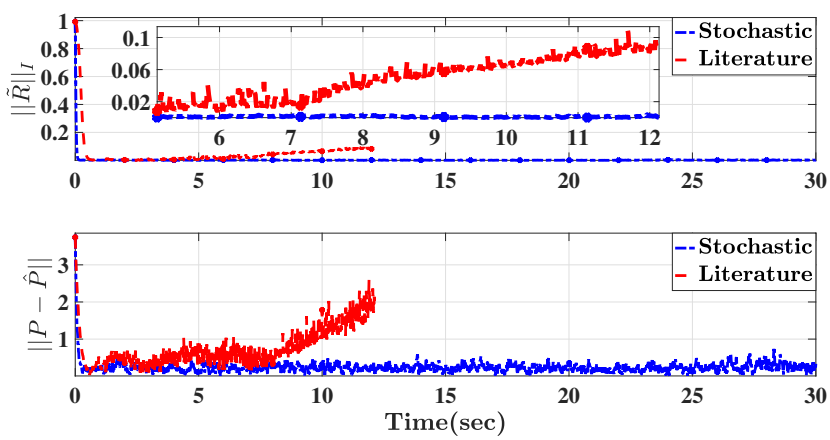

Figure 7.7: Tracking performance of normalized Euclidean distance error of $||\tilde{R}||_I$ and Euclidean distance $||P - \hat{P}||$.

Let $\mathring{\mathrm{v}}_1^{\mathcal{B}(\mathrm{L})} = R^\top \left(\mathrm{v}_1^{\mathcal{I}(\mathrm{L})} - P\right)$ and $\mathring{\mathrm{v}}_i^{\mathcal{B}(\mathrm{R})} = R^\top \mathrm{v}_i^{\mathcal{I}(\mathrm{R})}$ denote the true body-frame vectors for $i = 1, 2, 3$. Consider the error between the true and measured body-frame vectors $\tilde{\mathrm{v}}_1^{\mathcal{B}(\mathrm{L})} = \mathrm{v}_1^{\mathcal{B}(\mathrm{L})} - \mathring{\mathrm{v}}_1^{\mathcal{B}(\mathrm{L})}$ and $\tilde{\mathrm{v}}_i^{\mathcal{B}(\mathrm{R})} = \mathrm{v}_i^{\mathcal{B}(\mathrm{R})} - \mathring{\mathrm{v}}_i^{\mathcal{B}(\mathrm{R})}$. In the same spirit, let the error between the true and measured velocities be given by $\tilde{\Omega} = \Omega_m - \Omega$ and $\tilde{V} = V_m - V$. Table 7.1 provides mean and STD of the input measurements and the output data. It should be stressed that the mean errors of $||\tilde{R}||_I$ and $P - \hat{P}$ approach zero while the STD of $||\tilde{R}||_I$ is less than its mean, and the STD of $P - \hat{P} \approx 0.1$. Numerical results outlined in Table 7.1 affirm the robustness of the proposed nonlinear stochastic filter as demonstrated in Figure 7.5, 7.6, and 7.7.

Table 7.1: Statistical analysis of the noise and bias in input measurements and output data of the proposed filter.

Input measurements					
Index	$\tilde{\mathrm{v}}_1^{\mathcal{B}(\mathrm{L})}$	$\tilde{\mathrm{v}}_1^{\mathcal{B}(\mathrm{R})}$	$\tilde{\mathrm{v}}_2^{\mathcal{B}(\mathrm{R})}$	$\tilde{\Omega}$ (rad/sec)	$\tilde{V}$ (m/sec)
Mean	$\begin{bmatrix} 0.15 \\ 0.1 \\ -0.1 \end{bmatrix}$	$\begin{bmatrix} -0.1 \\ 0.1 \\ 0.05 \end{bmatrix}$	$\begin{bmatrix} 0 \\ 0 \\ 0.1 \end{bmatrix}$	$\begin{bmatrix} 0.1 \\ -0.1 \\ 0.1 \end{bmatrix}$	$\begin{bmatrix} 0.2 \\ 0.5 \\ 0.1 \end{bmatrix}$
STD	$0.1 \times \underline{\mathbf{1}}_3$	$0.1 \times \underline{\mathbf{1}}_3$	$0.1 \times \underline{\mathbf{1}}_3$	$0.15 \times \underline{\mathbf{1}}_3$	$0.15 \times \underline{\mathbf{1}}_3$

Output data over the period (1-30 sec)		
Index	$\|\|\tilde{R}\|\|_I$	$P - \hat{P}$ (m)
Mean	1.2×10^{-3}	$[-17.7, 2.6, -8.4]^\top \times 10^{-3}$
STD	8.5×10^{-4}	$[1.15, 1.07, 1.27]^\top \times 10^{-1}$

Simulations presented in this section demonstrate the robustness of the proposed stochastic filter in the sense of Stratonovich against high levels of bias and noise components introduced in angular velocity, translational velocity and vectorial measurements. Also, they show that the stochastic filter is capable of correcting its position and attitude even in presence of large initial error in a small amount of time. In addition, the stochastic filter is autonomous, and therefore no prior information about the upper bound of the covariance matrix $\mathcal{Q}^2$ is required to achieve impressive estimation performance.

7.5 Conclusion

Pose is naturally nonlinear and is modeled on the Special Euclidean Group $\mathbb{SE}(3)$. Pose estimators used to be designed as nonlinear deterministic filters neglecting the noise inherent to the model dynamics. This is reflected in the nonlinear deterministic filter design as well as in the potential function selection. In this work, the pose problem has been formulated as a nonlinear pose problem on $\mathbb{SE}(3)$. The problem is mapped from $\mathbb{SE}(3)$ to vector form using Rodriguez vector parameterization and position. The problem is defined stochastically in the sense of Stratonovich. Next, a nonlinear stochastic pose filter on $\mathbb{SE}(3)$ has been proposed. It has been shown that errors in position, Rodriguez vector and estimates are semi-globally uniformly ultimately bounded (SGUUB) in mean square and that they converge to the small neighborhood of the origin for the case when noise is attached to the pose dynamics. Simulation results prove fast convergence from large initialized pose error even when angular and translational velocity vectors as well as body-frame measurements are subject to high levels of noise and bias.

Chapter 8
Conclusion

In this thesis attitude and pose estimation problems were considered on the Lie groups of $\mathbb{SO}(3)$ and $\mathbb{SE}(3)$. The attitude and pose kinematics are naturally nonlinear and modelled on the Lie group of $\mathbb{SO}(3)$ and $\mathbb{SE}(3)$. Accordingly, these estimation problems were approached through nonlinear deterministic and stochastic filtering algorithms developed directly on $\mathbb{SO}(3)$ and $\mathbb{SE}(3)$. Deterministic attitude and pose filtering approaches proposed in this thesis allow for guaranteed and systematic convergence of the error which starts arbitrarily within a given large set and reduces systematically and smoothly to a given small residual set, whereas attitude and pose filtering methods described in the literature do not have clear measure of the transient and steady-state performance of the tracking error. Unlike the deterministic methods that disregard the noise in filter derivation, nonlinear stochastic attitude and pose filtering approaches allow to diminish the noise attached to angular velocity measurements such that the error is almost semi-globally uniformly ultimately bounded in mean square and is regulated to arbitrarily small neighborhood of the equilibrium point from almost any initial condition. As such, the proposed filters ensure superior convergence properties. In addition, the proposed nonlinear filters are autonomous, and therefore no prior information about the sensor uncertainties is required to achieve impressive estimation performance.

Addressing the inability of nonlinear deterministic attitude filters on $\mathbb{SO}(3)$ described in the literature to handle large error in initialization and to force the error function to follow predefined transient and steady-state measures, two different nonlinear deterministic filters on $\mathbb{SO}(3)$ have been proposed in ***Chapter*** 3. The attitude error function of the proposed filters is constrained to initially start within a known large set and reduce systematically and smoothly to a given small set. Trapping the attitude error within the dynamically reducing boundaries is achieved via an auxiliary variable known as transformed error. The transformed error helped to guarantee

boundedness of the closed loop error signals with the normalized distance of attitude error being regulated asymptotically to the origin from almost any initial condition. The first proposed filter required a rate gyroscope measurement and a set of two or more vectorial measurements to obtain online algebraic reconstruction of the attitude. The second proposed filter used the rate gyroscope measurement combined with the vectorial measurements directly avoiding the need for attitude reconstruction.

It is important to note that nonlinear attitude filter kinematics on $\mathbb{SO}(3)$ rely on angular velocity measurements. Therefore, another major shortcoming of the nonlinear deterministic attitude filters on $\mathbb{SO}(3)$ described in the literature is the assumption that angular velocity measurement is subject only to constant bias. To account for not only constant bias but also any noise components introduced during the measurement process two nonlinear stochastic attitude filters on $\mathbb{SO}(3)$ which improve the overall estimation quality have been proposed in ***Chapter*** 4. The first stochastic filter was driven in the sense of Ito and the second one was developed in the sense of Stratonovich. These filters showed that the error of rigid-body orientation is steered towards an arbitrarily small neighborhood of the identity in probability with the error being almost semi-globally uniformly ultimately bounded in mean square while the noise impact is reduced to a very low level for known or unknown bounded covariance.

Chapter 5 proposed an explicit nonlinear stochastic complementary filter on $\mathbb{SO}(3)$ driven in the sense of Ito, which, unlike filters introduced in ***Chapter*** 4, alleviated the need for online algebraic attitude reconstruction which is computationally expensive. Instead the rate gyroscope measurement and a set of two or more vectorial measurements directly are used. The explicit filter ensured that the error in rigid-body orientation is regulated towards an arbitrarily small neighborhood of the identity in probability and the error was almost semi-globally uniformly ultimately bounded in mean square. The attitude filters proposed in ***Chapter*** 3, 4 and 5 were able to provide reliable attitude estimates with remarkable convergence properties considering measurements obtained from low quality sensors such as low-cost IMUs devices.

The shortcoming of nonlinear deterministic pose filters on $\mathbb{SE}(3)$ described in the literature is their inability to force the pose error to initiate within a predefined large set and decay systematically and smoothly to a predefined small residual set.

To address this deficiency, two robust nonlinear deterministic pose filters on $\mathbb{SE}(3)$ with predefined transient and steady-state measures have been proposed in ***Chapter*** 6. The pose error function has been proven to be confined within dynamically reducing boundaries with the aid of an auxiliary variable termed transformed error. The proposed filters guaranteed boundedness of the closed loop error signals with constrained error and unconstrained transformed error being proven to be almost globally asymptotically stable such that the error in the homogeneous transformation matrix is regulated asymptotically to the identity from almost any initial condition. The proposed pose filters demonstrated faster convergence than any of the filters previously proposed in the literature. The first proposed filter required translational velocity measurements, rate gyroscope measurements, a set of two or more vectorial measurements, and one or more landmarks to obtain online algebraic reconstruction of the pose. The second proposed filter used the aforementioned set of measurements directly without the need of pose reconstruction.

An important factor to consider is that nonlinear deterministic pose filters on $\mathbb{SE}(3)$ presume that angular and translational velocity measurements are subject only to constant bias and ignore any noise introduced during the measurement process. In ***Chapter*** 7, a nonlinear stochastic pose filter on $\mathbb{SE}(3)$ has been introduced in the sense of Stratonovich to address the uncertainties present in velocity measurements. It has been shown that the error in the homogeneous transformation matrix was steered towards an arbitrarily small neighborhood of the identity in probability. Also, it has been proven that the error in the homogeneous transformation matrix be almost semi-globally uniformly ultimately bounded in mean square. The filters proposed in ***Chapter*** 6 and 7 were able to provide reliable pose estimates with superior convergence properties in case when measurements were obtained from low-cost inertial vision system such as low-cost IMUs systems and on-board cameras.

The simulation results in ***Chapter*** 3*,* 4*,* 5*,* 6*, and* 7 demonstrated the strong filtering capability of the proposed filters against high levels of bias and noise components introduced in velocity and vectorial measurements. Also, they showed that the proposed filters were capable of correcting attitude or pose estimates even in presence of large initial error in a short period of time. It should also be remarked that all gains associated with the filter design are adaptively tuned such that the filter gains become increasingly aggressive as the attitude or pose error increase.

8.1 Future Work

The following challenges could be further investigated to achieve even better filter performance:

1. Nonlinear stochastic filters on $\mathbb{SO}(3)$ and $\mathbb{SE}(3)$ able to handle large error in initialization with error function being forced to follow predefined transient and steady-state measures. These filters should be robust against high levels of bias and noise components introduced in velocity and vectorial measurements. Also, they should be able to correct attitude or pose estimates in presence of large initial error in a short period of time. This issue is still an open problem.

2. Nonlinear stochastic filters on $\mathbb{SO}(3)$ and $\mathbb{SE}(3)$ robust against angular velocity measurements and body-frame measurements corrupted with unknown constant bias and noise components.

3. Nonlinear stochastic filters on $\mathbb{SO}(3)$ and $\mathbb{SE}(3)$ able to tackle intermittent measurements.

4. Hybrid global exponential stabilization of nonlinear stochastic attitude filters on $\mathbb{SO}(3)$.

5. Hybrid global exponential stabilization of nonlinear stochastic pose filters on $\mathbb{SE}(3)$.

References

Anderson, B. D., & Moore, J. B. (1979). Optimal filtering. *Englewood Cliffs*, *21*, 22–95.

Aqeeli, E., Hashim, H. A., Anwer, H., & Shami, A. (2019). Optimal location management in LTE networks using evolutionary techniques. *International Journal of Communication Systems*, 1–17.

Arulampalam, M. S., Maskell, S., Gordon, N., & Clapp, T. (2002). A tutorial on particle filters for online nonlinear/non-gaussian bayesian tracking. *IEEE Transactions on Signal Processing*, *50*(2), 174–185.

Ayinde, B. O., & Hashim, H. A. (2018). Energy-efficient deployment of relay nodes in wireless sensor networks using evolutionary techniques. *International Journal of Wireless Information Networks*, *25*, 157–172.

Baerveldt, J., A, & Klang, R. (1997). A low-cost and low-weight attitude estimation system for an autonomous helicopter. In *Intelligent engineering systems, 1997. ines97. proceedings., 1997 ieee international conference on* (pp. 391–395).

Baldwin, G., Mahony, R., & Trumpf, J. (2009). A nonlinear observer for 6 dof pose estimation from inertial and bearing measurements. In *Robotics and automation, 2009. icra09. ieee international conference on* (pp. 2237–2242).

Baldwin, G., Mahony, R., Trumpf, J., Hamel, T., & Cheviron, T. (2007). Complementary filter design on the special euclidean group se (3). In *Control conference (ecc), 2007 european* (pp. 3763–3770).

Barrau, A., & Bonnabel, S. (2015). Intrinsic filtering on lie groups with applications to attitude estimation. *IEEE Transactions on Automatic Control*, *60*(2), 436–449.

Barrau, A., & Bonnabel, S. (2017). The invariant extended kalman filter as a stable observer. *IEEE Transactions on Automatic Control*, *62*(4), 1797–1812.

Bechlioulis, C. P., & Rovithakis, G. A. (2008). Robust adaptive control of feedback linearizable mimo nonlinear systems with prescribed performance. *IEEE Transactions on Automatic Control*, *53*(9), 2090–2099.

Black, H. D. (1964). A passive system for determining the attitude of a satellite. *AIAA journal*, *2*(7), 1350–1351.

Blanco, J.-L. (2010). A tutorial on se (3) transformation parameterizations and on-manifold optimization. *University of Malaga, Tech. Rep*, *3*.

Bonnable, S., Martin, P., & Salaun, E. (2009). Invariant extended kalman filter: theory and application to a velocity-aided attitude estimation problem. In *Decision and control, 2009 held jointly with the 2009 28th chinese control conference. cdc 2009. proceedings of the 48th ieee conference on* (pp. 1297–1304).

Bullo, F., & Lewis, A. D. (2004). *Geometric control of mechanical systems: modeling, analysis, and design for simple mechanical control systems* (Vol. 49). Springer Science & Business Media.

Cheng, Y., & Crassidis, J. (2004). Particle filtering for sequential spacecraft attitude estimation. In *Aiaa guidance, navigation, and control conference and exhibit* (p. 5337).

Chiuso, A., & Soatto, S. (2000). Monte carlo filtering on lie groups. In *Decision and control, 2000. proceedings of the 39th ieee conference on* (Vol. 1, pp. 304–309).

Choi, C., & Christensen, H. I. (2012). Robust 3d visual tracking using particle filtering on the special euclidean group: A combined approach of keypoint and edge features. *The International Journal of Robotics Research*, *31*(4), 498–519.

Choukroun, D., Bar-Itzhack, I. Y., & Oshman, Y. (2006). Novel quaternion kalman filter. *IEEE Transactions on Aerospace and Electronic Systems*, *42*(1), 174–190.

Crassidis, J. L., & Markley, F. L. (2003). Unscented filtering for spacecraft attitude estimation. *Journal of guidance, control, and dynamics*, *26*(4), 536–542.

Crassidis, J. L., Markley, F. L., & Cheng, Y. (2007). Survey of nonlinear attitude estimation methods. *Journal of guidance, control, and dynamics*, *30*(1), 12–28.

Deng, H., & Krsti, M. (1997). Stochastic nonlinear stabilization-i: a backstepping design. *Systems & Control Letters*, *32*(3), 143–150.

Deng, H., Krstic, M., & Williams, R. J. (2001). Stabilization of stochastic nonlinear systems driven by noise of unknown covariance. *IEEE Transactions on Automatic Control*, *46*(8), 1237–1253.

Dominguez, S. (2017). Simultaneous recognition and relative pose estimation of 3d objects using 4d orthonormal moments. *Sensors*, *17*(9), 2122.

El-Ferik, S., Hashim, H. A., & Lewis, F. L. (2018). Neuro-adaptive distributed con-

trol with prescribed performance for the synchronization of unknown nonlinear networked systems. *IEEE Transactions on Systems, Man, and Cybernetics: Systems*, *48*(12), 2135–2144.

Eltoukhy, A. E., Chan, F. T., & Chung, S. H. (2017). Airline schedule planning: a review and future directions. *Industrial Management & Data Systems*, *117*(6), 1201–1243.

Eltoukhy, A. E., Chan, F. T., Chung, S. H., & Niu, B. (2018). A model with a solution algorithm for the operational aircraft maintenance routing problem. *Computers & Industrial Engineering*, *120*, 346–359.

Eltoukhy, A. E., Chan, F. T., Chung, S. H., Niu, B., & Wang, X. (2017). Heuristic approaches for operational aircraft maintenance routing problem with maximum flying hours and man-power availability considerations. *Industrial Management & Data Systems*, *117*(10), 2142–2170.

Eltoukhy, A. E., Wang, Z., Chan, F. T., & Chung, S. (2018). Joint optimization using a leader–follower stackelberg game for coordinated configuration of stochastic operational aircraft maintenance routing and maintenance staffing. *Computers & Industrial Engineering*, *125*, 46–68.

Eltoukhy, A. E., Wang, Z., Chan, F. T., & Fu, X. (2019). Data analytics in managing aircraft routing and maintenance staffing with price competition by a stackelberg-nash game model. *Transportation Research Part E: Logistics and Transportation Review*, *112*, 143–168.

Ge, S. S., & Wang, C. (2004). Adaptive neural control of uncertain mimo nonlinear systems. *IEEE Transactions on Neural Networks*, *15*(3), 674–692.

Goodarzi, F. A., & Lee, T. (2016). Extended kalman filter on se (3) for geometric control of a quadrotor uav. In *Unmanned aircraft systems (icuas), 2016 international conference on* (pp. 1371–1380).

Grip, H. F., Fossen, T. I., Johansen, T. A., & Saberi, A. (2012). Attitude estimation using biased gyro and vector measurements with time-varying reference vectors. *IEEE Transactions on Automatic Control*, *57*(5), 1332–1338.

Hamel, T., & Mahony, R. (2006). Attitude estimation on so (3) based on direct inertial measurements. In *Robotics and automation, 2006. icra 2006. proceedings 2006 ieee international conference on* (pp. 2170–2175).

Hashim, H. A. (2019). Distributed adaptive consensus control of high order unknown nonlinear networked systems with guaranteed performance. *arXiv*, 1–11.

Hashim, H. A., & Abido, M. A. (2015). Fuzzy controller design using evolutionary techniques for twin rotor MIMO system: a comparative study. *Computational intelligence and neuroscience*, *2015*, 49.

Hashim, H. A., & Abido, M. A. (2019). Location management in LTE networks using multi-objective particle swarm optimization. *Computer Networks*, *157*, 78–88.

Hashim, H. A., Ayinde, B. O., & Abido, M. A. (2016). Optimal placement of relay nodes in wireless sensor network using artificial bee colony algorithm. *Journal of Network and Computer Applications*, *64*, 239–248.

Hashim, H. A., Brown, L. J., & McIsaac, K. (2018a). Nonlinear explicit stochastic attitude filter on SO(3). In *Proceedings of the 57th IEEE conference on Decision and Control (CDC)* (pp. 1210 –1216).

Hashim, H. A., Brown, L. J., & McIsaac, K. (2018b). Nonlinear stochastic attitude filters on the special orthogonal group 3: Ito and stratonovich. *IEEE Transactions on Systems, Man, and Cybernetics: Systems*, 1–13.

Hashim, H. A., Brown, L. J., & McIsaac, K. (2019a). Guaranteed performance of nonlinear attitude filters on the special orthogonal group SO(3). *IEEE Access*, *7*(1), 3731–3745.

Hashim, H. A., Brown, L. J., & McIsaac, K. (2019b). Guaranteed performance of nonlinear pose filter on SE(3). In *Proceedings of the American Control Conference (ACC)* (pp. 1–6).

Hashim, H. A., Brown, L. J., & McIsaac, K. (2019c). Nonlinear pose filters on the special euclidean group SE(3) with guaranteed transient and steady-state performance. *IEEE Transactions on Systems, Man, and Cybernetics: Systems*, 1–14.

Hashim, H. A., Brown, L. J., & McIsaac, K. (2019d). Nonlinear stochastic position and attitude filter on the special euclidean group 3. *Journal of the Franklin Institute*, *356*(7), 4144–4173.

Hashim, H. A., El-Ferik, S., & Abido, M. A. (2015). A fuzzy logic feedback filter design tuned with pso for L1 adaptive controller. *Expert Systems with Applications*, *42*(23), 9077–9085.

Hashim, H. A., El-Ferik, S., Ayinde, B. O., & Abido, M. A. (2017). Optimal tuning of fuzzy feedback filter for L1 adaptive controller using multi-objective particle swarm optimization for uncertain nonlinear MIMO systems. *arXiv preprint arXiv:1710.05423*.

Hashim, H. A., El-Ferik, S., & Lewis, F. L. (2017). Adaptive synchronisation of unknown nonlinear networked systems with prescribed performance. *International Journal of Systems Science*, *48*(4), 885–898.

Hashim, H. A., El-Ferik, S., & Lewis, F. L. (2019). Neuro-adaptive cooperative tracking control with prescribed performance of unknown higher-order nonlinear multi-agent systems. *International Journal of Control*, *92*(2), 445–460.

Haykin, S. S., et al. (2001). *Kalman filtering and neural networks*. Wiley Online Library.

He, S., Dai, S.-L., & Luo, F. (2018). Asymptotic trajectory tracking control with guaranteed transient behavior for msv with uncertain dynamics and external disturbances. *IEEE Transactions on Industrial Electronics*.

Hua, M.-D., & Allibert, G. (2018). Riccati observer design for pose, linear velocity and gravity direction estimation using landmark position and imu measurements. In *2018 ieee conference on control technology and applications*.

Hua, M.-D., Zamani, M., Trumpf, J., Mahony, R., & Hamel, T. (2011). Observer design on the special euclidean group se (3). In *Decision and control and european control conference (cdc-ecc), 2011 50th ieee conference on* (pp. 8169–8175).

Ito, K., & Rao, K. M. (1984). *Lectures on stochastic processes* (Vol. 24). Tata institute of fundamental research.

Jazwinski, A. H. (2007). *Stochastic processes and filtering theory*. Courier Corporation.

Ji, H.-B., & Xi, H.-S. (2006). Adaptive output-feedback tracking of stochastic nonlinear systems. *IEEE Transactions on Automatic Control*, *51*(2), 355–360.

Kalman, R. E. (1960). A new approach to linear filtering and prediction problems. *Journal of basic Engineering*, *82*(1), 35–45.

Keskin, C., Kirac, F., Kara, Y. E., & Akarun, L. (2013). Real time hand pose estimation using depth sensors. In *Consumer depth cameras for computer vision* (pp. 119–137). Springer.

Khasminskii, R. (1980). *Stochastic stability of differential equations*. Rockville, MD: S & N International.

Kwon, J., Choi, M., Park, F. C., & Chun, C. (2007). Particle filtering on the euclidean group: framework and applications. *Robotica*, *25*(6), 725–737.

Lee, T. (2012). Exponential stability of an attitude tracking control system on so (3) for large-angle rotational maneuvers. *Systems & Control Letters*, *61*(1),

231–237.

Lefferts, E. J., Markley, F. L., & Shuster, M. D. (1982). Kalman filtering for spacecraft attitude estimation. *Journal of Guidance, Control, and Dynamics*, *5*(5), 417–429.

Mahony, R., Hamel, T., & Pflimlin, J.-M. (2005). Complementary filter design on the special orthogonal group so (3). In *Decision and control, 2005 and 2005 european control conference. cdc-ecc05. 44th ieee conference on* (pp. 1477–1484).

Mahony, R., Hamel, T., & Pflimlin, J.-M. (2008). Nonlinear complementary filters on the special orthogonal group. *IEEE Transactions on Automatic Control*, *53*(5), 1203–1218.

Markley, F. L. (1988). Attitude determination using vector observations and the singular value decomposition. *Journal of the Astronautical Sciences*, *36*(3), 245–258.

Markley, F. L. (2003). Attitude error representations for kalman filtering. *Journal of guidance, control, and dynamics*, *26*(2), 311–317.

Menegaz, H. M., Ishihara, J. Y., Borges, G. A., & Vargas, A. N. (2015). A systematization of the unscented kalman filter theory. *IEEE Transactions on Automatic Control*, *60*(10), 2583–2598.

Mohamed, H. A. H. (2014). Improved robust adaptive control of high-order nonlinear systems with guaranteed performance. *M. Sc, King Fahd University Of Petroleum & Minerals*, *1*.

Mortensen, R. (1968). Maximum-likelihood recursive nonlinear filtering. *Journal of Optimization Theory and Applications*, *2*(6), 386–394.

Murray, R. M., Li, Z., Sastry, S. S., & Sastry, S. S. (1994). *A mathematical introduction to robotic manipulation*. CRC press.

Rehbinder, H., & Ghosh, B. K. (2003). Pose estimation using line-based dynamic vision and inertial sensors. *IEEE Transactions on Automatic Control*, *48*(2), 186–199.

Rehbinder, H., & Hu, X. (2000). Nonlinear state estimation for rigid-body motion with low-pass sensors. *Systems & Control Letters*, *40*(3), 183–190.

Rehbinder, H., & Hu, X. (2004). Drift-free attitude estimation for accelerated rigid bodies. *Automatica*, *40*(4), 653–659.

Salcudean, S. (1991). A globally convergent angular velocity observer for rigid body

motion. *IEEE transactions on Automatic Control*, *36*(12), 1493–1497.

Shuster, M. D. (1993). A survey of attitude representations. *Navigation*, *8*(9), 439–517.

Shuster, M. D., & Oh, S. D. (1981). Three-axis attitude determination from vector observations. *Journal of Guidance, Control, and Dynamics*, *4*, 70–77.

Srivatsan, R. A., Rosen, G. T., Mohamed, D. F. N., & Choset, H. (2016). Estimating se (3) elements using a dual quaternion based linear kalman filter. In *Robotics: Science and systems.*

Stratonovich, R. L. (1967). *Topics in the theory of random noise* (Vol. 2). CRC Press.

Thienel, J., & Sanner, R. M. (2003). A coupled nonlinear spacecraft attitude controller and observer with an unknown constant gyro bias and gyro noise. *IEEE Transactions on Automatic Control*, *48*(11), 2011–2015.

Vasconcelos, J. F., Cunha, R., Silvestre, C., & Oliveira, P. (2010). A nonlinear position and attitude observer on se (3) using landmark measurements. *Systems & Control Letters*, *59*(3), 155–166.

Vik, B., & Fossen, T. I. (2001). A nonlinear observer for gps and ins integration. In *Decision and control, 2001. proceedings of the 40th ieee conference on* (Vol. 3, pp. 2956–2961).

Wahba, G. (1965). A least squares estimate of satellite attitude. *SIAM review*, *7*(3), 409–409.

Wong, E., & Zakai, M. (1965). On the convergence of ordinary integrals to stochastic integrals. *The Annals of Mathematical Statistics*, *36*(5), 1560–1564.

Zamani, M., Trumpf, J., & Mahony, R. (2013). Minimum-energy filtering for attitude estimation. *IEEE Transactions on Automatic Control*, *58*(11), 2917–2921.

Zlotnik, D. E., & Forbes, J. R. (2017). Nonlinear estimator design on the special orthogonal group using vector measurements directly. *IEEE Transactions on Automatic Control*, *62*(1), 149–160.

Appendix A
Proof of Lemma 3.1, 5.1 and 6.1

The subsequent analysis is done in terms of Rodriquez parameters vector and is used only for the purpose of proving Lemma 3.1, 5.1 and 6.1. Let $R \in \mathbb{SO}(3)$ be the attitude of a rigid-body in 3D space. The attitude could be extracted for a given Rodriguez parameters vector $\rho \in \mathbb{R}^3$. The mapping from Rodriguez vector to $\mathbb{SO}(3)$ is defined by $\mathcal{R}_\rho : \mathbb{R}^3 \to \mathbb{SO}(3)$ (Shuster (1993))

$$\mathcal{R}_\rho(\rho) = \frac{1}{1+||\rho||^2}\left(\left(1-||\rho||^2\right)\mathbf{I}_3 + 2\rho\rho^\top + 2\left[\rho\right]_\times\right) \tag{A.1}$$

With direct substitution of (A.1) in (2.6) one easily obtains

$$||R||_I = \frac{||\rho||^2}{1+||\rho||^2} \tag{A.2}$$

Additionally, for $\mathcal{R}_\rho = \mathcal{R}_\rho(\rho)$ the anti-symmetric projection operator of the attitude in (A.1) is equivalent to

$$\boldsymbol{\mathcal{P}}_a(R) = \frac{1}{2}\left(\mathcal{R}_\rho - \mathcal{R}_\rho^\top\right) = 2\frac{1}{1+||\rho||^2}\left[\rho\right]_\times \tag{A.3}$$

Thus, the vex operator of (A.3) becomes

$$\mathbf{vex}\left(\boldsymbol{\mathcal{P}}_a(R)\right) = 2\frac{\rho}{1+||\rho||^2} \tag{A.4}$$

From the result in (A.2) one can obtain

$$\left(1-||R||_I\right)||R||_I = \frac{||\rho||^2}{\left(1+||\rho||^2\right)^2} \tag{A.5}$$

and from (A.4) it is easily shown that

$$||\mathbf{vex}\left(\boldsymbol{\mathcal{P}}_a\left(R\right)\right)||^2 = 4\frac{||\rho||^2}{\left(1+||\rho||^2\right)^2} \tag{A.6}$$

Therefore, (A.5) and (A.6) prove

$$||\mathbf{vex}\left(\boldsymbol{\mathcal{P}}_a\left(R\right)\right)||^2 = \left(1-||R||_I\right)||R||_I$$

Since it was assumed that $\sum_{i=1}^{N_{\mathrm{R}}} k_i^{\mathrm{R}} = 3$, this indicates that $\mathrm{Tr}\left\{\mathbf{M}_{\mathrm{R}}\right\} = 3$. Recall that the normalized Euclidean distance of $R\mathbf{M}_{\mathrm{R}}$ is $\|R\mathbf{M}_{\mathrm{R}}\|_I = \frac{1}{4}\mathrm{Tr}\left\{\left(\mathbf{I}_3 - R\right)\mathbf{M}_{\mathrm{R}}\right\}$. From the angle-axis parameterization in (2.7), one finds

$$\begin{aligned}\|R\mathbf{M}_{\mathrm{R}}\|_I &= \frac{1}{4}\mathrm{Tr}\left\{-\left(\sin(\theta)\left[u\right]_\times + \left(1-\cos(\theta)\right)\left[u\right]_\times^2\right)\mathbf{M}_{\mathrm{R}}\right\} \\ &= -\frac{1}{4}\mathrm{Tr}\left\{\left(1-\cos(\theta)\right)\left[u\right]_\times^2\mathbf{M}_{\mathrm{R}}\right\}\end{aligned} \tag{A.7}$$

where $\mathrm{Tr}\left\{\left[u\right]_\times\mathbf{M}_{\mathrm{R}}\right\} = 0$ as in identity (2.15). One has (Murray, Li, Sastry, and Sastry (1994))

$$\|R\|_I = \frac{1}{4}\mathrm{Tr}\left\{\mathbf{I}_3 - R\right\} = \sin^2\left(\theta/2\right) \tag{A.8}$$

The Rodriguez vector can be expressed in terms of angle-axis parameterization as (Shuster (1993))

$$u = \cot\left(\theta/2\right)\rho \tag{A.9}$$

From identity (2.14) and (A.9), the expression in (A.7) becomes

$$\|R\mathbf{M}_{\mathrm{R}}\|_I = \frac{1}{2}\|R\|_I\, u^\top\bar{\mathbf{M}}_{\mathrm{R}}u = \frac{1}{2}\|R\|_I\cot^2\left(\frac{\theta}{2}\right)\rho^\top\bar{\mathbf{M}}_{\mathrm{R}}\rho$$

Also, from (A.8), $\cos^2\left(\frac{\theta}{2}\right) = 1 - \|R\|_I$ which implies that

$$\tan^2\left(\frac{\theta}{2}\right) = \frac{\|R\|_I}{1-\|R\|_I}$$

Accordingly, the normalized Euclidean distance of $R\mathbf{M}_{\mathrm{R}}$ could be formulated in the sense of Rodriguez vector

$$\|R\mathbf{M}_{\mathrm{R}}\|_I = \frac{1}{2}\left(1 - \|R\|_I\right)\rho^\top \bar{\mathbf{M}}_{\mathrm{R}}\rho = \frac{1}{2}\frac{\rho^\top \bar{\mathbf{M}}_{\mathrm{R}}\rho}{1+\|\rho\|^2} \tag{A.10}$$

The anti-symmetric projection operator of $R\mathbf{M}_{\mathrm{R}}$ can be defined in terms of Rodriquez vector using identity (2.11) and (2.13) by

$$\begin{aligned}\boldsymbol{\mathcal{P}}_a\left(R\mathbf{M}_{\mathrm{R}}\right) &= \frac{\rho\rho^\top \mathbf{M}_{\mathrm{R}} - \mathbf{M}_{\mathrm{R}}\rho\rho^\top + \mathbf{M}_{\mathrm{R}}\left[\rho\right]_\times + \left[\rho\right]_\times \mathbf{M}_{\mathrm{R}}}{1+\|\rho\|^2} \\ &= \frac{\left[\left(\mathrm{Tr}\left\{\mathbf{M}_{\mathrm{R}}\right\}\mathbf{I}_3 - \mathbf{M}_{\mathrm{R}} - \left[\rho\right]_\times \mathbf{M}_{\mathrm{R}}\right)\rho\right]_\times}{1+\|\rho\|^2}\end{aligned}$$

Thereby, the vex operator of the above expression is

$$\mathbf{vex}\left(\boldsymbol{\mathcal{P}}_a\left(R\mathbf{M}_{\mathrm{R}}\right)\right) = \frac{\left(\mathbf{I}_3 + \left[\rho\right]_\times\right)}{1+\|\rho\|^2}\bar{\mathbf{M}}_{\mathrm{R}}\rho \tag{A.11}$$

Hence, the 2-norm of (A.11) is equivalent to

$$\|\mathbf{vex}\left(\boldsymbol{\mathcal{P}}_a\left(R\mathbf{M}_{\mathrm{R}}\right)\right)\|^2 = \frac{\rho^\top \bar{\mathbf{M}}_{\mathrm{R}}\left(\mathbf{I}_3 - \left[\rho\right]_\times^2\right)\bar{\mathbf{M}}_{\mathrm{R}}\rho}{\left(1+\|\rho\|^2\right)^2}$$

From the identity in (2.14), $\left[\rho\right]_\times^2 = -||\rho||^2\mathbf{I}_3 + \rho\rho^\top$ such that

$$\begin{aligned}\|\mathbf{vex}\left(\boldsymbol{\mathcal{P}}_a\left(R\mathbf{M}_{\mathrm{R}}\right)\right)\|^2 &= \frac{\rho^\top \bar{\mathbf{M}}_{\mathrm{R}}\left(\mathbf{I}_3 - \left[\rho\right]_\times^2\right)\bar{\mathbf{M}}_{\mathrm{R}}\rho}{\left(1+\|\rho\|^2\right)^2} \\ &= \frac{\rho^\top\left(\bar{\mathbf{M}}_{\mathrm{R}}\right)^2\rho}{1+\|\rho\|^2} - \frac{\left(\rho^\top \bar{\mathbf{M}}_{\mathrm{R}}\rho\right)^2}{\left(1+\|\rho\|^2\right)^2} \\ &\geq \underline{\lambda}\left(1 - \frac{\|\rho\|^2}{1+\|\rho\|^2}\right)\frac{\rho^\top \bar{\mathbf{M}}_{\mathrm{R}}\rho}{1+||\rho||^2} \\ &\geq 2\underline{\lambda}\left(1 - \|R\|_I\right)\|R\mathbf{M}_{\mathrm{R}}\|_I\end{aligned} \tag{A.12}$$

where $\underline{\lambda} = \underline{\lambda}\left(\bar{\mathbf{M}}_{\mathrm{R}}\right)$ is the minimum singular value of $\bar{\mathbf{M}}_{\mathrm{R}}$ and $\|R\|_I = \|\rho\|^2 / \left(1 + \|\rho\|^2\right)$ as in (A.2). One can find

$$1 - \|R\|_I = \frac{1}{4}\left(1 + \mathrm{Tr}\left\{R\mathbf{M}_{\mathrm{R}}\mathbf{M}_{\mathrm{R}}^{-1}\right\}\right) \tag{A.13}$$

Hence, from (A.12) and (A.13) the following inequality holds

$$\|\mathbf{vex}\left(\boldsymbol{\mathcal{P}}_a\left(R\mathbf{M}_{\mathrm{R}}\right)\right)\|^2 \geq \frac{\underline{\lambda}}{2}\left(1 + \mathrm{Tr}\left\{R\mathbf{M}_{\mathrm{R}}\mathbf{M}_{\mathrm{R}}^{-1}\right\}\right)\|R\mathbf{M}_{\mathrm{R}}\|_I$$

which completes the proof of Lemma 3.1, 5.1 and 6.1.

Appendix B
An Overview of Attitude Reconstruction via SVD

Let $R \in \mathbb{SO}(3)$ be the true attitude. The attitude can be reconstructed through a set of vectors given, for example, Chapter 5 equation (5.1). Let s_i be the confidence level of measurement i such that for n measurements we have $\sum_{i=1}^{n} s_i = 1$. In that case, the corrupted reconstructed attitude R_y can be obtained using Singular Value Decomposition (SVD) by

$$\begin{cases} \mathcal{J}(R) & = 1 - \sum_{i=1}^{n} s_i \left(\upsilon_i^{\mathcal{B}(\mathrm{R})}\right)^\top R^\top \upsilon_i^{\mathcal{I}(\mathrm{R})} \\ & = 1 - \mathrm{Tr}\left\{R^\top B^\top\right\} \\ B & = \sum_{i=1}^{n} s_i \upsilon_i^{\mathcal{B}(\mathrm{R})} \left(\upsilon_i^{\mathcal{I}(\mathrm{R})}\right)^\top = USV^\top \\ U_+ & = U \begin{bmatrix} 1 & 0 & 0 \\ 0 & 1 & 0 \\ 0 & 0 & \det(U) \end{bmatrix} \\ V_+ & = V \begin{bmatrix} 1 & 0 & 0 \\ 0 & 1 & 0 \\ 0 & 0 & \det(V) \end{bmatrix} \\ R_y & = V_+ U_+^\top \end{cases}$$

where $\upsilon_i^{\mathcal{I}(\mathrm{R})}$ and $\upsilon_i^{\mathcal{B}(\mathrm{R})}$ are given in Chapter 3, 4, 5, 6 and 7. For more details visit Hashim et al. (2018b); Markley (1988).

Appendix C
Detailed proofs

Lemma C.1 *Let $\rho \in \mathbb{R}^3$ be the Rodriguez vector associated with attitude $R \in \mathbb{SO}(3)$. Consider the following positive definite potential function*

$$V(\tilde{\rho}) = \left(\frac{\|\rho\|^2}{1 + \|\rho\|^2} \right)^2 \tag{C.1}$$

Thus, for $V_\rho = \partial V / \partial \rho$, the following holds

$$\frac{1}{2} V_\rho^\top \left(\mathbf{I}_3 + [\rho]_\times + \rho\rho^\top \right) \left(\mathbf{I}_3 - R^\top \right) \Omega = 0 \tag{C.2}$$

Proof. From equation (C.1), one obtains

$$V_\rho = 4 \frac{\|\rho\|^2}{\left(1 + \|\rho\|^2\right)^3} \tilde{\rho} \tag{C.3}$$

Consider R in Rodriguez vector representation as given in (A.1), as such, one has

$$
\begin{aligned}
&2\frac{\|\rho\|^2\rho^\top}{\left(1+\|\rho\|^2\right)^3}\rho^\top\left(\mathbf{I}_3+[\rho]_\times+\rho\rho^\top\right)\left(\mathbf{I}_3-\tilde{R}^\top\right)\Omega\\
&=2\frac{\|\rho\|^2}{\left(1+\|\rho\|^2\right)^3}\left(\rho^\top\left(\mathbf{I}_3+\rho\rho^\top\right)-\frac{\rho^\top\left(\mathbf{I}_3+\rho\rho^\top\right)\left(\left(1-\|\tilde{\rho}\|^2\right)\mathbf{I}_3+2\rho\rho^\top-2\left[\rho\right]_\times\right)}{1+\|\tilde{\rho}\|^2}\right)\Omega\\
&=2\frac{\|\rho\|^2}{\left(1+\|\rho\|^2\right)^3}\left(\left(1+\|\rho\|^2\right)\tilde{\rho}^\top-\frac{\left(1+\|\rho\|^2\right)\rho^\top\left(\mathbf{I}_3-\|\rho\|^2\mathbf{I}_3+2\rho\rho^\top\right)}{1+\|\tilde{\rho}\|^2}\right)\Omega\\
&=2\frac{\|\rho\|^2}{\left(1+\|\rho\|^2\right)^3}\tilde{\rho}^\top\left(\left(1+\|\rho\|^2\right)-\frac{\left(1+\|\rho\|^2\right)^2}{1+\|\rho\|^2}\right)\Omega\\
&=0
\end{aligned}
$$

which shows (C.2).

Lemma C.2 *Let $\rho\in\mathbb{R}^3$ be Rodriguez vector and let*

$$g=\frac{1}{2}\left(\mathbf{I}_3+[\rho]_\times+\rho\rho^\top\right)$$

Define $\boldsymbol{\mathcal{W}}_i(\rho)$ as follows

$$\boldsymbol{\mathcal{W}}_i(\rho)=\sum_{k=1}^{3}\sum_{j=1}^{3}\frac{\mathcal{Q}_{j,j}^2}{2}g_{kj}(\rho)\frac{\partial g_{ij}(\rho)}{\partial\rho_k} \tag{C.4}$$

for all $i,j,k=1,2,3$, also, one can find is $\boldsymbol{\mathcal{W}}(\rho)$ to be equivalent to

$$\boldsymbol{\mathcal{W}}(\rho)=\frac{1}{4}\left(\mathbf{I}_3+[\rho]_\times+\rho\rho^\top\right)\mathcal{Q}^2\rho \tag{C.5}$$

Proof. It could be shown that

$$
\begin{aligned}
g(\rho)\,\mathcal{Q} &= \frac{1}{2}\left(\mathbf{I}_3 + [\rho]_\times + \rho\rho^\top\right) \\
&= \begin{bmatrix} 1+\rho_1^2 & -\rho_3+\rho_1\rho_2 & \rho_2+\rho_1\rho_3 \\ \rho_3+\rho_1\rho_2 & 1+\rho_2^2 & -\rho_1+\rho_2\rho_3 \\ -\rho_2+\rho_1\rho_3 & \rho_1+\rho_2\rho_3 & 1+\rho_3^2 \end{bmatrix} \mathcal{Q} \\
&= \begin{bmatrix} \left(1+\rho_1^2\right)\mathcal{Q}_{1,1} & \left(-\rho_3+\rho_1\rho_2\right)\mathcal{Q}_{2,2} & \left(\rho_2+\rho_1\rho_3\right)\mathcal{Q}_{3,3} \\ \left(\rho_3+\rho_1\rho_2\right)\mathcal{Q}_{1,1} & \left(1+\rho_2^2\right)\mathcal{Q}_{2,2} & \left(-\rho_1+\rho_2\rho_3\right)\mathcal{Q}_{3,3} \\ \left(-\rho_2+\rho_1\rho_3\right)\mathcal{Q}_{1,1} & \left(\rho_1+\rho_2\rho_3\right)\mathcal{Q}_{2,2} & \left(1+\rho_3^2\right)\mathcal{Q}_{3,3} \end{bmatrix}
\end{aligned} \tag{C.6}
$$

From (C.4) and (C.6), one has for $i = 1$

$$
\begin{aligned}
&\sum_{k=1}^{3}\sum_{j=1}^{3} \frac{\mathcal{Q}_{j,j}^2}{2} g_{kj}(\rho)\frac{\partial g_{ij}(\rho)}{\partial \rho_k} \\
&= \frac{1}{8}\begin{bmatrix} \left(1+\rho_1^2\right)\mathcal{Q}_{1,1} \\ \left(\rho_3+\rho_1\rho_2\right)\mathcal{Q}_{1,1} \\ \left(-\rho_2+\rho_1\rho_3\right)\mathcal{Q}_{1,1} \end{bmatrix}^\top \begin{bmatrix} 2\rho_1\mathcal{Q}_{1,1} \\ 0 \\ 0 \end{bmatrix} + \frac{1}{8}\begin{bmatrix} \left(-\rho_3+\rho_1\rho_2\right)\mathcal{Q}_{2,2} \\ \left(1+\rho_2^2\right)\mathcal{Q}_{2,2} \\ \left(\rho_1+\rho_2\rho_3\right)\mathcal{Q}_{2,2} \end{bmatrix}^\top \begin{bmatrix} \rho_2\mathcal{Q}_{2,2} \\ \rho_1\mathcal{Q}_{2,2} \\ -1\mathcal{Q}_{2,2} \end{bmatrix} \\
&\quad + \frac{1}{8}\begin{bmatrix} \left(\rho_2+\rho_1\rho_3\right)\mathcal{Q}_3 \\ \left(-\rho_1+\rho_2\rho_3\right)\mathcal{Q}_3 \\ \left(1+\rho_3^2\right)\mathcal{Q}_3 \end{bmatrix}^\top \begin{bmatrix} \rho_3\mathcal{Q}_{3,3} \\ \mathcal{Q}_{3,3} \\ \rho_1\mathcal{Q}_{3,3} \end{bmatrix} \\
&= \frac{1}{8}\left(2\rho_1+2\rho_1^3\right)\mathcal{Q}_{1,1}^2 + \frac{1}{8}\left(-\rho_3\rho_2+\rho_1\rho_2^2+\rho_1+\rho_1\rho_2^2-\rho_1-\rho_2\rho_3\right)\mathcal{Q}_{2,2}^2 \\
&\quad + \frac{1}{8}\left(\rho_2\rho_3+\rho_1\rho_3^2-\rho_1+\rho_2\rho_3+\rho_1+\rho_1\rho_3^2\right)\mathcal{Q}_{3,3}^2 \\
&= \frac{1}{4}\left(\left(1+\rho_1^2\right)\rho_1\mathcal{Q}_{1,1}^2 + \left(\rho_1\rho_2-\rho_3\right)\rho_2\mathcal{Q}_{2,2}^2 + \left(\rho_2+\rho_1\rho_3\right)\rho_3\mathcal{Q}_{3,3}^2\right)
\end{aligned} \tag{C.7}
$$

for $i = 2$

$$
\begin{aligned}
&\sum_{k=1}^{3}\sum_{j=1}^{3}\frac{\mathcal{Q}_{j,j}^{2}}{2}g_{kj}\left(\rho\right)\frac{\partial g_{ij}\left(\rho\right)}{\partial\rho_{k}} \\
&\quad=\frac{1}{8}\begin{bmatrix}\left(1+\rho_{1}^{2}\right)\mathcal{Q}_{1}\\ \left(\rho_{3}+\rho_{1}\rho_{2}\right)\mathcal{Q}_{1}\\ \left(-\rho_{2}+\rho_{1}\rho_{3}\right)\mathcal{Q}_{1}\end{bmatrix}^{\top}\begin{bmatrix}\rho_{2}\mathcal{Q}_{1,1}\\ \rho_{1}\mathcal{Q}_{1,1}\\ \mathcal{Q}_{1,1}\end{bmatrix}+\frac{1}{8}\begin{bmatrix}\left(-\rho_{3}+\rho_{1}\rho_{2}\right)\mathcal{Q}_{2,2}\\ \left(1+\rho_{2}^{2}\right)\mathcal{Q}_{2,2}\\ \left(\rho_{1}+\rho_{2}\rho_{3}\right)\mathcal{Q}_{2,2}\end{bmatrix}^{\top}\begin{bmatrix}0\\ 2\rho_{2}\ \ \mathcal{Q}_{2,2}\\ 0\end{bmatrix} \\
&\qquad+\frac{1}{8}\begin{bmatrix}\left(\rho_{2}+\rho_{1}\rho_{3}\right)\mathcal{Q}_{3}\\ \left(-\rho_{1}+\rho_{2}\rho_{3}\right)\mathcal{Q}_{3}\\ \left(1+\rho_{3}^{2}\right)\mathcal{Q}_{3}\end{bmatrix}^{\top}\begin{bmatrix}-\mathcal{Q}_{3,3}\\ \rho_{3}\mathcal{Q}_{3,3}\\ \rho_{2}\mathcal{Q}_{3,3}\end{bmatrix} \\
&\quad=\frac{1}{8}\left(\rho_{2}+\rho_{1}^{2}\rho_{2}+\rho_{3}\rho_{1}+\rho_{1}^{2}\rho_{2}-\rho_{2}+\rho_{1}\rho_{3}\right)\mathcal{Q}_{1}^{2} \\
&\qquad+\frac{1}{8}\left(2\rho_{2}+2\rho_{2}^{3}\right)\mathcal{Q}_{2,2}^{2}+\frac{1}{8}\left(-\rho_{2}-\rho_{1}\rho_{3}-\rho_{1}\rho_{3}+\rho_{2}\rho_{3}^{2}+\rho_{2}+\rho_{2}\rho_{3}^{2}\right)\mathcal{Q}_{3,3}^{2} \\
&\quad=\frac{1}{4}\left(\left(\rho_{1}\rho_{2}+\rho_{3}\right)\rho_{1}\mathcal{Q}_{1}^{2}+\left(1+\rho_{2}^{2}\right)\rho_{2}\mathcal{Q}_{2,2}^{2}+\left(\rho_{2}\rho_{3}-\rho_{1}\right)\rho_{3}\mathcal{Q}_{3,3}^{2}\right)
\end{aligned}
\tag{C.8}
$$

for $i = 3$

$$
\begin{aligned}
&\sum_{k=1}^{3}\sum_{j=1}^{3}\frac{\mathcal{Q}_{j,j}^{2}}{2}g_{kj}\left(\rho\right)\frac{\partial g_{ij}\left(\rho\right)}{\partial\rho_{k}} \\
&\quad=\frac{1}{8}\begin{bmatrix}\left(1+\rho_{1}^{2}\right)\mathcal{Q}_{1,1}\\ \left(\rho_{3}+\rho_{1}\rho_{2}\right)\mathcal{Q}_{1,1}\\ \left(-\rho_{2}+\rho_{1}\rho_{3}\right)\mathcal{Q}_{1,1}\end{bmatrix}^{\top}\begin{bmatrix}\rho_{3}\mathcal{Q}_{1,1}\\ -\mathcal{Q}_{1,1}\\ \rho_{1}\mathcal{Q}_{1,1}\end{bmatrix}+\frac{1}{8}\begin{bmatrix}\left(-\rho_{3}+\rho_{1}\rho_{2}\right)\mathcal{Q}_{2,2}\\ \left(1+\rho_{2}^{2}\right)\mathcal{Q}_{2,2}\\ \left(\rho_{1}+\rho_{2}\rho_{3}\right)\mathcal{Q}_{2,2}\end{bmatrix}^{\top}\begin{bmatrix}\mathcal{Q}_{2,2}\\ \rho_{3}\mathcal{Q}_{2,2}\\ \rho_{2}\mathcal{Q}_{2,2}\end{bmatrix} \\
&\qquad+\frac{1}{8}\begin{bmatrix}\left(\rho_{2}+\rho_{1}\rho_{3}\right)\mathcal{Q}_{3,3}\\ \left(-\rho_{1}+\rho_{2}\rho_{3}\right)\mathcal{Q}_{3,3}\\ \left(1+\rho_{3}^{2}\right)\mathcal{Q}_{3,3}\end{bmatrix}^{\top}\begin{bmatrix}0\\ 0\\ 2\rho_{3}\mathcal{Q}_{3,3}\end{bmatrix} \\
&\quad=\frac{1}{4}\left(\left(\rho_{1}\rho_{3}-\rho_{2}\right)\rho_{1}\mathcal{Q}_{1,1}^{2}+\left(\rho_{1}+\rho_{2}\rho_{3}\right)\rho_{2}\mathcal{Q}_{2,2}^{2}+\left(1+\rho_{3}^{2}\right)\rho_{3}\mathcal{Q}_{3,3}^{2}\right)
\end{aligned}
\tag{C.9}
$$

Combining the results in (C.7), (C.8) and (C.9) yield

$$
\begin{aligned}
\mathcal{W}(\rho) &= \frac{1}{4}\begin{bmatrix} \left(1+\rho_1^2\right)\rho_1 & \left(\rho_1\rho_2-\rho_3\right)\rho_2 & \left(\rho_2+\rho_1\rho_3\right)\rho_3 \\ \left(\rho_1\rho_2+\rho_3\right)\rho_1 & \left(1+\rho_2^2\right)\rho_2 & \left(\rho_2\rho_3-\rho_1\right)\rho_3 \\ \left(\rho_1\rho_3-\rho_2\right)\rho_1 & \left(\rho_1+\rho_2\rho_3\right)\rho_2 & \left(1+\rho_3^2\right)\rho_3 \end{bmatrix}\begin{bmatrix} \mathcal{Q}_{1,1}^2 \\ \mathcal{Q}_{2,2}^2 \\ \mathcal{Q}_{3,3}^2 \end{bmatrix} \\
&= \frac{1}{4}\begin{bmatrix} 1+\rho_1^2 & \rho_1\rho_2-\rho_3 & \rho_2+\rho_1\rho_3 \\ \rho_1\rho_2+\rho_3 & 1+\rho_2^2 & \rho_2\rho_3-\rho_1 \\ \rho_1\rho_3-\rho_2 & \rho_1+\rho_2\rho_3 & 1+\rho_3^2 \end{bmatrix}\begin{bmatrix} \mathcal{Q}_{1,1}^2 & 0 & 0 \\ 0 & \mathcal{Q}_{2,2}^2 & 0 \\ 0 & 0 & \mathcal{Q}_{3,3}^2 \end{bmatrix}\begin{bmatrix} \rho_1 \\ \rho_2 \\ \rho_3 \end{bmatrix} \\
&= \frac{1}{4}\left(\mathbf{I}_3+[\rho]_\times+\rho\rho^\top\right)\begin{bmatrix} \mathcal{Q}_{1,1}^2 & 0 & 0 \\ 0 & \mathcal{Q}_{2,2}^2 & 0 \\ 0 & 0 & \mathcal{Q}_{3,3}^2 \end{bmatrix}\begin{bmatrix} \rho_1 \\ \rho_2 \\ \rho_3 \end{bmatrix} \\
&= \frac{1}{4}\left(\mathbf{I}_3+[\rho]_\times+\rho\rho^\top\right)\mathcal{Q}^2\rho
\end{aligned}
$$

which shows (C.5).

Lemma C.3 *For* $\boldsymbol{T}, \boldsymbol{T}_1, \boldsymbol{T}_2 \in \mathbb{SE}(3)$ *and* $\mathcal{Y} = \left[y_1^\top, y_2^\top\right] \in \mathbb{R}^6 \forall y_1, y_2 \in \mathbb{R}^3$ *, the following identities hold:*

$$
\boldsymbol{T}\left[\mathcal{Y}\right]_\wedge \boldsymbol{T}^{-1} = \left[\overline{\breve{\mathbf{Ad}}}_{\boldsymbol{T}}\mathcal{Y}\right]_\wedge, \quad \boldsymbol{T} \in \mathbb{SE}, \mathcal{Y} \in \mathbb{R}^6 \tag{C.10}
$$

$$
\boldsymbol{\Upsilon}\left(\mathbf{Ad}_{\boldsymbol{T}}\left(\left[\mathcal{Y}\right]_\wedge\right)\right) = \overline{\breve{\mathbf{Ad}}}_{\boldsymbol{T}}\boldsymbol{\Upsilon}\left(\left[\mathcal{Y}\right]_\wedge\right) \in \mathbb{R}^6 \tag{C.11}
$$

$$
\overline{\breve{\mathbf{Ad}}}_{\boldsymbol{T}}\overline{\breve{\mathbf{Ad}}}_{\boldsymbol{T}^{-1}} = \overline{\breve{\mathbf{Ad}}}_{\boldsymbol{T}^{-1}}\overline{\breve{\mathbf{Ad}}}_{\boldsymbol{T}} = \mathbf{I}_6, \quad \boldsymbol{T} \in \mathbb{SE}(3) \tag{C.12}
$$

Proof. Recall the preliminaries in Chapter

$$
\begin{aligned}
\left[\mathcal{Y}\right]_\wedge &= \begin{bmatrix} [y_1]_\times & y_2 \\ \underline{\mathbf{0}}_3^\top & 0 \end{bmatrix} \\
\mathbf{Ad}_{\boldsymbol{T}}\left(\left[\mathcal{Y}\right]_\wedge\right) &= \boldsymbol{T}\left[\mathcal{Y}\right]_\wedge \boldsymbol{T}^{-1} \in \mathfrak{se}(3) \\
\overline{\breve{\mathbf{Ad}}}_{\boldsymbol{T}} &= \begin{bmatrix} R & \mathbf{0}_{3\times 3} \\ [P]_\times R & R \end{bmatrix} \in \mathbb{R}^{6\times 6}
\end{aligned}
$$

It is straight forward to show that

$$
\begin{aligned}
\mathrm{Ad}_{\boldsymbol{T}}\left([\mathcal{Y}]_{\wedge}\right) &= \boldsymbol{T}\,[\mathcal{Y}]_{\wedge}\,\boldsymbol{T}^{-1} \\
&= \begin{bmatrix} R & P \\ 0_{1\times 3} & 1 \end{bmatrix} \begin{bmatrix} [y_1]_{\times} & y_2 \\ \underline{\mathbf{0}}_3^{\top} & 0 \end{bmatrix} \begin{bmatrix} R^{\top} & -R^{\top}P \\ 0_{1\times 3} & 1 \end{bmatrix} \\
&= \begin{bmatrix} R\,[y_1]_{\times}\,R^{\top} & Ry_2 - R\,[y_1]_{\times}\,R^{\top}P \\ 0_{1\times 3} & 0 \end{bmatrix} \\
&= \begin{bmatrix} [Ry_1]_{\times} & Ry_2 - [Ry_1]_{\times}\,P \\ 0_{1\times 3} & 0 \end{bmatrix}
\end{aligned} \tag{C.13}
$$

Similarly, one can verify that

$$
\begin{aligned}
\left[\overline{\breve{\mathbf{Ad}}}_{\boldsymbol{T}}\mathcal{Y}\right]_{\wedge} &= \left[\begin{bmatrix} R & 0 \\ [P]_{\times}\,R & R \end{bmatrix} \begin{bmatrix} y_1 \\ y_2 \end{bmatrix}\right]_{\wedge} \\
&= \begin{bmatrix} Ry_1 \\ [P]_{\times}\,Ry_1 + Ry_2 \end{bmatrix}_{\wedge} \\
&= \begin{bmatrix} Ry_1 \\ -\,[Ry_1]_{\times}\,P + Ry_2 \end{bmatrix}_{\wedge} \\
&= \begin{bmatrix} [Ry_1]_{\times} & Ry_2 - [Ry_1]_{\times}\,P \\ 0_{1\times 3} & 0 \end{bmatrix}
\end{aligned} \tag{C.14}
$$

Accordingly, (C.13) and (C.14) show (C.10). From (C.13) one obtains

$$
\boldsymbol{\Upsilon}\left(\mathbf{Ad}_{\boldsymbol{T}}\left([\mathcal{Y}]_{\wedge}\right)\right) = \begin{bmatrix} Ry_1 \\ Ry_2 - [Ry_1]_{\times}\,P \end{bmatrix} \tag{C.15}
$$

From (C.14) one has

$$
\overline{\breve{\mathbf{Ad}}}_{\boldsymbol{T}}\boldsymbol{\Upsilon}\left([\mathcal{Y}]_{\wedge}\right) = \begin{bmatrix} R & \mathbf{0}_{3\times 3} \\ [P]_{\times}\,R & R \end{bmatrix} \begin{bmatrix} y_1 \\ y_2 \end{bmatrix} = \begin{bmatrix} Ry_1 \\ Ry_2 - [Ry_1]_{\times}\,P \end{bmatrix} \tag{C.16}
$$

Therefore, (C.15) and (C.16) justify (C.11). The last identity

$$
\begin{aligned}
\overline{\breve{\mathbf{Ad}}}_{\boldsymbol{T}}\overline{\breve{\mathbf{Ad}}}_{\boldsymbol{T}^{-1}} &= \begin{bmatrix} R & \mathbf{0}_{3\times 3} \\ [P]_\times R & R \end{bmatrix} \begin{bmatrix} R^\top & \mathbf{0}_{3\times 3} \\ \left[-R^\top P\right]_\times R^\top & R^\top \end{bmatrix} \\
&= \begin{bmatrix} \mathbf{I}_3 & \mathbf{0}_{3\times 3} \\ [P]_\times + R\left[-R^\top P\right]_\times R^\top & \mathbf{I}_3 \end{bmatrix} \\
&= \mathbf{I}_6
\end{aligned}
$$

which justifies the result in (C.12).

Curriculum Vitae

Name:	Hashim Abdellah Hashim Mohamed
Post-Secondary Education and Degrees:	University of Western Ontario London, ON, Canada 2019 Doctor of Philosophy in Robotics and Control Electrical and Computer Engineering King Fahd University of Petroleum & Minerals Dhahran, Saudi-Arabia 2015 Master of Science in Systems and Control Engineering College of Computer Sciences and Engineering Helwan University Cairo, Egypt 2009 Bachelor of Science (First rank with Honour) Mechatronics, Mechanical Engineering

Selected Journal Publications

- Hashim, H. A., Brown, L. J., & McIsaac, K. (2019). Nonlinear Pose Filters on the Special Euclidean Group SE(3) with Guaranteed Ttransient and Steady-state Performance. IEEE Transactions on Systems, Man, and Cybernetics: Systems, PP (PP), 1-14.
- Hashim, H. A., Brown, L. J., & McIsaac, K. (2018). Nonlinear Stochastic Attitude filters on the Special Orthogonal Group 3: Ito and stratonovich. IEEE Transactions on Systems, Man, and Cybernetics: Systems, PP (PP), 1-13.
- Hashim, H. A., Brown, L. J., & McIsaac, K. (2019). Nonlinear stochastic position and attitude filter on the special euclidean group 3. Journal of the Franklin Institute, 356 (7), 4144-4173.
- Hashim, H. A., El-Ferik, S., & Lewis, F. L. (2019). Neuro-adaptive Cooperative Tracking Control with Prescribed Performance of Unknown Higher-order Nonlinear Multi-agent Systems. International Journal of Control , 92 (2), 445-460.

- Hashim, H. A. & Abido, M. A. (2019). Location Management in LTE Networks using Multi-Objective Particle Swarm Optimization. Computer Networks, Vol. 157 (1), 78-88.
- Hashim, H. A. & Abido, M. A. (2016). Optimal placement of relay nodes in wireless sensor network using artificial bee colony algorithm. Journal of Network and Computer Applications, 64 (21), 239–248.